CHAPTER 1
INTRODUCTION

1.1. Cancer overview

Cancer is an anarchistic proliferation of a homeostatic cell escaping the regulations. Two facts are observed when the cancerous cell grows: Firstly, intense and uncontrolled multiplication leading to a tumour which invades certain sites. Secondly, it has the capacity of evasion of control mechanisms to colonize other sites and produce metastases.

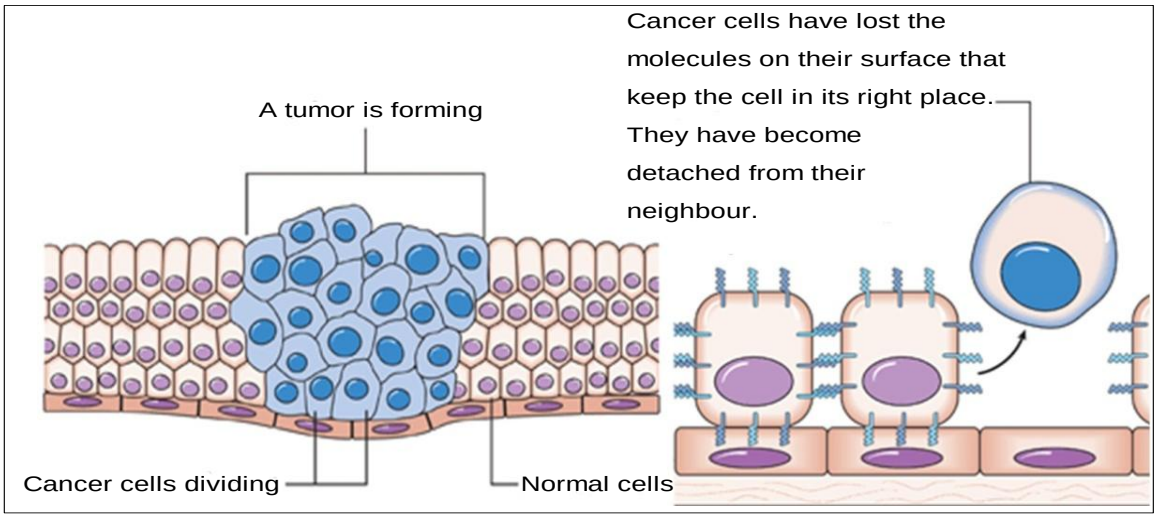

Figure 1.1: Cancer cells[1]

The canceration of a cell results from the disordered state of genetic control of the cellular division. It is characterized by a great genetic instability. This genetic disease is expressed by unspecific signs, i.e. symptoms met in other none-cancerous pathological afflictions. The specific absence of character of the cancerous cell is accompanied by an absence of specific diagnostics, and, as a consequence, lead to an absence of specific therapeutic approaches.

Three main therapeutic techniques for cancer treatment are available; these include: surgery, radiation therapy and chemotherapy.

a) Surgery[2,3] :

Surgery was the first mode of the cancer therapy, consisting of removing the primary tumor; it is by far the most efficient cancer cure. Although offering the greatest chance to treat various types of cancer by removing the primary tumors, surgery is ineffective for metastasized or disseminated tumors. Surgery can proceed to withdraw a tumor tissue when it appears to be confined to one area; a typical case is breast removal. It may be used along with chemotherapy or radiation therapy, which can be given before or after the operation.

Reconstructive surgery is used to restore a person's appearance or the function of an organ or body part after primary surgery. Typical examples are breast re-enactment after mastectomy or the use of tissue flaps, bone grafts, or prosthetic (metal or plastic) materials after surgery for oral cavity cancers.

b) Radiation therapy[2,4] :

This is a therapeutic technique that requires an exposure of a precise part of the body to radiation, notably ionizing radiations such as X-rays or gamma rays. Because of the risks related to the action of radiation, radiotherapy is less used for the treatment of the afflictions which are not cancerous. The ionizing radiations destroy the malignant cells, but unfortunately, they affect also the normal cells; thus radiotherapy requires the precise location of the tumours.

c) Chemotherapy[5,6,7,11]:

In the battle against cancer, one of the main therapeutic techniques used for treatment is chemotherapy. This involves the use of chemicals to destroy cancer cells. Chemotherapy works by interfering with the cancer cell's ability to grow.

To understand chemotherapy, the cell cycle must first be understood. Chemotherapy is effective because the drugs used affect some phase of the cell life cycle. Each cell goes through a four-phase cycle in order to replicate itself. The first phase, 'the Ribonucleic acid (RNA) and protein synthesis phase' (called G_1), is when the cell prepares to replicate its chromosomes. In the second stage, 'the Deoxyribonucleic acid (DNA) replicating phase' (called S), the DNA synthesis occurs and the DNA is duplicated. The next phase, 'the cell pre-splitting phase' (called G_2), is when the RNA and protein duplicate. The final stage is the mitotic phase (called M), which is the stage of the cell division. In this final stage, the duplicated DNA and RNA split and move to separate ends of the cell, and the cell actually divides into two identical, functional cells[11].

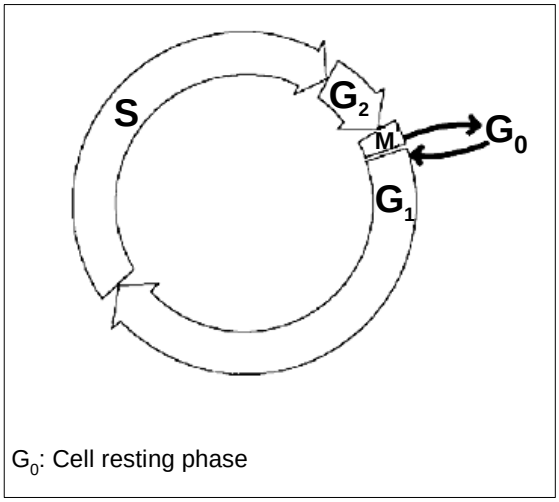

Figure 1.2: Cell cycle phases[13]

The drug acts more on the cancerous cells than on the normal cells because:
Cancerous cells multiply more quickly than normal cells and are thus more sensitive to the anti-cancer drugs; cancerous cells acquire abnormal functions which modify their usual metabolic capacities. But chemotherapy is not specific, which explains its side effects. The majority of drugs used in chemotherapy are administered intravenously but they can also be given in tablets. This therapy can also be used in conjunction with radiotherapy and surgery to increase the treatment efficiency. Currently, more than fifty different drugs are in oncological use. Frequently, several drugs are used simultaneously to prevent the tumour from becoming resistant to the treatment; one may also mix drugs to avoid cross resistance thus allowing for a better antitumor effectiveness. This situation stimulated researchers worldwide to investigate the use of macromolecular drug delivery systems to enhance the efficiency of anti-tumor agents (see Chapter 2). This research, part of the effort of the polymer research group in the School of Chemistry of the University of the Witwatersrand, contributes to the development of macromolecules which reduce drug toxicity and other drug deficiencies in cancer chemotherapy.

1.2. Aims of the project

The aim of the present thesis is the development of macromolecular anticancer drugs composed of a polymeric carrier to which antineoplastic agents are tied via biodegradable hydrazone links. Drug release in the cancerous cell, which is strongly pH dependent, proceeds hydrolytically in the acidic intracellular compartment, and this, represents an advanced drug delivery method in cancer chemotherapy.

Experimental goals contributing to the aims of the present project were set as follows:

1. Synthesis of water-soluble macromolecular carriers equipped with hydrazine side groups.
2. Conjugation of selected drugs to carriers via Hydrazone bridges.
3. Evaluation of the stability of hydrazone bridges.

C H A P T E R 2
BACKGROUND AND LITERATURE REVIEW

2.1. Cancer Chemotherapy

2.1.1. Introduction

The available anticancer drugs have different mechanisms of action which may vary at different drug concentrations and in their effects on different types of normal and cancer cells. A single "cure" for cancer has proved elusive since there is not a single type of cancer but many different types of cancer. In addition, there are very few demonstrable biochemical differences between cancerous cells and normal cells; so the effectiveness of many anticancer drugs is limited by their toxicity to normal cells. A final problem is that cancerous cells which are initially suppressed by a specific drug may develop a resistance to that drug. For this reason cancer chemotherapy may consist of using a combination of drugs over varying lengths of time.

2.1.2. Cancer Chemotherapy[8,9]

Chemotherapeutic drugs are sometimes feared because of a patient's concern of toxic effects. Their role is to slow and hopefully halt the growth and spread of a cancer[8]. The anticancer agents affect malignant cells in one of the three ways, depending on the drug chosen:

1. Damaging the DNA of the affected cancer cells.
2. Inhibiting the synthesis of new DNA strands to stop the cell from replicating, because the replication of the cell is what allows the tumor to grow.
3. Stopping the mitotic processes of the cell so that the cancer cell cannot divide into two cells.

Current chemotherapy drugs act in one of these ways to achieve the goal of killing cancer cells in the body. Unfortunately, the majority of drugs currently on the market are not specific, which leads to many common side effects associated with cancer chemotherapy. The common aim of all chemotherapy is to decrease the growth rate (cell division) of cancer cells. Side effects are typically seen in body systems that naturally have a rapid turnover of cells, including skin, hair, gastrointestinal, and bone marrow. These healthy, normal cells also end up damaged by the chemotherapy program.

2.1.3. Categories of Chemotherapy drugs[10,11,12]

Most chemotherapy agents work by interfering with DNA synthesis or function. Each chemotherapy drug works during different phases of the cell cycle. Based on their action, chemotherapy agents can be classified as cell-cycle specific agents (effective during certain phases of cell cycle) and cell-cycle nonspecific agents (effective during all phases of cell cycle). Depending on their characteristics and nature of action, chemotherapy agents can be categorized as alkylating agents, antimetabolites, anthracyclines, antitumor antibiotics, monoclonal antibodies, platinum drugs, or plant alkaloids (Figure 2.1).

2.1.3.1. Alkylating agents[10]

Alkylating agents are one of the earliest and most commonly used chemotherapy agents used for cancer treatments. Their use in cancer treatments started in early 1940s[10]. These agents work directly on the damaging of DNA to prevent the cancer cell from reproducing. As a class of drugs, these agents are not phase-specific; in other words, they work in all phases of the cell cycle. Those agents are used to treat many different cancers, including acute and chronic leukemia, lymphoma, hodgkins disease, multiple myeloma, sarcoma, as well as cancers of the lung, breast, and ovary. They can cause long-term damage to the bone marrow. There are many different alkylating agents, including: nitrogen mustards, nitrosoureas, alkyl sulfonates, triazines, and ethylenimines.

2.1.3.2. Antimetabolites[10,11]

Antimetabolites were first discovered in the year 1948, when Dr. Sidney Farber found that folic acid analog can reduce childhood leukemia. Out of 16 patients he tested, 10 displayed hematologic improvement. This discovery laid the foundation that enabled scientists to synthesize many new agents that could inhibit biological enzymatic reactions [10]. Antimetabolites block cell growth by interfering with DNA synthesis. These drugs work by mimicking a substance involved in DNA synthesis, inhibiting production of an acid necessary for DNA to be synthesized. These drugs affect the “S” phase of the cell cycle, and are used for the treatment of tumors of the gastrointestinal tract, breast, and ovary. The antimetabolite chemotherapy drugs include: methotrexate, 6-mercaptopurine, 5-fluorouracil, thioguanine, cytarabine, cladribine, gemcitabine, fludarabine, and pemetrexed.

2.1.3.3. Anthracyclines[10,11]

Anthracyclines were developed between 1970s and 1990s and include daunosamine and tetra-hydronaphthacenedione-based chemotherapy agents[10]. Anthracycline drugs work by forming free oxygen radicals that break DNA strands thereby inhibiting DNA synthesis and function. These chemotherapeutic agents form a complex with DNA and enzyme to inhibit the topoisomerase enzyme. One of the side effects of anthracyclines is that it can damage heart muscle cells along with the DNA of a cancer cell leading to cardiac toxicity. These drugs are used to treat a large number of cancers including lymphomas, leukemia, and uterine carcinomas. Examples of anthracyclines include daunorubicin, doxorubicin, epirubicin, mitoxantrone, and idarubicin.

2.1.3.4. Antitumor antibiotics[10,11]

Antitumor antibiotics are developed from the soil fungus Streptomyces[10]. They work by binding with DNA to prevent RNA synthesis. They also prevent cell growth by preventing

DNA replication. These drugs prevent the DNA from reattaching itself together, and this causes the cell to die. This category of drugs is used to treat a wide variety of cancers including testicular cancer and leukemia. Examples of those chemotherapy agents are: doxorubicin, mitomycin-C, and bleomycin.

2.1.3.5. Monoclonal antibodies[10,11]

Monoclonal antibodies are one of the newer chemotherapy agents approved for cancer treatment by the Food and Drug Administration (FDA) in 1997[10]. They work by attaching to certain parts of the tumor-specific antigens and make them easily recognizable by the host's immune system. They also prevent growth factors' attachment promoting cell growth. They can be combined with radioactive particles and other powerful anticancer drugs to deliver them directly to cancer cells. This treatment can be given to patients without causing any serious harm to other healthy cells of the body. The treatment is useful in treating colon, lung, neck, and breast cancers, chronic lymphocylic leukemia, acute myelogenous leukemia, and non-hodgkin's lymphoma. Chemotherapy agents include: alemtuzumab, bevacizumab, cetuximab, gemtuzumab, ibritumomab, panitumumab, rituximab, tositumomab, and trastuzumab.

2.1.3.6. Platinum drugs[10,11]

Platinum-based metal derivatives were found to be useful for cancer treatments, as first demonstrated with the synthesis of cisplatin. These chemotherapy agents work by cross-linking subunits of DNA. They act during any part of cell cycle and help in treating cancer by impairing DNA synthesis, transcription, and function. Cisplatin was found to be useful in treating testicular, lung cancer, and colon cancer. The platinum drugs (cisplatin, carboplatin, and oxaliplatin) are sometimes grouped with alkylating agents because they kill cells in a similar way.

2.1.3.7. Plant alkaloids[10,11]

Plant alkaloids, as the name suggests, are plant derivatives. They are cell-specific chemotherapy agents, but the cycle affected varies from drug to drug. Vincristine (Oncovin) is a plant alkaloid of interest in mesothelioma treatment[10]. They are categorized into four groups:

- Topoisomerase inhibitors: These chemotherapy agents are categorized into Type I (extracted from the bark and wood of the Chinese tree Camptotheca accuminata) and Type II (extracted from the alkaloids found in the roots of May apple plants). They work in the late S and G2 phases of the cell cycle by interfering with DNA transcription, duplication, and function to avoid DNA supercoiling. They are used to treat certain leukemias, as well as lung, ovarian, gastrointestinal, and other cancers.

- Vinca alkaloids: Vinca alkaloids are derived from the periwinkle plant, Vinca rosea (Catharanthus roseus) and are known to be used by the people of Madagascar to treat diabetes. Although not helpful in controlling diabetes, vinca alkaloids are useful in treating leukemias. They are efficient in the M phase of the cell cycle and work by inhibiting tubulin assembly in microtubules[10]. The usually used vinca alkaloid chemotherapy agents are Vincristine, Vinblastine, Vinorelbine, and Vindesine.

- Taxanes: Taxanes are plant alkaloids that were first developed in 1963 upon isolation from the bark of the Pacific yew tree, Taxus brevifolia in 1963. Paclitaxel, which is the active component of taxanes, was first discovered in 1971 and was made available for clinical use in the year 1993[10]. Paclitaxel and docetaxel are generally used taxanes. These chemotherapy agents are used to cure a large group of cancers including breast, ovarian, lung, head and neck, gastric, esophageal, prostate and gastric cancers.

- Epipodophyllotoxins: Epipodophyllotoxins chemotherapy agents are extracted from the American May Apple tree (Podophyllum peltatum). They prevent DNA replication by stopping the cell from entering the G1 phase and stop DNA replication in the S phase[10].

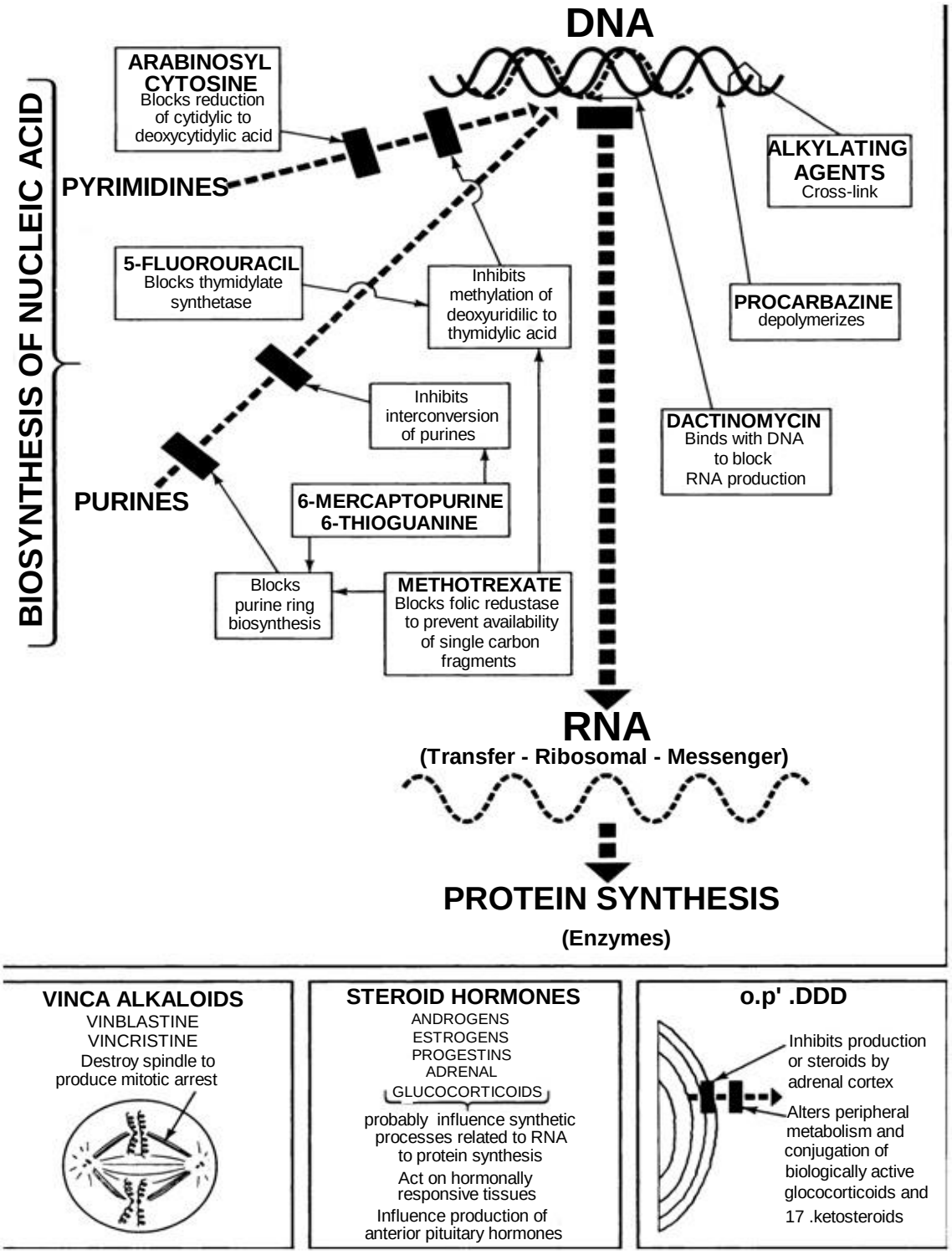

Figure 2.1 mechanism of action for selected anticancer drugs[12]

2.1.3.8. The ferrocenyl drug system

Bio-organometallic chemistry is an emergent area in medicinal therapy due to varied biological applications of organometallic compounds[14,15]. The first organometallic compound used, over the past 30 years, were platinum-based drugs, notably cisplatin and carboplatin, which have dominated the treatment of various cancers by chemical agents. However, these drugs cause serious side effects, including renal impairment, neurotoxicity and ototoxicity (loss of balance/hearing). Thus, there has been considerable interest and increased research activity in developing other transition metal compounds as anticancer drugs, which are less toxic than the platinum-based drugs. Among different organometallic systems, metallocenes and metallocene dihalides proved to be particularly active against a number of tumors[16]. Despite the fact that their activity seems to follow mechanistic paths which differ from those of cisplatin, both drugs have a DNA intracellular target.

The first metallocene discovered was ferrocene, and its particular structure was brought out by Wilkinson[17] in the early 1950s. Ferrocene, a stable, synthetic, iron-containing compound, induces in vitro and in vivo activation of mouse lymphocytes and macrophages; it also shows an antitumor effect in mice, due to its immune-stimulatory property[18]. Ever since, there has been a rapid growth in the study of ferrocene compounds for several reasons, which include the excellent stability of the ferrocene moiety in biological media, their lipophilicity, and their reversible redox chemistry. Unlike the platinum-based compounds, the cytotoxic activity of ferrocene compounds, namely ferricenium salts, is probably not based on their direct binding to DNA, but on their ability to regenerate oxygen-active species which induce oxidative DNA damage. Free-radical chemistry plays a vital role in cancer generation and in various phases of growth and control of neoplasia. Effective inhibition and detoxification processes in the cancerous organism may well be involved in the superoxide and free radical-scavenging reactions (see scheme 2.2). A deactivating recombination of ferrocene in its oxidized state with the

free-radical from ribonucleotide reductase, an important enzymatic link in DNA synthesis, may represent another potential contribution to the inhibition of the cell's proliferation process.

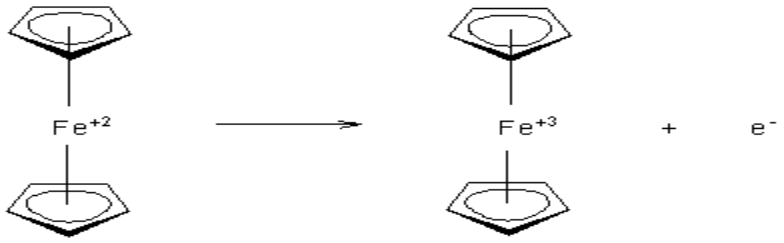

Scheme 2.1: Reversible oxidation/reduction[19]

In addition, ferrocene could readily form a variety of stable conjugated species, like anticancer drugs (ferrocifen: ferrocene conjugated tamoxifen) and antimalarial drugs (ferroquine: ferrocene-attached chloroquine) (figure 2.2).

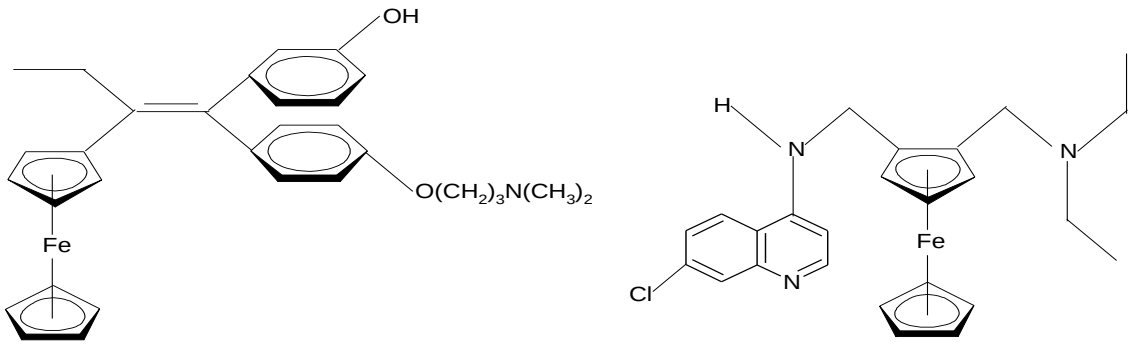

Hydroxy-Ferrocifen

Ferroquine

Figure 2.2: Ferroquine and ferrocifen structures[20]

The cytoxicity of tamoxifen and ferroquine is greatly enhanced due to the presence of a ferrocenyl moiety which shows anticancer and antimalarial activities respectively.

Moreover, bioconjugates of metallocenes with protein, peptide, DNA, RNA, and sugar are being subject to various biochemical researches. In view of this, ferrocene compounds were the investigated drug systems in this project, and will be discussed in detail.

2.1.3.8.1. Ferrocene-Ferricenium system behavior in the biological environment

One of the key features of the ferrocene molecule is the ready donation of an electron from an essentially non-bonding, high-energy molecular orbital, transforming the neutral, diamagnetic compound to the positively charged, paramagnetic ferricenium ion radical. This one-electron transfer reaction is reversible (path a), and has some implications in the biological realm. In the biological environment, ferrocene is oxidized by hydrogen peroxide in the presence of horseradish peroxidase[21]. The cation may form charge transfer complexes by reactions with donor groups in proteins, such as tryptophan[22]. The reverse reaction in Scheme 2.2 has been shown to proceed:

1) Through the pH-controlled action of the flash-photolytically generated superoxide anion radical, the latter being converted in the process to dioxygen[23] (path b)
2) Through oxidation of metalloproteins, such ferrocytochrome[24,25] (path c),
3) Through oxidation of NADH to NAD^+ [26,27] (path d and scheme 2.3), and
4) With formation of the hydroxyl free radical in the presence of glutathione, GSH[28] (path e).

The ferricenium reactions are the characteristic feature of free-radical compounds to react with other radical species through recombination. Ferricenium cation interacting with a free radical •R (biological radical), can convert with loss of a proton to a substituted ferrocene compound (scheme 2.2). This reaction obviously constitutes a free radical-scavenging process in contact with suitable biological partners and, hence, may well have significant implications for the ferricenium cation in the living organism.

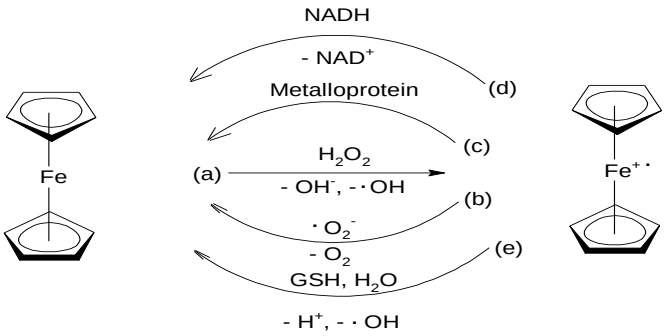

Scheme 2.2 Biological interactions involving the ferrocene-ferricenium system[29]

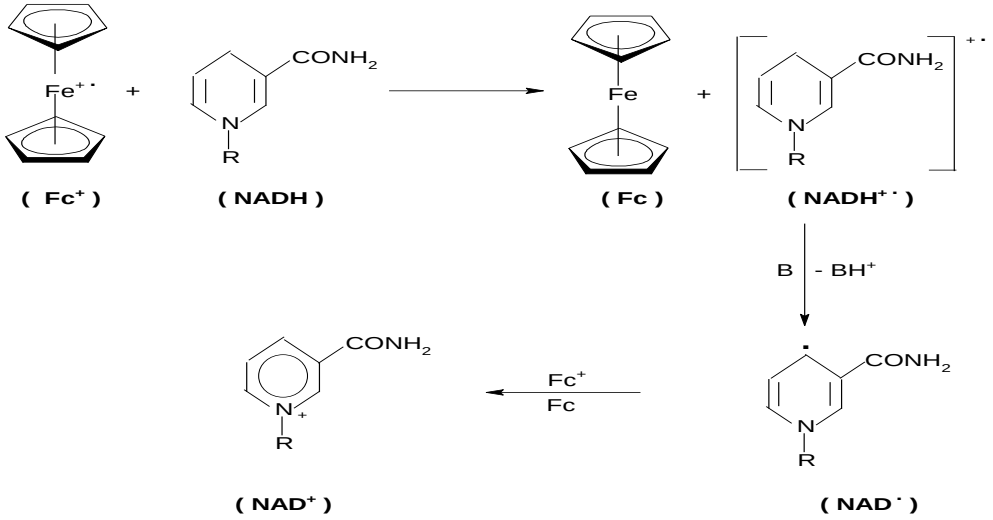

Scheme 2.3 Ferricenium reduction by NADH[29]

2.1.3.8.2. Ferrocene-Ferricenium system as candidate anticancer drug model

Although the biological processes controlling carcinogenicity and cancer growth are diverse in the extreme and only partially understood even at this present time, reactive oxygen species and associated free-radical reactions are significant contributors to the overall interplay of these processes[29,30]. Reduction of dioxygen in the respiring aerobic cell produces reactive oxygen derivatives including hydrogen peroxide, superoxide radical anion, and the highly destructive hydroxyl free radical. In the healthy organism these species will be modulated by the detoxifying action of a diversity of cell protective

enzymes, such as superoxide dismutase (SOD), catalase, GSH peroxidase, or heme oxidase, mobilized by the host's defence mechanisms[31,32]. If thus kept under control, reactive oxygen species, such as hydrogen peroxide, may in fact perform a vital role in sustaining homeostasis, and thus healthy equilibrium, through induction of apoptosis of detrimental cells. If left unchecked, on the other hand, the very same species can be found to operate against the host's well being. Strongly reduced SOD activity, for example, was observed in many cancer cells[32], and the generation of superoxide and secondary free radicals in elevated concentrations may initiate pathological reactions, as these species bind to the cell's DNA with resultant replication errors during the mitotic stage[30]. Carcinogenesis may thus be triggered. Both carcinogenic[29,30,32,33,34] and metastatic[35] processes may, in turn, be inhibited by antioxidants and free-radical scavengers, including SOD-mimetic agents functioning as superoxide traps.

Diverse clinically used anticancer drugs, in fact, may react as free radicals or undergo in vivo metabolism via free radical steps[35,36,37], and their antineoplastic activity may well involve a radical-scavenging mechanism. It should be clear from these observations that any compound existing as a free radical or being capable of in vivo transformation into a free-radical metabolite, could in principle interfere with free-radical activity in the cancerous cell and thereby act as a cell growth-inhibiting agent.

The preparation of several ferricenium compounds and their assessment for antiproliferative activity against ascitic murine tumors and several human tumor clonogenic cultures are reported in review articles[38,39]. For those salts tested that were insoluble, like the ferrocene parent itself, no activity was revealed in the screens. In contrast, ferricenium salts comprising the picrate, tetrachloroferrate (III), μ-oxo-bis(trichloroferrate(III)), trichloroacetate, or chloride counter ions, were found to be active, and they all showed good water solubility with high saturation limits. Under optimal conditions, in the Ehrlich ascites screening test, best results (cure rates of 100%) were displayed by the picrate and the trichloroacetate salts. The oxidation-reduction equilibrium distribution of ferricenium and ferrocene species in any body compartment is probably exclusively under the control of the biological environment[40], *i.e.* pH and enzymatic

activity in that compartment, and not of the oxidation state in which the ferrocene compound was initially administered. Thus, the biological effects encountered in vitro should also be shown in vivo irrespective of the compounds' initial oxidation state, the only requirement being water solubility of the compound, which should be highly adequate for rapid dissolution and dissipation in the aqueous fluid system.

A strategy designed to achieve ferrocene administration in a water-soluble dosis form could logically involve conversion of the compound to a prodrug constructed so as to possess water solubility and enough stability in circulation to survive transport to, and into, the tumors cell. There the original compound would be released for action, rapidly undergoing the particular ferrocene-ferricenium equilibrium distribution dictated by the lysosomal environment. This prodrug concept can indeed be reduced to practice through the expediency of conjugating the ferrocene unit bioreversibly to a suitable carrier that is polymeric, water-soluble, and possesses the necessary chemical and physical prerequisites prescribed by the rules of biomedicine.

2.2. Polymer – Drug Conjugation

2.2.1. Conjugation systems

After more than 40 years of research and development of drug delivery systems, polymer carriers have proved their value in the design and preparation of controlled drug release formulations[41] (extensively reviewed by Duncan[42], Satchi-Fainaro et al[43], and Vicent and Duncan[44]). They should ideally deliver a drug to a specific site in a specific time and release pattern. Initially, constant or sustained drug release was the feature pursued by most of the drug delivery studies in order to avoid problems associated with conventional administration in chronic treatments. This concept has evolved into the trend of developing drug delivery systems that fit the circadian rhythm by using the so-called stimuli responsive polymer or 'intelligent' polymer. In this sense, the main advantages of polymers are their great versatility from a structure point of view, the possibilities to combine hydrophobic and hydrophilic components, as well as the interactions polymer-

polymer, polymer-drug and, polymer-solvent that offer many possibilities to design and prepare formulations with specific properties and functions.

Water-soluble conjugates of synthetic copolymers with anticancer drugs and antibodies provide a potential drug delivery system facilitating specific drug delivery to model tumors in mice[45,46]. In the system, an anti-cancer drug is attached to the polymer through a biodegradable spacer susceptible to enzymatic hydrolysis enabling intracellular drug release at a controlled rate, and a specific antibody is attached as a homing device, recognizing specific receptors expressed on the surface of the target cells. Water-soluble drug carriers based on non-degradable copolymers were designed as lysosomotropic drug delivery systems. Various structures of the carriers and polymer drugs have been synthesized and studied. In a classic structure, an anti-cancer drug and a targeting antibody are attached to the hydrophilic back bone via enzymatically degradable oligopeptide sequences randomly distributed along the polymer chain. Such conjugates provide a potential and powerful drug delivery system facilitating specific drug delivery to tumor cells or model tumors inoculated in mice[47]. Despite its significant anti-cancer activity, the system has some drawbacks, such as a poorly defined branched structure, high molecular weight and broad distribution of molecular weights. These drawbacks are minimized in the second systems, called star structure of the conjugate. The star conjugates differ in the degree of antibody substitution and the length of the polymer chain synthesized. All antibody conjugates of star structure had lower molecular weights and a significantly narrower molecular weight distribution than the conjugates of a classic structure. The rate of drug release from the classic conjugates incubated in the presence of lysosomal enzyme strongly depended on the structure of the oligopeptide space[48,49].

Both classic and star systems enable drug release only in secondary lysosomes after contact with lysosomal enzymes. Biological activity of all conjugates depends on the detailed structure of the conjugate and the ability of the system to release active drug in the target cells. A prerequisite for biological activity of the classic and star conjugates is the presence of lysosomal enzymes at the polymer drug target.

In the third system (hydrazone conjugates), the drug is attached to the biodegradable backbone via a spacer containing a hydrazone group. The hydrazone conjugates are stable under physiological conditions (blood circulation, pH 7.4), but hydrolytically degradable in a mildly acidic environment (e.g., in endosomes and lysosomes, pH ~ 5 - 6) (figure 2.3). The systems can circulate in the blood stream for a long time and are specifically activated (drug is released) in the target cells, including those not exhibiting enzymatic activity.

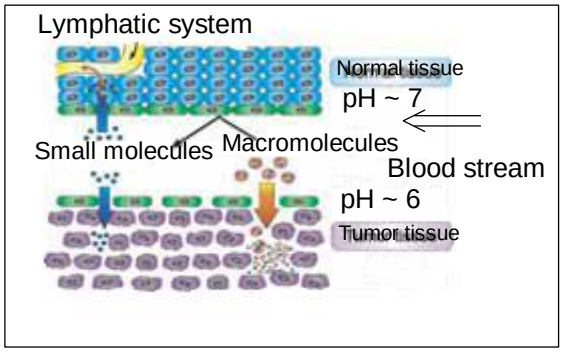

Figure 2.3 Pathophysiology of tumor tissue[50]

2.2.1.1. **Lysosomotropic conjugates**.

Lysosomotropic agent was established by De Duve and co-workers (1974) to designate substances that are taken up selectively into lysosomes. This definition leaves open the chemical nature of a lysosomotropic substance and the mechanism of its uptake. However, almost all agents with lysosomotropic properties based on cell permeation rather than endocytotic uptake belong to the class of weak bases. This has led to the assumption that the specific uptake of lysosomotropic substances into lysosomes depends on the acidic pH of these compartments, ion-trapping weak bases. The ion-trapping mechanism depends on the proton gradient between the cytosol and the lysosomal compartment.

2.2.1.2. Hydrazone conjugates.

Hydrazones have been demonstrated to possess, among others, antimicrobial, anticonvulsant, analgesic, antiinflammatory, antiplatelet, antitubercular and antitumoral activities. As iron is necessary for the biochemical reactions of living organisms, researchers have synthesized hydrazones by using various aldehydes and their iron complexes and evaluated these complexes for their antitumoral activity. The mechanism of antitumoral activity of iron complexes is the inhibition of ribonucleotide reductase, which is an important enzyme for conversion of ribonucleotides to deoxyribonucleotides. Hydrazones possessing an azometine –NHN=C**H**- proton constitute an important class of compounds for new drug development.

Drug release from the conjugates containing hydrazone spacer at pH < 6 is faster than those with ester bonds[51]. Cytotoxicity of the conjugates of treated cells depended on the detailed structure of the spacer and the used antibody. The hydrazone conjugates had more cytotoxic potency than those with ester bonds.

2.2.2. Polymers as Drug Carriers

Modification of biologically active compounds with polymers is one of the methods for altering and controlling pharmacokinetics, bio-distribution, and toxicity[52]. Polymers chosen as drug carriers are either natural or synthetic macromolecules. Certain requirements must be met in order to maximize their potential as polymeric drug carriers by decreasing the toxicity and (or) increasing the therapeutic index of the anticancer drug. Synthetic macromolecules may be preferred as drug carriers because they can be tailor-made to have properties matching the requirements of the biological situation.

For the preparation of macromolecular prodrugs, the cytotoxic component should:
(i) show enough cytotoxicity at relatively low doses in order to decrease the load of a carrier macromolecule; (ii) be chemically stable in the conjugated form until released; and (iii) have adequate functional groups in its molecular structure for chemical fixation[13].

2.2.2.1. Requirements for a polymeric drug carrier

The carrier should: (i) be biodegradable; (ii) lack intrinsic toxicity and antigenicity;
(iii) Show no accumulation in the body; (iv) have adequate functional groups for chemical fixation; (v) retain the original specificity for target; and (vi) keep the original activity of the delivered drug, until it reaches the site of action. These can be summarized by biodegradability; biocompatibility, hydrosolubility, and chemical composition.

2.2.2.1.1. Hydrosolubility for intravenous drug delivery

Solubility in aqueous media is a necessary criterion for any polymer intended to be used as a drug carrier in the biomedical field (as blood is largely made up of water). Such polymer should be linear and highly flexible. This will have the advantage of increasing the positive entropy of the solution, and therefore favour the dissolution process, and the presence of intra- or extrachain hydrophilic entities such hydroxyl- and amino- terminals. These hydrophilic entities are of excellent utility as they are capable of undergoing effective hydration. The ability to incorporate charged species into the polymer also leads to its hydrosolubility property.

2.2.2.1.2. Biodegradability

The candidate carriers must be eliminated from the body once they have performed their function or metabolized to small fragments that are below the renal threshold and are subsequently eliminated. However, their backbone must comprise of segments amenable to hydrolytic and enzymatic cleavage in order to allow for the biodegradation and resultant catabolic elimination following drug release. If non-biodegradable polymers are used such as the synthetic polymers with carbon-carbon backbone, the polymer should have a molecular weight not exceeding the renal threshold 30 000 - 50 000. The failure to comply with this requirement will result in deposit and accumulation in various organs.

2.2.2.1.3. Biocompatibility

The polymeric backbone must be non-toxic, non-immunogenic, and non-thrombogenic in order to avoid any carrier-generated toxic, immunogenic and blood-clotting side effects. Indeed, failure to meet these requirements will result in premature destruction of the carrier through attack by the host defense systems, which renders the drug delivery system useless. Metabolic products generated from the parent polymers must also be biocompatible.

2.2.2.1.4. Chemical composition

The carrier macromolecule must comprise of reactive functional groups suitable for drug anchoring and release. These groups should be separated from the principal chain by short side chains or spacers. The presence of spacers will decrease the steric inaccessibility due to the polymeric backbone. By their nature, the spacers should be stable in the blood stream[53] but susceptible to either enzymatically catalyzed or pH-dependent hydrolysis in the lysosomal compartment[54]. Likewise, polymeric carriers should display the ability to be directed to predetermined cell types. This can be achieved by the incorporation of targeting moieties such as cationic functions and antibodies[55]. The presence of cationic functions, including tertiary amino groups, is required either in the carrier backbone or as side groups. This will facilitate adsorptive pinocytotic cell entry[56] and therefore prevent problems related to potential ionicity or polarity of the monomeric drug, and on the other hand, increase drug selectivity for the transformed cell, given that many types of cancer cell are characterized by negative surface charge. Also the macromolecular carrier should incorporate an interposition, between the spacer-bearing units, of subunits lacking drug-binding abilities along the principal chain. This will prevent multifunctional drug binding by reducing spacer density in the molecule.

2.2.3. Natural polymers as drug carriers.

Before the use of synthetic polymers, natural polymer made life possible. Thus, in 1871, Purdon used some proteolytic enzymes to inhibit bacterial infection during surgery[57]; and in 1953, Kidd[58] conceived the use of L-asparginase in the treatment of acute lymphoblastic leukemia. Polymers of this class are being widely used due to their similarities with the extracellular environment, high chemical versatility, typically good biological performance and inherent cellular interaction and, also very significantly, the cell or enzyme-controlled degradability. These biocharacteristics classify the natural-origin polymers as one of the most attractive options to be used in the tissues engineering field and drug delivery applications. Natural polymers include:

a) Protein-origin polymers

- Collagen: is defined by high mechanical strength, good biocompatibility, low antigenicity and ability of being crosslinked, and tailored for its mechanical, degradation and water-uptake properties. Collagen is hard to process, and the extent and rate of degradability is hard to control. For the latter, several factors have an impact on the degradability of collagen, for instance, the penetration of cells into the structure causes contraction, as well as the fact that, besides collagenase and gelatinase; several other non-specific proteinases are able to digest collagen[59]. Crosslinking is necessary in order to tailor the degradation of collagen, and this has obviously to take into account the application, as fluid movement, pressure and nature of the tissue where the material is implanted contributing to a faster degradation rate. In addition to the difficulties in processability, the sterilization of collagen is also a problem, as nearly all sterilization methods incur some degree of alteration of collagen[59].

- Gelatin: is a natural polymer that is derived from collagen, and is commonly used for pharmaceutical and medical applications because of its biodegradability and biocompatibility in physiological environments as reviewed by Tabata and Mkos[60,61]. These characteristics have contributed to gelatin's safety as a component in drug

formulations or as a sealant for vascular prostheses[62]. The strategies range from the co-implatation of loaded microspheres[63] to the incorporation of the cells into porous scaffolds [64] and, in general, the in vivo results show the high efficiency of using gelatin carriers-based technology. There are several commercially available gelatin-based carriers for drug delivery that are being applied in tissue engineering applications[64-66].

- Silk fibroin: is generally defined as protein polymers that are spun into fibers by some Lepidoptera larvae such as silkworms, spiders, scorpions, mites and flies[67]. Degradable silk is a mechanically robust biomaterial that offers a wide range of mechanical and functional properties for biomedical applications including drug delivery [68-69].

- Fibrin: due to its biochemical characteristics, mainly in cellular interactions, fibrin-based materials also found applications in the field of drug delivery with special focus on cell delivery. Fibrin is a protein matrix produced from fibrinogen, which can be autologously harvested from the patient[70], providing an immunocompatible carrier for delivery of active biomolecules, specially cells.

- Other protein-based polymers: There are other very interesting and attractive protein-origin polymers, namely elastin and soybean.

b) Polysaccharidic polymers:

Polysaccharides are a class of biopolymers constituted by simple sugar monomers[71].

- Chitosan: is a cationic polymer obtained from chitin comprising of copolymers of β (1→4)-glucosamine and N-acetyl-D-glucosamine. Chitin is a natural polysaccharide found particularly in the shell of crustacean, cuticles of insects and cell walls of fungi and it is the second most abundant polymerized carbon found in nature. Chitosan, the fully or partially deacetylated form of chitin, due to its properties has attracted much attention in tissue engineering and drug delivery fields with a wide variety of applications ranging from skin,

bone, cartilage and vascular grafts to substrates for mammalian cell culture. It has been proved to be biologically renewable, biodegradable, biocompatible, non-antigenic, non-toxic and biofunctional[72]. Chitosan exhibits a pH-sensitive behavior as a weak poly-base due to the large quantities of amino groups on its chain. Chitosan dissolves easily at a low pH while it is insoluble at higher pH ranges. The mechanism of pH-sensitive swelling involves the protonation of amine groups of chitosan under low pH conditions. This property has held chitosan to be widely investigated as a delivery matrix. Crosslinking is often used to tailor chitosan-based material properties. The most common crosslinkers used to crosslink chitosan are dialdehydes such as glyoxal[73] and glutaraldehyde[74]. The aldehyde groups form covalent imine bonds with the amino groups of chitosan due to the resonance established with adjacent double ethylenic bonds via a Schiff reaction[75]. Dialdehydes allow the crosslinking to happen by direct reaction in aqueous media and under mild conditions. Moreover, dialdehydes such as glutaraldehyde, stabilize the collagen structure, prevent tissue digestion by enzymes or bacteria and reduce the antigenicity of the material[76]. They also add to retention of the biocompatibility of the polymer. Natural crosslinkers like genipin[77] are gaining wide acceptance for crosslinking chitosan.

- Starch: is one of the most promising natural polymers because of its inherent biodegradability, overwhelming abundance and renewability. It is composed of a mixture of glycans that plants synthesize and deposit in the chloroplasts as their principal food reserve. Over the years several materials have been blended with starch to improve its processability, including, but not restricted to, several synthetic polymers, such as polyethylene[78], polycaprolactone[79], polyethylene-co-vinyl alcohol[80], poly (hydroxybutyrate-co-valerate)[81], among others[82-83], or even other natural origin materials such as other polysaccharides[84] and proteins[85].

- Alginate: Alginate-based materials are pH-sensitive. Biomolecule releases from alginate-based materials in low pH solutions, is significantly reduced which could be advantageous in the development of a delivery system. Theoretically, alginate shrinks at a low pH and the encapsulated drugs are not released. This pH dependent behavior of

alginate is exploited to tailor release profiles and in the development of ‘smart’ systems. However, at a higher pH, alginate undergoes a rapid dissolution which may result in burst release of protein drugs and subsequently their denaturation by proteolytic enzymes. Therefore, many modifications in the physicochemical properties are needed for the prolonged controlled release of protein drugs[86-87].

Natural polymers have the advantage of easy availability and biocompatibility, although their preparation may be restricted by the need for several purification steps, and their use is limited by their high immunogenicity. Many of them have been identified and have been or are being used as possible drugs or possess an intrinsic anticancer activity. Their modification with synthetic macromolecules dramatically increases their therapeutic effectiveness.

2.2.4. Synthetic polymers as drug carriers.

For many years, the polymer research laboratory of this university has focused its research on synthesizing polymeric carriers for delivering drugs to cancer cells. The research has mostly concentrated on the synthesis of water-soluble carriers, such as polyaspartamides and polyamidoamines, and on their conjugation with a number of antineoplastic agents, as well as synthesizing suitable monomers for these polymers[88-104]. Synthetic polymers are advantageously used as drug carriers since they are clearly more susceptible to modifications than natural macromolecules. They are tailor-made in accordance with the general requirements (including molecular weight, biodegradability, toxicity, the possibility for drug attachment/ release and for targeting) to be fulfilled by any polymer in an attempt to serve in a biological environment. The molecular-weight distribution must be under the kidney threshold (30 000 - 50 000) if they are not biodegradable. This will have the advantage of minimizing storage. Additionally, they must be designed in such a way as to be effortlessly internalized by fluid-phase pinocytosis in order to prevent their non-specific re-uptake after being released into the bloodstream following cell death. Indeed, the absence of non-specific interactions with

plasma membranes minimizes the probability of accumulation of the carrier in nontarget cells, and thus increases its biocompatibility.

The concept of synthetic polymeric drugs or pharmacologically active polymers was first introduced by Helmut Ringsdorf in 1975[105]. His model is based on the covalent link between the drug and a macromolecular backbone through a labile bond.

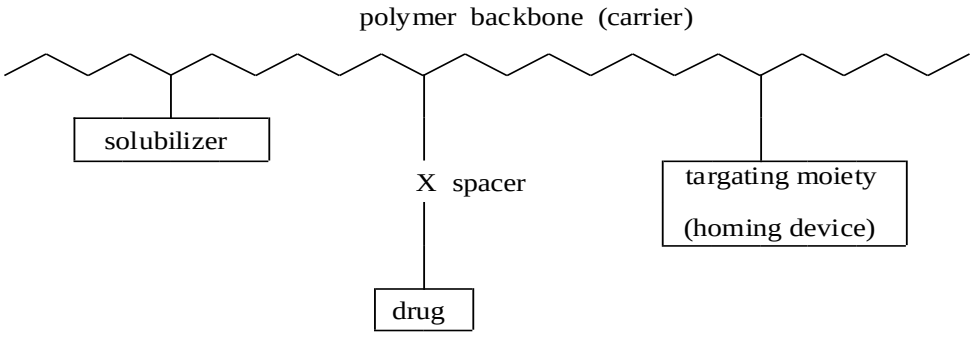

Figure 2.4. Ringsdorf model of synthetic polymer drugs[105]

Figure 2.4 shows the structure of the Ringsdorf model where a biostable or biodegradable polymer backbone carries three different units. A hydrophilic area used to make the whole macromolecule soluble and non-toxic, a second region in which the drug is linked to the polymer chain, and a third area that incorporates a transport system whose function is to carry the whole polymer to the target cells or site of pharmacological action. The separation of the different areas along the macromolecular chain may be accomplished by statistical terpolymerization or block copolymerization. In addition, polymer properties can be induced by the polymer specific structural characteristics such as high molecular weight, coil structure, neighbouring groups' effects, copolymer composition, variable polyelectrolyte charges, flexibility of polymer chains, and microstructure. In this sense, the advantages of this type of drug delivery systems are their diversity in composition, molecular structure and molecular weight, being predominantly used hydrophilic systems with polar or ionic groups, which lead to polymer water solubility and reactivity for conjugation with bioactive molecules. This model provides the most relevant guidelines of designing and synthesizing a potential water-soluble carrier molecule.

2.2.4.1. Pharmacokinetic of macromolecular prodrugs

Ringsdorf's model, as the possibility of drug delivery systems are able to achieve both controlled release of the drug, through optimization of its pharmacokinetics, and drug targeting, through a moiety that is able to drive the carrier-bound drug to specific organs and tissues, rapidly became a main target, especially in cancer chemotherapy. A schematic representation of the drug's transport from carrier-anchoring to delivery in intracellular space is set up in scheme 2.4.

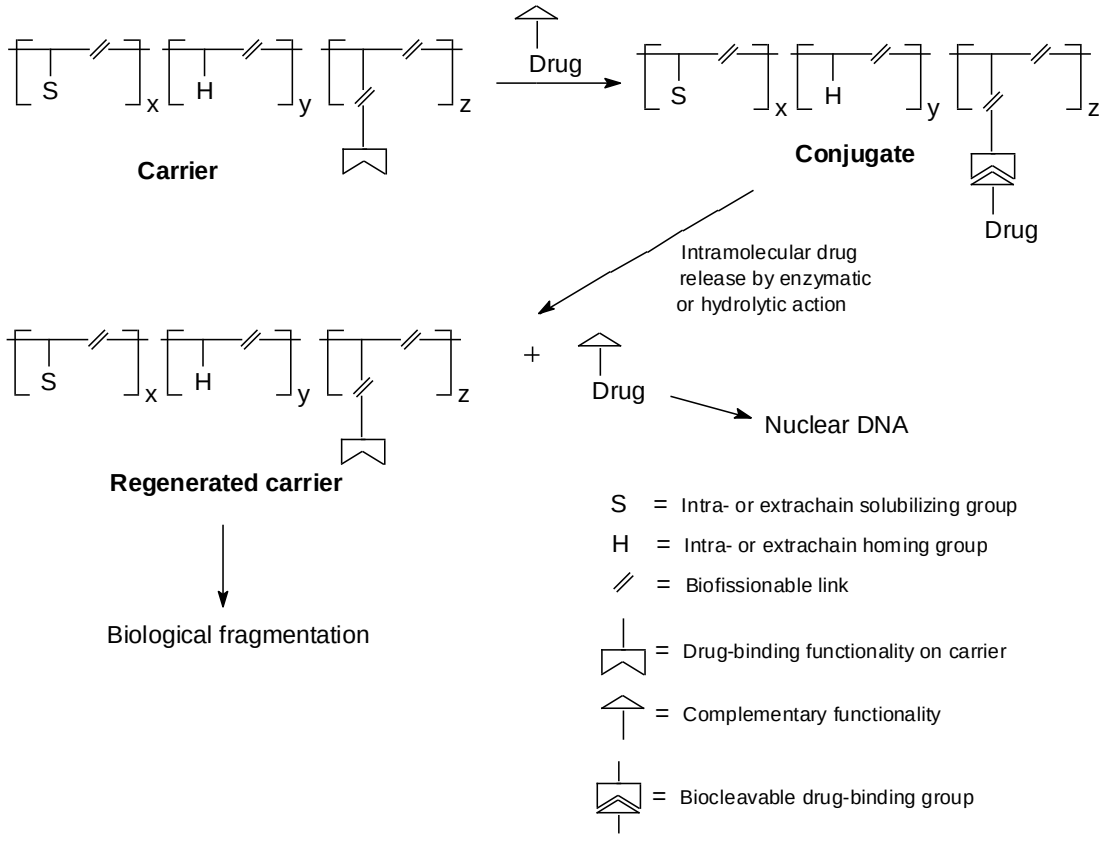

Scheme 2.4: Flow chart describing drug conjugate pharmacokinetics[106].

The efficacy of drug therapy depends on identifying a target and designing a pharmaceutical agent that will be able to reach that target. The increased understanding of molecular pathology provides us with many targets relating to the primary cause of diseases.

The information tells us that no subcellular compartment can claim to be free from being implicated in the cause or effect of at least one disease. Drugs may therefore need to be delivered not only to specific organs and cells but also to distinct subcellular compartments or microenvironments (Figure 2.5). The major challenge for pharmacology is therefore to identify the subcellular target and then design drug delivery strategies based on an ability to understand, utilise, modify and exploit membrane trafficking pathways.

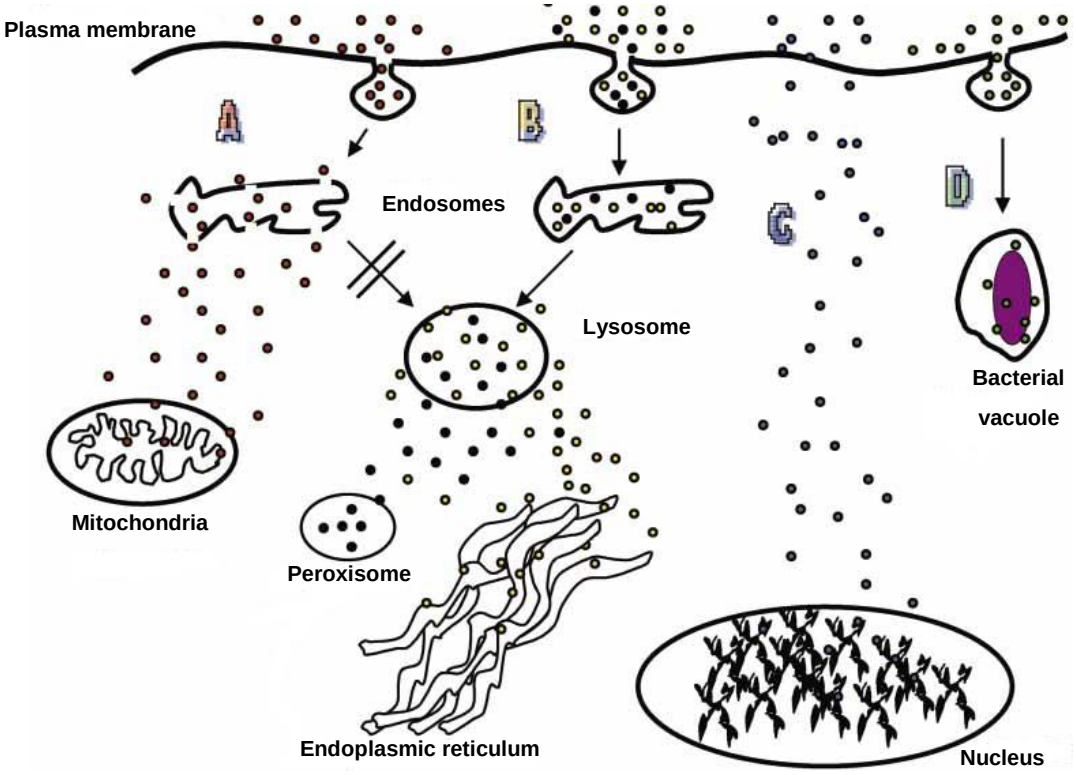

(A,B) Internalisation of the drug or drug complex into the endocytic pathway precedes drug release into the cytosol. This may be mediated by cleavage of a labile drug-complex linker or physical membrane destabilisation by, for example, a virus or a liposome. In A, the drug complex is endosomotropic, and the drug needs to be released prior to encountering the degrading proteases and nucleases of the lysosome.
(B) The endoplasmic reticulum and peroxisome-targeted drugs are lysosomotropic; there is a requirement for them to be first delivered to the lysosomes.
(C) The nuclear-targeted drug permeates through biological membranes or alternatively is attached to a membrane-permeable carrier.
(D) The drug is targeted via the endocytic pathway to a bacterium inside the vacuole.

Figure 2.5: Examples of targets, barriers and strategies for intracellular drug delivery.[107]

2.2.4.2. Pharmacokinetics of macromolecules at body and organ levels

Distribution of macromolecules is usually restricted to the intravascular space after intravenous injection, due to low capillary permeability in most organs with continuous capillary bed. The kidney, where fenestrated capillaries are present, plays an important role in the disposition of macromolecules circulating in the blood stream. Since the fenestrated capillaries are devoid of diaphragms in glomerular capillaries, macromolecules can easily cross the fenestrated capillaries. In the glomerulus, the continuous basement membrane functions primarily as size and charge-dependent barriers for glomerular filtration of macromolecules. Hence, the shape, flexibility and deformability of macromolecules are also important factors[108]. Macromolecules with molecular weights of less than 50 000 (approximately 6 nm in diameter) are subject to glomerular filtration. Positively charged macromolecules show higher glomerular permeability than anionic ones with similar molecular weight. For macromolecules of molecular weight >50 000, which escape from sieving through the glomerulus, the liver plays an important role in their disposition. In contrast to most other organs in which the capillary presents a substantial barrier between the vascular and interstitial spaces, the liver has discontinuous endothelial capillaries which are characterized by approximately 100 nm fenestrated with a porosity of 64%[109]. This structure brings any macromolecule circulating in the bloodstream into free contact with the surface of parenchymal cells. Due to this anatomical characteristic which offers a wide surface area for electrostatic interaction, cationic macromolecules are widely distributed in the liver due to ionic interaction with the negatively charged cell surface. On the other hand, strongly anionic macromolecules are known to be taken up by the liver's non-parenchymal sinusoidal cells, by scavenger receptor - mediated endocytosis[110].

2.2.4.3. Pharmacokinetics of macromolecules at the cellular level

Since macromolecules normally cannot enter cells by passive diffusion across the plasma membrane, the general mechanism for their passage through the cell membrane is

endocytosis (figure 2.6). Endocytosis is the process of cell surface invagination and subsequent internalization of the plasma membrane as vacuoles that are associated with transport of extracellular solutes into the cell. Fluid phase endocytosis is a useful non-specific process for transporting macromolecules dissolved in the extracellular fluid to the cells at a relatively slow rate. Macromolecular carriers without any special affinity to target cells are considered to be endocytosed by this mechanism. On the other hand, macromolecular carries for active targeting, such as glycoproteins, are rapidly and effectively internalized by receptor-mediated endocytosis, which proceeds via clathrin-coated pits. After formation of clathrin-coated vesicles, the coat is generally shed and uncoated endosomes are formed[111].

The size of these vesicles is relatively small (100nm in diameter) and hence the size of the ligand macromolecule cannot exceed the internal diameter of these vesicles. Although there are several fates for ligands utilizing the coated pit pathway following internalization, fusion with lysosome enriched with hydrolytic enzymes yields the digested vacuole, and the macromolecules are subjected to degradation. Although little is known about the intracellular pharmacokinetics of macromolecules, apart from lysosomal degradation, processes such as release from the endosomal or lysosomal compartments and translocation to the cytosol or nucleus are equally important (Figure 2.6). With regard to the nuclear transport, it should be noted that direct entry into the nucleus occurs via nuclear pores which are smaller than 40 nm in diameter. This implies that macromolecules targeted to the nucleus should be smaller than this pore size. The sites of action of drugs conjugated to macromolecular carriers are usually located in the intracellular compartments, such as the cytosol and the nucleus. Therefore, the therapeutic efficacy of drug-carrier complexes greatly depends on cellular uptake and intracellular trafficking, as well as on intracellular release of active drug component[111].

Meanwhile, polymers with varying chemical and biological properties have been investigated. These include polymer carrier-bound drugs, where a physiologically active substance is bonded to a polymeric chain and so becomes a macromolecular prodrug.

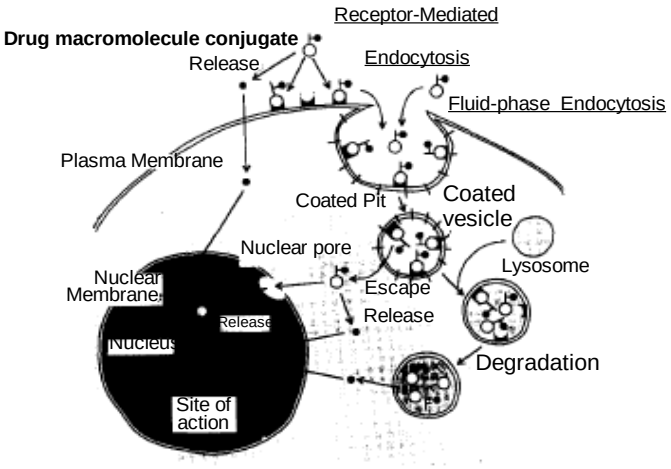

Figure 2.6: Schematic representation of the intracellular fate of macromolecule drug conjugate after endocytosis[112]

2.2.3.4. Pharmacokinetic benefits of macromolecular prodrugs

A water-soluble polymer conjugate, designed in complete compliance with a variety of biomedical specifications, will provide some or all of the following pharmacokinetic benefits:

(1) Efficacious drug distribution in the aqueous fluid system for the intravenously or intraperitoneally administrated drug, and facilitated access to the target cell.

(2) Amenability to covalent conjugation with pharmacological agents (with optimal drug loading) such that the drug-carrier linkage is stable during transport to the target cell, but hydrolysable within the cell.

(3) Easier endocytotic[113] cell entry will be experienced by the water-soluble conjugate irrespective of the structural peculiarities (such as ionicity, polarity or electrical) of the drug, especially for pinocytic capture by cells (ideally the carrier would include inherent properties to enable it to target the particular cell types or, alternatively, be suitable for chemical modification to facilitate targeting). Unless associated with a specialized carrier-mediated transport system, such polar or salt-like molecules, therefore, fail to reach intracellular space effectively, and most of them will be wasted as medicinal agents.

(4) Good biocompatibility, being nonimmunogenic, noncarcinogenic, or displaying general cytotoxic properties.
(5) Metabolizability for removal from the organism once fulfilling its drug delivery function.

2.2.5. Drug systems based on carrier-conjugated

The drug systems submitted to investigation within the framework of this project have been conjugated to various polymeric carriers, and the conjugation, which is achieved by formation of hydrazone biocleavable bond, is extensively reported.
The abovementioned considerations led to the strategy of conjugating the inherently hydrophobic ferrocene complex reversibly to water-soluble macromolecular carriers. The reversible anchoring of the complex to the polymeric carrier can lead to significantly enhanced therapeutic effectiveness of the therapeutic agent, as crucially important factors combined to increase bioavailability at the target site while reducing toxicity and the risk of resistance build-up. Following Ringsdorf's model of macromolecular prodrugs, the ferrocene complex was conjugated to various polymeric carriers in our polymer laboratory under Professor E.W. Neuse supervision. Conjugation was achieved with ferrocenylcarboxylic acids and either amine- functionalized carriers leading to amide-bonded[114] ferrocene conjugates, or hydroxyl-functionalized carriers affording ester-bonded[115] ferrocene conjugates. A more recent article from the same laboratory reported the cytotoxic activity of macromolecular ferrocene conjugates against Colo 320 DM human colon cancer line[116]. In the present study, Ferrocenylpropenal, ferrocenyl-aldehyde, and acetylferrocene were anchored to hydrazine-functionalized polymers, using hydrazone bridge approaches.

2.3. Branched hydrazone linkers

These linkers are used to prepare drug-linker molecules and biologically active conjugates composed of a targeting ligand, a therapeutically active drug, and a branched linker capable of recognizing a selected target cell population via targeting ligand. Hydrazones have been studied as a group of the most useful spectrophotometric

reagents[117]. Combining appropriate starting materials (carbonyl compounds and hydrazine), the sensitivity as an analytical reagent and/ or solubility of hydrazones could be improved and the donating environment could be changed. The ferrocenyl drug is chemically modified to contain an aldehyde or keto group.

2.3.1. Strategy for the synthesis of polymeric carriers containing the hydrazone Bridge

Step 1: Modification of biomolecules

Biomolecule A (figure 2.7) is modified to hold aldehyde or ketone functions, and separately, biomolecule B is covalently modified to contain hydrazine group. The target biomolecules are reacted through primary amine groups[118].

Step 2: Conjugation of biomolecules

When the modified biomolecules are mixed at acidic pH, a stable covalent hydrazone bond is formed, and the resulting conjugate is ready for use[118].

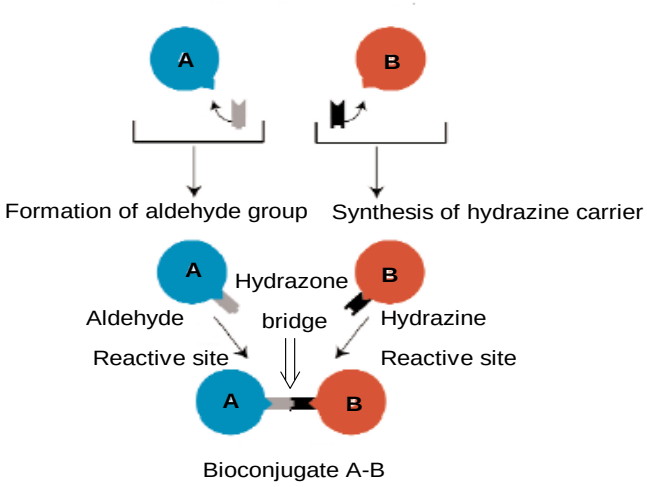

Figure 2.7 Formation of Hydrazone Bridge[118]

Scheme 2.5 shows the reaction a hydrazine carrier and an aldehyde drug to form a hydrazone conjugate.

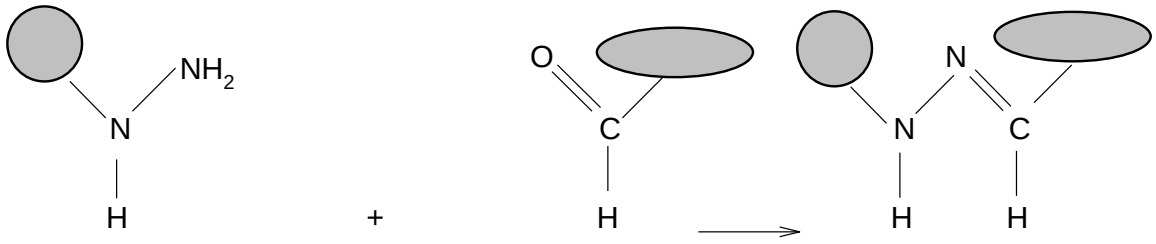

Hydrazine group Aldehyde group Hydrazone

Scheme 2.5: Interaction between hydrazine and aldehyde groups

2.3.2. Hydrazone linker's stability

The linker component of antibody-drug conjugates required higher stability in the systemic circulation, and efficient to release drug at the target site. The mechanisms of drug release depend on the linker stability. Because of this, significant effort has been directed toward balancing the stability of these linkers in the central circulation, while still allowing them to be sufficiently labile for activation at the target site.

2.3.3. Cancer cell's pH and ferrocenyl hydrazone drugs

2.3.3.1. pH and cancer cells

A normal cell shows healthy oxygen tension (aerobic state) and respiration across the cell membrane. There is free exchange across the cell membrane and its pH is in the range of 7.35 (figure 2.8). But a tumor cell's state is anaerobic, oxygen cannot enter the cell, glucose undergoes fermentation to lactic acid; cell pH drops to 6.5. Lactic acid attacks the DNA, destroying template action. Messenger RNA is changed and the control mechanism of the cell is crushed. In the acid medium, enzymes within the cell become toxic,

eventually bringing about the death of the cell as well as the host. Cancerous tissues are acidic, whereas healthy tissues are alkaline.

2.3.3.2. pH-responsive hydrazone-ferrocenyl conjugates

pH responsive linkers can be used to control the releases of drugs to kill cancer. Stable under physiological conditions (blood circulation, pH 7.35), but hydrolytically degradable in mildly acidic environment (in endosomes and lysosomes, pH 5 – 6.5), hydrazone-ferrocenyl conjugates can offer a number of attractive features: 1) decreased non-specific release in the systemic circulation, 2) increased cell uptake through modified surface charge, and 3) increase drug release efficiency. The focus of our research was to develop a therapeutical device which will release active drug under pH control.

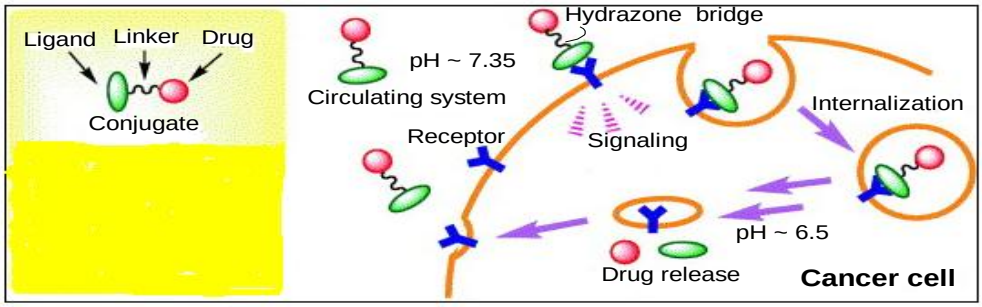

Figure 2.8: pH control of hydrazone-ferrocenyl conjugates[119]

CHAPTER 3
RESULTS AND DISCUSSION

In accordance with the experimental aims outlined in chapter one, this thesis project was carried out within the framework of the following steps:

1) Synthesis of special aldehydes and ketones as potential anticancer drugs to be incorporated into the polymer backbone and synthesis of water-soluble macromolecular carriers containing the hydrazine group. Procedures developed in previous projects and improved where necessary were used in this investigation.

2) Conjugation of the hydrazine-functionalized carriers prepared in step one with ferrocenylaldehyde, cinnamaldehyde and curcumin.

3) Evaluation of selected conjugates for drug delivery assessment.

3.1. Synthesis of Aldehyde and Ketone Drugs

3.1.1. Synthesis of ferrocenylpropenal

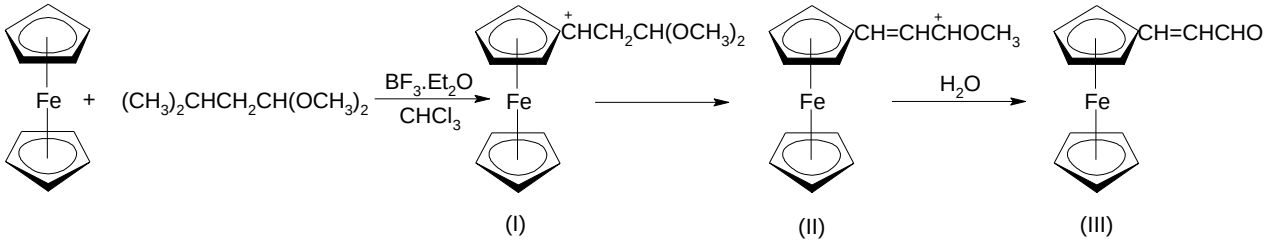

Scheme 3.1: Synthesis of 3-ferrocenylpropenal

3-Ferrocenylpropenal was prepared, as shown on scheme 3.1, according to the procedure of Dudnik et al (1969), by the treatment of a solution of ferrocene and 1,1,3,3-tetramethoxypropane in $CHCl_3$ at 2^0C with slight excess of BF_3-Et_2O. The 3-ferrocenylpropenal was a three step reaction. In the first step the reaction involved the synthesis of 3-ferrocenyl-dimethoxypropane under nitrogen atmosphere. The cation (II) rather than (I) was apparently the final product of the reaction since the aldehyde (III) was isolated under basic as well as acid workup conditions. The final product was obtained in yields of 56 – 61 %, and the melting point ranged between 97 and 98 ^0C. The experimental conditions and ^1H NMR data are summarized in Tables 3.1 and 3.2 respectively.

3.1.2. Synthesis of Acetylferrocene

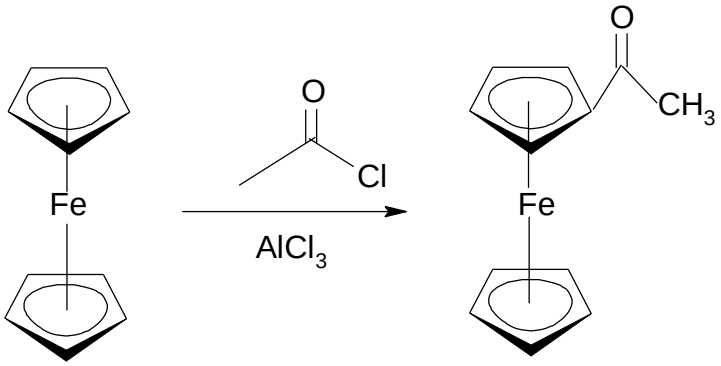

Scheme 3.2: *Synthesis* acetylferrocene

Acetylferrocene was prepared, as shown on scheme 3.2, by Friedel-crafts acetylation of ferrocene. Ferrocene was acetylated by acetyl chloride in the presence of $AlCl_3$ to produce a mixture which was purified. The acetylation products and any unreacted ferrocene all have significantly different polarities, so are easily separated by liquid-solid chromatography; and crystallized from hexane/ ethylacetate mixture. The yield of the final product was 49 – 58 %, and the melting point was 85 – 86 ^0C. The experimental conditions and ^1H NMR data are summarized in Tables 3.1 and 3.2 respectively.

Table 3.1: Summary of experimental data for Ferrocenyl drugs

Drugs Designation	Molar Ratios[a]			Reaction time & Temperature[c]		Yield %	mp ^{0}C
	Fc	TMP[b]	CH_3OCl[b]	1st Step	2nd Step		
Fcp[d]	1.00	1.4	-	2 ^{0}C, 0.5 h, N_2	- 2 ^{0}C, 0.25 h - RT, 1 h - 64 ^{0}C, 1 h	56-61	97-98
Fca[e]	1.00	-	1.2	RT, 1 h	70-80 ^{0}C, 0.25 h	49-58	85-86

[a] *Base molar Fc*

[b] *TMP: tetramethoxypropane and CH_3OCl: acetyl chloride*

[c] *RT: room temperature and N_2: nitrogen gas ;* [d] *Fcp: Ferrocenylpropenal and* [e] Fca: *Acetylferrocene*

Table 3.2: ^{1}H NMR of ferrocenyl drugs

Drug Designation	Assignment	^{1}H NMR[a,b]		
		Shift range δ(ppm)	Proton count	
			Found	Expected
Fcp[c]	**Fc** **CHCH**CHO CHCH**CHO**	4.2 – 4.1 5.5 – 5.4 9.1 – 7.8	9.1 1.9 0.9	9 2 1
Fca[d]	**Fc** CO**CH_3**	4.2 – 4.1 2.9 – 2.4	8.8 3.2	9 3

[a] *In D_2O, pD 10 – 11. Chemical shifts, δ (ppm), referenced against internal sodium 3-(trimethylsilyl)-2,2,3,3-d_4-propionate;*

[b] *Integration error limit ± 15%; and* [c] *Fcp: Ferrocenylpropenal* [d] Fca: *Acetylferrocene*

3.2. Synthesis of Macromolecular Carriers

3.2.1. Introduction

In the present project an effort was made to generate macromolecular drug carriers, such as polyaspartamides. The synthesis of these polymeric structures was performed in strict accordance with biomedically prescribed specifications, and toward the development of the kind and sequence of chemical reaction steps required to reduce these designs to practice. The following considerations support the choice of the structural polymers:

- The carrier must posses a highly flexible backbone and the presence of intrachain-type or side group-attached solubilizing groups capable of undergoing effective hydration required for rapid dissipation in the central circulation system.
- The main-chain construction should be non-toxic, non-immunogenic, and non-thrombogenic to prevent side effects, and to ensure catabolic elimination of the polymer upon drug release.
- The presence of functional groups as binding sites to ensure proper drug attachment and subsequent release in the biological environment.
- The presence of cationic functions (or precursor groups, such as tertiary amines) to cause facilitated cell entry by endocytosis, thus circumventing potential problems caused by drug polarity or ionicity. This mode of cell entry may assume unique significance where drug resistance has emerged.
- The sizes of macromolecular carrier, generally in the molecular mass range of 20 000 – 30 000, are sufficiently low to avoid toxic side effects frequently observed with high molecular mass, and yet high enough to retard renal clearance.
- Delayed and controlled drug release concerning the polymer-drug connective link,

thereby ensuring restriction of drug serum conjugate concentration well within pharmacologically dictated limits with concomitant reduction of organ toxicity. Features are also built into the molecules that provide conjugate stability in the plasma and drug release upon endocytotic cell entry.

The carrier polymers preferentially used in this project for the anchoring of the selected drug models are aliphatic polyamides of the schematic structure shown in scheme 3.3

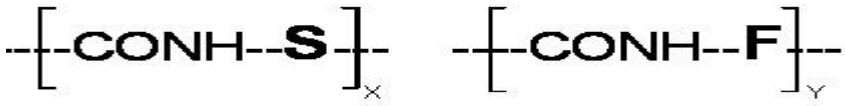

Scheme 3.3: Basic carrier model

In this model, S represents an intra-chain or extra-chain type of hydrosolubilizing moiety, comprising selected amine, hydroxyl, or carboxyl functions, capable to provide water solubility of the ultimate conjugate. The group F comprises extra-chain type functionality capable of forming a bridge with a drug species. In this project, polymers possessing NH_2 as the drug-connecting group were chosen for conjugation work.

3.2.1. Polyaspartamides

In the early ‘Seventies Drobnick[120] and collaborators published the potential value of polysuccinimide and derived aspartamide polymers as drug carriers. For a number of years, polyaspartamides were preferred for use as macromolecular carriers for a number of antineoplastic drug systems, in the polymer research laboratory of the University of the Witwatersrand. For this reason the polymers synthesized in this project were based on this type.

3.2.1.1. Poly-DL-Succinimide

The basic polymer educt for the synthesis of polyaspartamides was prepared by the method of Neri and collaborators[121]. This involved the polycondensation of DL-aspartic acid in the presence of orthophosphoric acid at high temperature (180^0–220^0 C). The reaction yielded poly-DL-succinimide (PSI), as seen in step 1 of the scheme 3.4. The crude polymer product was subsequently subjected to carbodiimide-mediated chain extension[122] (see step 2 of scheme 3.4) and the final product obtained by precipitating out of the reaction mixture with cold water. Inherent viscosities of polysuccinimide prepared ranged from 36-48 mL/g.

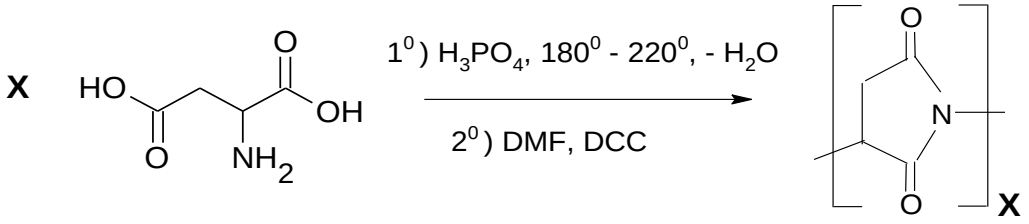

D, L - Aspartic acid

Poly - D, L - succinimide

Scheme 3.4: Polycondensation *of DL-aspartic acid*.

3.2.1.2. Poly-α,β-DL-aspartamides

The succeptibility of PSI to nucleophilic imide ring opening mediated by amines was considered a key factor in the synthesis of polyaspartamides in this project, as developed by Neuse and Perlwitz[123]. Polyaspartamides are readily prepared from the treatment of poly-DL-succinimide with amines in anhydrous, dipolar aprotic medium, such as N,N-dimethylformamide (DMF), giving rise to a mixture of D- and L- enantiomeric forms, consisting of both α- and β- peptidic repeat units[124] (Scheme 3.5).

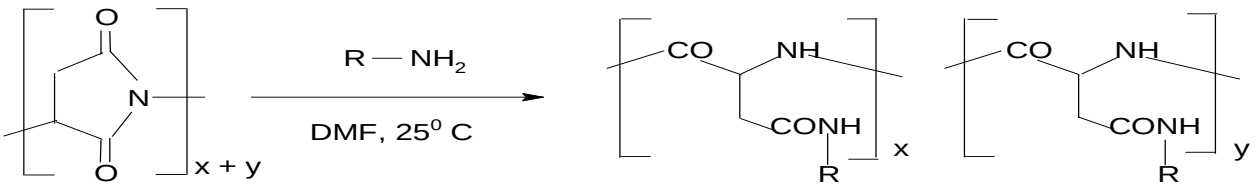

Scheme 3.5: *Reaction scheme of formation of homopoly(α, β-DL-aspartamides)*

The aminolytic ring-opening reaction of polysuccinimide developed a generation of polyaspartamides through a stepwise, sequential addition of two amine nucleophile reactants, NH_2-R_1 and NH_2-R_2, in prearranged stoichiometric ratios. Occasionally a third amine, NH_2-R_3, may be used in this operation. The copolyaspartamides produced are composed of randomly distributed aspartamide repeat units bearing N-attached substituents (R_1, R_2 etc.) as introduced by the amine nucleophiles selected. Scheme 3.6 illustrates this sequence of ring opening steps.

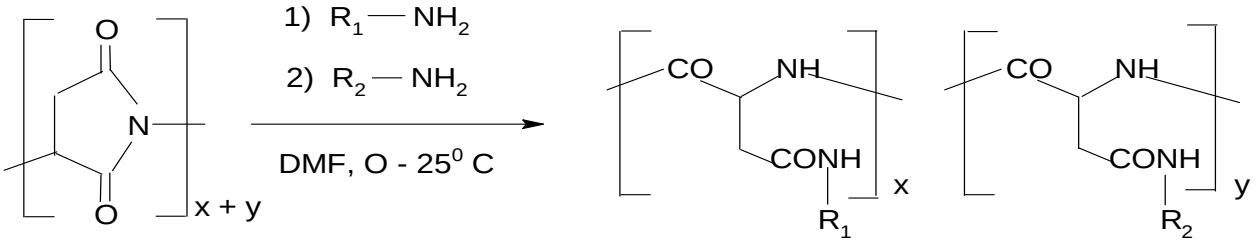

Scheme 3.6: *Aminolytic ring opening reaction leading to the formation of copolyaspartamide.*

In general, R_1 is selected to represent a hydrosolubilizing moiety (e.g. hydroxyl or tertiary amino groups), and R_2 represents a drug-biding site (e.g. primary or secondary amine, carboxyl or hydroxyl) functionality.

Polyaspartamides were preferred as they meet the general requirements for designing macromolecular carriers given above. The preferential use of such poly-α,β-DL-aspartamide in this project is supported by the following considerations:

(i) The molecular mass, which generally ranges from about 25000 to 35000, is well within the required range that is adequately low to suppress inherent polymer toxicity, and yet high enough to delay renal clearance.

(ii) The intrachain amide groups allow a gradual backbone cleavage for ease of catabolic elimination of the spent polymer. The D-type polymers are known to be more resistant to the enzymatic attack, while L-type polymers are exposed to enzyme attack and consequently undergo rapid degradation. The presence of D-configurated CH groups and β-peptide units in the chain prevents unduly rapid α-peptidase-mediated “unzipping” of the chain from its terminals brought about by the exopeptidases[125] group of enzymes, whose function is to cleave the terminal residues from polypeptides, ensuring that fragmentation of the polymer is delayed.

(iii) Polyaspartamides are essentially non-toxic, and immunogenicity of these synthetic peptide-type polymers is expected to be significantly lower than that observed with high molecular proteinaceous biopolymers. In addition, the ultimate backbone degradation product being an essential amino acid, L-aspartic acid, is acceptable as a “body-friendly” catabolite.

(iv) The S-modified subunits, which bear the hydrosolubilizing group (R_1), can be introduced advantageously as the majority component ($x > y$), as this will provide an effective insulation of the F-modified subunits (those bearing R_2 group) from each other and, thus, will reduce the risk of intramolecular interaction of closest drug species.

(v) The introduction of tertiary amine functions as side groups will provide the special functions of pinocytotic cell entry and target cell affinity.

3.2.1.2.1. Polyaspartamide Carriers bearing one hydrosolubilizing group

The first series of p*olyaspartamide drug carrier polymers* (Schemes 3.7 and 3.8) were synthesized under experimental conditions similar to previous work performed in this laboratory, with improved synthesis methods. The side chains represented by R_1 in this group were 3-(dimethylamino)propylamine (DMP), 3-(diethylamino)propylamine (DEP), 2-(dimethylamino)ethylamine (DMEA), 2-(diethylamino)ethylamine (DEEA), 2-(2-aminoethoxy)ethanol (AEE), or 4-amino-2,2,6,6-tetramethylpiperidine (ATP), whereas the diamine nucleophilic representing R_2 group was hydrazine as shown in Scheme 3.6. In accordance with the general principle outlined before, DMP, DMEA, DEP, DEEA, ATP and AEE were used as major reactants (x > y). The aminolysis reactions were performed in a two-step reaction. In the first step, a given amount of R_1 group reactant was allowed to react with polysuccinimide for 6 hours at ambient temperature. Thereafter, in the second step, the reaction mixture was added drop-wise to an excess amount of hydrazine solution at 0^oC. The reaction continued for a specified time, ~48 hours, at 0^oC under nitrogen atmosphere. The relative amount of Hy (three times the stoichiometric amount) was found necessary to achieve the desired percentage incorporation with complete ring opening and substitution of the remaining succinimide units of the substrate polymer.

Agreement of expected with calculated data in the NMR spectra was satisfactory and confirmed the structural compositions indicated in Schemes 3.7 and 3.8.
The polymeric reaction products, 2a – 2f, were obtained routinely in a sequence of the following operations: solvent volume reduction, polymer precipitation, aqueous dialysis in membrane tubing possessing molecular mass cut-off limits of 12 000, and freeze-drying to isolate the polymer as solids. The yields of the water-soluble carriers collected were 58 – 77 %.

Table 3.3 lists individual experimental details, mole ratios, inherent viscosity and yields, while ^1H NMR data are presented in table 3.4. Inherent viscosities, measured in water solutions and averaged from three identically performed experiments, ranged from 8 to 14 mL/g. Carriers 2a, 2b, 2c, 2d, 2e and 2f were used for drug anchoring.

In general, lower viscosity was observed for the polymer derived from DMP (Table 3.4). Note that the DMP is a strong base which means that the protonation will be evident even under weakly basic condition. Protonation will render the amino group to be positively charged. This will favor the adsorptive pinocytotic cellular uptake of the macromolecules as reported by Shen. Toxicological tests of selected PSI-DMP-Hy and PSI-DMP-PDA carriers, done in the department of Immunology of the University of Pretoria, revealed higher toxicity of these DMP carriers. DMP as a good hydrosolubilizing and cell-selecting group, was added with others solubilizing groups in the preparation of terpolyaspartamides, with possibility of lowering the toxicity of DMP and increasing the solubility of the polymer carriers.

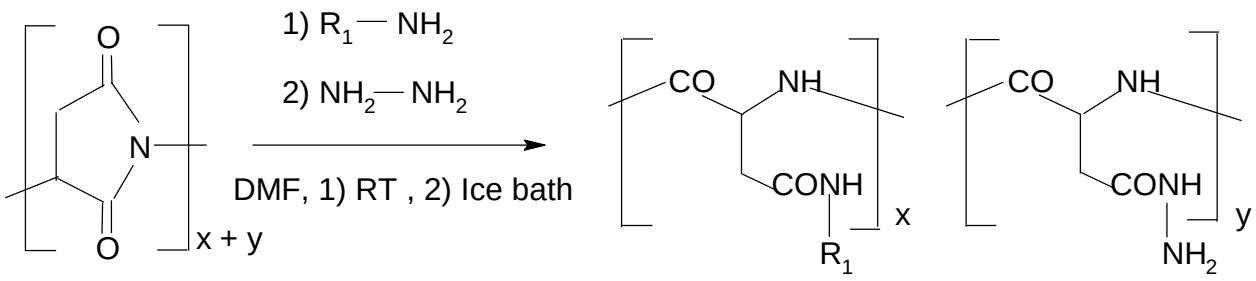

2a (80)	R_1:	NMe_2	x / y = 4
2b (80)	R_1:	NMe_2	x / y = 4
2c (80)	R_1:	NEt_2	x / y = 4
2d (80)	R_1:	NEt_2	x / y = 4
2e (80)	R_1:	NH	x / y = 4
2f (80)	R_1:	O OH	x / y = 4

Scheme 3.7: *Synthesis of copolyaspartamide carriers 2a (80) – 2f (80)*

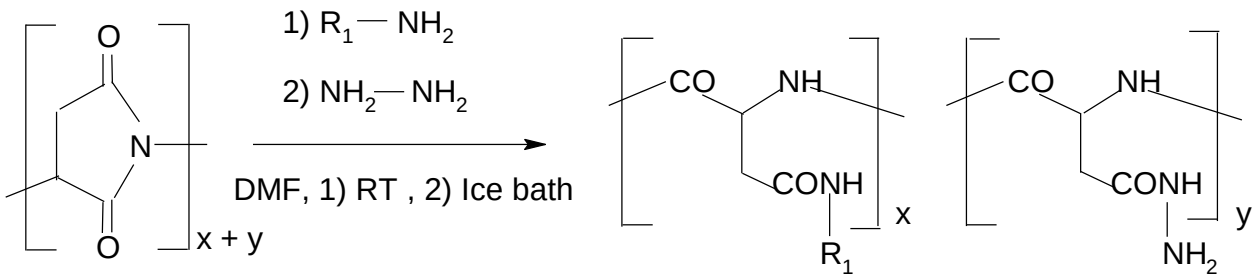

2a (90)	R_1:	NMe_2	x / y = 9
2b (90)	R_1:	NMe_2	x / y = 9
2c (90)	R_1:	NEt_2	x / y = 9
2d (90)	R_1:	NEt_2	x / y = 9
2e (90)	R_1:	NH	x / y = 9
2f (90)	R_1:	O OH	x / y = 9

Scheme 3.8: *Synthesis of copolyaspartamide carriers 2a (90) – 2f (90)*

Table 3.3: Summary of experimental data for copolyaspartamide Carriers

Polymer Designation	Molar Ratios[a]								Reaction time & Temperature[b]		Yield %	η_{inh}[c] mL/g	x/y
	PSI	DMP[d]	DMEA[d]	DEP[d]	DEEA[d]	ATP[d]	AEE[d]	Hy[d]	1st Step	2nd Step			
2a(80)	1.00	0.80	-	-	-	-	-	0.20	6h, RT	48h, IB	72.1	8.4	4
2b(80)	1.00	-	0.80	-	-	-	-	0.20	6h, RT	48h, IB	64.5	10.6	4
2c(80)	1.00	-	-	0.80	-	-	-	0.20	6h, RT	48h, IB	59.2	11.9	4
2d(80)	1.00	-	-	-	0.80	-	-	0.20	6h, RT	48h, IB	63.3	11.2	4
2e(80)	1.00	-	-	-	-	0.80	-	0.20	6h, RT	48h, IB	58.7	14.0	4
2f(80)	1.00	-	-	-	-	-	0.80	0.20	6h, RT	48h, IB	59.1	9.6	4
2a(90)	1.00	0.90	-	-	-	-	-	0.10	6h, RT	48h, IB	61.9	8.1	9
2b(90)	1.00	-	0.90	-	-	-	-	0.10	6h, RT	48h, IB	60.3	9.1	9
2c(90)	1.00	-	-	0.90	-	-	-	0.10	6h, RT	48h, IB	59.6	10.3	9
2d(90)	1.00	-	-	-	0.90	-	-	0.10	6h, RT	48h, IB	67.9	9.6	9
2e(90)	1.00	-	-	-	-	0.90	-	0.10	6h, RT	48h, IB	76.7	13.1	9
2f(90)	1.00	-	-	-	-	-	0.90	0.10	6h, RT	48h, IB	58.2	8.9	9

[a] *Base molar **PSI*** [b] IB*: Ice Bath; RT: room temperature* [c] *At 30.0^{0}C ± 0.5^{0}C in dist H_2O; conc = 0.2mg/100mL*

[d] *DMP: 3-(dimethylamino)propylamine; DMEA: 2-(dimethylamino)ethylamine; DEP: 2-(dimethylamino)ethylamine; DEEA: 2-(diethylamino)ethylamine; ATP: 4-amino-2,2,6,6-tetramethylpiperidine; AEE: 2-(2-aminoethoxy)ethanol;*

Table 3.4: ^{1}H NMR of copolyaspartamides 2**a(80), 2b(80), 2c(80), 2d(80), 2e(80),2f(80), 2a(90), 2b(90), 2c(90), 2d(90), 2e(90)** and **2f(90)**

Polymer Designation	Assignment	^{1}H NMR[a,b]		
		Shift range δ(ppm)	Proton count	
			Found	Expected
2a(80)	CONHCH$_2$**CH$_2$**CH$_2$NMe$_2$ N**Me$_2$** **CH$_2$**NMe$_2$ **CH$_2$**CONH CONH**CH$_2$**	1.7 – 1.5 2.3 – 2.1 2.4 – 2.3 2.8 – 2.6 3.3 – 3.1	8.5 24.0 7.1 7.8 8.1	8.0 24.0 8.0 8.0 8.0
2b(80)	N**Me$_2$** **CH$_2$**NMe$_2$ **CH$_2$**CONH CONH**CH$_2$**	2.3 – 2.1 2.4 – 2.3 2.8 – 2.6 3.3 – 3.1	24.0 8.1 7.7 8.5	24.0 8.0 8.0 8.0
2c(80)	CH$_2$N(CH$_2$**CH$_3$**)$_2$ CONHCH$_2$**CH$_2$**CH$_2$NEt$_2$ **CH$_2$**N(**CH$_2$**CH$_3$)$_2$ **CH$_2$**CONH CONH**CH$_2$**	1.1 – 0.9 1.7 – 1.5 2.7 – 2.5 2.9 – 2.7 3.4 – 3.2	24.0 7.7 24.0 8.1 8.2	24.0 8.0 24.0 8.0 8.0
2d(80)	CH$_2$N(CH$_2$**CH$_3$**)$_2$ **CH$_2$**N(**CH$_2$**CH$_3$)$_2$ **CH$_2$**CONH CONH**CH$_2$**	1.2 – 0.9 2.7 – 2.5 2.9 – 2.7 3.4 – 3.2	24.0 24.1 7.4 8.1	24.0 24.0 8.0 8.0
2e(80)	[C(**CH$_3$**)$_2$]-NH; CONHCH(**CH$_2$**)$_2$ **CH$_2$**CONH CONH**CH**	1.5 – 0.9 2.9 – 2.7 4.1 – 4.0	64.0 7.5 3.94	64.0 8.0 4.0
2f(80)	**CH$_2$**CONH CONH**CH$_2$** **CH$_2$**O**CH$_2$CH$_2$**OH	2.8 – 2.6 3.5 – 3.1 3.8 – 3.5	7.8 7.9 24.0	8.0 8.0 24.0

[a] *In D_2O, pD 10 – 11. Chemical shifts, δ (ppm), referenced against internal sodium 3-(trimethylsilyl)-2,2,3,3-d_4-propionate;*

[b] *Integration error limit ± 15%*

Table 3.4 continued

Polymer Designation	Assignment	^{1}H NMR[a,b]		
		Shift range δ(ppm)	Proton count	
			Found	Expected
2a(90)	$CONHCH_2\mathbf{CH_2}CH_2NMe_2$ $N\mathbf{Me_2}$ $\mathbf{CH_2}NMe_2$ $\mathbf{CH_2}CONH$ $CONH\mathbf{CH_2}$	1.7 – 1.5 2.3 – 2.1 2.4 – 2.3 2.8 – 2.6 3.3 – 3.1	18.5 54.6 16.3 18.7 18.0	18.0 54.0 18.0 18.0 18.0
2b(90)	$N\mathbf{Me_2}$ $\mathbf{CH_2}NMe_2$ $\mathbf{CH_2}CONH$ $CONH\mathbf{CH_2}$	2.3 – 2.1 2.4 – 2.3 2.8 – 2.6 3.3 – 3.1	54.0 18.5 18.8 18.8	54.0 18.0 18.0 18.0
2c(90)	$CH_2N(CH_2\mathbf{CH_3})_2$ $CONHCH_2\mathbf{CH_2}CH_2NEt_2$ $\mathbf{CH_2}N(\mathbf{CH_2}CH_3)_2$ $\mathbf{CH_2}CONH$ $CONH\mathbf{CH_2}$	1.3 – 0.9 1.7 – 1.5 2.7 – 2.5 2.9 – 2.7 3.4 – 3.2	54.0 17.7 52.7 18.2 18.4	54.0 18.0 54.0 18.0 18.0
2d(90)	$CH_2N(CH_2\mathbf{CH_3})_2$ $\mathbf{CH_2}N(\mathbf{CH_2}CH_3)_2$ $\mathbf{CH_2}CONH$ $CONH\mathbf{CH_2}$	1.4 – 0.9 2.7 – 2.5 2.9 – 2.7 3.4 – 3.2	54.0 53.3 19.1 19.1	54.0 54.0 18.0 18.0
2e(90)	$[C(\mathbf{CH_3})_2]$-NH $CONHCH(\mathbf{CH_2})_2$ $CONH\mathbf{CH}$	1.2 – 0.9 1.5 – 1.3 4.1 – 4.0	108.0 15.3 7.8	108.0 16.0 9.0
2f(90)	$\mathbf{CH_2}CONH$ $CONH\mathbf{CH_2}$ $\mathbf{CH_2}O\mathbf{CH_2}\mathbf{CH_2}OH$	2.8 – 2.6 3.5 – 3.1 3.8 – 3.5	17.4 19.3 54.0	18.0 18.0 54.0

[a] *In D_2O, pD 10 – 11. Chemical shifts, δ (ppm), referenced against internal sodium 3-(trimethylsilyl)-2,2,3,3-d_4-propionate;*

[b] *Integration error limit ± 15%*

3.2.1.2.2. Terpolyaspartamide Carriers

The possibility of modifying the general structure of copolyaspartamides to terpolyasparmides (*Polyaspartamide Carriers bearing two* hydrosolubilizing groups) was previously demonstrated in this laboratory[123]. The same procedure as described for copolymers **2a(80), 2b(80), 2c(80), 2d(80), 2e(80), 2f(80), 2a(90), 2b(90), 2c(90), 2d(90), 2e(90)** and **2f(90)** was used for the preparation of the terpolyaspartamides carriers **3a(60)**, **3b(60)**, **3c(60), 3d(60)**, **3e(60)** and **3a(50)**, **3b(50)**, **3c(50), 3d(50)**, **3e(50)** (Schemes 9 and 10), but a different mode of addition was used. A three-step treatment of poly-DL-succinimide with AEE or ATP and DMP, DEP, DEEA or DMEA, in the same solvent at ambient temperature over various periods of time was utilized. The polymeric products were obtained in typical yields of 57 - 72%, and possessed inherent viscosities in the range of 12 – 19 mL/g. Their experimental details and viscosity results are presented in table 3.5, whereas ^{1}H NMR data are compiled in table 3.6.

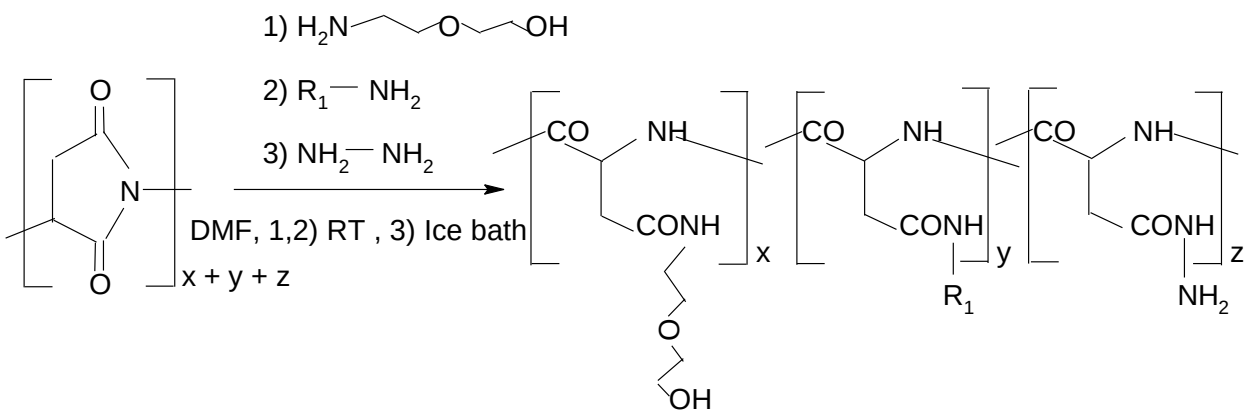

3a (60)	R_1:	NMe_2	x / y / z = 3 / 1 / 1
3b (60)	R_1:	NMe_2	x / y / z = 3 / 1 / 1
3c (60)	R_1:	NEt_2	x / y / z = 3 / 1 / 1
3d (60)	R_1:	NEt_2	x / y / z = 3 / 1 / 1
3e (60)	R_1:	NH	x / y / z = 3 / 1 / 1

Scheme 3.9: Synthesis of terpolyaspartamide carriers 3a (60) – 3e (60)

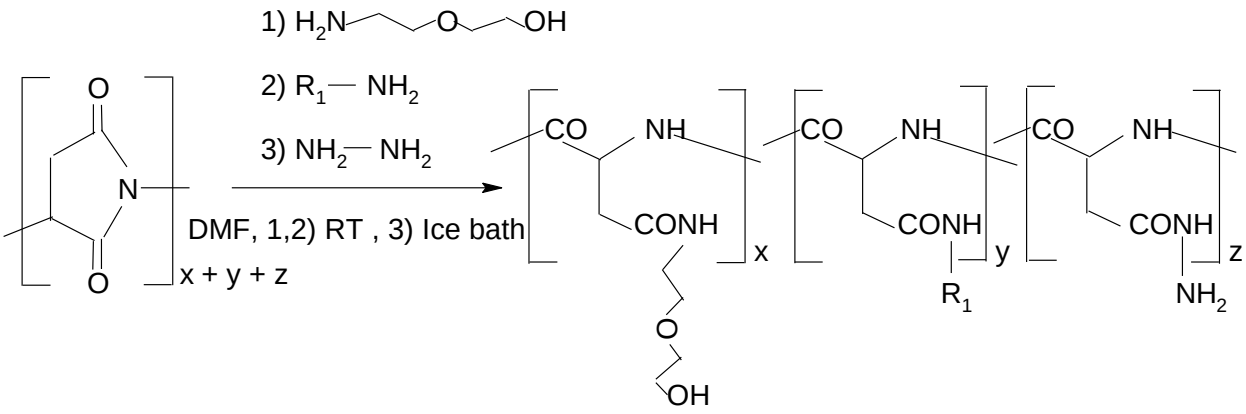

3a (50)	R_1:	NMe_2	x / y / z = 5 / 4 / 1
3b (50)	R_1:	NMe_2	x / y / z = 5 / 4 / 1
3c (50)	R_1:	NEt_2	x / y / z = 5 / 4 / 1
3d (50)	R_1:	NEt_2	x / y / z = 5 / 4 / 1
3e (50)	R_1:	NH	x / y / z = 5 / 4 / 1

Scheme 3.10: *Synthesis of terpolyaspartamide carriers 3a (50) – 3e (50)*

Table 3.5: Summary of experimental data for terpolyaspartamide carriers 3

Polymer Designation	Molar Ratios[a]							Reaction time & Temperature[b]		Yield %	η_{inh}[c] mL/g	x/y/z
	PSI	DMP	DMEA	DEP	DEEA	ATP	AEE	1st Step	2nd Step			
3a(60)	1.00	0.60	-	-	-	-	0.20	**AEE, RT**	**DMP, RT**	57.2	12.6	3/1/1
3b(60)	1.00	-	0.60	-	-	-	0.20	**AEE, RT**	**DMEA, RT**	65.7	12.9	3/1/1
3c(60)	1.00	-	-	0.60	-	-	0.20	**AEE, RT**	**DEEA, RT**	68.4	13.1	3/1/1
3d(60)	1.00	-	-	-	0.60	-	0.20	**AEE, RT**	**DEP, RT**	57.9	13.2	3/1/1
3e(60)	1.00	-	-	-	-	0.60	0.20	**AEE, RT**	**ATP, RT**	71.1	15.9	3/1/1
3a(50)	1.00	0.40	-	-	-	-	0.50	**AEE, RT**	**DMP, RT**	59.4	13.8	5/4/1
3b(50)	1.00	-	0.40	-	-	-	0.50	**AEE, RT**	**DMEA, RT**	66.3	13.8	5/4/1
3c(50)	1.00	-	-	0.40	-	-	0.50	**AEE, RT**	**DEEA, RT**	61.2	14.2	5/4/1
3d(50)	1.00	-	-	-	0.40	-	0.50	**AEE, RT**	**DEP, RT**	59.4	15.2	5/4/1
3e(50)	1.00	-	-	-	-	0.40	0.50	**AEE, RT**	**ATP, RT**	67.3	18.1	5/4/1

[a] *Base molar **PSI*** [b] IB*: Ice Bath; RT: room temperature* [c] *At 30.0^{0}C ± 0.5^{0}C in dist H_2O; conc = 0.2mg/100mL*

[d]*DMP: 3-(dimethylamino)propylamine; DMEA: 2-(dimethylamino)ethylamine; DEP: 2-(dimethylamino)ethylamine; DEEA: 2-(diethylamino)ethylamine; ATP: 4-amino-2,2,6,6-tetramethylpiperidine; AEE: 2-(2-aminoethoxy)ethanol; Hy: hydrazine hydrate*

Table 3.6: ^{1}H NMR of terpolyaspartamides 3a (50) –3e (50) and 3a (60) – 3e (60)

Polymer Designation	Assignment	^{1}H NMR[a,b]		
		Shift range δ(ppm)	Proton count	
			Found	Expected
3a(50)	$CONHCH_2\mathbf{CH_2}CH_2NMe_2$ $N\mathbf{Me_2}$; $\mathbf{CH_2}NMe_2$ $CONH\mathbf{CH_2}$ $\mathbf{CH_2}O\mathbf{CH_2CH_2}OH$	1.7 – 1.5 2.5 – 2.1 3.3 – 3.1 3.8 – 3.5	7.8 32.0 19.8 26.8	8.0 32.0 18.0 30.0
3b(50)	$N\mathbf{Me_2}$; $\mathbf{CH_2}NMe_2$ $\mathbf{CH_2}CONH$ $CONH\mathbf{CH_2}$ $\mathbf{CH_2}O\mathbf{CH_2CH_2}OH$	2.5 – 2.1 2.8 – 2.6 3.3 – 3.1 3.8 – 3.5	13.9 15.7 18.7 30.0	32.0 18.0 18.0 30.0
3c(50)	$CH_2N(CH_2\mathbf{CH_3})_2$ $CONHCH_2\mathbf{CH_2}CH_2NEt_2$ $\mathbf{CH_2}N(\mathbf{CH_2}CH_3)_2$ $CONH\mathbf{CH_2}$ $\mathbf{CH_2}O\mathbf{CH_2CH_2}OH$	1.2 – 0.9 1.7 – 1.5 2.7 – 2.5 3.4 – 3.2 3.8 – 3.5	25.2 9.1 26.0 20.5 30.0	24.0 8.0 24.0 18.0 30.0
3d(50)	$CH_2N(CH_2\mathbf{CH_3})_2$ $\mathbf{CH_2}N(\mathbf{CH_2}CH_3)_2$; $\mathbf{CH_2}CONH$ $CONH\mathbf{CH_2}$ $\mathbf{CH_2}O\mathbf{CH_2CH_2}OH$	1.2 – 0.9 2.9 – 2.5 3.4 – 3.2 3.8 – 3.5	21.0 42.0 19.4 30.0	24.0 42.0 18.0 30.0
3e(50)	$NH[C(\mathbf{CH_3})_2]_2$; $CONHCH(\mathbf{CH_2})_2$ $CONH\mathbf{CH_2}$ $\mathbf{CH_2}O\mathbf{CH_2CH_2}OH$ $CONH\mathbf{CH}$	1.5 – 0.9 3.4 – 3.2 3.8 – 3.5 4.1 – 4.0	66.4 9.5 30.0 3.98	64.0 10.0 30.0 4.0

Table 3.6 continued

Polymer Designation	Assignment	^{1}H NMR[a,b]		
		Shift range δ(ppm)	Proton count	
			Found	Expected
3a(60)	$CONHCH_2\mathbf{CH_2}CH_2NMe_2$ $N\mathbf{Me_2}$; $\mathbf{CH_2}NMe_2$ $CONH\mathbf{CH_2}$ $\mathbf{CH_2}O\mathbf{CH_2}\mathbf{CH_2}OH$	1.7 – 1.5 2.5 – 2.1 3.4 – 3.2 3.8 – 3.5	5.9 24.0 8.1 6.6	6.0 24.0 8.0 6.0
3b(60)	$N\mathbf{Me_2}$; $\mathbf{CH_2}NMe_2$ $CONH\mathbf{CH_2}$ $\mathbf{CH_2}O\mathbf{CH_2}\mathbf{CH_2}OH$	2.5 – 2.1 3.4 – 3.2 3.8 – 3.5	21.7 8.0 6.4	24.0 8.0 6.0
3c(60)	$CH_2N(CH_2\mathbf{CH_3})_2$ $CONHCH_2\mathbf{CH_2}CH_2NEt_2$ $\mathbf{CH_2}N(\mathbf{CH_2}CH_3)_2$ $CONH\mathbf{CH_2}$ $\mathbf{CH_2}O\mathbf{CH_2}\mathbf{CH_2}OH$	1.2 – 0.9 1.7 – 1.5 2.7 – 2.5 3.4 – 3.2 3.8 – 3.5	17.9 5.8 18.3 8.8 6.0	18.0 6.0 18.0 8.0 6.0
3d(60)	$CH_2N(CH_2\mathbf{CH_3})_2$ $\mathbf{CH_2}N(\mathbf{CH_2}CH_3)_2$ $CONH\mathbf{CH_2}$ $\mathbf{CH_2}O\mathbf{CH_2}\mathbf{CH_2}OH$	1.2 – 0.9 2.7 – 2.5 3.4 – 3.2 3.8 – 3.5	18.0 18.1 7.7 5.1	18.0 18.0 8.0 6.0
3e(60)	$NH[C(\mathbf{CH_3})_2]_2$; $CONHCH(\mathbf{CH_2})_2$ $CONH\mathbf{CH_2}$ $\mathbf{CH_2}O\mathbf{CH_2}\mathbf{CH_2}OH$ $CONH\mathbf{CH}$	1.5 – 0.9 3.4 – 3.2 3.8 – 3.5 4.1 – 4.0	46.2 1.8 6.0 2.5	48.0 2.0 6.0 3.0

[a] *In D_2O, pD 10 – 11. Chemical shifts, δ (ppm), referenced against internal sodium 3-(trimethylsilyl)-2,2,3,3-d_4-propionate*

[b] *Integration error limit ± 15%*

The synthetic pathway chosen for the synthesis of terpolyspartamide carriers 4 in this project is shown in schemes 11 and 12. The terpolyspartamides **4a (60), 4b (60), 4c (60), 4d (60), 4e (60), 4a (50), 4b (50), 4c (50), 4d (50)** and **4e (50)** were obtained in the same procedure as described for terpolyspartamide carriers 3. The aminolytic ring opening of PSI with the addition of ATP in the first step (slowly step), followed by another tertiary amine (DMP, DMEA, DEP, DEE or AEE) in the second step, adjusted the hydrosolubilizing and cell selective functionalities. The first step required a reaction time of 1 day at ambient temperature while the second step involved a shorter reaction time of 6 hours at ambient temperature. The compositions which represented the amine-functionalized unit were ascertained from relative peak intensities in the ^{1}H NMR spectra as shown in table 3.8. The polymeric products were obtained in typical yields of 54 - 71 %, and possessed inherent viscosities in the range of 18 – 28 mL/g. Table 3.7 summarize the experimental conditions and viscosity.

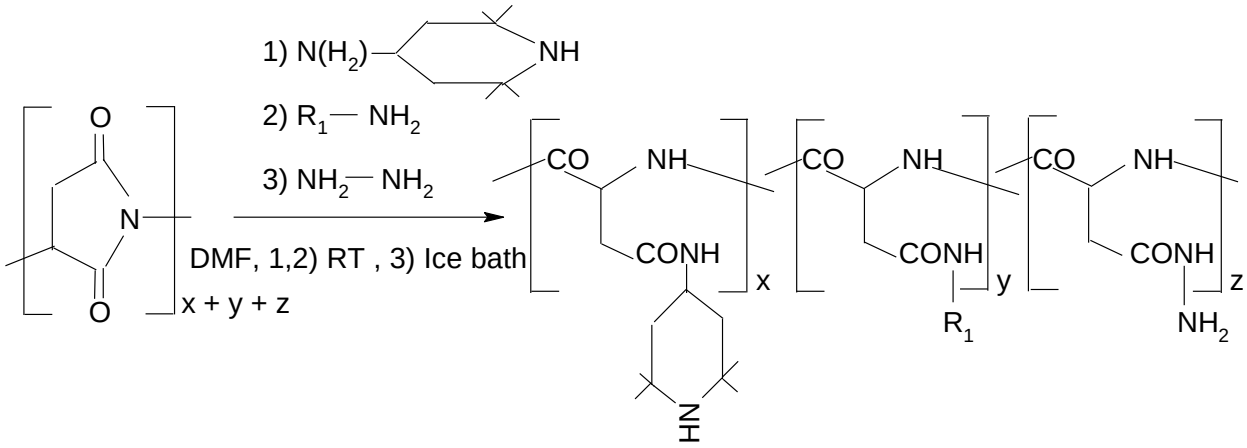

4a (60)	R_1:	NMe_2	x / y / z = 3 / 1 / 1
4b (60)	R_1:	NMe_2	x / y / z = 3 / 1 / 1
4c (60)	R_1:	NEt_2	x / y / z = 3 / 1 / 1
4d (60)	R_1:	NEt_2	x / y / z = 3 / 1 / 1
4e (60)	R_1:	O OH	x / y / z = 3 / 1 / 1

Scheme 3.11: *Synthesis of terpolyaspartamide carriers 4a (60) – 4e (60)*

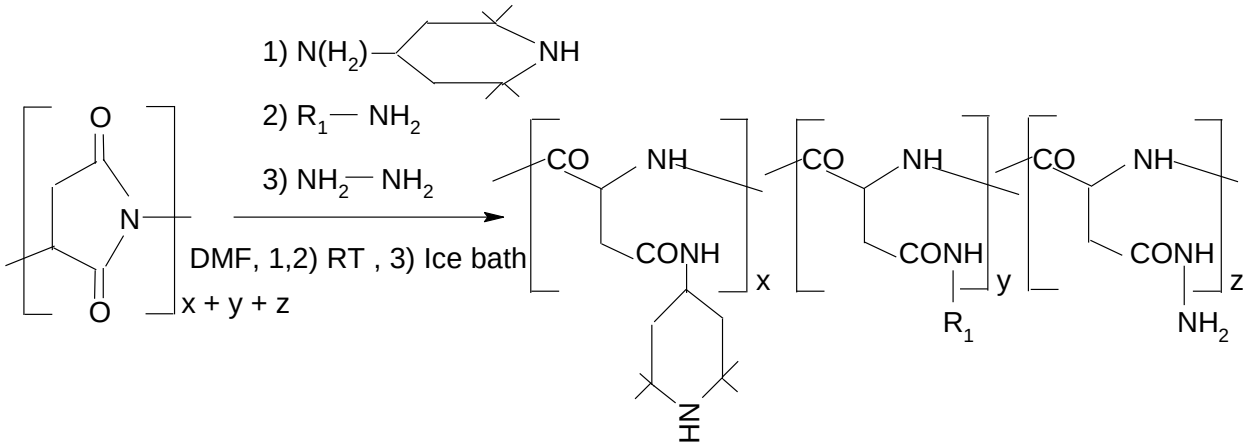

4a (50)	R_1:	NMe_2	x / y / z = 5 / 4 / 1
4b (50)	R_1:	NMe_2	x / y / z = 5 / 4 / 1
4c (50)	R_1:	NEt_2	x / y / z = 5 / 4 / 1
4d (50)	R_1:	NEt_2	x / y / z = 5 / 4 / 1
4e (50)	R_1:	O OH	x / y / z = 5 / 4 / 1

Scheme 3.12: Synthesis of terpolyaspartamide carriers 4a (50) – 4e (50)

Table 3.7: Summary of experimental data for terpolyaspartamide carriers 4

Polymer Designation	Molar Ratios[a]							Reaction time & Temperature[b]		Yield %	η_{inh}[c] mL/g	x/y
	PSI	DMP	DMEA	DEP	DEEA	AEE	ATP	1st Step	2nd Step			
4a(60)	1.00	0.20	-				0.60	ATP, RT	DMP, RT	66.5	20.8	3/1/1
4b(60)	1.00		0.20				0.60	ATP, RT	DMEA, RT	61.5	19.3	3/1/1
4c(60)	1.00			0.20			0.60	ATP, RT	DEEA, RT	54.4	21.6	3/1/1
4d(60)	1.00				0.20		0.60	ATP, RT	DEP, RT	55.7	24.6	3/1/1
4e(60)	1.00					0.20	0.60	ATP, RT	AEE, RT	70.1	21.3	3/1/1
4a(50)	1.00	0.40					0.50	ATP, RT	DMP, RT	59.2	21.7	5/4/1
4b(50)	1.00		0.40				0.50	ATP, RT	DMEA, RT	65.1	18.6	5/4/1
4c(50)	1.00		-	0.40		-	0.50	ATP, RT	DEEA, RT	60.9	24.7	5/4/1
4d(50)	1.00	-			0.40	-	0.50	ATP, RT	DEP, RT	67.3	27.9	5/4/1
4e(50)	1.00		-			0.40	0.50	ATP, RT	AEE, RT	61.9	21.4	5/4/1

[a] *Base molar **PSI***

[b] *RT: room temperature*

[c] *At 30.0^0C ± 0.5^0C in dist H_2O; conc = 0.2mg/100mL*

Table 3.8: ^{1}H NMR of terpolyaspartamides carrier's 4a (50)-4e (50) and 4a (60)-4e (60)

Polymer Designation	Assignment	^{1}H NMR[a,b]		
		Shift range δ(ppm)	Proton count	
			Found	Expected
4a (50)	$CH(\mathbf{CH_2})_2$; $NH[C(\mathbf{CH_3})_2]_2$ $CONHCH_2\mathbf{CH_2}CH_2NMe_2$ $N\mathbf{Me_2}$ $\mathbf{CH_2}NMe_2$ $CONH\mathbf{CH_2}$ $CONH\mathbf{CH}$	1.5 – 0.9 1.7 – 1.5 2.3 – 2.1 2.4 – 2.3 3.3 – 3.1 4.1 – 4.0	80.0 9.4 23.5 9.4 9.4 4.7	80.0 8.0 24.0 8.0 8.0 5.0
4b (50)	$CH(\mathbf{CH_2})_2$; $NH[C(\mathbf{CH_3})_2]_2$ $N\mathbf{Me_2}$ $\mathbf{CH_2}NMe_2$ $CONH\mathbf{CH_2}$ $CONH\mathbf{CH}$	1.5 – 0.9 2.3 – 2.1 2.4 – 2.3 3.3 – 3.1 4.1 – 4.0	80.0 22.9 7.6 7.6 3.8	80.0 24.0 8.0 8.0 5.0
4c (50)	$CH_2N(CH_2\mathbf{CH_3})_2$; $NH[C(\mathbf{CH_3})_2]_2$; $CH(\mathbf{CH_2})_2$ $CONHCH_2\mathbf{CH_2}CH_2NEt_2$ $\mathbf{CH_2}N(\mathbf{CH_2}CH_3)_2$; $\mathbf{CH_2}CONH$ $CONH\mathbf{CH_2}$ $CONH\mathbf{CH}$	1.5 – 0.9 1.7 – 1.5 2.9 – 2.5 3.3 – 3.1 4.1 – 4.0	104.0 8.0 42.0 8.6 6.5	104.0 8.0 42.0 8.0 5.0
4d (50)	$CH_2N(CH_2\mathbf{CH_3})_2$; $NH[C(\mathbf{CH_3})_2]_2$; $CH(\mathbf{CH_2})_2$ $\mathbf{CH_2}N(\mathbf{CH_2}CH_3)_2$; $\mathbf{CH_2}CONH$ $CONH\mathbf{CH_2}$ $CONH\mathbf{CH}$	1.5 – 0.9 2.9 – 2.5 3.3 – 3.1 4.1 – 4.0	104.0 46.9 7.6 4.8	104.0 42.0 8.0 5.0
4e (50)	$NH[C(\mathbf{CH_3})_2]_2$; $CH(\mathbf{CH_2})_2$ $\mathbf{CH_2}CONH$ $CONH\mathbf{CH_2}$; $\mathbf{CH_2}O\mathbf{CH_2}\mathbf{CH_2}OH$ $CONH\mathbf{CH}$	1.5 – 0.9 2.9 – 2.6 3.8 – 3.1 4.1 – 4.0	80.0 18.5 36.4 5.7	80.0 18.0 32.0 5.0

Table 3.8 continued

Polymer Designation	Assignment	^{1}H NMR[a,b]		
		Shift range δ(ppm)	Proton count	
			Found	Expected
4a (60)	CH(**CH_2**)$_2$; NH[C(CH_3)$_2$]$_2$ CONHCH$_2$**CH_2**CH_2NMe_2 N**Me_2** **CH_2**NMe_2 CONH**CH_2** CONH**CH**	1.5 – 0.9 1.7 – 1.5 2.3 – 2.1 2.4 – 2.3 3.3 – 3.1 4.1 – 4.0	48.0 2.3 6.4 2.4 2.3 2.9	48.0 ‘2.0 6.0 2.0 2.0 3.0
4b (60)	CH(**CH_2**)$_2$; NH[C(CH_3)$_2$]$_2$ N**Me_2** **CH_2**NMe_2 CONH**CH_2** CONH**CH**	1.5 – 0.9 2.3 – 2.1 2.4 – 2.3 3.3 – 3.1 4.1 – 4.0	48.0 6.7 2.5 2.5 2.5	48.0 6.0 2.0 2.0 3.0
4c (60)	$CH_2N(CH_2$**CH_3**$)_2$; NH[C(**CH_3**)$_2$]$_2$; CH(**CH_2**)$_2$ CONHCH$_2$**CH_2**CH_2NEt_2 **CH_2**N(**CH_2**CH_3)$_2$ CONH**CH_2** CONH**CH**	1.5 – 0.9 1.7 – 1.5 2.7 – 2.5 3.3 – 3.1 4.1 – 4.0	54.0 2.5 6.3 1.9 3.0	54.0 2.0 6.0 2.0 3.0
4d (60)	$CH_2N(CH_2$**CH_3**$)_2$; NH[C(**CH_3**)$_2$]$_2$; CH(**CH_2**)$_2$ **CH_2**N(**CH_2**CH_3)$_2$ CONH**CH_2** CONH**CH**	1.5 – 0.9 2.7 – 2.5 3.3 – 3.1 4.1 – 4.0	54.0 6.2 2.4 2.7	54.0 6.0 2.0 3.0
4e (60)	NH[C(**CH_3**)$_2$]$_2$; CH(**CH_2**)$_2$ CONH**CH_2** **CH_2**O**CH_2****CH_2**OH CONH**CH**	1.5 – 0.9 3.4 – 3.1 3.8 – 3.5 4.1 – 4.0	48.0 2.4 5.5 2.4	48.0 2.0 6.0 3.0

[a] *In D_2O, pD 10 – 11. Chemical shifts, δ (ppm), referenced against internal sodium 3-(trimethylsilyl)-2,2,3,3-d_4-propionate;* [b] *Integration error limit ± 15%*

3.2.2. Polymer-Drug Anchoring

In the effort of enhancing the specificity of drug action, different strategies involving chemical modification of drug with water-soluble polymers are being investigated in this laboratory. Synthetic biocompatible and biodegradable polymers carriers, for low risk of immunogenicity and toxicity, have been given preference over natural polymers. Polymer-anchored structures will be discussed in which partaking drug models are represented by organoiron compounds derived from ferrocene, and by curcumin.

3.2.2.1. Polymer-ferrocene conjugation

The antiproliferative and antineoplastic action of ferrocene, as described previously, prompted the initiation of an extended synthetic program in this laboratory aiming at the development and routine synthesis of such ferrocene conjugates for biomedical investigation[126-128]. The ferrocene derivatives employed in this project were acetylferrocene, 3-Ferrocenylpropenal, and ferrocenecarboxyaldehyde. The above ferrocene derivatives were chosen because of their low reduction potential[128] which ensure ease of reduction in the biological environment.

All carrier polymers used in this project were pre-dried prior to conjugation reactions, and were initially water-soluble solids. Degrees of coupling were assessed from the relative intensity of the ferrocene proton signals in the “window” at 4.3-4.1 ppm in ^{1}H NMR spectra, which correlated with UV analysis.

The basic coupling models used in this project are shown below (figure 3.1)

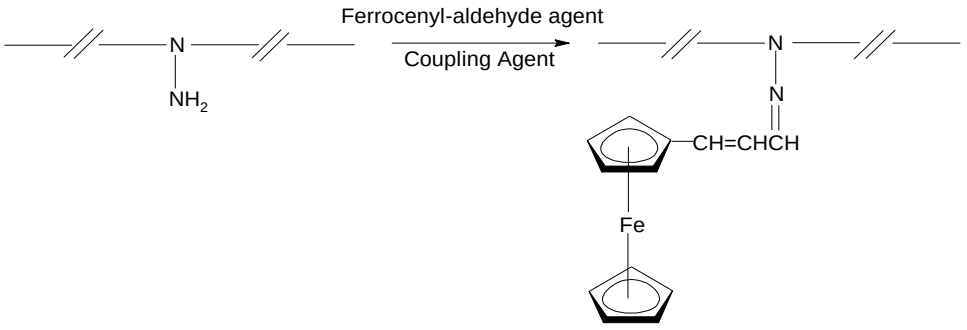

Model 1

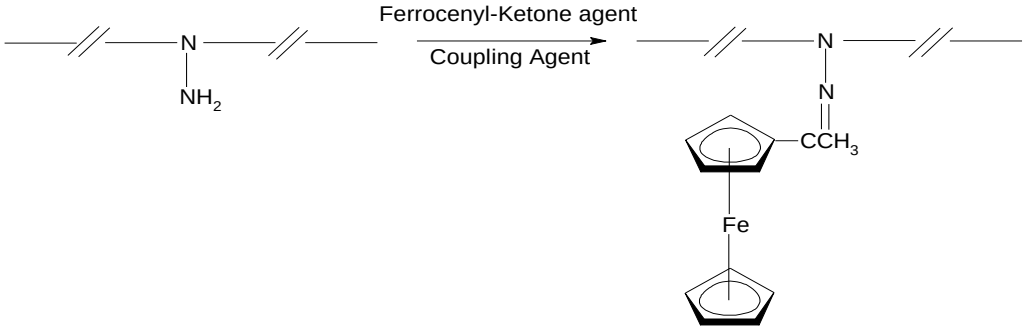

Model 2

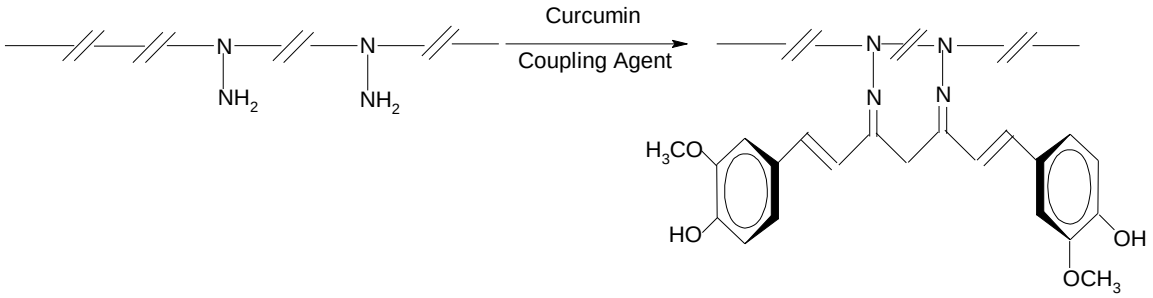

Model 3

Figure 3.1: *Models of Hydrazone-conjugates*

Conjugates **2a (80)-Fcp – 2f (80)-Fc, 2a (90)-Fcp – 2f (90)-Fcp, 3a (60)-Fcp, 3b (60)-Fcp, 3a (50)-Fcp, 3b (50)-Fcp, 4a (50)-Fcp – 4e (50)-Fcp, and 4a (60)-Fcp – 4e (60)-Fcp** were derived from carriers **2a (80) – 2f (80), 2a (90) – 2f (90), 3a (60)- 3e (60), 3a (50)** - **3e (50), 4a (60)- 4e (60), and 4a (50) – 4e (50)**. The carriers were treated with 3-Ferrocenylpropenal, ferrocenecarboxyaldehyde, or acetylferrocene in a mixture of methanol (predominant proportion) and DMF, according to schemes 13, 14 and 15 under controlled experimental conditions of time, temperature and acidity. In order to suppress the hydrolysis of the carrier catalyzed by lower pH or hydroxo bridging which causes insolubility of the final conjugate at high pH, the pH was carefully adjusted and maintained in the range of pH 6.5 - 7. The water-soluble product conjugates were obtained by precipitation from the reaction solution, fractionation and purification by aqueous dialysis, and isolation by freeze-drying. The structures were confirmed by ^{1} H NMR spectroscopy. The ^{1}H NMR spectra of the conjugates displayed the signals of the respective carriers and those of the incorporated ferrocenylation agent, especially the ferrocenyl (C-H) protons whose signal (4.3 – 4.1 ppm) was used for the evaluation of the drug content in comparison with other important signals. For the ferrocene conjugates, the drug incorporation was between 63% and 100%. Independent determination by UV spectroscopy using the molar extinction coefficient (ϵ = 100 mol^{-1} cm^{-1}) and the absorbance at λ 440 nm in H_2O confirmed the ^{1}H NMR results. The molar feed ratio, experimental conditions, viscosities, and ferrocene content data are summarized in Table 3.9.

In these experiments, the ratio of ferrocene/polymer repeat unit was in the 1.2 – 1.4 range. The hydrazone based coupling method afforded ferrocene conjugates an inherent viscosities varying from 14 to 29 mL g^{-1}. In accordance with the presence of the drug molecules, the viscosities of these conjugates were higher when compared with those of the forerunner carriers. The solid-state IR spectra of these conjugates showed the bands of stretching vibrations of the N=C bonds (1625-1642 cm^{-1}) which showed the presence in these materials of the hydrazone bridges.

The copolyaspartamide conjugates PSI-DMP(90)-Hy-Fcp **(2a (90) – Fcp),** PSI-DEEA(90)-Hy-Fcp **(2d (90) – Fcp),** PSI-AEE(90)-Hy-Fcp **(2f (90) – Fcp)** and PSI-AEE(90)-Hy-Fcp **(2f (80) – Fcp)** were obtained in yields of 65.3 %, 53.2 %, 58.9 %, 51.7 % and 57.8 % under the same experimental conditions as above. Listed in table 3.9 are preparative data, and in table 3.10 are summarized the characteristic ^{1}H NMR data. The UV analysis determined ferrocene contents for **2a (90) – Fcp, 2d (90) – Fcp, 2f (90) – Fcp** and **2f (80) – Fcp** are 3.1 % lower, 2.0 % lower, 8.9 % lower and 1.5 % higher respectively than calculated. The ^{1}H NMR results confirmed ferrocene contents ranging from 1.6 to 36.9 % lower than those calculated from the idealized structures.

The water-soluble conjugates **2e (90) – Fca, 2f (90) – Fcc, 2a (80) – Cyn, 2e (80) – Cyn, 2c (90) – Cyn** and **2f (90) – Cur** were obtained in yields of 58.3 %, 52.1 %, 61.9 %, 60.3 %, 59.7 % and 61.5 %, under experimental conditions similar to the above conjugation method. Their experimental details are presented in table 3.9, whereas ^{1}H NMR data are compiled in table 3.10.

The terpolyaspartamide conjugates PSI-DMP(40)-AEE(50)-Hy-Fcp **(3a (50) – Fcp),** PSI-DMP(60)-AEE(20)-Hy-Fcp **(3a (60) – Fcp),** PSI-DEEA(60)-AEE(20)-Hy-Fcp **(3d (60) – Fcp),** PSI-DEEA(40)-AEE(50)-Hy-Fcp **(3d (50) – Fcp),** PSI-DEP(20)-ATP(60)-Hy-Fcp **(4c (50) – Fcp),** PSI-DEP(20)-ATP(60)-Hy-Fcp **(4c (60) – Fcp),** PSI-DEEA(40)-ATP(50)-Hy-Fcp **(4d (50) – Fcp),** PSI-AEE(40)-ATP(50)-Hy-Fcp **(4e (50) – Fcp),** PSI-DMEA(20)-ATP(60)-Hy-Fcp **(4b (50) – Fca),** PSI-AEE(40)-ATP(50)-Hy-Fcp **(4e (50) – Fca),** PSI-DEP(40)-ATP(50)-Hy-Fcp **(4c (60) – Fcc)** and PSI-DMP(20)-ATP(60)-Hy-Fcp **(4a (60) – Cur)** were obtained in yields of 56.3 %, 62.7 %, 48.1 %,64.8%, 50.2 %, 57.1 %, 58.8 %, 52.7 %, 49.2 %, 55.1%, 58.2%, 66.9% and 52.3 % under the same experimental conditions as above. Listed in table 3.9 are experimental data, and in table 3.10 are summarized characteristic ^{1}H NMR data. The UV analysis determined ferrocene contents for **3a (50) – Fcp, 3a (60) – Fcp, 3d (60) – Fcp, 3d (50) – Fcp, 4c (50) – Fcp, 4c (60) – Fcp, 4d (50) – Fcp, 4e (50) – Fcp, 4b (50) – Fca, 4e (50) – Fca,** and **4c (60) – Fcc** are 13.8 % lower, 27.7 % lower, 25.8 % lower, 0.77 % lower, 5.06 % lower, 2.12 % lower, 3.54 % lower, 4.35 % lower, 7.56 % lower, 6.33 % lower and 45.21 % lower respectively than calculated. The ^{1}H NMR results correlated with ferrocene contents which ranged from 1.30 to 29.2 % higher than those calculated for the idealized structures.

Curcumin having antioxidant properties (may decrease inflammation) can play a role in cancer therapy. A small number of curcumin conjugation showed the possibility of incorporated curcumin into hydrazine carriers with possibilities of forming hydrazone bond. Efforts are necessary to establish realistic conclusion.

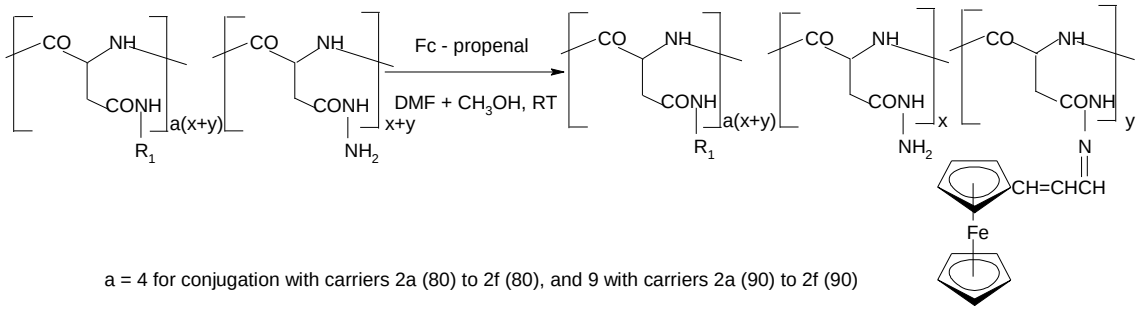

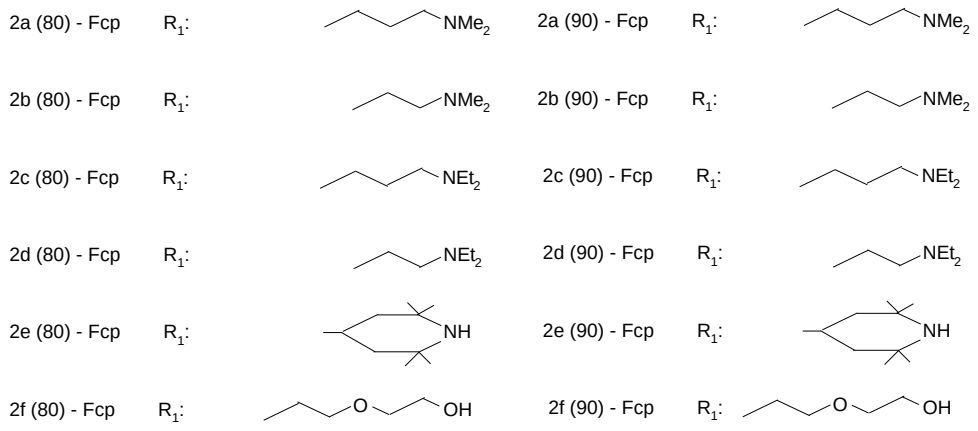

Scheme 3.13: *Synthesis of conjugates 2a (80)-Fcp – 2f (90)-Fcp*

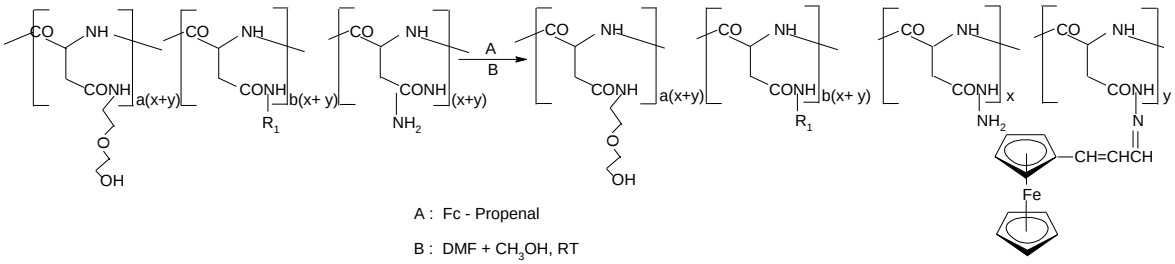

A : Fc - Propenal

B : DMF + CH_3OH, RT

a = 3 and b = 1 for carriers with 3a (60) to 3e (60)

a = 5 and b = 4 for carriers with 3a (50) to 3e (50)

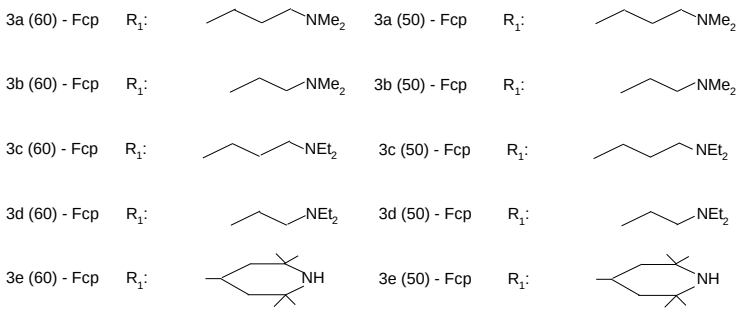

Scheme 3.14: *Synthesis of conjugates 3a (60)-Fcp – 3e (50)-Fcp*

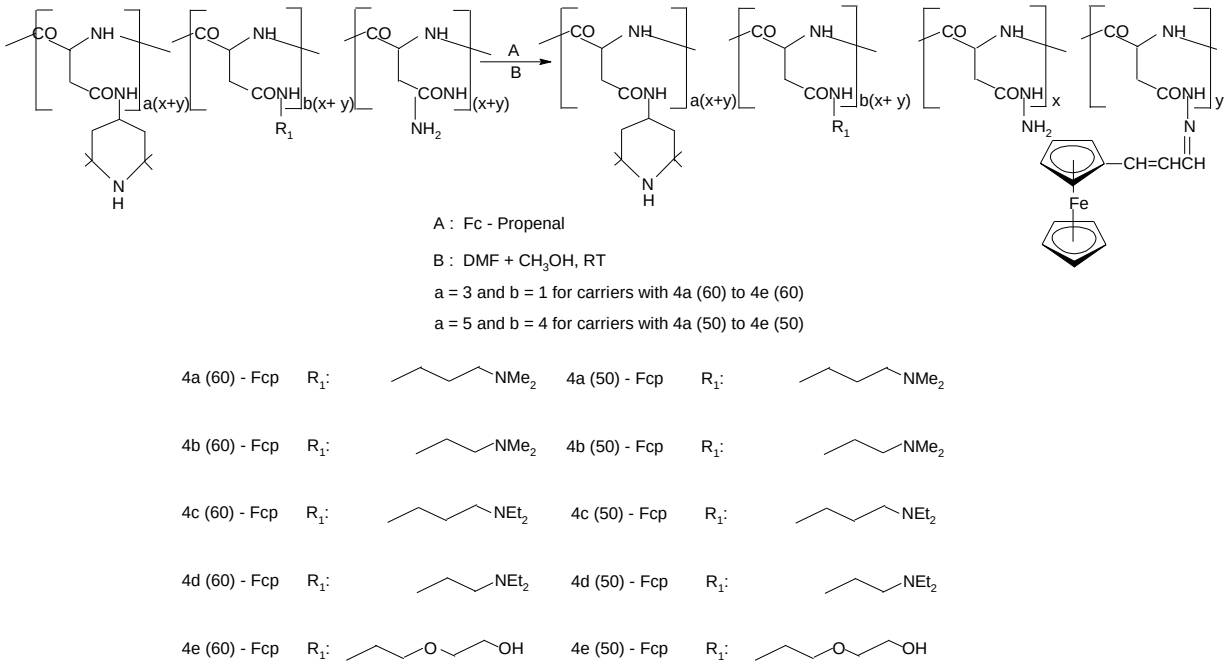

Scheme 3.15: *Synthesis of conjugates* ***4a (60)-Fcp*** *–* *4e* ***(50)-Fcp***

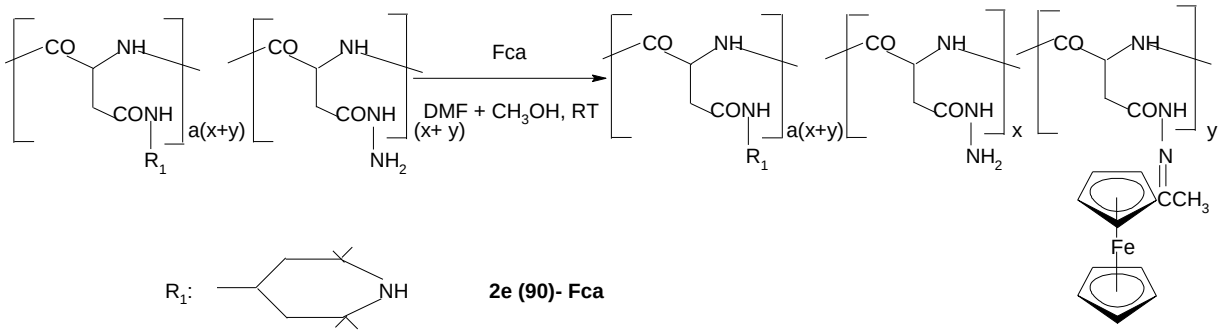

scheme 16.1: Conjugation with acetylferrocene

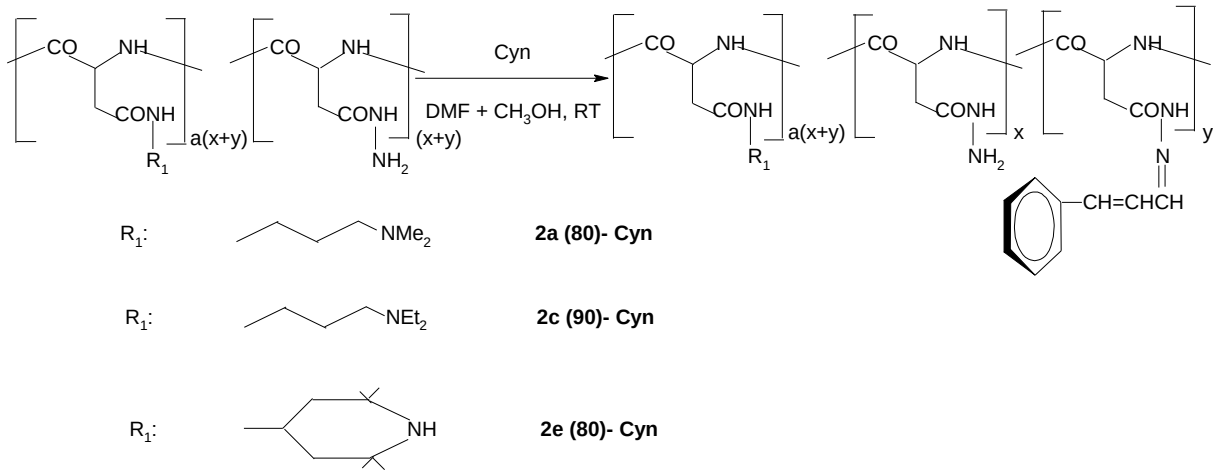

scheme 16.2: Conjugation with Cinnamaldehyde

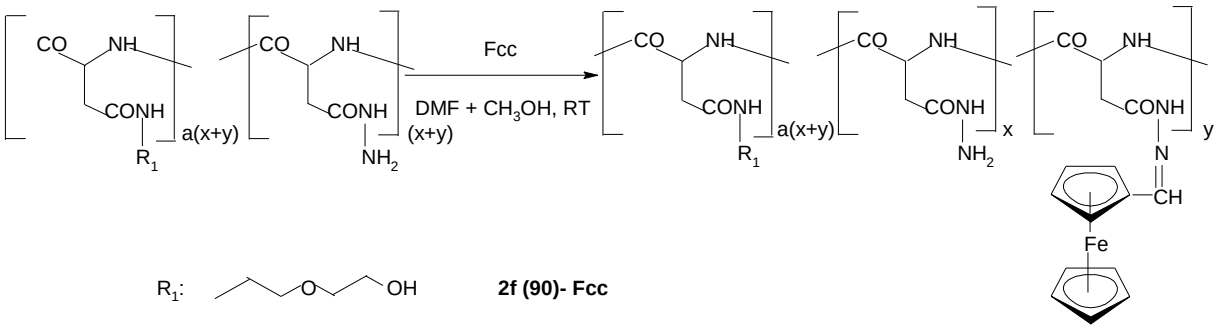

scheme 16.3: Conjugation with Ferrocenecarboxyaldehyde

With a = 4 for 2a (80) and 2e (80) carriers, and 9 for 2c (90), 2e (90) and 2f (90)

Scheme 3.16: *Synthesis of conjugates with Fca, Fcc and Cyn*

Table 3.9: *Preparative and Analytical data of drug-conjugates.*

Conjugate Designation	Molar Ratios		Reaction time & Temperature		Yield %	Base Molecular Mass[a]	η_{inh}[b] mL/g	x/y[c]	Drug (Fe or Cyn) %	
	Carrier	Drug	Fist Step	Second Step					Found[d]	Calcd[e]
2a(90)-Fcp	1.0	1.2	3d, RT	2h, 50^{0}C	65.3	1936.758	14.8	1.04	2.76	2.88
2a(90)-Fcp	1.0	1.4	3d, RT	2h, 50^{0}C	53.2	2143.894	15.1	1.00	2.60	2.60
2d(90)-Fcp	1.0	1.2	3d, RT	2h, 50^{0}C	58.9	2270.164	21.3	1.01	2.44	2.46
2f(90)-Fcp	1.0	1.2	3d, RT	2h, 50^{0}C	51.7	2170.534	16.2	1.60	1.62	2.57
2f(80)-Fcp	1.0	1.2	3d, RT	2h, 50^{0}C	57.8	2097.418	18.4	1.21	2.19	2.66
2e(90)-Fca	1.0	1.2	3d, RT	2h, 50^{0}C	58.3	2630.704	24.2	1.37	1.55	2.12
2f(90)-Fcc	1.0	1.2	3d, RT	2h, 50^{0}C	52.1	2170.534	17.3	1.47	1.75	2.57
2a(80)-Cyn	1.0	1.2	3d, RT	2h, 50^{0}C	61.9	1965.856	15.1	0.89	6.60	5.90
2e(80)-Cyn	1.0	1.2	3d, RT	2h, 50^{0}C	60.3	2398.576	24.4	1.19	4.07	4.84
2c(90)-Cyn	1.0	1.2	3d, RT	2h, 50^{0}C	59.7	1909.942	16.7	1.04	5.84	6.08
2f(90)-Cur	1.0	2.2	3d, RT	2h, 50^{0}C	61.5	2258.748	20.2	1.00	13.82	13.82

Table 3.9 continued

Conjugate Designation	Molar Ratios		Reaction time & Temperature		Yield %	Base Molecular Mass[a]	η_{inh}[b] mL/g	x/y[c]	Drug (Fe or Cyn) %	
	Carrier	drug	Fist Step	Second Step					Found[d]	Calcd[e]
3a(50)-Fcp	1.0	1.2	3d, RT	2h, 50^0C	56.3	2158.694	21.2	1.25	2.07	2.59
3a(60)-Fcp	1.0	1.2	3d, RT	2h, 50^0C	62.7	2091.498	18.7	1.12	2.38	2.67
3d(60)-Fcp	1.0	1.2	3d, RT	2h, 50^0C	48.1	2119.558	21.1	1.35	1.95	2.63
3d(50)-Fcp	1.0	1.2	3d, RT	2h, 50^0C	64.8	2144.074	20.3	1.39	1.87	2.60
4c(50)-Fcp	1.0	1.2	3d, RT	2h, 50^0C	50.2	2358.224	26.2	1.11	2.13	2.37
4c(50)-Fcp	1.0	1.4	3d, RT	2h, 50^0C	57.1	2358.224	24.1	1.05	2.26	2.37
4c(60)-Fcp	1.0	1.2	3d, RT	2h, 50^0C	58.8	2370.218	28.1	1.04	2.27	2.36
4d(50)-Fcp	1.0	1.2	3d, RT	2h, 50^0C	52.7	2470.464	24.5	1.01	2.24	2.26
4e(50)-Fcp	1.0	1.2	3d, RT	2h, 50^0C	49.2	2426.182	28.2	1.00	2.30	2.30
4b(50)-Fca	1.0	1.2	3d, RT	2h, 50^0C	55.1	2345.386	21.4	1.10	2.17	2.38
4e(50)-Fca	1.0	1.2	3d, RT	2h, 50^0C	58.2	2357.290	22.3	1.12	2.11	2.37
4c(60)-Fcc	1.0	1.2	3d, RT	2h, 50^0C	66.9	2428.470	23.1	1.17	1.06	2.30
4a(60)-Cur	1.0	2.2	3d, RT	2h, 50^0C	52.3	2518.492	23.8	1.62	8.44	13.67

[a] *Molecular mass of the simple recurring unit; structures normalized to y = 1*

[b] *At 30.0^0 C ± 0.5^0 C in distilled water; conc = 2mg/mL*

[c] *Ferrocene content for complete incorporation of the drug*

[d] *% protons calculated from H NMR*

[e] *% protons calculated for complete incorporation*

Table 3.10: ^{1}H NMR of drug-conjugates

Conjugate Designation	% Fe			Protons counted[d] (expected)[e] chemical shift range δ (ppm)						
	calcd[a]	^{1}H NMR[b]	UV[c]	δ: 4.2-4.1	δ: 3.8-3.6 0r [4.1-4.0]	δ: 3.3-3.1	δ: 2.9-2.6	δ: 2.5-2.3	δ: 2.3-2.1	δ: 1.2-0.9
2a(90)-Fcp	2.88	2.76	2.79	8.6 (9)	-	17.8(18)	17.2(18)	-	54(54)	-
2a(90)-Fcp'	2.60	2.60	2.58	9.0(9)	-	19.5(18)	17.5(18)	-	54(54)	-
2d(90)-Fcp	2.46	2.44	2.41	8.9(9)	-	-	18.0(18)	53.3(54)	54(54)	-
2f(90)-Fcp	2.57	1.62	2.34	5.7(9)	54(54)	-	17.8(18)	-	-	-
2f(80)-Fcp	2.66	2.19	2.70	7.4(9)	24.0(24)	-	7.8(8.0)	-	-	-
2e(90)-Fca	2.12	1.55	1.95	6.6(9)	[9.0(9)]	-	-	-	-	108(108)
2f(90)-Fcc	2.57	1.75	2.50	6.1(9)	54.0(54)	16.8(18)	-	-	-	-
3a(50)-Fcp	2.59	2.07	2.23	7.2(9)	30.0(30)	-	-	24.0(24)	-	-
3a(60)-Fcp	2.67	2.38	1.93	8.0(9)	6.0(6)	-	-	18.0(18)	-	-
3d(60)-Fcp	2.63	1.95	2.04	6.7(9)	-	5.8(6)	6.1(6)	-	18.0(18)	-
3d(50)-Fcp	2.60	1.87	2.58	6.5(9)	34.6(30)	18.6(18)	-	-	-	24(24)
4c(50)-Fcp	2.37	2.13	2.25	8.1(9)	-	-	24.0(24)	18.0(18)	-	63.4(60)
4c(50)-Fcp'	2.37	2.26	2.30	8.6(9)	-	-	24.0(24)	18.0(18)	-	63.4(60)

Table 3.10 continued

Conjugate Designation	% Drug (Fe, Cyn or Cur)			Protons counted[d] (expected)[e] chemical shift range δ (ppm)							
	calcd[a]	^{1}H NMR[b]	UV[c]	δ: 7.6-7.2	δ: 6.7-6.5	δ: 4.3-4.1	δ: 4.1-4.0	δ: 3.8-3.6	δ: 3.4-3.3 or [3.3-3.1]	δ: 1.9-1.7 or [2.3-2.1]	δ: 1.2-0.9
4c(60)-Fcp	2.36	2.27	2.31	-	-	8.6(9)	-	-	1.9(2)	-	54.0(54)
4d(50)-Fcp	2.26	2.24	2.18	-	-	8.9(9)	-	-	7.6(8)	-	60.0(60)
4e(50)-Fcp	2.30	2.30	2.20	-	-	9.1(9)	-	23.9(24)	-	-	60.0(60)
4b(50)-Fca	2.38	2.17	2.20	-	-	8.2(9)	-	-	8.8(8)	-	60.0(60)
4e(50)-Fca	2.37	2.11	2.22	-	-	8.0(9)	-	5.7(5)	-	-	60.0(60)
4c(60)-Fcc	2.30	1.06	1.26	-	-	4.1(9)	3.4(3)	-	-	-	54.0(54)
2a(80)-Cyn	5.90	6.60	5.88	5.6(5)	-	-	-	-	[7.6(9)]	[24.0(24)]	-
2e(80)-Cyn	4.84	4.07	4.71	4.2(5)	-	-	3.5(4)	-	-	-	48.0(48)
2c(90)-Cyn	6.08	5.84	5.90	4.8(5)	-	-	-	-	-	17.9(18)	54.0(54)
2f(90)-Cur	13.82	13.82	13.79	-	6.1(6)	-	-	54.0(54)	20.2(18)	-	-
4a(60)-Cur	13.61	8.44	11.20	-	3.7(6)	2.8(3)	-	-	-	-	48.0(48)

a Mass percentage of Fe calculated for 100% acylation. *b Mass percentage of Fe derived from 1H NMR spectrum (error limit ± 15%).*

c Mass percentage derived from UV absorbance of bound Fc, Cur and Cyn in H_2O at 440 nm(ε =100 $cm^{-1}M^{-1}$), 430 nm (ε =2.5× 10^4 $cm^{-1}M^{-1}$), and 280nm (ε =3.7× 10^4 $cm^{-1}M^{-1}$), respectively.

d In D_2O, pH 10-11, chemical shifts, δ/ppm, referenced against internal sodium 3-trimethylsilyl-2,2,3,3-d4-propionate; integration error limits ± 12 %.Protons are calculated for structural representations in Table 3.9.

e Expected count for composition in accordance with recurring unit.

3.3.2. Polymer multidrug conjugation

As part of the tasks assigned to this project, the anticancer compounds (folic acid (FA) or curcumin (Cur), and ferrocene) were anchored to the same polymeric carrier backbone. The drug systems operate by different cell killing mechanisms, and it was of interest here to establish additive effects or to increase the efficiency of the drug systems. The conjugation was achieved by hydrazone bond formation and the co-conjugates were the pairs FA-Fcp and Cur-Fcp. In the first two pairs, folic acid (FA) used different coupling methods. FA was used as an additional targeting moiety, given that the folate cellular uptake occurs by a natural endocytosis pathway mediated by folate receptor. The presence of these entities suggests competitive mechanisms of cellular uptake. No modification in the work-up steps was observed (excepting for FA conjugation), this was done as discussed in the foregoing paragraph. The experimental conditions, viscosities, and ferrocene content data are summarized in Table 3.11, whereas ^{1}H NMR data are compiled in table 3.12.

As can be seen in table 3.11, the polyaspartamide co-drug conjugates were obtained in yields of 47 - 58 %. They were characterized by inherent viscosities in the range of 20 – 24 mL g^{-1}. These were higher than those of their precursor carriers (**2a (90), 2a (80) and 4c (60)**). The UV determination of Fc content using the molar extinction coefficient value (ε = 100 M^{-1} cm^{-1}) and the absorbance at λ = 440 nm in H_2O, showed the co-drug conjugates **2a (90) – FA – Fcp, 2a (80) – FA – Fcp and 4c (60) – Cur – Fcp** to contain 2.38, 2.10 and 1.96 % Fe by mass, respectively. The ^{1}H NMR results correlated with Fc content which ranged from 1.96 to 2.32 % Fe by mass.

The clear correspondence of drug contents in the co-drug conjugates determined by the different analytical methods demonstrates that the polyaspartamides types polymers were effective co-drug carriers, although only a small number of carriers were investigated.

The drug model is displayed in figure 3.2

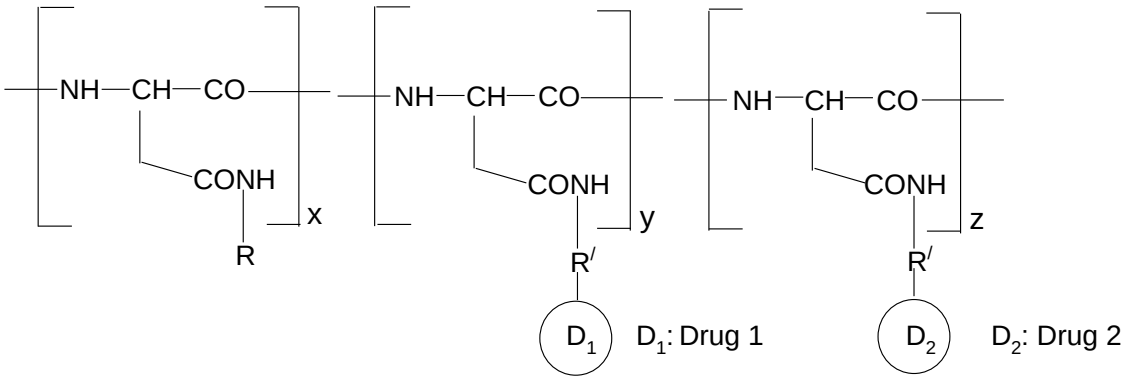

Figure 3.2: Multidrug conjugation

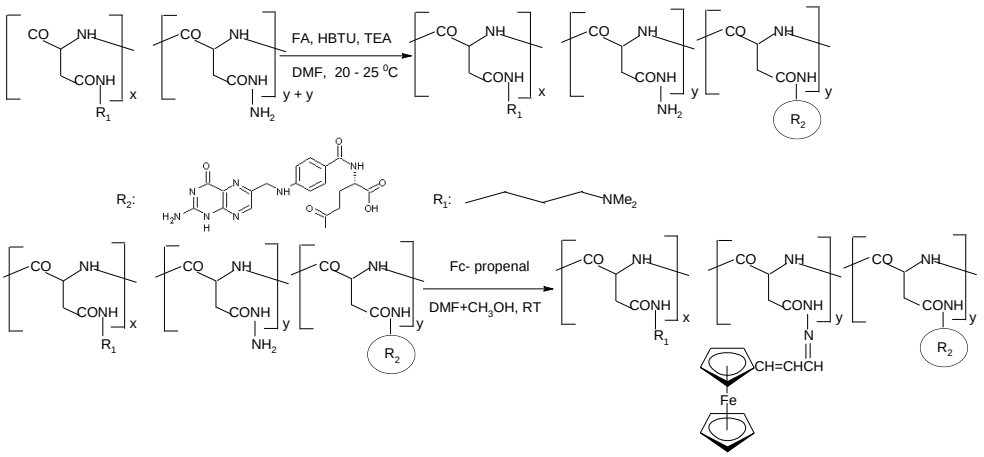

Scheme 18. 1: 2a (80)- FA- Fcp / 2a (90)- FA- Fcp

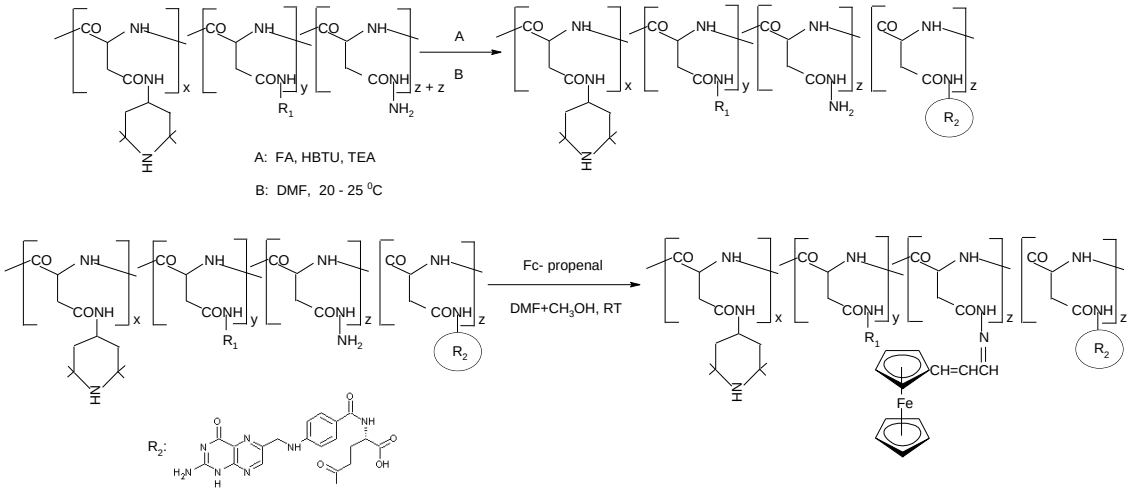

Scheme 18. 2: 4c (60) - Cur- Fcp

Scheme 3.17: *Synthesis of co-conjugates 2a(80)-FA-Fcp, 2a(90)-FA-Fcp and 4c(60)-Cur-Fcp*

Table 3.11: *Analytical data of drug-conjugates*

Conjugate Designation	Molar Ratios (carrier: 1 mole)		Reaction time & Temperature		Yield %	Base Molecular Mass [a]	η_{inh} [b] mL/g	x/y [c] (Fe; Z)	Drugs %			
	Drug 1	Drug 2	First Step	Second Step					% Fe Found [d]	% Fe Calcd [e]	% Z [d] Found [d]	% Z [d] Calcd [e]
2a (90)-FA-Fcp	0.5	0.8	1d, RT	3 d, 50^{0}C	47.8	2263.934	20.3	(1.12;1.07)	2.20	2.47	17.42	18.73
2a (80)-FA-Fcp	0.5	0.8	1d, RT	3 d, 50^{0}C	46.6	2616.990	22.4	(1.01;1.03)	2.11	2.13	15.79	16.20
4c (60)-Cur-Fcp	0.5	0.8	1d, RT	3 d, 50^{0}C	57.5	2818.964	23.8	(1.01;1.02)	1.96	1.98	11.68	11.92

[a] *Molecular mass of the simple recurring unit; structures normalized to y = 1*

[b] *At 30.0^0 C ± 0.5^0 C in distilled water; conc = 2mg/mL*

[c] *Drug content for complete incorporation of the drug*

[d] *Z = FA or Cur*

Table 3.12: ^{1}H NMR for selected PAsA co-conjugates

Conjugate Designation	% Fe			Protons counted[d] (expected)[e] chemical shift range δ (ppm)						
	calcd[a]	^{1}H NMR[b]	UV[c]	δ: 8.6-6.5	δ: 6.7-6.5	δ: 4.3-4.1	δ: 2.9-2.7 or [3.9-3.7]	δ: 2.3-2.1	δ: 1.8-1.6	δ: 1.2-0.9
2a (90)-FA-Fcp	2.47	2.20	2.38	2.8(3)	-	3.2(3.6)	-	53.8(54)	18.0(18)	-
2a (80)-FA-Fcp	2.13	2.11	2.10	3.9(4)	-	1.78(1.8)	7.8(8.0)	19.6(18)	7.5(8.0)	-
4c (60)-Cur-Fcp	1.98	1.96	1.96	-	1.76(1.8)	2.97(3.0)	[5.97(6)]	-	7.5(8)	54(54)

Conjugate Designation	% FA			% Cur		
	calcd[a]	^{1}H NMR[b]	UV[c]	calcd[a]	^{1}H NMR[b]	UV[c]
2a (90)-FA-Fcp	18.73	17.42	18.68	-	-	-
2a (80)-FA-Fcp	16.20	15.79	16.08	-	-	-
4c (60)-Cur-Fcp	-	-	-	11.92	11.68	11.80

a Mass percentage of Fe calculated for 100% acylation. *b Mass percentage of Fe derived from 1H NMR spectrum (error limit ± 15%).*

c Mass percentage derived from UV absorbance of bound Fc, Cur and FA in H_2O at 440 nm(ε =100 $cm^{-1}M^{-1}$), 430 nm (ε =2.5× 10^4 $cm^{-1}M^{-1}$), and 370nm (ε = 6500 $cm^{-1}M^{-1}$), respectively.

d In D_2O, pH 10-11, chemical shifts, δ/ppm, referenced against internal sodium 3-trimethylsilyl-2,2,3,3-d4-propionate; integration error limits ± 12 %.Protons are calculated for structural representations in Table 3.11.

e Expected count for composition in accordance with recurring unit.

3.3 Evaluation of the stability of hydrazone linkage at various pH

3.3.1 In vitro stability test at pH 7.4

To investigate the stability of the hydrazone linkage in aqueous solutions at neutral pH, 10 mg of conjugate's samples were dissolved in 20 mL of pH 7.4 phosphate buffer solution, and then placed in a stirred bath at 29 ^{0}C temperature, pH and agitation control (the pH was determined using a glass electrode). At appropriate intervals of time, each sample was filtered and the release medium was assayed spectrophotometrically at 440 nm in order to determine the amount of released drug. The non-bound ferrocenyl moieties are totally insoluble in water so that they cannot interfere with the reading of UV absorbance. The absorbance was converted to concentration using a calibration curve. All measurements were carried out in triplicate using samples prepared under the same conditions. The results agreed with each other within 6.25 % error.

3.3.2 In vitro released test at pH 6.5

To examine the instability of the carrier-drug bridge, 10 mg of conjugate samples were dissolved in 20 mL of pH 6.5 lactate buffer solution at room temperature, pH and agitation control. At appropriate intervals of time, each sample was filtered and the release medium was evaluated spectrophotometrically at 440 nm in order to determine the amount of released drug. The absorbance was converted to concentration using a calibration curve. All measurements were carried out in triplicate using samples prepared under the same conditions. The results agreed with each other within 12 % error. A similar experiment was performed at pH 5.5.

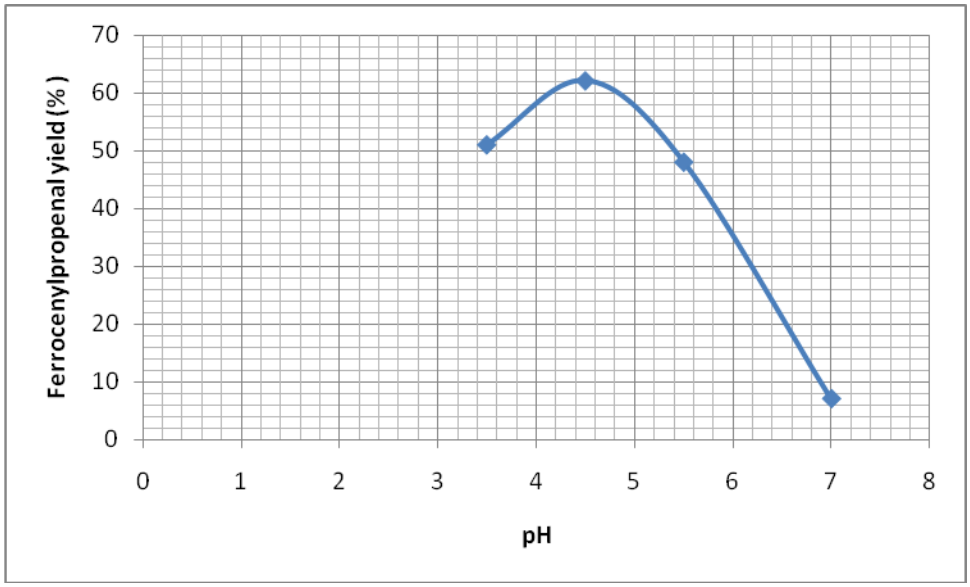

Figure 3.3 : Percentage of hydrazone formation at pH values from 3.5 to 7
(It was perfomed in 50 mM CH_3COOK buffer (acidic pH) and H_2O (neutral pH))

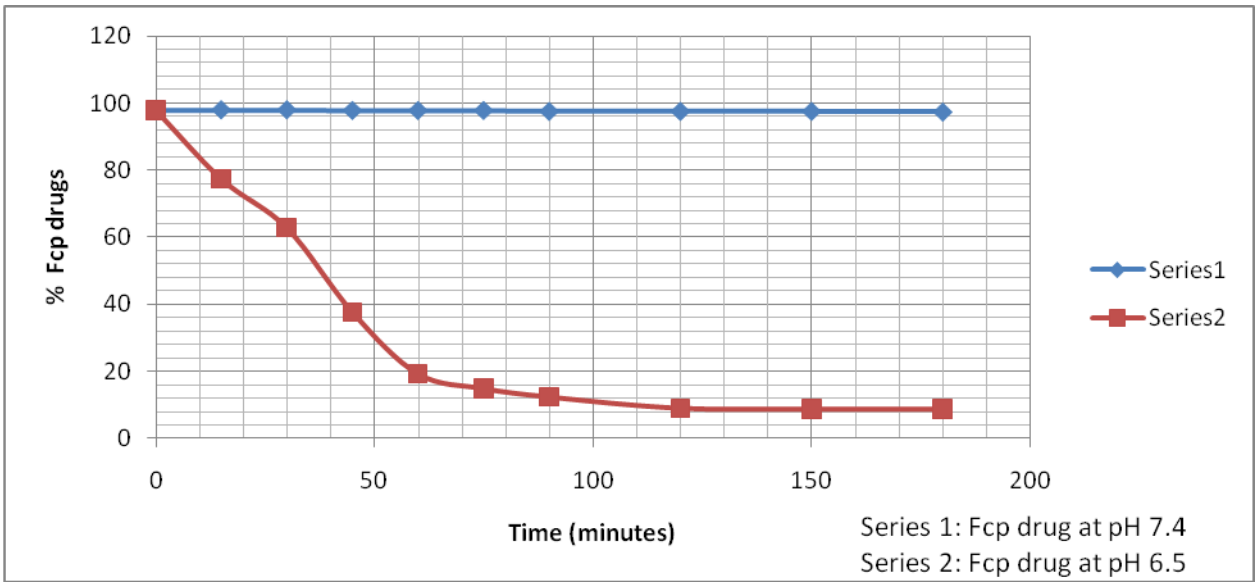

Figure 3.4: Fc-p concentration against time at neutral and acid pH

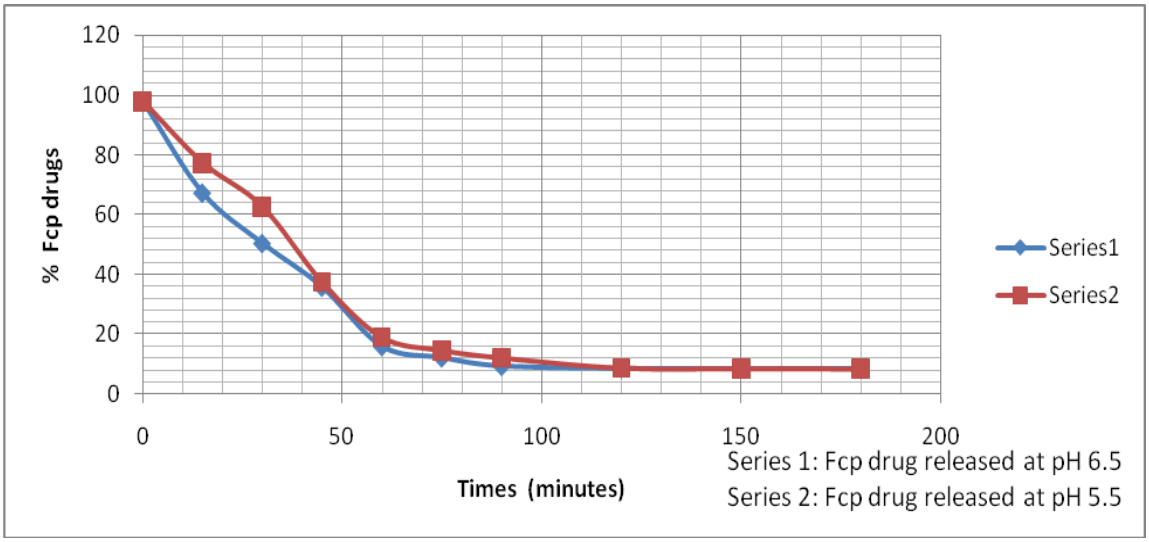

Figure 3.5: Fc-p concentration against time at different pH

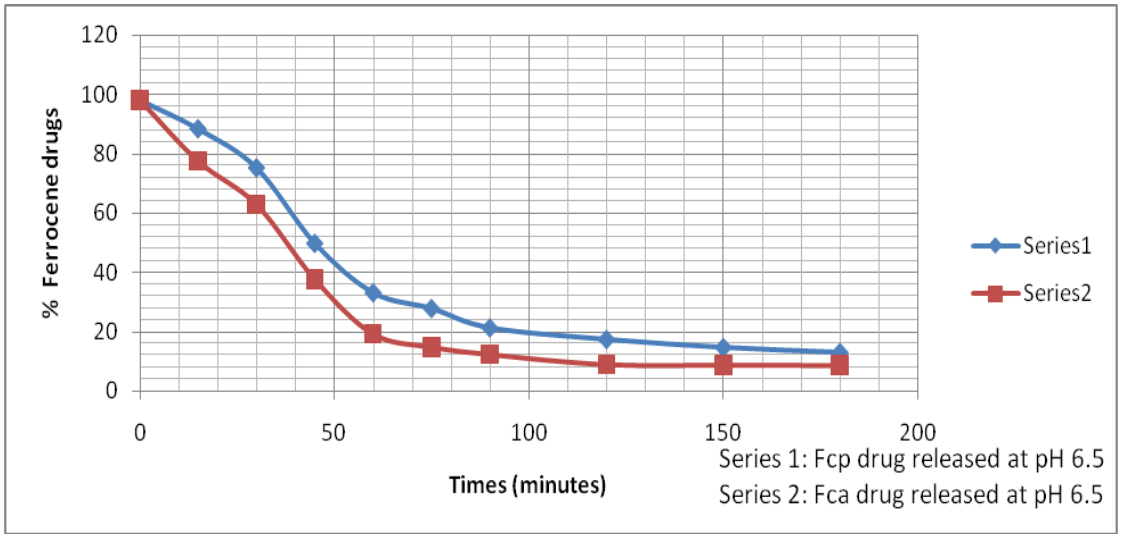

Figure 3.6: Release of aldehyde and ketone drugs at pH 6.5

3.3.3 Discussion:

The stability studies carried out in aqueous buffered medium revealed high stability under neutral conditions. The studies carried out in vitro release of ferrocenylpropenal at low pH, for different parameters (pH, drug concentration and times). It was shown that the hydrazone bridge was weak at cancer cell's pH; because significant amounts of ferrocenylpropenal are liberated at acidic pH (figure 3.6). The release rates of ferrocenyl drugs were faster with aldehyde than ketone-base. The release of drug from the conjugates incubated in a buffer at pH 5.5 was faster when compared with that at pH 6.5 (see figure 3.5). The delivery was more pronounced for aldehyde conjugates.

The hydrazone link is expected to be not only sensitive, but also generally chemoselective. The hydrazones are fairly stable under neutral conditions, and thus presumably in vivo. However, they are formed and cleaved under acidic conditions (equilibrium) [129]. This is in accordance with the chemoselectivity of hydrazone formation on a preparative scale as described in the literature[130-133]. The hydrazone formation between ferrocenylpropenal and hydrazine carriers showed high yields in an acidic pH range (figure 3.3). Low yield at neutral pH reflect the dependence of hydrazone formation on proton catalysis. It is important to note that hydrazone cleavage is also proton-catalyzed. The low labeling yield found under neutral condition can consequently be explained by the lack of catalyzing protons needed for effective hydrazone formation, which on the other hand accounts for the relatively high stability of hydrazones at neutral pH. The stability studies carried out in aqueous buffered medium revealed high stability under neutral conditions (blood pH) (see figure 3.4). Obviously, further studies have to be performed to evaluate the stability in vivo.

CHAPTER 4

EXPERIMENTAL

4.1. General Procedures

^{1}H NMR spectra (300 MHz or 400 MHz unless stated otherwise) were recorded on D_2O solutions. Chemical shifts, δ in ppm, were given relative to sodium 3-(trimethylsilyl)-2,2,3,3-d_4- propionate with δ= 0.00 ppm as internal standard (Integration error limits ±15%). In order to eliminate protonation effects, spectral sample solutions were adjusted to pD 10 – 11 with NaOH (unless stated otherwise).

Inherent viscosities, η_{inh}, were determined at 30.0 ± 0.5^{0}C in Cannon-Fenske viscometer tubes. Distilled water was used as solvent; the concentration was 0.2 g/100 mL, and the results, averages of three runs, are given in units of mL/g. Dialysis operations were performed with the aid of cellulose membranes tubing (Spectrum Industry Inc., Los Angeles, USA) of type Spectra/Por 4 (12 000 – 14 000 molecular mass cut-off limit), and type Spectra/Por 6 (25 000 molecular mass cut-off limit), against several batches of distilled water.

Freeze drying operations were perfomed with the aid of a Virtis Bench Top 3 freeze drier (operating at -40^{0}C, 10 – 15 Pa). The freeze-dried polymer samples were routinely subjected to a post-drying in an infrared drying apparatus and kept in a desiccator. Analytical samples of the conjugates were normally dried for 2 days at 50 – 60^{0}C under reduced pressure in an Abderhalden tube ($CaCl_2$ as a drying agent). Hydrazine determinations were made in German by Mr. W. Dindorf (microanalytisches laboratorium) and the hydrazone link was identified by solid-state IR. Melting points were obtained on sealed capillary tubes using the Gallenkamp apparatus.

4.2. Solvents and Reagents

Distilled water was used in washing the polymer after polymerization of D,L aspartic acid, precipitation of PSI-DCC and dialysis work. N,N'-dimethylformamide (DMF), freshly distilled under reduced pressure in a faint stream of N_2, with a fore-run of around 10% being discarded, was dried over molecular sieves 4Å prior to use. All additional solvents were laboratory grade, received from commercial sources.

The following reagents were used as received: 2-(2-aminoethoxy)ethanol (AEE), DL-aspartic acid, N,N'-dicyclohexylcarbodiimide (DCC), 4-amino-2,2,6,6-tetramethylpiperidine (ATP), diethylaminopropylamine (DEP), 3-(dimethylamino)propylamine (DMP), 2-dimethylaminoethylamine (DMEA), 2-diethylaminoethylamine (DEEA). Orthophosphoric acid (85 %) was also used as received (Fluka AG, Aldrich Chemie GmbH). Ferrocene (Strem Chemicals Inc.), methylene chloride, toluene, methanol, ethyl acetate, and acetone were pre-dried over molecular sieves 4 Å. Diethyl ether, ethanol, and petroleum ether were used as supplied (SAAR CHEM).

4.3. Experimental procedures

4.3.1. Preparation of ferrocenyl drugs

4.3.1.1. Ferrocenylpropenal: Freshly distilled boron trifluoride etherate (50 mL) was added drop-wise to a cooled solution prepared from ferrocene (20.00 g, 0.107 mol) and 1,1,3,3-tetramethoxypropane (20.00 g, 0.122 mol) in chloroform (400 mL) over a period of 0.5 hour, in nitrogen atmosphere. The purple solution was stirred at 2^oC for 15 minutes, than at room temperature for 1 hour and finally at 64^oC for an additional hour. The solution was poured into 100 mL of water and extracted three times with diethyl ether. The organic phase was washed with water until the aqueous phase reached pH 7, dried over magnesium sulfate and finally concentrated to red oil. Chromatographic treatment on a column (alumina activity 2) and elution with ether gave a major band of 3-ferrocenylpropenal. Several crops were collected and in total yield of 22.8 g (57%); mp 97 – 98^0C.

^{1}H NMR ($CDCl_3$), δ/ppm (expected proton counts in parentheses): 4.2 – 4.1, 9.1H (9H, **Fc**); 5.5 – 5.4, 1.9H (2H, **CHCH**CHO); 9.1 – 7.8, 0.9H (1H, CHCH**CH**O).

4.3.1.2. Acethylferrocene: Ferrocene (20 g, 0.107mol), acetyl chloride (70 mL) and phosphoric acid (20 mL) were mixted, and then heated in a 70 – 80^{o}C water bath for 15 minutes. Crushed ice of roughly equal volume was added, and the mixture was stirred until the ice melted, then the aqueous suspension was extracted with diethyl ether. The solution was dried over anhydrous K_2CO_3, and decanted into a clean flask. The formation of the product was checked by TLC (using ethyl acetate/hexane 1:1). The solution was concentrated and transferred, using Pasteur pipette, onto a chromatographic column. The orange-yellow fraction (starting material) and reddish fraction (acetylferrocene) was collected in different flasks. The product was crystallized with diethyl ether. Several crops were collected in a total yield of 61.2 %; mp 85 – 86^{0}C. TLC test: acetyferrocene R_f: 0.34 (starting material R_f: 0.80).

^{1}H NMR ($CDCl_3$), δ/ppm (expected proton counts in parentheses): 4.2 – 4.1, 8.8H (9H, **Fc**); 2.9 – 2.4, 3.2H (3H, CO**CH_3**).

4.3.2. Preparation of polymeric carriers

4.3.2.1. Poly-DL-succinimide

The Polysuccinimide (PSI) was prepared using the method of Neri and Antoni[121]. This method involved the polymerization of DL-aspartic acid in orthophosphoric acid at high temperature. The crude product, 62.70 g (72 %), was dissolved in DMF (231.35 mL), the solution was cooled. In order to achieve chain extension, the end carboxylic groups were coupled with N,N'-dicyclohexylcarbodiimide (DCC) (6.32 g) while the solution was stirred in a stoppered vessel at ice bath temperature for 4 hours; then at room temperature overnight (16 hours). The precipitated urea derivate was removed by centrifugation. The supernatant DMF solution was poured with stirring into cold water for precipitation of the polymeric product. Thorough washing with water for removal of DMF was followed by a drying process in an oven (65^{o}C) for 48 hours. Yield: 55.176 g (88 %); Inherent viscosity

(η_{inh}, determined in DMF): 52 mL/g. For the purpose of this project, the products with viscosities ranging from 46 – 54 mL/g from several preparations were combined.

4.3.2.2. Synthesis of copolyaspartamides

Carrier 2a (80): The designation 2**a (80)** indicates a (80:20) mole % ratio of DMP to Hy in the polymer product. 3-dimethylaminopropylamine (DMP) (2.452 g, 24 mmol) in N,N'-dimethylformamide (DMF) (10 mL) was added drop-wise, with rapid stirring, to polysuccinimide (2.910 g, 30 mmol) dissolved in DMF (20 mL). The solution was saturated under N_2 for 5 h at room temperature (RT). Then PSI-DMP was added drop-wise to the stirred solution of hydrazine hydrate (Hy) (0.901 g, 18 mmol) in DMF (30 mL), cooled in an ice bath. Re-saturated with N_2, the solution was stirred for 40 hours in an ice bath and another 5 hours at ambient temperature. The solution was concentrated on rotary-evaporator (bath 60-65^{0}C) to approximately 20 mL. The polymer product was precipitated from solution with diethyl ether (Et_2O):Hexane (2:1), and the precipitate washed with hot toluene and acetone, and redissolved in H_2O (40 mL). The pH was adjusted from pH~12 to pH~7.0 with conc. HCl. The solution was dialyzed successively for 2 days in Spectra/Por 4 and another 2 days in Spectra/Por 6 tubing. The water-soluble polymer was then freeze-dried, post-dried, and kept in a desiccator. The yield of the post-dried polymer was 4.516 g (72.1 %), and η_{inh} = 8.4 mL/g.

^{1}H NMR (D_2O), δ/ppm (expected proton counts in parentheses): 1.7 – 1.5, 8.5H (8H, $CONHCH_2\mathbf{CH_2}CH_2NMe_2$); 2.3 – 2.1, 24H (24H, $N\mathbf{Me_2}$); 2.4 – 2.3, 7.1H (8H, $\mathbf{CH_2}NMe_2$); 2.8 – 2.6, 7.8H (8H, $\mathbf{CH_2}CONH$); 3.3 – 3.1, 8.1H (8H, $CONH\mathbf{CH_2}$).

Carrier 2b (80): By a similar procedure as before 2-(dimethylamino)ethylamine (DMEA) (2.116 g, 24 mmol) in DMF (5 mL) was added to polysuccinimide (2.910 g, 30 mmol) dissolved in DMF (15 mL). The solution was saturated with N_2 and stirred for 5h, thereafter the solution was added drop-wise to the stirred Hy (0.901 g, 18 mmol) in DMF (30 mL), cooled in an ice bath; then the final solution was re-saturated with N_2 and stirred for 40 hours in an ice bath and another 5 hours at ambient temperature. Further work-up as before resulted in the copolymer **2b (80)** in a yield of 3.823 g (64.5 %), and η_{inh} = 10.6 mL/g.

^{1}H NMR (D_2O), δ/ppm (expected proton counts in parentheses): 2.3 – 2.1, 24H (24H, N**Me$_2$**); 2.4 – 2.3, 8.1H (8H, **CH$_2$**NMe_2); 2.8 – 2.6, 7.7H (8H, **CH$_2$**CONH); 3.3 – 3.1, 8.5H (8H, CONH**CH$_2$**).

Carrier 2c (80): The same reaction conditions, procedure and stoichiometry as used for the preparation of carrier **2a (80)** were adopted. 3-Diethylaminopropylamine (DEP) (3.126 g, 24 mmol) in DMF (8 mL) was added to polysuccinimide (2.910 g, 30 mmol) dissolved in DMF (15 mL). The solution was saturated with N_2 and stirred for 5 h, thereafter it was added drop-wise to the stirred solution of Hy (0.901 g, 18 mmol) in DMF (30 mL) (cooled in an ice bath); the final solution was re-saturated with N_2 and stirred for 40 hours in an ice bath and another 5 hours at ambient temperature. Conventional work-up gave the copolymer **2c (80)** in a yield of 4.106 g (59.2 %), and with η_{inh} = 11.9 mL/g.

^{1}H NMR (D_2O), δ/ppm (expected proton counts in parentheses): 1.1 – 0.9, 19.6 (24H, $CH_2N(CH_2$**CH$_3$**$)_2$); 1.7 – 1.5, 7.7H (8H, CONHCH_2**CH$_2$**CH_2NEt_2); 2.7 – 2.5, 24H (24H, **CH$_2$**N(**CH$_2$**$CH_3)_2$); 2.9 – 2.7, 8.1H (8H, **CH$_2$**CONH); 3.4 – 3.2, 8.2H (8H, CONH**CH$_2$**).

Carrier 2d (80): By the procedure leading to copolymer **2a (80)**, polysuccinimide (2.910 g, 30 mmol) in DMF (15 mL), was treated with 2(diethylamino)ethylamine (DEEA) (2.789 g, 24 mmol). Then the solution was added drop-wise to the stirred solution of hydrazine hydrate (Hy) (0.901 g, 18 mmol) in DMF (30 mL), cooled in an ice bath. Re-saturated with N_2, the solution was stirred for 40 hours in an ice bath and another 5 hours at ambient temperature. The resultant solution was treated and worked up as before, giving 4.184 g (63.3 %) of **2d (80)** as a water soluble solid. η_{inh} = 11.2 mL/g.

^{1}H NMR (D_2O), δ/ppm (expected proton counts in parentheses): 1.2 – 0.9, 24H (24H, $CH_2N(CH_2$**CH$_3$**$)_2$); 2.7 – 2.5, 24.1H (24H, **CH$_2$**N(**CH$_2$**$CH_3)_2$); 2.9 – 2.7, 7.4H (8H, **CH$_2$**CONH); 3.4 – 3.2, 8.1H (8H, CONH **CH$_2$**).

Carrier 2e (80): Following the same procedure as above, polysuccinimide (2.910 g, 30 mmol) in DMF (15 mL) was treated with 4-amino-2,2,6,6 tetramethylpiperidine (ATP) (3.750 g, 24 mmol) in DMF (8 mL) in the first step, and in the second step the solution

was added drop-wise to the stirred solution of hydrazine hydrate (Hy) (0.901 g, 18 mmol) in DMF (30 mL), cooled in an ice bath. The resulting solution was re-saturated with N_2 and stirred for 40 hours in an ice bath and another 5 hours at ambient temperature, and conventional work-up resulted in a water-soluble polymer, **2e (80)**, in a yield of 4.438 g (58.7 %). η_{inh} = 14.0 mL/g.

^{1}H NMR (D_2O), δ/ppm (expected proton counts in parentheses):1.2 – 0.9, 48H (48H, [C(**CH_3)$_2$**]NH); 1.5 – 1.3, 16H (16H, CONHCH(**CH_2)$_2$**); 2.9 – 2.7, 7.5H (8H, **CH_2**CONH); 4.1 – 4.0, 3.94H (4H, CONH**CH**).

Carrier 2f (80): By a similar procedure as above, 2-(2-aminoethoxy)ethanol (AEE) (2.523 g, 24 mmol) in DMF (5 mL) was added to polysuccinimide (2.910g, 30 mmol) dissolved in DMF (15 mL). The solution saturated with N_2 and stirred for 5 h, thereafter the solution was added drop-wise to the stirred solution of hydrazine hydrate (Hy) (0.901 g, 18 mmol) in DMF (30 mL), cooled in an ice bath. The resulting solution was re-saturated with N_2 and stirred for 40 hours in an ice bath and another 5 hours at ambient temperature. Conventional work-up gave copolymer **2f (80)** in a yield of 3.743 g (59.1 %). η_{inh} = 9.6 mL/g.

^{1}H NMR (D_2O), δ/ppm (expected proton counts in parentheses): 2.8 – 2.6, 7.8H (8H, **CH_2**CONH); 3.5 – 3.1, 7.9H (8H, CONH**CH_2**); 3.8 – 3.5, 24H (24H, **CH_2**O**CH_2CH_2**OH).

Carrier 2a (90): The same basic procedure was used to prepare this carrier. Polysuccinimide (2.910 g, 30 mmol) in DMF (15 mL) was treated with DMP (2.759 g, 27 mmol) in DMF (5 mL), thereafter the solution was added drop-wise to the stirred solution of Hy (0.450 g, 9 mmol) in DMF (15 mL), cooled in an ice bath; the solution was then re-saturated with N_2 and stirred for 40 hours in an ice bath and another 5 hours at ambient temperature, and this resulted in a water-soluble polymer, **2a (90)**, in a yield of 3.788 g (61.9 %). η_{inh} = 8.1 mL/g.

^{1}H NMR (D_2O), δ/ppm (expected proton counts in parentheses): 1.7 – 1.5, 18.5H (18H, $CONHCH_2\mathbf{CH_2}CH_2NMe_2$); 2.3 – 2.1, 54.6H (54H, $N\mathbf{Me_2}$); 2.4 – 2.3, 16.3H (18H, $\mathbf{CH_2}NMe_2$); 2.8 – 2.6, 18.7H (18H, $\mathbf{CH_2}CONH$); 3.3 – 3.1, 18H (18H, $CONH\mathbf{CH_2}$).

Carrier 2b (90): By a similar procedure as before 2-(dimethylamino)ethylamine (DMEA) (2.380 g, 27 mmol) in DMF (5 mL) was added to polysuccinimide (2.910 g, 30 mmol) dissolved in DMF (15 mL). The solution was saturated with N_2 and stirred for 5h, thereafter the solution was added drop-wise to the stirred solution of Hy (0.450 g, 9 mmol) in DMF (15 mL), cooled in an ice bath; the final solution was re-saturated with N_2 and stirred for 40 hours in an ice bath and another 5 hours at ambient temperature. This resulted in the copolymer **2b (90)** in a yield of 3.461 g (60.3 %), and η_{inh} = 9.1 mL/g.

^{1}H NMR (D_2O), δ/ppm (expected proton counts in parentheses): 2.3 – 2.1, 54H (54H, $N\mathbf{Me_2}$); 2.4 – 2.3, 18.5H (18H, $\mathbf{CH_2}NMe_2$); 2.8 – 2.6, 18.8H (18H, $\mathbf{CH_2}CONH$); 3.3 – 3.1, 18.8H (18H, $CONH\mathbf{CH_2}$).

Carrier 2c (90): The same procedure used in carrier **2a (80)** was adopted. 3-Diethylaminopropylamine (DEP) (3.516 g, 27 mmol) in DMF (8 mL) was added to polysuccinimide (2.910 g, 30 mmol) dissolved in DMF (15 mL). The solution saturated with N_2 and stirred for 5 h, thereafter the solution was added drop-wise to the stirred solution of Hy (0.450 g, 9 mmol) in DMF (15 mL), cooled in an ice bath; the final solution was re-saturated with N_2 and stirred for 40 hours in an ice bath and another 5 hours at ambient temperature. This gave the copolymer **2c (90)** in a yield of 4.098 g (59.6 %), and η_{inh} = 10.3 mL/g.

^{1}H NMR (D_2O), δ/ppm (expected proton counts in parentheses): 1.3 – 0.9, 54 (54H, $CH_2N(CH_2\mathbf{CH_3})_2$); 1.7 – 1.5, 17.7H (18H, $CONHCH_2\mathbf{CH_2}CH_2NEt_2$); 2.7 – 2.5, 52.7H (54H, $\mathbf{CH_2}N(\mathbf{CH_2}CH_3)_2$); 2.9 – 2.7, 18.2H (18H, $\mathbf{CH_2}CONH$); 3.4 – 3.2, 18.4H (18H, $CONH\mathbf{CH_2}$).

Carrier 2d (90): By the procedure leading to copolymer **2a (80)**, polysuccinimide (2.910 g, 30 mmol) in DMF (15 mL), was treated with 2(diethylamino)ethylamine (DEEA) (3.138 g, 27 mmol). Then PSI-DEEA solution was added drop-wise to the stirred solution of hydrazine hydrate (Hy) (0.450 g, 9 mmol) in DMF (15 mL), cooled in an ice bath. Re-

saturated with N_2, the resultant solution was stirred for 40 hours in an ice bath and another 5 hours at ambient temperature. The resultant solution was treated and worked up as before, giving 4.412 g (67.9 %) of **2d (90)** as a water soluble solid. η_{inh} = 9.6 mL/g.

^{1}H NMR (D_2O), δ/ppm (expected proton counts in parentheses): 1.2 – 0.9, 54H (54H, $CH_2N(CH_2\mathbf{CH_3})_2$); 2.7 – 2.5, 53.3H (54H, $\mathbf{CH_2}N(\mathbf{CH_2}CH_3)_2$); 2.9 – 2.7, 19.1H (18H, $\mathbf{CH_2}$CONH); 3.4 – 3.2, 19.1H (18H, CONH$\mathbf{CH_2}$).

Carrier 2e (90): Following the same procedure as above, polysuccinimide (2.910 g, 30 mmol) in DMF (15 mL) was treated with 4 amino 2,2,6,6 tetramethylpiperidine (ATP) (4.219 g, 27 mmol) in DMF (8 mL) in the first step, and in the second step the PSI-ATP solution was added drop-wise to the stirred solution of hydrazine hydrate (Hy) (0.450 g, 9 mmol) in DMF (15 mL), cooled in an ice bath. The solution was re-saturated with N_2, the resultant solution was stirred for 40 hours in an ice bath and another 5 hours at ambient temperature, and this resulted in a water-soluble polymer, **2e (90)**, in a yield of 5.813 g (76.7 %). η_{inh} = 13.1 mL/g.

^{1}H NMR (D_2O), δ/ppm (expected proton counts in parentheses):1.2 – 0.9, 108H (108H, [C($\mathbf{CH_3}$)$_2$]NH); 1.5 – 1.3, 15.3H (16H, CONHCH($\mathbf{CH_2}$)$_2$); 4.1 – 4.0, 7.8H (9H, CONH**CH**).

Carrier 2f (90): By a similar experimental procedure as before, 2-(2-aminoethoxy)ethanol (AEE) (2.839 g, 27 mmol) in DMF (5 mL) was added to polysuccinimide (2.910g, 30 mmol) dissolved in DMF (15 mL). The solution saturated with N_2 and stirred for 5 h, was added drop-wise to the stirred solution of hydrazine hydrate (Hy) (0.450 g, 9 mmol) in DMF (15 mL), cooled in an ice bath. The resultant solution was re-saturated with N_2 and stirred for 40 hours in an ice bath and another 5 hours at ambient temperature. This resulted in the copolymer **2f (90)** in a yield of 3.608 g (58.2 %). η_{inh} = 8.9 mL/g.

^{1}H NMR (D_2O), δ/ppm (expected proton counts in parentheses): 2.9 – 2.6, 17.4H (18H, $\mathbf{CH_2}$CONH); 3.5 – 3.3, 19.3H (18H, CONH$\mathbf{CH_2}$); 3.7 – 3.5, 54H (54H, $\mathbf{CH_2}O\mathbf{CH_2CH_2}$OH).

4.3.2.3. Synthesis of terpolyaspartamides

Carrier 3a (60): To the stirred solution of polysuccinimide (1.500 g, 15.5 mmol) in DMF (10 mL), AEE (0.325 g, 3.09 mmol) in DMF (2 mL) was added drop-wise. The solution was saturated with N_2 and stirred for 1day at room temperature, thereafter DMP (0.9481 g, 9.28 mmol) in DMF (5 mL) was added drop-wise to this solution. Resaturated with N_2, the mixture was stirred for 5 h at room temperature (RT). Then the solution was added drop-wise to the stirred solution of hydrazine hydrate (Hy) (0.4645 g, 9.278 mmol) in DMF (10 mL), cooled in an ice bath. Re-saturated with N_2, the solution was stirred for 40 hours in an ice bath and another 5 hours at ambient temperature. The solution was concentrated on rotary-evaporator (bath 60-65^{0}C) to approximately 20 mL. The polymer product was precipitated from solution with diethyl ether (Et_2O):Hexane (2:1), and the precipitate washed with hot toluene and acetone, and redissolved in H_2O (40 mL). The pH was adjusted from 12 to 7.0 with conc. HCl. The solution was dialyzed successively for 2 days in Spectra/Por 4 and another 2 days in Spectra/Por 6 tubing. Freeze-drying of the retentate and IR post-drying gave 1.852 g (57.2 %) of water-soluble **3a (60)**. η_{inh} = 12.6 mL/g.

^{1}H NMR (D_2O), δ/ppm (expected proton counts in parentheses): 1.7 – 1.5, 5.9H (6H, CONHCH$_2$**CH$_2$**CH$_2$NMe$_2$); 2.5 – 2.1, 24H (24H, N**Me$_2$**; **CH$_2$**NMe$_2$); 3.4 – 3.2, 8.1H (8H, CONH**CH$_2$**); 3.7 – 3.5, 6.6H (6H, **CH$_2$**O**CH$_2$CH$_2$**OH).

Carrier 3b (60): Following the same procedure as above, polysuccinimide (1.500 g, 15.464 mmol) in DMF (15 mL), was reacted with AEE (0.325 g, 3.09 mmol) in DMF (2 mL), and DMEA (0.818 g, 9.278 mmol) in DMF (5 mL) was then added, and the mixture was treated and worked up as before, giving 2.042 g (65.7 %) of **3b (60)** as a water-soluble solid. η_{inh} = 12.9 mL/g.

^{1}H NMR (D_2O), δ/ppm (expected proton counts in parentheses): 2.5 – 2.1, 21.7H (24H, N**Me$_2$**; **CH$_2$**NMe$_2$); 3.4 – 3.2, 8H (8H, CONH**CH$_2$**); 3.7 – 3.5, 6.4H (6H, **CH$_2$**O**CH$_2$CH$_2$**OH).

Carrier 3c (60): By the procedure leading to **3a (60)**, this carrier was prepared from polysuccinimide (1.500g, 15.464 mmol) dissolved in DMF (15 mL), in which AEE(0.325 g, 3.09 mmol) in DMF (2 mL) was added dropwise, and then DEP (1.208 g, 9.278 mmol) dissolved in DMF (5 mL) was then added to the mixture. The final mixture was added to the hydrazine solution, giving 2.392 g (68.4 %) of **3c (60)** as a water-soluble solid. η_{inh} = 13.1 mL/g.

^{1}H NMR (D_2O), δ/ppm (expected proton counts in parentheses): 1.2 – 0.9, 17.9H (18H, $CH_2N(CH_2\mathbf{CH_3})_2$; 1.7 – 1.5, 5.8H (6H, $CONHCH_2\mathbf{CH_2}CH_2NEt_2$); 2.7 – 2.5, 18.3H (18H, $\mathbf{CH_2}N(\mathbf{CH_2}CH_3)_2$); 3.4 – 3.2, 8.8H (9H, $CONH\mathbf{CH_2}$); 3.7 – 3.5, 6H (6H, $\mathbf{CH_2}O\mathbf{CH_2CH_2}OH$) .

Carrier 3d (60): Following the same procedure as above, AEE (0.325 g, 3.09 mmol) in DMF (2 mL) was added dropwise to polysuccinimide (1.500 g, 15.464 mmol) in DMF (15 mL); thereafter DEEA (1.078 g, 9.278 mmol) was added to the solution,and mixture was treated and worked up as before, giving 1.950 g (57.9 %) of **3d (60)** as a water soluble-solid. η_{inh} = 13.2 mL/g.

^{1}H NMR (D_2O), δ/ppm (expected proton counts in parentheses): 1.2 – 0.9, 18H (18H, $CH_2N(CH_2\mathbf{CH_3})_2$; 2.7 – 2.5, 18.1H (18H, $\mathbf{CH_2}N(\mathbf{CH_2}CH_3)_2$); 3.4 – 3.2, 7.7H (9H, $CONH\mathbf{CH_2}$); 3.7 – 3.5, 5.1H (6H, $\mathbf{CH_2}O\mathbf{CH_2CH_2}OH$) .

Carrier 3e (60): By an analogous procedure described in the previous experiment, AEE (0.325 g, 3.09 mmol) in DMF (2 mL) was added dropwise to polysuccinimide (1.500 g, 15.464 mmol) in DMF (15 mL), and allowed to react for 1 day. Re-saturated with N_2, ATP (1.450 g, 9.278 mmol) was then added and the solution allowed to react for another day. The solution was treated and worked up as before, giving 2.659 g (71.1 %) of **3e (60)** as a water-soluble solid. η_{inh} = 15.9 mL/g.

^{1}H NMR (D_2O), δ/ppm (expected proton counts in parentheses): 1.5 – 0.9, 46.2H (48H, $NH[C(\mathbf{CH_3})_2]_2$; $CONHCH(\mathbf{CH_2})_2$); 3.4 – 3.2, 1.8H (2H, $CONH\mathbf{CH_2}$); 3.8 – 3.5, 6H (6H, $\mathbf{CH_2}O\mathbf{CH_2CH_2}OH$); 4.1 – 4.0, 2.5H (3H, $CONH\mathbf{CH}$). .

Carrier 3a (50): By the procedure leading to **3a (60)**, this carrier was prepared from polysuccinimide (1.500 g, 15.464 mmol) in DMF (15 mL), treated with AEE (0.650 g, 6.19 mmol) in DMF (4 mL). Re-saturated with N_2, DMP (0.790 g, 7.732 mmol) was then added to the solution. Then hydrazine hydrate (Hy) (0.232 g, 4,639 mmol) in DMF (10 mL) was added drop-wise to the stirred solution cooled in an ice bath. Re-saturated with N_2, the solution was stirred for 40 hours in an ice bath and another 5 hours at ambient temperature. The solution was treated and worked up as before, giving 1.884 g (59.4 %) of **3a (50)** as a water-soluble solid. η_{inh} = 13.8 mL/g.

^{1}H NMR (D_2O), δ/ppm (expected proton counts in parentheses): 1.7 – 1.5, 7.8H (8H, $CONHCH_2\mathbf{CH_2}CH_2NMe_2$); 2.5 – 2.1, 32H (32H, $N\mathbf{Me_2}$; $\mathbf{CH_2}NMe_2$); 3.3 – 3.1, 19.8H (18H, $CONH\mathbf{CH_2}$); 3.7 – 3.5, 26.8H (30H, $\mathbf{CH_2}O\mathbf{CH_2CH_2}OH$).

Carrier 3b (50): By an analogous procedure described in the forgoing experiment, polysuccinimide (1.5 g, 15.464 mmol) in DMF (15 mL), was reacted with AEE (0.650 g, 6.190 mmol) in DMF (4mL). DMEA (0.682 g, 7.732 mmol) in DMF (5 mL) was then added; 5 hours later hydrazine hydrate (Hy) (0.2322 g, 4.639 mmol) in DMF (15 mL) was added drop-wise to the stirred solution cooled in an ice bath. Re-saturated with N_2, the solution was stirred for 40 hours in an ice bath and another 5 hours at ambient temperature; and the mixture was treated and worked up as before, giving 2.031 g (66.3 %) of **3b (50)** as a water-soluble solid. η_{inh} = 13.8 mL/g.

^{1}H NMR (D_2O), δ/ppm (expected proton counts in parentheses): 2.5 – 2.1, 13.9H (32H, $N\mathbf{Me_2}$; $\mathbf{CH_2}NMe_2$); 2.8 – 2.6, 15.7H (18H, $\mathbf{CH_2}CONH$), 3.3 – 3.1, 18.7H (18H, $CONH\mathbf{CH_2}$); 3.7 – 3.5, 30H (30H, $\mathbf{CH_2}O\mathbf{CH_2CH_2}OH$).

Carrier 3c (50): The same conditions and procedure used in the preparation of **3a (60)** were adopted in the synthesis of **3c (50).** AEE (0.650 g, 6.190 mmol) in DMF (4 mL) was added dropwise to polysuccinimide (1.500 g, 15.464 mmol) in DMF (15 mL), and allowed to react for 1 day. Re-saturated with N_2, DEP (1.208 g, 9.278 mmol) in DMF (5mL) was then added to the resultant solution; 5 hours later hydrazine hydrate (Hy) (0.2322 g, 4.639

mmol) in DMF (15 mL) was added drop-wise to the stirred solution cooled in an ice bath. Re-saturated with N_2, the solution was stirred for 40 hours in an ice bath and another 5 hours at ambient temperature. This resulted in the terpolymer **3c (50)** in a yield of 2.197 g (61.2 %). η_{inh} = 14.2 mL/g.

^{1}H NMR (D_2O), δ/ppm (expected proton counts in parentheses): 1.2 – 0.9, 25.2H (24H, $CH_2N(CH_2\mathbf{CH_3})_2$; 1.7 – 1.5, 9.1H (8H, $CONHCH_2\mathbf{CH_2}CH_2NEt_2$); 2.7 – 2.5, 26H (24H, $\mathbf{CH_2}N(\mathbf{CH_2}CH_3)_2$); 3.4 – 3.2, 20.5H (18H, $CONH\mathbf{CH_2}$); 3.7 – 3.5, 30H (30H, $\mathbf{CH_2}O\mathbf{CH_2CH_2}OH$) .

Carrier 3d (50): By a similar experimental procedure described before, 2-(2-aminoethoxy)ethanol (AEE) (0.650 g, 6.190 mmol) in DMF (4 mL) was added dropwise to polysuccinimide (1.500 g, 15.464 mmol) dissolved in DMF (15 mL). The solution saturated with N_2 and stirred for 24 hours. DEEA (0.898 g, 7.732 mmol) in DMF (5 mL) was then added to the solution, 5 hours later hydrazine hydrate (Hy) (0.2322 g, 4.639 mmol) in DMF (15 mL) was added drop-wise to the stirred solution cooled in an ice bath. Re-saturated with N_2, the solution was stirred for 40 hours in an ice bath and another 5 hours at ambient temperature. This resulted in the terpolymer **3d (50)** in a yield of 1.948 g (59.4 %). η_{inh} = 15.2 mL/g.

^{1}H NMR (D_2O), δ/ppm (expected proton counts in parentheses): 1.2 – 0.9, 21H (24H, $CH_2N(CH_2\mathbf{CH_3})_2$; 2.9 – 2.5, 42H (42H, $\mathbf{CH_2}N(\mathbf{CH_2}CH_3)_2$; $\mathbf{CH_2}CONH$); 3.4 – 3.2, 19.4H (19H, $CONH\mathbf{CH_2}$); 3.7 – 3.5, 30H (30H, $\mathbf{CH_2}O\mathbf{CH_2CH_2}OH$) .

Carrier 3e (50): By the procedure leading to **3a (60)**, this carrier was prepared from polysuccinimide (1.5 g, 15.464 mmol) dissolved in DMF (15 mL), treated with AEE (0.650 g, 6.190 mmol) in DMF (4 mL). ATP (1.208 g, 7.732 mmol) dissolved in DMF (5 mL) was then added to the solution; 5 hours later hydrazine hydrate (Hy) (0.2322 g, 4.639 mmol) in DMF (15 mL) was added drop-wise to the stirred solution cooled in an ice bath. Re-saturated with N_2 and stirred for 40 hours in an ice bath and another 5 hours at ambient temperature. This resulted in the terpolymer **3e (50)** in a yield of 2.416 g (67.3 %). η_{inh} = 18.1 mL/g.

^{1}H NMR (D_2O), δ/ppm (expected proton counts in parentheses): 1.5 – 0.9, 66.4H (64H, NH[C(**CH_3**)$_2$]$_2$; CONHCH(**CH_2**)$_2$); 3.4 – 3.2, 9.5H (10H, CONH**CH_2**); 3.8 – 3.5, 30H (30H, **CH_2**O**CH_2CH_2**OH); 4.1 – 4.0, 3.98H (4H, CONH**CH**).

Carrier 4a (60): To the stirred solution of polysuccinimide (1.980 g, 20.41 mmol) in DMF (10 mL), ATP (1.914 g, 12.25 mmol) in DMF (4 mL) was added drop-wise. The solution was saturated with N_2 and stirred for 1day at room temperature, thereafter DMP (0.420 g, 4.082 mmol) in DMF (2 mL) was added drop-wise to this solution. Re-saturated with N_2, the mixture was stirred for 5 h at room temperature (RT). Then hydrazine hydrate (Hy) (0.6131 g, 12.25 mmol) in DMF (10 mL) was added drop-wise to the stirred solution cooled in an ice bath. Re-saturated with N_2, the solution was stirred for 40 hours in an ice bath and another 5 hours at ambient temperature. The solution was concentrated on rotary-evaporator (bath 60-65^{0}C) to approximately 20 mL. The polymer product was precipitated from solution with diethyl ether (Et_2O):Hexane (2:1), and the precipitate washed with hot toluene and acetone, and redissolved in H_2O (40 mL). The pH was adjusted from 12 to 7.0 with conc. HCl. The solution was dialyzed successively for 2 days in Spectra/Por 4 and another 2 days in Spectra/Por 6 tubing. Freeze-drying of the retentate and IR post-drying gave 3.276 g (66.5 %) of water-soluble **4a (60)**. η_{inh} = 20.8 mL/g.

^{1}H NMR (D_2O), δ/ppm (expected proton counts in parentheses): 1.5 – 0.9, 48H (48H, NH[C(**CH_3**)$_2$]$_2$; CH(**CH_2**)$_2$); 1.7 – 1.5, 2.3H (2H, CONHCH$_2$**CH_2**CH_2NMe_2); 2.3 – 2.1, 6.4H (6H, N**Me_2**); 2.4 – 2.3, 2.4(2H, **CH_2**NMe_2); 3.3 – 3.1, 2.3H (2H, CONH**CH_2**); 4.1 – 4.0, 2.9H (3H, CONH**CH**).

Carrier 4b (60): By a similar procedure as before 2-(dimethylamino)ethylamine DMEA (0.360 g, 4.082 mmol) in DMF (2 mL) was added drop-wise to the stirred mixture of polysuccinimide (1.980 g, 20.41 mmol) and ATP (1.914 g, 12.25 mmol). The solution was saturated with N_2 and stirred for 5h, thereafter Hy (0.6131 g, 12.25 mmol) in DMF (10 mL) was added drop-wise to the stirred solution cooled in an ice bath, the solution re-saturated with N_2 and stirred for 40 hours in an ice bath and another 5 hours at ambient

temperature. This resulted in the terpolymer **4b (60)** in a yield of 2.993 g (61.5 %), and η_{inh} = 19.3 mL/g.

^{1}H NMR (D_2O), δ/ppm (expected proton counts in parentheses): 1.5 – 0.9, 48H (48H, NH[C(**CH_3**)$_2$]$_2$; CH(**CH_2**)$_2$); 2.3 – 2.1, 6.7H (6H, N**Me_2**); 2.4 – 2.3, 2.5(2H, **CH_2**NMe_2); 3.3 – 3.1, 2.5H (2H, CONH**CH_2**); 4.1 – 4.0, 2.5H (3H, CONH**CH**).

Carrier 4c (60): Same reaction conditions, procedure and stoichiometry used in carrier **4a (60)** was adopted. 3-diethylamino propylamine DEPA (0.532 g, 4.082 mmol) in DMF (2 mL) was added drop-wise to the stirred mixture of polysuccinimide (1.980 g, 20.41 mmol) and ATP (1.914 g, 12.25 mmol). The solution saturated with N_2 and stirred for 5 h, thereafter Hy (0.6131 g, 12.25 mmol) in DMF (10 mL) was added drop-wise to the stirred solution cooled in an ice bath, the solution re-saturated with N_2 and stirred for 40 hours in an ice bath and another 5 hours at ambient temperature. This gave the terpolymer **4c (60)** in a yield of 2.741 g (54.4 %), and η_{inh} = 21.6 mL/g.

^{1}H NMR (D_2O), δ/ppm (expected proton counts in parentheses): 1.5 – 0.9, 54H (54H, $CH_2N(CH_2$**CH_3**$)_2$; NH[C(**CH_3**)$_2$]$_2$; CH(**CH_2**)$_2$); 1.7 – 1.5, 2.5H (2H, CONHCH_2**CH_2**CH_2NEt_2); 2.7 – 2.5, 6.3H (6H, **CH_2**N(**CH_2**CH_3)$_2$); 3.3 – 3.1, 1.9H (2H, CONH**CH_2**); 4.1 – 4.0, 3H (3H, CONH**CH**).

Carrier 4d (60): By the procedure leading to terpolyaspartamide **4a (60)**, A mixture of polysuccinimide (1.980 g, 20.41 mmol) and ATP (1.914 g, 12.25 mmol) in DMF, was treated with 2(diethylamino)ethylamine DEEA (0.474 g, 4.082 mmol). Then hydrazine hydrate (Hy) (0.6131 g, 12.25 mmol) in DMF (10 mL) was added drop-wise to the stirred solution cooled in an ice bath. Re-saturated with N_2, the solution was stirred for 40 hours in an ice bath and another 5 hours at ambient temperature. The resultant solution was treated and worked up as before, giving 2.774 g (55.7 %) of **4d (60)** as a water soluble solid. η_{inh} = 24.6 mL/g.

^{1}H NMR (D_2O), δ/ppm (expected proton counts in parentheses): 1.5 – 0.9, 54H (54H, $CH_2N(CH_2\mathbf{CH_3})_2$; $NH[C(\mathbf{CH_3})_2]_2$; $CH(\mathbf{CH_2})_2$); 2.7 – 2.5, 6.2H (6H, $\mathbf{CH_2}N(\mathbf{CH_2}CH_3)_2$); 3.3 – 3.1, 2.4H (2H, CONH$\mathbf{CH_2}$); 4.1 – 4.0, 2.7H (3H, CONH**CH**).

Carrier 4e (60): By a similar procedure as above, 2-(2-aminoethoxy)ethanol (AEE) (0.4291 g, 4.082 mmol) in DMF (2 mL) was added drop-wise to the stirred mixture of polysuccinimide (1.980 g, 20.41 mmol) and ATP (1.914 g, 12.25 mmol) in DMF. The solution saturated with N_2 and stirred for 5 h, thereafter hydrazine hydrate (Hy) (0.6131 g, 12.25 mmol) in DMF (10 mL) was added drop-wise to the stirred solution cooled in an ice bath. Re-saturated with N_2, the solution was stirred for 40 hours in an ice bath and another 5 hours at ambient temperature. This resulted in the terpolymer **4e (60)** in a yield of 3.460 g (70.1 %). η_{inh} = 21.3 mL/g.

^{1}H NMR (D_2O), δ/ppm (expected proton counts in parentheses): 1.5 – 0.9, 48H (48H, $NH[C(\mathbf{CH_3})_2]_2$; $CH(\mathbf{CH_2})_2$); 3.4 – 3.1, 2.4H (2H, CONH$\mathbf{CH_2}$); 3.8 – 3.5, 5.5H (6H, $\mathbf{CH_2}O\mathbf{CH_2CH_2}OH$); 4.1 – 4.0, 2.4H (4H, CONH**CH**).

Carrier 4a (50): The same basic procedure used in **4a (60)** was adopted to prepare this carrier, A mixture of polysuccinimide (1.980 g, 20.41 mmol) and ATP (1.595 g, 10.21 mmol) in DMF was treated with DMP (0.8341 g, 8.165 mmol) in DMF (2 mL), thereafter Hy (0.3066 g, 6.124 mmol) in DMF (10 mL) was added drop-wise to the stirred solution cooled in an ice bath. Re-saturated with N_2, the solution was stirred for 40 hours in an ice bath and another 5 hours at ambient temperature, and this resulted in a water-soluble polymer, **4a (50)**, in a yield of 2.792 g (59.2 %). η_{inh} = 21.7 mL/g.

^{1}H NMR (D_2O), δ/ppm (expected proton counts in parentheses): 1.5 – 0.9, 80H (80H, $NH[C(\mathbf{CH_3})_2]_2$; $CH(\mathbf{CH_2})_2$); 1.7 – 1.5, 9.4H (8H, $CONHCH_2\mathbf{CH_2}CH_2NMe_2$); 2.3 – 2.1, 23.5H (24H, N$\mathbf{Me_2}$); 2.4 – 2.3, 9.4(8H, $\mathbf{CH_2}NMe_2$); 3.3 – 3.1, 9H (8H, CONH$\mathbf{CH_2}$); 4.1 – 4.0, 4.7H (5H, CONH**CH**).

Carrier 4b (50): By a similar procedure as before 2-(dimethylamino)ethylamine DMEA (0.720 g, 8.165 mmol) in DMF (2 mL) was added drop-wise to the stirred mixture of

polysuccinimide (1.980 g, 20.41 mmol) and ATP (1.595 g, 10.21 mmol) in DMF. The solution was saturated with N_2 and stirred for 5h, thereafter Hy (0.3066 g, 6.124 mmol) in DMF (10 mL) was added drop-wise to the stirred solution cooled in an ice bath. Re-saturated with N_2, the solution was stirred for 40 hours in an ice bath and another 5 hours at ambient temperature. This resulted in the copolymer **4b (50)** in a yield of 2.996 g (65.1 %), and η_{inh} = 18.6 mL/g.

^{1}H NMR (D_2O), δ/ppm (expected proton counts in parentheses): 1.5 – 0.9, 80H (80H, NH[C(**CH_3**)$_2$]$_2$; CH(**CH_2**)$_2$); 2.3 – 2.1, 22.9H (24H, N**Me_2**); 2.4 – 2.3, 7.6(8H, **CH_2**NMe_2); 3.3 – 3.1, 7.6H (8H, CONH**CH_2**); 4.1 – 4.0, 3.8H (5H, CONH**CH**).

Carrier 4c (50): The same procedure used in carrier **4a (60)** was adopted. 3-(diethylamino)propylamine DEP (1.063 g, 8.165 mmol) in DMF (2 mL) was added drop-wise to the stirred mixture of polysuccinimide (1.980 g, 20.41 mmol) and ATP (1.595 g, 10.21 mmol) in DMF. The solution saturated with N_2 and stirred for 5 h, thereafter Hy (0.3066 g, 6.124 mmol) in DMF (10 mL) was added drop-wise to the stirred solution cooled in an ice bath. Re-saturated with N_2, the solution was stirred for 40 hours in an ice bath and another 5 hours at ambient temperature. This gave the copolymer **4b (50)** in a yield of 3.011 g (60.9 %), and η_{inh} = 24.7 mL/g.

^{1}H NMR (D_2O), δ/ppm (expected proton counts in parentheses): 1.5 – 0.9, 104H (104H, CH_2N(CH_2**CH_3**)$_2$; NH[C(**CH_3**)$_2$]$_2$; CH(**CH_2**)$_2$); 1.7 – 1.5, 8H (8H, CONHCH_2**CH_2**CH_2NEt_2); 2.9 – 2.5, 42H (42H, **CH_2**N(**CH_2**CH_3)$_2$; **CH_2**CONH); 3.3 – 3.1, 8.6H (8H, CONH**CH_2**); 4.1 – 4.0, 6.5H (5H, CONH**CH**).

Carrier 4d (50): By the procedure leading to terpolyaspartamide **4a (60)**; a mixture of polysuccinimide (1.980 g, 20.41 mmol) and ATP (1.595 g, 10.21 mmol) in DMF, was treated with 2(diethylamino)ethylamine DEEA (0.949 g, 8.165 mmol). Then hydrazine hydrate (Hy) (0.3066 g, 6.124 mmol) in DMF (10 mL) was added drop-wise to the stirred solution cooled in an ice bath. Re-saturated with N_2, the solution was stirred for 40 hours in an ice bath and another 5 hours at ambient temperature. The resultant solution was

treated and worked up as before, giving 2.990 g (61.9 %) of **4d (50)** as a water soluble solid. η_{inh} = 27.9 mL/g.

^{1}H NMR (D_2O), δ/ppm (expected proton counts in parentheses): 1.5 – 0.9, 104H (104H, $CH_2N(CH_2\mathbf{CH_3})_2$; $NH[C(\mathbf{CH_3})_2]_2$; $CH(\mathbf{CH_2})_2$); 2.9 – 2.5, 46.9H (42H, $\mathbf{CH_2}N(\mathbf{CH_2}CH_3)_2$; $\mathbf{CH_2}CONH$); 3.3 – 3.1, 7.6H (8H, $CONH\mathbf{CH_2}$); 4.1 – 4.0, 4.8H (5H, CONH**CH**).

Carrier 4e (50): By a similar experimental procedure as before, 2-(2-aminoethoxy)ethanol (AEE) (0.8585 g, 8.165 mmol) in DMF (2 mL) was added drop-wise to the stirred mixture of polysuccinimide (1.980 g, 20.41 mmol) and ATP (1.595 g, 10.21 mmol) in DMF. The solution saturated with N_2 and stirred for 5 h, thereafter hydrazine hydrate (Hy) (0.3066 g, 6.124mmol) in DMF (10 mL) was added drop-wise to the stirred solution cooled in an ice bath. Re-saturated with N_2 and stirred for 40 hours in an ice bath and another 5 hours at ambient temperature. This resulted in the copolymer **4e (50)** in a yield of 2.934 g (61.9 %). η_{inh} = 21.4 mL/g.

^{1}H NMR (D_2O), δ/ppm (expected proton counts in parentheses): 1.5 – 0.9, 48H (48H, $NH[C(\mathbf{CH_3})_2]_2$; $CH(\mathbf{CH_2})_2$); 3.4 – 3.1, 2.4H (2H, $CONH\mathbf{CH_2}$); 3.8 – 3.5, 5.5H (6H, $\mathbf{CH_2}O\mathbf{CH_2CH_2}OH$); 4.1 – 4.0, 2.4H (4H, CONH**CH**).

4.3.3. Preparation of polymeric conjugates

4.3.3.1. Polyaspartamides-ferrocenyl anchoring

Conjugate 2a (90)-Fcp: To the N_2-saturated solution of carrier **2a (90)** (0.586 g, 0.305 mmol) in DMF-MeOH (1:3) (5 mL), Fcp (0.0878 g, 0.366 mmol) in MeOH (5 mL) was added. After adding a drop of acetic acid, upon re-saturation with N_2, the solution was light protected, and stirred for 3 days at RT with the pH of the solution maintained between 5 and 6. The solution was precipitated and dialyzed for 2 d in Spectra/Por 4 tubing. The retentate was freeze-dried, to give 0.382 g (65.3 %) of water-soluble solid **2a (90)-Fcp**. η_{inh} = 14.8 mL/g.

^{1}H NMR (D_2O), δ/ppm (expected proton counts in parentheses): 4.2 – 4.1, 8.6H (9H, protons of **Fcp**); 3.3 – 3.1, 17.8H (18H, CONH**CH_2**); 2.9 – 2.6, 17.2H (18H, **CH_2**CONH); 2.3 – 2.1, 54H (54H, N**Me_2**). These data indicate 96 % Fc incorporation. Found: Fc, 2.79 % (UV), 2.76 % (H NMR). Calcd: Fc, 2.88 %.

Conjugate 2d (90)-Fcp: By the same preceding procedure as described in the foregoing experiment, carrier **2d (90)** (0.32 g, 0.44 mmol) in DMF-MeOH (1:3) (5 mL) was used instead of carrier **2a (90)**, and Fcp (0.099 g, 0.413 mmol) in MeOH (5mL) was added to the stirred polymeric solution. The solution was treated and worked up as before, giving conjugate **2d (90)-Fcp** as a water-soluble solid in a yield of 0.247 g (58.9 %). η_{inh} = 21.3 mL/g.

^{1}H NMR (D_2O), δ/ppm (expected proton counts in parentheses): 4.2 – 4.1, 8.9H (9H, protons of **Fcp**); 2.9 – 2.6, 18H (18H, **CH_2**CONH); 2.5 – 2.3, 53.3H (54H, **CH_2**N(**CH_2**CH_3)$_2$; 2.3 – 2.1, 54H (54H, N**Me_2**). These data indicate 99 % Fc incorporation. Found: Fc, 2.42 % (UV), 2.44 % (H NMR). Calcd: Fc, 2.46 %.

Conjugate 2f (90)-Fcp: By an analogous procedure as described in the forgoing experiment, carrier **2f (90)** (0.296 g, 0.284 mmol) was used instead of carrier **2a (90)** and Fcp (0.082g, 0.341 mmol). The solution was treated and worked up as before, giving conjugate **2f (90)-Fcp** as a water-soluble solid in a yield of 0.195 g (51.7 %). η_{inh} = 16.2 mL/g.

^{1}H NMR (D_2O), δ/ppm (expected proton counts in parentheses): 4.2 – 4.1, 5.7H (9H, protons of **Fcp**); 3.8 – 3.6, 54H (54H, **CH_2**O**$CH_2$$CH_2$**OH); 2.9 – 2.6, 17.8H (18H, **CH_2**CONH). These data indicate 63 % Fc incorporation. Found: Fc, 2.34 % (UV), 1.62 % (H NMR). Calcd: Fc, 2.57 %.

Conjugate 2f (80)-Fcp: Conjugate **2f (80)-Fcp** was obtained by the same procedure as described in the forgoing experiment. A solution of carrier **2f (80)** (0.316 g, 0.317 mmol) was treated with Fcp (0.091 g, 0.380 mmol) and resulted in a water-soluble conjugate **2f (80)-Fcp** in a yield of 0.235 g (57.8 %). η_{inh} = 18.4 mL/g.

^{1}H NMR (D_2O), δ/ppm (expected proton counts in parentheses): 4.2 – 4.1, 7.4H (9H, protons of **Fcp**); 3.8 – 3.6, 24H (24H, **CH_2OCH_2CH_2**OH); 2.9 – 2.6, 7.8H (8H, **CH_2**CONH). These data indicate 82 % Fc incorporation. Found: Fc, 2.70 % (UV), 2.19 % (H NMR). Calcd: Fc, 2.66 %.

Conjugate 2e (90)-Fca: To a stirred aqueous solution (5 mL) of carrier **2e (90)** (0.300 g, 0.151 mmol), saturated with N_2, light protected, was added Fca (0.043 g, 0.181 mmol). After adding a drop of acetic acid, the solution was re-saturated with N_2, stirred for 3d at RT and then stirred for another 2 h in the incubator at 50^{0}C. During the process, the pH was carefully monitored and maintained at ~5.5 - 6. The routinely filtered solution was dialyzed in Spectra/Por 4 tubing for 2d, and the conjugate isolated as a water-soluble solid by freeze-drying in a yield of 0.200 g (58.3 %). η_{inh} = 24.2 mL/g.

^{1}H NMR (D_2O), δ/ppm (expected proton counts in parentheses): 4.2 – 4.1, 6.6H (9H, protons of **Fca**); 4.1 – 4.0, 9H (9H, CONH**CH**); 1.2 – 0.9, 108H (108H, [C(**CH_3**)$_2$]-NH). These data indicate 73 % Fc incorporation. Found: Fc, 1.95 % (UV), 1.55 % (H NMR). Calcd: Fc, 2.12 %.

Conjugate 2f (90)-Fcc: By the same preceding procedure as described in the forgoing experiment, carrier **2f (90)** (0.284 g, 0.153 mmol) in H_2O (5 mL) was used instead of carrier **2a (90)**, and Fcc (0.044 g, 0.184 mmol) in H_2O (5 mL) was added to the stirred polymeric solution. The solution was treated and worked up as before, giving conjugate **2f (90)-Fcc** as a water-soluble solid in a yield of 0.171 g (52.1 %). η_{inh} = 17.3 mL/g.

^{1}H NMR (D_2O), δ/ppm (expected proton counts in parentheses): 4.2 – 4.1, 6.1H (9H, protons of **Fcc**); 3.8 – 3.6, 54H (54H, **CH_2OCH_2CH_2**OH); 3.3 – 3.1, 16.8H (18H, CONH

CH_2). These data indicate 68 % Fc incorporation. Found: Fc, 2.50 % (UV), 1.75 % (H NMR). Calcd: Fc, 2.57 %.

Conjugate 2a (80)-Cyn: Conjugate **2a (80)-Cyn** was obtained by the same procedure as described in the forgoing experiment. A solution of carrier **2a (80)** (0.300 g, 0.142 mmol) was treated with Cyn (0.022 g, 0.171 mmol) instead of Fc, and resulted in a water-soluble conjugate **2a (80)-Cyn** in a yield of 0.199 g (61.9 %). η_{inh} = 15.1 mL/g.

^{1}H NMR (D_2O), δ/ppm (expected proton counts in parentheses): 7.6 – 7.2, 5.6H (5H, aromatic **CH** of Cyn); 3.3 – 3.1, 7.6H (9H, CONH**CH_2**); 2.3 – 2.1, 24H (24H, N**Me_2**). These data indicate 112% Cyn incorporation. Found: Cyn, 5.88 % (UV), 6.60 % (H NMR). Calcd: Cyn, 5.90 %.

Conjugate 2e (80)-Cyn: By an analogous procedure as described in the forgoing experiment, carrier **2a (80)** (0.320 g, 0.159 mmol) was used instead of carrier **2a (90),** and Cyn (0.025 g, 0.191 mmol) was added to the stirred polymeric solution. The solution was treated and worked up as before, giving conjugate **2e (80)-Cyn** as a water-soluble solid in a yield of 0.208 g (60.3 %). η_{inh} = 24.4 mL/g.

^{1}H NMR (D_2O), δ/ppm (expected proton counts in parentheses): 7.6 – 7.2, 4.2H (5H, aromatic **CH** of Cyn); 4.1 – 4.0, 3.5H (4H, CONH**CH**); 1.2 – 0.9, 48H (48H, [C(**CH_3**)$_2$]-NH). These data indicate 84 % Cyn incorporation. Found: Cyn, 4.71 % (UV), 4.07 % (H NMR). Calcd: Cyn, 4.84 %.

Conjugate 2c (90)-Cyn: The light protected solution (5 mL) of carrier **2c (90)** (0.314 g, 0.255 mmol) was saturated with N_2, then treated with a solution of Cyn (0.040 g, 0.306 mmol) dissolved in CH_3OH (5 mL). After adding a drop of acetic acid, the solution was stirred for 3 d at RT, the pH monitored and maintained at ~5.5 – 6. The solution was filtered and dialyzed for 2 d in Spectra/Por 4 tubing against regular changing of distilled water. The retentate was freeze-dried, to give 0.211 g (59.7 %) of water-soluble, solid **2c (90)-Cyn**. η_{inh} = 16.7 mL/g.

^{1}H NMR (D_2O), δ/ppm (expected proton counts in parentheses): 7.6 – 7.2, 4.8H (5H, aromatic **CH** of Cyn); 1.9 – 1.7, 17.9H (18H, $CONHCH_2\mathbf{CH_2}CH_2Net_2$); 1.2 – 0.9, 54H (54H, $CH_2N(CH_2\mathbf{CH_3})_2$). These data indicate 96 % Cyn incorporation. Found: Cyn, 5.90 % (UV), 5.84 % (H NMR). Calcd: Cyn, 6.08 %.

Conjugate 2f (90)-Cur: The light protected solution (5 mL) of carrier **2f (90)** (0.4733 g, 0.255 mmol) was saturated with N_2, then treated with a solution of Cur (0.113 g, 0.306 mmol) dissolved in CH_3OH (5 mL). After adding a drop of acetic acid, the solution was stirred for 3 d at RT, the pH monitored and maintained at ~5.5 – 6. The solution was filtered and dialyzed for 2 d in Spectra/Por 4 tubing against regular changing of distilled water. The retentate was freeze-dried, to give 0.361 g (61.5 %) of water-soluble, solid **2f (90)-Cur**. η_{inh} = 20.2 mL/g.

^{1}H NMR (D_2O), δ/ppm (expected proton counts in parentheses): 6.7 – 6.5, 6.1H (6H, proton of Cur); 3.8 – 3.6, 54H (54H, $\mathbf{CH_2}O\mathbf{CH_2CH_2}OH$); 3.4 – 3.3, 20.2H (18H, $CONH\mathbf{CH_2}$). These data indicate 100 % Cur incorporation. Found: Cur, 13.79 % (UV), 13.82 % (H NMR). Calcd: Cur, 13.82 %.

Conjugate 3a (50)-Fcp: By the same abovementioned procedure as described in the forgoing experiment, carrier **3a (50)** (0.4958 g, 0.256 mmol) in DMF-MeOH (5 mL) was used instead of carrier **2a (90)**, and Fcp (0.0737 g, 0.307 mmol) in MeOH (5 mL) was added to the stirred polymeric solution. The solution was treated and worked up as before, giving conjugate **3a (80)-Fcp** as a water-soluble solid in a yield of 0.3206 g (56.3 %). η_{inh} = 21.2 mL/g.

^{1}H NMR (D_2O), δ/ppm (expected proton counts in parentheses): 4.2 – 4.1, 7.2H (9H, protons of **Fcp**); 3.8 – 3.6, 30H (30H, $\mathbf{CH_2}OCH_2CH_2OH$); 2.5 – 2.3, 24H (24H, $\mathbf{CH_2}NMe_2$). These data indicate 80 % Fc incorporation. Found: Fc, 2.23 % (UV), 2.07 % (H NMR). Calcd: Fc, 2.59 %.

Conjugate 3a (60)-Fcp: To the N_2-saturated solution of carrier **3a (60)** (0.570 g, 0.305 mmol) in DMF-MeOH (1:3) (5 mL), Fcp (0.0878 g, 0.366 mmol) in MeOH (5 mL) was added. After adding a drop of acetic acid, upon re-saturation with N_2, the solution was light protected, and stirred for 3 days at RT with the pH of the solution maintained between 5 and 6. The solution was precipitated and dialyzed for 2 d in Spectra/Por 4 tubing. The retentate was freeze-dried, to give 0.445 g (62.7 %) of water-soluble solid **3a (60)-Fcp**. η_{inh} = 18.7 mL/g.

^{1}H NMR (D_2O), δ/ppm (expected proton counts in parentheses): 4.2 – 4.1, 8H (9H, protons of **Fcp**); 3.8 – 3.6, 6H (6H, **CH_2**OCH_2CH_2OH); 2.5 – 2.3, 18H (18H, **CH_2**NMe_2). These data indicate 89 % Fc incorporation. Found: Fc, 1.93 % (UV), 2.38 % (H NMR). Calcd: Fc, 2.67 %.

Conjugate 3d (60)-Fcp: By the same preceding procedure as described in the foregoing experiment, carrier **3d (60)** (0.835 g, 0.440 mmol) in DMF-MeOH (1:3) (5 mL) was used instead of carrier **2a (90)**, and Fcp (0.0991 g, 0.413 mmol) in MeOH (5mL) was added to the stirred polymeric solution. The solution was treated and worked up as before, giving conjugate **3d (60)-Fcp** as a water-soluble solid in a yield of 0.449 g (48.1 %). η_{inh} = 21.1 mL/g.

^{1}H NMR (D_2O), δ/ppm (expected proton counts in parentheses): 4.2 – 4.1, 6.7H (9H, protons of **Fcp**); 3.3 – 3.1, 5.8H (6H, CONH**CH_2**); 2.9 – 2.6, 6.1H (6H, **CH_2**CONH); 2.4 – 2.1, 18H (18H, $CH_2N(CH_2CH_3)_2$). These data indicate 74 % Fc incorporation. Found: Fc, 2.04 % (UV), 1.95 % (H NMR). Calcd: Fc, 2.63 %.

Conjugate 3d (50)-Fcp: By an analogous procedure as described in the forgoing experiment, carrier **3d (50)** (0.546 g, 0.284 mmol) was used instead of carrier **2a (90)** and Fcp (0.0818g, 0.341 mmol). The solution was treated and worked up as before, giving conjugate **3d (50)-Fcp** as a water-soluble solid in a yield of 0.210 g (64.8 %). η_{inh} = 20.3 mL/g.

^{1}H NMR (D_2O), δ/ppm (expected proton counts in parentheses): 4.2 – 4.1, 6.5H (9H, protons of **Fcp**); 3.8 – 3.6, 34.6H (30H, **CH_2OCH_2CH_2**OH); 3.3 – 3.1, 18.6H (18H, CONH**CH_2**); 1.2 – 0.9, 24H (24H, $CH_2N(CH_2$**$CH_3)_2$**). These data indicate 72 % Fc incorporation. Found: Fc, 2.58 % (UV), 1.87 % (H NMR). Calcd: Fc, 2.60 %.

Conjugate 4c (50)-Fcp: Conjugate **4c (50)-Fcp** was obtained by the same procedure as described in the forgoing experiment. A solution of carrier **4c (50)** (0.677 g, 0.317 mmol) was treated with Fcp (0.0912 g, 0.380 mmol) and resulted in a water-soluble conjugate **4c (50)-Fcp** in a yield of 0.3856 g (50.2 %). η_{inh} = 26.2 mL/g.

^{1}H NMR (D_2O), δ/ppm (expected proton counts in parentheses): 4.2 – 4.1, 8.1H (9H, protons of **Fcp**); 2.9 – 2.6, 24H (24H, **CH_2**CONH); 2.5 – 2.3, 18H (18H, **CH_2**N(**CH_2**$CH_3)_2$). These data indicate 90 % Fc incorporation. Found: Fc, 2.25 % (UV), 2.13 % (H NMR). Calcd: Fc, 2.37 %.

Conjugate 4c (60)-Fcp: To a stirred aqueous solution (5 mL) of carrier **4c (60)** (0.324 g, 0.151 mmol), saturated with N_2, light protected, was added Fcp (0.0434 g, 0.181 mmol). After adding a drop of acetic acid, the solution was re-saturated with N_2, stirred for 3d at RT and then stirred for another 2 h in the incubator at 50^{0}C. During the process, the pH was carefully monitored and maintained at ~5.5 - 6. The routinely filtered solution was dialyzed in Spectra/Por 4 tubing for 2d, and the conjugate isolated as a water-soluble solid by freeze-drying in a yield of 0.191 g (58.8 %). η_{inh} = 28.1 mL/g.

^{1}H NMR (D_2O), δ/ppm (expected proton counts in parentheses): 4.2 – 4.1, 8.6H (9H, protons of **Fcp**); 3.4 – 3.3, 1.9H (2H, CONH**CH_2**); 1.2 – 0.9, 54H (54H, $CH_2N(CH_2$**$CH_3)_2$**). These data indicate 96 % Fc incorporation. Found: Fc, 2.31 % (UV), 2.27 % (H NMR). Calcd: Fc, 2.36 %.

Conjugate 4d (50)-Fcp: By the same preceding procedure as described in the forgoing experiment, carrier **4d (50)** (0.344 g, 0.153 mmol) in H_2O (5 mL) was used instead of

carrier **2a (90)**, and Fcp (0.0441 g, 0.184 mmol) in H_2O (5 mL) was added to the stirred polymeric solution. The solution was treated and worked up as before, giving conjugate **4d (50)-Fcp** as a water-soluble solid in a yield of 0.204 g (52.7 %). η_{inh} = 24.5 mL/g.

^{1}H NMR (D_2O), δ/ppm (expected proton counts in parentheses): 4.2 – 4.1, 8.9H (9H, protons of **Fcp**); 3.4 – 3.3, 7.6H (8H, CONH**CH_2**); 1.2 – 0.9, 60H (60H, $CH_2N(CH_2$**CH_3**$)_2$). These data indicate 99 % Fc incorporation. Found: Fc, 2.18 % (UV), 2.24 % (H NMR). Calcd: Fc, 2.26 %.

Conjugate 4e (50)-Fcp: Conjugate **4e (50)-Fcp** was obtained by the same procedure as described in the forgoing experiment. A solution of carrier **4e (50)** (0.313 g, 0.142 mmol) was treated with Fcp (0.0410 g, 0.171 mmol), and resulted in a water-soluble conjugate **4e (50)-Fcp** in a yield of 0.174 g (49.2 %). η_{inh} = 28.2 mL/g.

^{1}H NMR (D_2O), δ/ppm (expected proton counts in parentheses): 4.3 – 4.1, 9.1H (9H, protons of **Fcp**); 3.8 – 3.6, 23.9H (24H, **CH_2**O**CH_2CH_2**OH); 1.2 – 0.9, 60H (60H, $N(CH_2$**CH_3**$)_2$). These data indicate 100 % Fc incorporation. Found: Fc, 2.20 % (UV), 2.30 % (H NMR). Calcd: Fc, 2.30 %.

Conjugate 4b (50)-Fca: By an analogous procedure as described in the forgoing experiment, carrier **4b (50)** (0.340 g, 0.159 mmol) was used instead of carrier **2a (90),** and Fca (0.0435 g, 0.191 mmol) was added to the stirred polymeric solution. The solution was treated and worked up as before, giving conjugate **4b (50)-Fca** as a water-soluble solid in a yield of 0.211 g (55.0 %). η_{inh} = 21.4 mL/g.

^{1}H NMR (D_2O), δ/ppm (expected proton counts in parentheses): 4.3 – 4.1, 8.2H (9H, protons of **Fca**); 3.4 – 3.3, 8.8H (8H, CONH**CH_2**); 1.2 – 0.9, 60H (60H, [C(**CH_3**$)_2$]-NH). These data indicate 91 % Fc incorporation. Found: Fc, 2.20 % (UV), 2.17 % (H NMR). Calcd: Fc, 2.38 %.

Conjugate 4e (50)-Fca: The light protected solution (5 mL) of carrier **4e (50)** (0.562 g, 0.255 mmol) was saturated with N_2, then treated with a solution of Fca (0.0697 g, 0.306

mmol) dissolved in CH_3OH (5 mL). After adding a drop of acetic acid, the solution was stirred for 3 d at RT, the pH monitored and maintained at ~5.5 – 6. The solution was filtered and dialyzed for 2 d in Spectra/Por 4 tubing against regular changing of distilled water. The retentate was freeze-dried, to give 0.368 g (58.2 %) of water-soluble, solid **4e (50)-Fca**. η_{inh} = 22.3 mL/g.

^{1}H NMR (D_2O), δ/ppm (expected proton counts in parentheses): 4.3 – 4.1, 8H (9H, protons of **Fca**); 3.6 – 3.3, 5.7H (5H, **CH_2OCH_2CH_2**OH); 1.2 – 0.9, 60H (60H, NH(**CH_3**)$_2$). These data indicate 89 % Fc incorporation. Found: Fc, 2.22 % (UV), 2.11 % (H NMR). Calcd: Fc, 2.37 %.

Conjugate 4c (60)-Fcc: The light protected solution (5 mL) of carrier **4c (60)** (0.548 g, 0.255 mmol) was saturated with N_2, then treated with a solution of Fcc (0.0655 g, 0.306 mmol) dissolved in CH_3OH (5 mL). After adding a drop of acetic acid, the solution was stirred for 3 d at RT, the pH monitored and maintained at ~5.5 – 6. The solution was filtered and dialyzed for 2 d in Spectra/Por 4 tubing against regular changing of distilled water. The retentate was freeze-dried, to give 0.410 g (66.9 %) of water-soluble, solid **4c (60)-Fcc**. η_{inh} = 23.1 mL/g.

^{1}H NMR (D_2O), δ/ppm (expected proton counts in parentheses): 4.3 – 4.1, 4.1H (9H, protons of **Fcc**); 4.1 – 4.0, 3.4H (3H, CONH**CH**); 1.2 – 0.9, 54H (54H, NH[C(**CH_3)$_2$]**). These data indicate 46 % Fc incorporation. Found: Fc, 1.26 % (UV), 1.06 % (H NMR). Calcd: Fc, 2.30 %.

Conjugate 4a (60)-Cur: By the same abovementioned procedure as described in the forgoing experiment, carrier **4a (60)** (0.557 g, 0.256 mmol) in DMF-MeOH (5 mL) was used instead of carrier **2a (90)**, and Cur (0.113 g, 0.307 mmol) in MeOH (5 mL) was added to the stirred polymeric solution. The solution was treated and worked up as before, giving conjugate **4a (60)-Cur** as a water-soluble solid in a yield of 0.350 g (52.3 %). η_{inh} = 23.8 mL/g.

^{1}H NMR (D_2O), δ/ppm (expected proton counts in parentheses): 6.7 – 6.5, 3.7H (6H, protons of **Cur**); 4.3 – 4.1, 2.8H (3H, CONH**CH**); 1.2 – 0.9, 48H (48H, CH(**CH_2**)$_2$; NH[C(CH_3)$_2$]). These data indicate 62 % Cur incorporation. Found: Cur, 11.20 % (UV), 8.44 % (H NMR). Calcd: Cur, 13.61 %.

4.3.3.1. Polyaspartamides multidrug conjugation

Conjugate 2a (90) – FA - Fcp: Step (1): The reaction of carrier **2a (90)** (0.392 g, 0.204mmol) with FA (0.063 g, 0.143 mmol), HBTU (0.046 g, 0.122 mmol), and TEA (0.041g, 0.408 mmol), after worked-up in conventional method, gave a yellow, completely water-soluble, homoconjugate 2a (90) **- FA** in a yield of 0.271 g (61.8 %).

^{1}H NMR (D_2O), δ/ppm: 8.5-6.5, 4.8H (Expected: 5H; aromatic and heteroaromatic CH of FA); 1.8-1.6, 18H (expected: 18H; CONHCH$_2$**CH$_2$**CH$_2$NMe$_2$). FA incorporation: 96 %.

Step (2): The target co-conjugate was obtained by reacting the homoconjugate with Fcp. Thus, homoconjugate (0.239 g, 0.102 mmol) treated with Fcp (0.039 g, 0.163 mmol), and a drop of acetic acid, afforded 2a (90) **– FA - Fcp** as water-soluble compound, in a yield of 0.133 g (47.8 %), possessing the following characteristics: η_{inh}, 20.3 mL g-1.

^{1}H NMR (D2O), δ/ppm: 8.5 - 6.5, 2.8H (Expected: 3H; aromatic and heteroaromatic CH of FA); 4.3 - 4.1, 3.2 (Expected: 3.6H, CH of ferrocenyl); 2.3 - 2.1, 53.8H (Expected: 54H, N**Me$_2$**); 1.8 - 1.6, 18H (expected: 18H; CONHCH$_2$**CH$_2$**CH$_2$NMe$_2$), showing 93 % FA and 89 % Fc incorporation. Found: FA, 18.68 % (UV), 17.42 % (^{1}H NMR); Fe, 2.38 % (UV), 2.20 % (^{1}H NMR).

Conjugate 2a (80) – FA - Fcp: By the same abovementioned procedure as described in the forgoing experiment, carrier **2a (80) - FA** (0.582 g, 0.256 mmol) in DMF-MeOH (5 mL) was used instead of carrier **2a (90) - FA**, and Fcp (0.0984 g, 0.410 mmol) in MeOH (5 mL) was added to the stirred polymeric solution. The solution was treated and worked up

as before, giving conjugate **2a (80) – FA - Fcp** as a water-soluble solid in a yield of 0.317 g (46.6 %). η_{inh} = 22.4 mL/g.

^{1}H NMR (D2O), δ/ppm: 8.5 - 6.5, 3.9H (Expected: 4H; aromatic and heteroaromatic CH of FA); 4.3 - 4.1, 1.78 (Expected: 1.8H, CH of ferrocenyl); 2.9 - 2.7, 7.8H (expected: 8H; **CH_2**CONH); 2.3 - 2.1, 19.6H (Expected: 18H, N**Me_2**); 1.8 - 1.6, 7.5H (expected: 8H; CONHCH$_2$**CH_2**CH$_2$NMe$_2$), showing 97 % FA and 99 % Fc incorporation. Found: FA, 16.08 % (UV), 15.79 % (^{1}H NMR); Fe, 2.10 % (UV), 2.11 % (^{1}H NMR).

Conjugate 4c (60) – Cur - Fcp: Step (1): The light protected solution (5 mL) of carrier **4c (60)** (0.548 g, 0.255 mmol) was saturated with N_2, then treated with a solution of Cur (0.111 g, 0.307 mmol) dissolved in CH_3OH (5 mL). After adding a drop of acetic acid, the solution was stirred for 2 d at RT, the pH monitored and maintained at ~5.5 – 6.

Step (2): By the same abovementioned procedure as described in step (1), homoconjugate **4c (60) - Cur** (0.637 g, 0.256 mmol) in DMF-MeOH (5 mL) was used instead of carrier **2a (90)**, and Fcp (0.098 g, 0.410 mmol) in MeOH (5 mL) was added to the stirred polymeric solution. The solution was treated and worked up as before, giving conjugate **4c (60) – Cur - Fcp** as a water-soluble solid in a yield of 0.423 g (57.5 %). η_{inh} = 23.8 mL/g.

^{1}H NMR (D_2O), δ/ppm (expected proton counts in parentheses): 6.7 – 6.5, 1.76H (1.8H, C**H** of Cur); 4.3 – 4.1, 2.97H (3H, CH of **Fcp**); 1.2 – 0.9, 54H (54H, $CH_2N(CH_2$**CH_3**$)_2$; NH[c(**CH_3**$)_2]_2$; CH(**CH_2**$)_2$). These data indicate 98 % Cur and 99 % Fc incorporation. Found: Cur, 11.80 % (UV), 11.68 % (^{1}H NMR); Fe, 1.96 % (UV), 1.96 % (^{1}H NMR).

CHAPTER 5

CONCLUSION

Polymer-drug conjugates have enormous potential for researchers and clinicians. The great versatility of these macromolecular drugs enables the design and development of effective treatments for a variety of human pathologies. From macromolecular prodrugs of established anticancer agents, the applications of polymer-drug conjugates have expanded dramatically in recent years. Delivery of new anticancer agents, novel polymer architectures, and the use of molecular targets are the most exciting and promising areas. However, the possibility of inhibiting the excess of cell death, at least in an acute form, is just beginning to be explored. It is hoped that in the near future some of these new approaches will reach clinical evaluation.

The project has demonstrated the practicability of synthesizing water-soluble macromolecules fitted with hydrosolubilizing agents such as DMP, DMEA, DEP, DEE, ATP and AEE, and drug binding functionalities such as hydrazine. The syntheses of carriers were brought about by aminolytic ring-opening of PSI (exemplified by copolyaspartamide and terpolyaspartamide).

Derivatives of the organoiron compound (ferrocene aldehydes and ketone), which represented the predominant drug species for carrier conjugation in this project, together with other drug systems, such as cinnamaldehyde, curcumin and folic acid, were synthesized and conjugated on selected carrier polymers. The practicability for the development of macromolecular conjugates, which are water-soluble, chemically stable and structurally defined, demonstrated the release of drugs in acidic environment. The stability of the bond was adapted to the mode and site of action of the agent, the necessity for release, and the availability of hydrolytic enzymes which can break the linkage and release the agent.

On the other hand, the success of such conjugates synthesized according to this strategy depended on:

(1) the physicochemical properties of the conjugates such as molecular size, electrical charge, and solubility;
(2) the chemical stability of active components of the conjugates and linkages;
(3) proper interaction with tumor cells;
(4) pharmacokinetics in the body(circulating, identification of cancer cells and mode of elimination).

Future research should be focused on investigating in vitro then in vivo screens in order to draw realistic conclusions; Cytotoxicity of ferrocene-folic acid conjugates should be investigated in order to evaluate the advantages associated with the co-conjugation of these two drug models. This would open up the possibility of extending the multidrug co-conjugation approach to other anticancer compounds.

REFERENCES

1. Cancer Research UK. 2002. The cancer cell Internet sources: available at http://www.cancerhelp.org.uk/help/menuforthistopic.asp?page=85. (accessed on December, 02 2008).
2. Pazdur, R.; Coia, L. R.; Hoskins, W. J.; Wagman, L. D.; eds. *Cancer Management*: A Multidisciplinary Approach, Medical Surgical and Radiation Oncology. Huntington: NY, PRR, 1996.
3. Eyre, H. J.; Lange, D.; Morris, L. B.; in *Informed Decisions*. 2nd Ed. Atlanta, GA: American Cancer Society, 1996.
4. Cancer, http://en.wikipedia.org/wiki/cancer. (accessed on September, 17 2009).
5. Chabner, B.; in *Pharmacologic Principles of Cancer Treatment*, W.B. Saunders Co., Philadelphia, 1982.
6. Chabner, B.A.; Long, D.L.; in *Cancer Chemotherapy and Biotherapy*, 2nd Edn. , Eds., Lippincott-Raven Publ., Philadelphia, 1996.
7. Foye, W.D.; in *Cancer Chemotherapeutic Agents*, Ed., Am. Chem. Soc., Washington, DC, 1995.
8. Anti-Cancer Drugs, http://www.elmhurst.edu/~chm/vchembook/650drugs.html (accessed on September, 17 2009).
9. American cancer society Inc. 2009. Chemotherapy Principles, Internet sources: available at http://www.cancer.org/docroot/home/index.asp (accessed on April, 06 2009).
10. Mesothelioma: Categories of chemotherapy drugs. Internet sources: available at http://www.mesotheliomaweb.org/categories.htm(accessed on July, 18 2009).
11. Ryan J. Burri and Nancy Y. Lee. 2009. Anticancer Therapy, Concurrent Chemotherapy and Radiotherapy for head and neck cancer.

Internet sources: available at http://www.oralcancerfoundation.org/facts/chemotherapy.htm (accessed on July, 18 2009).

12. David A. Karnofsky. Mechanism of Action of Anticancer Drugs at a Cellular Level. *CA Cancer Journal for Clinicians.* 1968; 18; 232-234 (The online version of this article, along with updated information and services, is located at http://caonline.amcancersoc.org . American cancer society Inc. July 2009).
13. D.D. N'da, Synthesis of methotrexate and ferrocene conjugates as potential anticancer agents, Ph D. dissertation, School of Chemistry, Wits University, (2004) p. 8, 52.
14. Guo,Z; Sadler, P.J. Angew,chem., Int. Ed. 1999,38,1512-1531.
15. Strohfeldt,K.;Tacke,M.Chem.Soc.Rev.2008,37,1174-1187).
16. Köpf-Maier, P.; *Eur. J. Clin. Pharmacol*. 47 (1994) 1.
17. Wilkinson, G.; Rosenblum, M.; Whiting, M. C.; Woodward, R. B.; *J. Am. Chem. Soc.* 74 (1952) 2123-2124.
18. Riva kovjazin, Tova Eldar, Miriam Patya, Alexey Vanichkin, Harry M. Lander, and Abraham Novogrodsky. Ferrocene-induced lymphocyte activation and antitumor activity is mediated by redox-sensitive signaling. Internet sources: available at http://www.fasebj.org/cgi/content/abstract/02-0558fjev1 (accessed on February, 05 2009).
19. Reversible oxidation/reduction. Internet sources: available at http://www.phys.jyu.fi/research/accelerator/ionsources/mivoc/image/picture1.jpg (accessed on July, 17 2009).
20. Ferrocene a short overview by Jens-Michael Breuning, JWG- University of Frankfurt. Internet sources: available at http://www.kishhospital.org/images/page_img/sleep_lab.jpg (accessed on July, 17 2009).
21. R. Epton, M. E. Hobson, and G. Marr, J. Organomet. Chem. 134, C23 (1977).
22. W. A. Kornicker and B. L. Vallee, Ann. N.Y. Acad. Sci. USA. 153, 689 (1968).

23. M. S. McDowell, J. H. Espenson, and A. Bak_c, Inorg. Chem. 23, 2232 (1984).

24. J. R. Pladziewicz and M. J. Carney, J. Am. Chem. Soc. 104, 3544 (1982).
25. J. R. Pladziewicz, M. S. Brenner, D. A. Rodeberg, and M. D. Likar, Inorg. Chem. 24, 1450 (1985).
26. B. W. Carlson and L. L. Miller, J. Am. Chem. Soc. 105, 7453 (1983).
27. T. Matsue, M. Suda, I. Uchida, T. Kato, U. Akiba, and T. Osa, J. Electroanal. Chem. 234, 163 (1987).
28. A. M. Joy, D. M. L. Goodgame, and I. J. Stratford, Int. J. Radiation Oncol. Biol. Phys. 16, 1053 (1989).
29. W. Troll, G. Witz, B. Goldstein, D. Stone, T. Sugimura, in Carcinogenesis, Vol. 7, E. Hecker et al. eds., (Raven Press, New York, 1982) p. 593.
30. P. J. O'Brien, Environ. Health Persp. 64, 219 (1985).
31. I. Fridovich, Annu. Rev. Biochem. 44, 147 (1976).
32. L. W. Oberley and G. R. Buettner, Cancer Res. 39, 1141 (1979).
33. G. Powis, Free Radical Biol. Med. 6, 63 (1989).
34. E. W. Neuse, R. Loonat, and J. C. A. Boeyens, Transition Met. Chem. 9, 12 (1984).
35. M. D. Sevilla, P. Neta, and L. J. Marnett, Biochem. Biophys. Res. Commun. 115, 800 (1983).
36. P. Kovacic, W. J. Popp, J. R. Ames, and M. D. Ryan, Anti-Cancer Drug Design. 3, 205 (1988).
37. B. Halliwell and J. M. C. Gutteridge, Free Radicals in Biology and Medicine (Clarendon Press, Oxford, 1985).
38. Köpf-Maier, P.; Köpf, H.; *Struct. Bonding* **70** (1998) 103.
39. Neuse, E. W.; Kanzawa, F.; *Appl. Organomet. Chem*. **4** (1990) 19.
40. Neuse, E. W.; Mbonyana, C. W. N.; In: Inorganic and *Metal-Containing Polymeric Materials*, Sheats, J., et al. Eds., Plenum Press, New York, 1990, p.139.
41. Mathiowitz, E. Encyclopedia of Controlled Drug Delivery; Willey -interscience: New York, 1999. 3. Baker, R. Controlled release of Biologically Active Agents; Academic Press: New York, 1987.).

42. Duncan R . Polymer conjugates as anticancer nanomedicines. *Nat Rev Cancer* . 2006 ; 6 : 688 – 701.

43. Satchi-Fainaro R , Duncan R , Barnes CM . Polymer therapeutics for cancer: current status and future challenges. *Adv Polym Sci* . 2006 ; 193 : 1 – 65.

44. Vicent MJ , Duncan R . Polymer conjugates: nanosized medicines for treating cancer. *Trends Biotechnol* . 2006 ; 24 : 39 – 47.

45. K. Ulbrich, V. Subr, J. Strohalm, D. Plocova, M. Jelinkova, B. Rihova, Polymeric Drugs Based on Conjugates of Synthetic and Natural Macromolecules I. Synthesis and Physico-chemical Characterisation. J. Controlled Release 64 (2000) 63-79.

46. M. Pechar, K. Ulbrich, V. Subr, L. W. Seymour, E. Schacht; Poly(Ethylene Glycol) Multiblock Copolymers as a Carrier of Anticancer Drug Doxorubicin. Bioconjugate Chemistry, 11 (2000) 131-139.

47. M. Kovar, T. Mrkvan, J. Strohalm, K. Ulbrich, T. Etrych, B. Rihova, HPMA Copolymer-Bound Doxorubicin Conjugate Target to Tumor Specific Antigen of BCLI Mouse B Cell Leukemia. J. Controlled Release, submitted 2003.

48. B. Rihova, J. Strohalm, K. Kubackova, M. Jelinkova, O. Hovorka, M. Kovar, D. Plocova, M. Sirova, M. St'astny, L. Rozprimova, K. Ulbrich, Acquired and Specific Immunological Mechanisms Co-responsible for Efficacy of Polymer-bound Drugs. J. Controlled Release 78 (2002) 97-114.

49. P.A. Vasey, S.B. Kaye, R. Morrison, C. Twelves, P. Wilson, R. Duncan, A.H. Thomson, L.S. Murray, T.E. Hilditch, T. Murray, S. Burtles, D. Fraier, E. Frigerio, J. Cassidy, Phase I clinical and pharmacokinetic study of PK 1 [N-(2-hydroxypropyl)methacrylamide copolymer doxorubicin]: First member of a new class of chemotherapeutic agents-Drug-polymer conjugates, Clin. Cancer Res. 5 (1999) 83-94.

50. Angew. Chem. 118, 1218 (2006)

51. T. Etrych, P. Chytil, M. Jelinkova, B. Rihova, K. Ulbrich, Synthesis of HPMA Copolymers Containing Doxorubicin Bound via Hydrazone Linkage. Effect of Spacer on Drug Release and in vitro Cytotoxicity. Macromol. Biosci. 2 (2002) 43-52.
52. Duncan, R.; and Kopeček, J.; *Adv. Polym. Sci.* 57 (1984) 53-101.
53. Rejmanová, P.; Kopeček, J.; Duncan, R.; Lloyd, J. B.; *Biomaterials* 6 (1985) 45-48.
54. Kopeček, J.; *Biomaterials* 5 (1984) 19-25.
55. Krinick, N. L.; Říhová, B.; Ulbrich, K.; Strohalm, J.; Kopeček, J.; *Makromol. Chem*. 191 (1990) 839.
56. McCormick, L. A.; Seymour, L. C. W.; Duncan, R.; Kopeček, J.; *J. Bioact. Comp. Polym.* 1 (1986) 4.
57. H.H.Westhall, D.A. Cooney, in Enzymes as Drugs, I.S.Holcenbery, J.Roberts, eds., Wiley, New York, p 395(1981).
58. D.A. Cooney, R.S. Rosenblath, Adv. Pharmcol. Chem. 12, 185(1975).
59. W. Friess, Collagen: biomaterial for drug delivery, Eur. J. Pharm. Biopharm. 45 (1998) 113–136.
60. Y. Tabata, Y. Ikada, Protein release from gelatin matrices, Adv. Drug Deliv. Rev. 31 (1998) 287–301.
61. S. Young, M.Wong, Y. Tabata, A.G. Mikos, Gelatin as a delivery vehicle for the controlled release of bioactive molecules, J. Control. Release 109 (2005) 256–274.
62. K.B. Djagny, Z. Wang, S. Xu, Gelatin: a valuable protein for food and pharmaceutical industries: review, Crit. Rev. Food Sci. Nutr. 41 (2001) 481–492.
63. Y. Kimura, M. Ozeki, T. Inamoto, Y. Tabata, Adipose tissue engineering based on human preadipocytes combined with gelatin microspheres containing basic fibroblast growth factor, Biomaterials 24 (2003) 2513–2521.
64. M.S. Ponticiello, R.M. Schinagl, S. Kadiyala, F.P. Barry, Gelatin-based resorbable sponge as a carrier matrix for human mesenchymal stem cells in cartilage regeneration therapy, J. Biomed. Mater. Res. 52 (2000) 246–255.

65. H.A. Awad, M. Quinn Wickham, H.A. Leddy, J.M. Gimble, F. Guilak, Chondrogenic differentiation of adipose-derived adult stem cells in agarose, alginate, and gelatin scaffolds, Biomaterials 25 (2004) 3211 –3222.

66. J. Malda, E. Kreijveld, J.S. Temenoff, C.A.V. Blitterswijk, J. Riesle, Expansion of human nasal chondrocytes on macroporous microcarriers enhances redifferentiation, Biomaterials 24 (2003) 5153–5161.

67. G.H. Altman, F. Diaz, C. Jakuba, T. Calabro, R.L. Horan, J. Chen, H. Lu, J. Richmond, D.L. Kaplan, Silk-based biomaterials, Biomaterials 24 (2003) 401–416.

68. S. Hofmann, C. Foo, F. Rossetti, M. Textor, G. Vunjak-Novakovic, D.L. Kaplan, H.P. Merkle, L. Meinel, Silk fibroin as an organic polymer for controlled drug delivery, J. Control. Release 111 (2006) 219–227.

69. S. Sofia, M.B. MacCarthy, G. Gronowiz, D.L. Kaplan, Functionalized silk based biomaterials, J. Biomed. Mater. Res. 54 (2001) 139–148.

70. T. Aper, A. Schmidt, M. Duchrow, H.-P. Bruch, Autologous blood vessels engineered from peripheral blood sample, Eur. J. Vasc. Endovasc. Surg.33 (2007) 33–39.

71. K. Nishinari, R. Takahashi, Interaction in polysaccharide solutions and gels, Curr. Opin. Colloid Interface Sci. 8 (2003) 396–400.

72. E. Khor, L.Y. Lim, Implantable applications of chitin and chitosan, Biomaterials 24 (2003) 2339–2349.

73. V.R. Patel, M.M. Amiji, Preparation and characterization of freezedried chitosan- poly(ethylene oxide) hydrogels for site-specific antibiotic delivery in the stomach, Pharmac. Res. 13 (1996) 588–593.

74. P.B. Malafaya, A. Pedro, A. Peterbauer, C. Gabriel, H. Redl, R. Reis, Chitosan particles agglomerated scaffolds for cartilage and Osteochondral tissue engineering approaches with adipose tissue derived stem cells, J. Mater. Sci., Mater. Med. 16 (2005) 1077–1085.

75. M. George, T.E. Abraham, Polyionic hydrocolloids for the intestinal delivery of protein drugs: alginate and chitosan — a review, J. Control. Release 114 (2006) 1–14.

76. M. Julien, D.R. Letouneau, Y. Marois, A. Cardou, M.W. King, R. Guidoin,

D. Chachra, J.M. Lee, Shelf-life of bioprosthetic heart valves: a structural and mechanical study, Biomaterials 18 (1997) 605–612.

77. S.C. Chen, Y.C.Wu, F.L. Mi, Y.H. Lin, L.C. Yu, H.W. Sung, A novel pHsensitive hydrogel composed of N,O-carboxymethyl chitosan and alginate cross-linked by genipin for protein drug delivery, J. Control. Release 96 (2004) 285–300.
78. P.A. Dell, W.G. Kohlman, Effects of water-content on the properties of starch poly(ethylene vinyl alcohol) blends, J. Appl. Polym. Sci. 52 (1994) 353–363.
79. C. Bastioli, A. Cerutti, I. Guanella, G.C. Romano, M. Tosin, Physical state and biodegradation behavior of starch–polycaprolactone systems, J. Environ. Polym. Degrad. 3 (1995) 81–95.
80. M.A. Villar, E.L. Thomas, R.C. Armstrong, Rheological properties of thermoplastic starch and starch poly(ethylene-co-vinyl alcohol) blends, Polymer 36 (1995) 1869– 1876.
81. M.A. Kotnis, G.S. Obrien, J.L. Willett, Processing and mechanical properties of biodegradable poly(hydroxybutyrate-co-valerate)-starch compositions, J. Environ. Polym. Degrad. 3 (1995) 97–105.
82. J.M. Mayer, G.R. Elion, C.M. Buchanan, B.K. Sullivan, S.D. Pratt, D.L. Kaplan, Biodegradable blends of cellulose–acetate and starch: production and properties, J. Macromol. Sci., Part A, Pure Appl. Chem. 32 (1995) 775–785.
83. D. Trimnell, G.F. Fanta, Formulations prepared from polyacrylamide and starch, J. Polym. Mater. 11 (1994) 271–277.
84. J. Nakamatsu, F.G. Torres, O.P. Troncoso, M.L. Yuan, A.R. Boccaccini, Processing and characterization of porous structures from chitosan and starch For tissue engineering scaffolds, Biomacromolecules 7 (2006) 3345–3355.
85. A.K. Bajpai, J. Shrivastava, alpha-Amylase induced enhanced enzymatic degradation of binary polymeric blends of crosslinked starch and gelatin, J. Macromol. Sci., Part A, Pure Appl. Chem. 41 (2004) 949–969,

86. C.K. Kuo, P.X. Ma, Ionically crosslinked alginate hydrogels as scaffolds for tissue engineering: part 1. structure, gelation rate and mechanical properties, Biomaterials 22 (2001) 511–521.

87. T. Pongjanyakul, S. Puttipipatkhachorn, Xanthan-alginate composite gel beads: molecular interaction and in vitro characterization, Int. J. Pharm. 331 (2007) 61–71.

88. M.G. Meirim, E.W. Neuse, D.D. N'Da, *J. Appl. Polm. Sci.,* **82**, 1844 (2001).

89. G. Caldwell, E.W. Neuse, *S. Afr. J. Chem.,* **45** (4), 93 (1992).

90. G. Caldwell, .W. Neuse, A.G. Perlwitz, *Journal of Inorganic and Organometallic Polymers,* Vol. 7, **2**, (1997).

91. G. Caldwell, E.W. Neuse, A. Stephanou, *J. Appl. Polym. Sci.,* **50**, 393 (1993).

92. E.W. Neuse, A.G. Perlwitz, in *Water-Soluble Polymers,* S.W. Shalaby, C.L. McCormick and G.B. Butler, Eds., American Chemical Society, Washigton, DC, (1991), Chap. 25.

93. D.D. N'Da, *Synthesis of Polymeric iron and platinum compounds for anticancer activity screening.* MSc Thesis, University of the Witwatersrand (2000).

94. M.G. Meirim, *Polymer-conjugated anticancer drugs.* MSc Thesis, University of the Witwatersrand (2002); and references cited.

95. G. Caldwell, M.G. Meirim, and E.W. Neuse, *Fourth International Symposium on Polymers for Advanced Technologies (PAT'97)*, Leipzig, Germany, August 31 – September 4, 1997; Abstr. P PVII.5.

96. E.W. Neuse, *Fourth International Symposium on Polymers for Advanced Technologies (PAT'97)*, Leipzig, Germany, August 31 – September 4, 1997; Abstr. P PVII.5.

97. G. Caldwell, M.G. Meirim, E.W. Neuse, C.E.J. van Rensburg, *Appl. Organomet. Chem.*, **12**, 793 (1998).

98. E.W. Neuse, *Polym. Advan. Technol.*, **9**, 786 (1998). See also: *Chemical Perspective,* **1**, 69 (2000).

99. M.G. Meirim, E.W. Neuse, G. Caldwell, *J. Inorg. Organometal. Polym.*, **8**, 225 (1998).

100. G. Caldwell, E.W. Neuse, C.E.J. van Rensburg, *Appl. Organomet. Chem.,* **13**, 189 (1999).

101. M.G. Meirim, E.W. Neuse, G. Caldwell, *J. Appl. Polym. Sci.*, **73**, 2143 (1999).

102. E.W. Neuse, M.G. Meirim, H.M. Netshifhefhe, W.-C. Shen, *40th Microsymposium "Polymers in Medicine"*, Prague, 17-20 July 2000; Abstr. P34.

103. M.G. Meirim, D.D. N'Da, E.W. Neuse, W.-C. Shen, and C.E.J. van Rensburg, *40th Microsymposium "Polymers in Medicine"*, Prague, 17-20 July 2000; Abstr. P34.

104. M.G. Meirim, E.W. Neuse, D.D. N'Da, *J. Appl. Polm. Sci.,***82**, 1844 (2001).

105. H. Ringsdorf. *J. Polym. Sci. Symp.,* **51**, 135 (1975).

106. E.W. Neuse, in *Macromolecules containing metal-like elements,* Volume 3: Biomedical applications*,* A.S. Abd-El-Aziz, C.E. Carraher, C.U. Pittman, J.E. Sheats, M. Zeldin, Eds., Wiley & Sons, New York (2004), Chap. 6.

107. Arwyn T. Jones, Intracellular drug delivery. Workshop report from the 28th international symposium on controlled released of bioactive materials, San Diego, 23-24 June 2001

108. Taylor A.E. and Granger .D.N.[1983] equivalent pore modeling vesicles and channels federation proc.42.2440-2445.

109. Wisse .E. and de Leeuw, A.M. (1984). Structural elements determining transport and exchange processes in the liver. In: s.s.Davis,L.IIlum,j.g.Mc vie and E. Tomlinson (Eds.), microsphere and drug therapy: Pharmaceutical, Immunological and medical aspects .elsevier , Amsterdam, pp.1-23].

110. Takakura Y., Furisu H., Nishikawa M., Sezaki H. and Hashida M. (1994). Pharmacokinetics of succinylated proteins and dextran sulfate in mice: implications for hepatictargeting of proteindrugs by direct succinylation via scavenger receptors Int. J. Pharm. 105. 19-29.//10 kawabata K., Takakura,Y.and Hashida.M.{1995}The fate of plasmid DNA after intravenous injection in mice:involvement of scavenge receptors in its hepatic uptake.pharm.Res.12,825 – 830.

111. Control of pharmacokinetic profiles of drug-macromolecule conjugates Yoshinobu Taakakura,Ram I.Mahato,Makiya nishikawa,Mitsuru

Hashida'' Department of drug Delivery Research,Faculty of pharmaceutical Sciences,Kyoto-ku,Kyoto 60641. Japan,Advanced Drug Delivery Reviews 19 (1996) 377-399.

112. Yoshinobu Takakura, Ram I. Mahato, Makiya Nishikawa, Mitsuru Hashida Control of pharmacokinetic profiles of drug-macromolecule conjugates. Advanced Drug Delivery Reviews 19 (1996) 377-399

113. Duncan, R.; Dimithjevic, S.; and Evagorou, E. G.; *STP Pharma Sci.* **6** (1996) 234-263.

114. Neuse, E. W., *Macromol. Symp.* **172** (2001) 127-138.

115. Neuse, E. W.; Meirim, M. G.; N'Da, D. D.; Caldwell, G.; *J. Inorg. Organometal. Polym.* **9** (1999) 221-230.

116. Jonhson, M. T.; Kreft, E.; N'Da, D. D.; Neuse, E. W.; van Rensburg, C. E. J.; *J. Inorg. Organometal. Polym.* **13** (2003) 225.

117. Bull. Inst. Chem. Res.; Kyoto Univ., Vol. 64, No. 4, 1986

118. SureLINK^{TM} Bioconjugation Kit and linkers deliver. Internet sources: available at www.kpl.com (accessed on January, 20 2010).

119. Stanislav Jaracz, Jin Chen, Larisa V. Kuznetsova and Iwao Ojima, Recent advances in tumor-targeting anticancer drug conjugates. Department of Chemistry and Institute of Chemical Biology and Drug Discovery, State University of New York at Stony Brook, Stony Brook, NY (2005) 11794-3400, USA

120. J. Drobník, V. Saudek, J. Vlasák, and J. Kala, *J. Polym. Sci., Polym. Symp.,* **66**, 65 (1979).

121. P. Neri, G. Antoni, *Macromol. Synth.,* **8**, (1982), 25.

122. C.J. Chang and G.Swift, *J.M.S. Pure Appl. Chem.* **A36** (7 & 8), 949-961 (1999).

123. E.W. Neuse, A.G Perlwitz, A.P. Barbosa, J. Appl. Polym. Sci, 54, 57 (1994)

124. A. Gelasco, S.J. Lippard, in *Metallopharmaceuticals I DNA interactions: Topics in Biological Inorganic Chemistry,* **1**, M.J. Clarke, P.J. Sadler, Eds., Springer, New York, (1999), 1.

125. J. Drobník, V. Saudek, J. Vlasák, and J. Kala, *J. Polym. Sci., Polym. Symp.,* **66**, 65 (1979).

126. C.W.N. Mboyama and E.W. Neuse, in 'Inorganic and Metal-containing

Polymeric Materials'. J. Sheats, et al., Eds., Plenum press, New York, 1990, p. 139.

127. G.A. Caldwell, E.W. Neuse, and M.G. Meirim, J. Inorg. *Organometal*. Chem. 2, 129 (1988).

128. J.C. Swarts, E.W. Neuse, and G.A. Caldwell, J. Inorg. Organometal. Polym. 7, 71 (1991).

129. Padilla De Jesu´ s OL, Ihre HR, Gagne L, Fre´chet JMJ, Szoka FC. Polyester dendritic systems for drug delivery applications: in vitro and in vivo evaluation. Bioconjug Chem 2002;13:453– 61.

130. Gras-Masse H. Chemoselective ligation and antigen vectorization. Biologicals 2001;29:183– 8.

131. Bourel-Bonnet L, Pe´cheur EI, Grandjean C, Blanpain A, Baust T, Melnyk O, et al. Anchorage of synthetic peptides onto liposomes via hydrazone and a-oxo hydrazone bonds. Preliminary functional investigations. Bioconjug Chem 2005;16:450– 7.

132. Zubin EM, Stetsenke DA, Zatsepin TS, Gait MJ, Oretskaya TS. Oligonucleotides containing 2V-O-[2-(2,3-dihydroxypropyl)amino-2-oxoethyl]uridine as suitable precursors of 2V- aldehyde oligonucleotides for chemoselective ligation. Bioorg Med Chem 2005;13: 4912– 20.

133. Chang YS, Jeong JM, Lee YS, Kim HW, Rai GB, Lee SJ, et al. Preparation of 18F-human serum albumin: a simple and efficient protein labeling method with 18F using a hydrazone- formation method. Bioconjug Chem 2005;16:1329– 33.

APPENDIX

SELECTED ^{1}H NMR

(^{1}H NMR spectrum were processed by MestRec 4.8.6 NMR PROCESSOR)

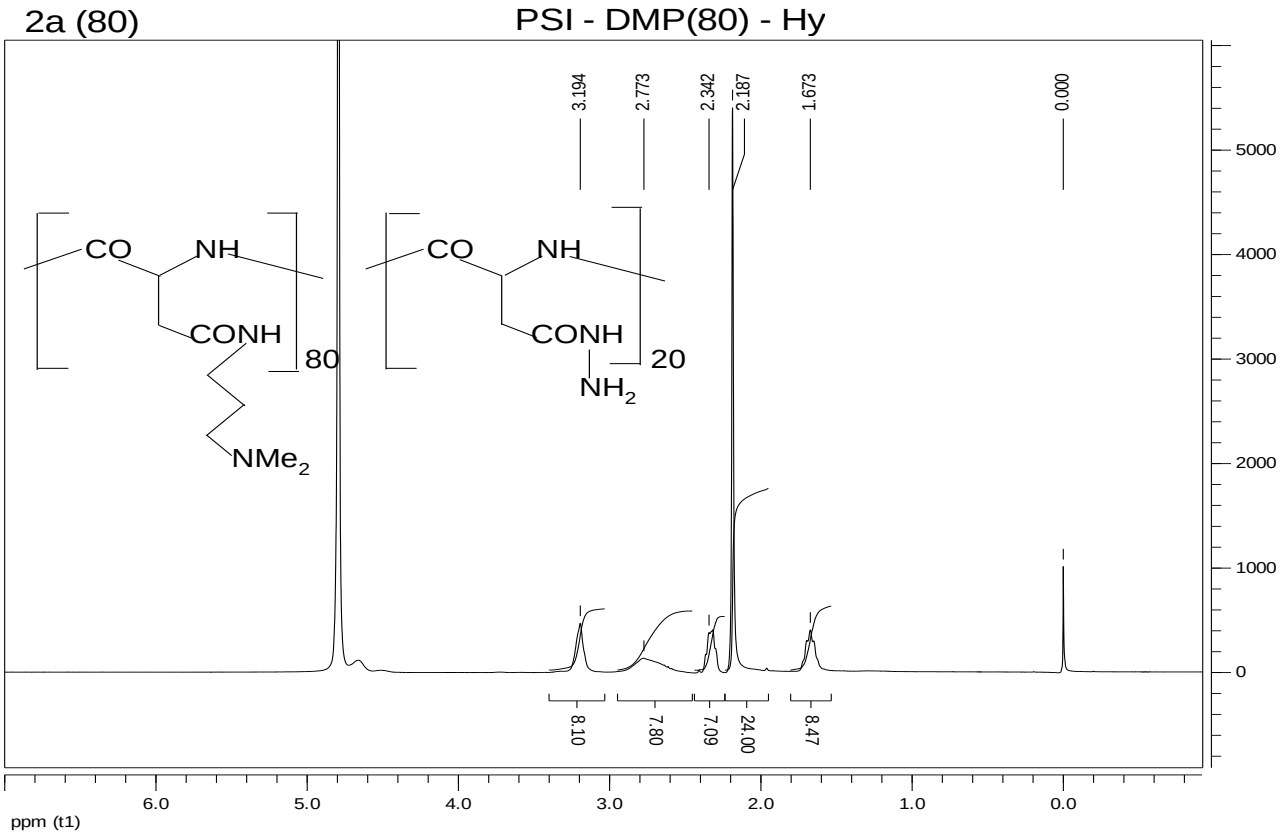
2a (80)
PSI - DMP(80) - Hy
3.194
2.773
2.342
2.187
1.673
0.000
CO
NH
CONH
80
NMe2
CO
NH
CONH
20
NH2
8.10
7.80
7.09
24.00
8.47
ppm (t1)

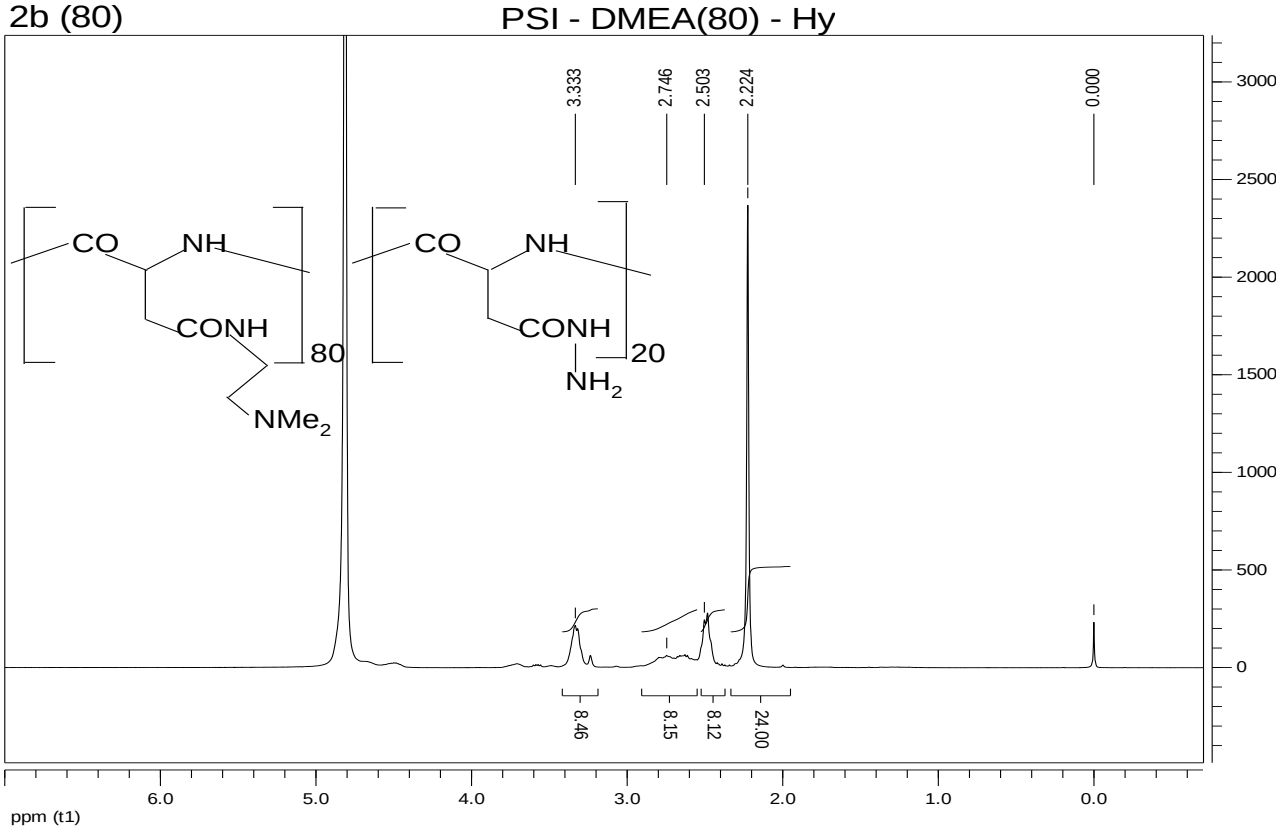
2b (80)
PSI - DMEA(80) - Hy
3.333
2.746
2.503
2.224
0.000
CO
NH
CONH
80
NMe2
CO
NH
CONH
20
NH2
8.46
8.15
8.12
24.00
ppm (t1)

2c (80)

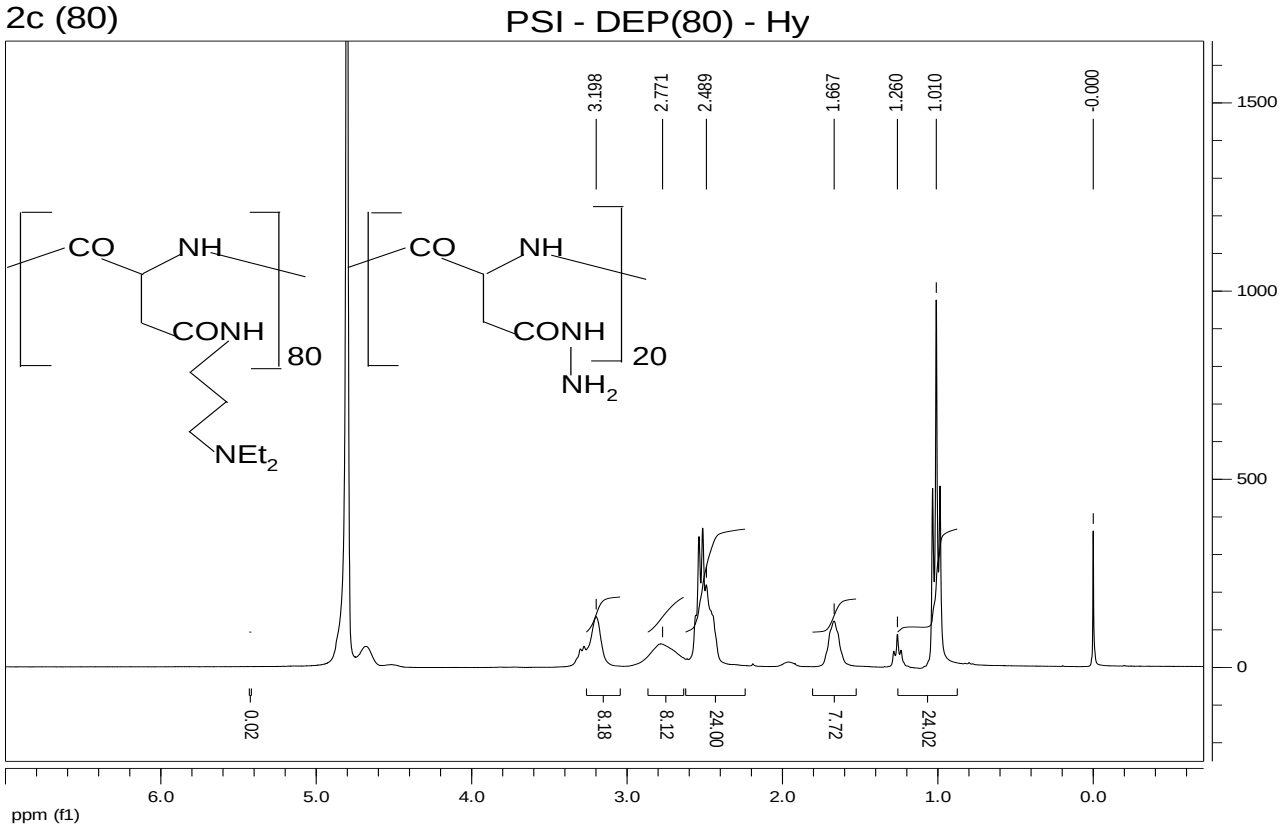
PSI - DEP(80) - Hy
3.198
2.771
2.489
1.667
1.260
1.010
-0.000
CO
NH
CONH
80
CONH
NH2
20
NEt2
0.02
8.18
8.12
24.00
7.72
24.02
1500
1000
500
0
6.0
5.0
4.0
3.0
2.0
1.0
0.0
ppm (f1)

2d (80)

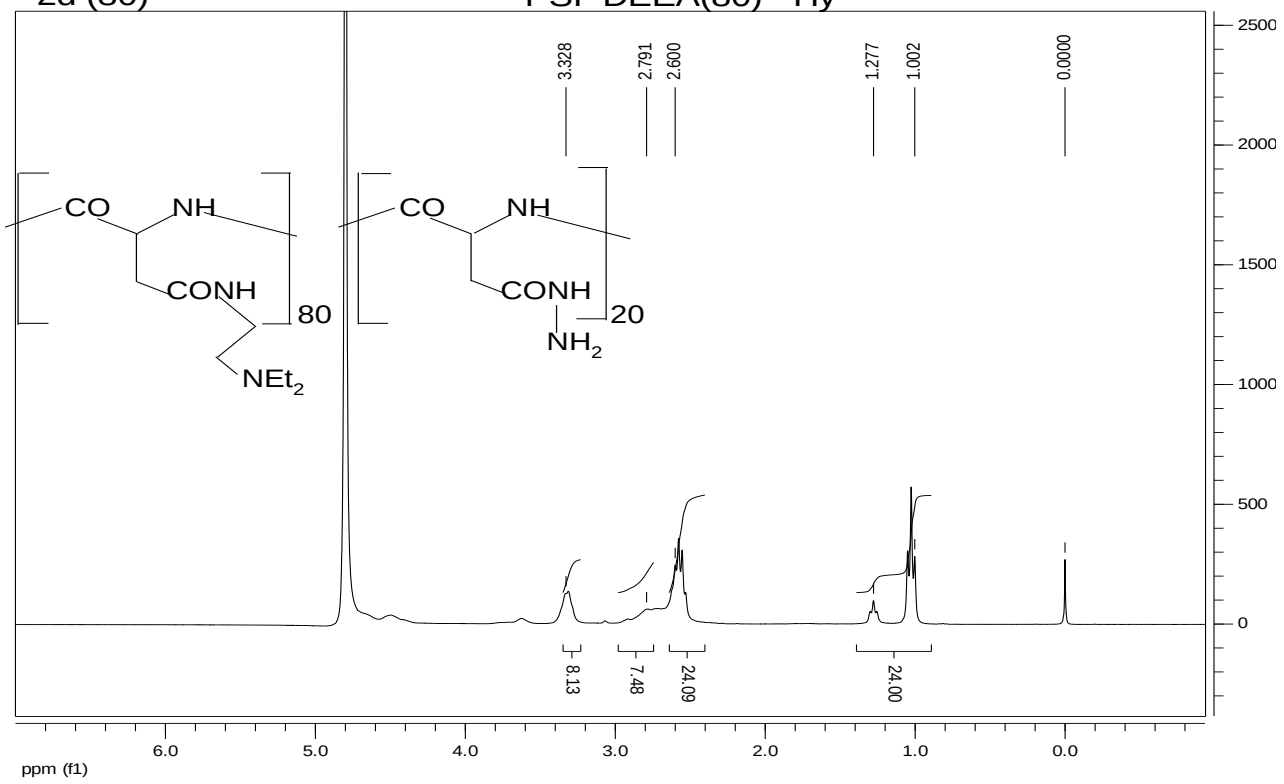
PSI -DEEA(80) - Hy
3.328
2.791
2.600
1.277
1.002
0.0000
CO
NH
CONH
80
CONH
NH2
20
NEt2
8.13
7.48
24.09
24.00
2500
2000
1500
1000
500
0
6.0
5.0
4.0
3.0
2.0
1.0
0.0
ppm (f1)

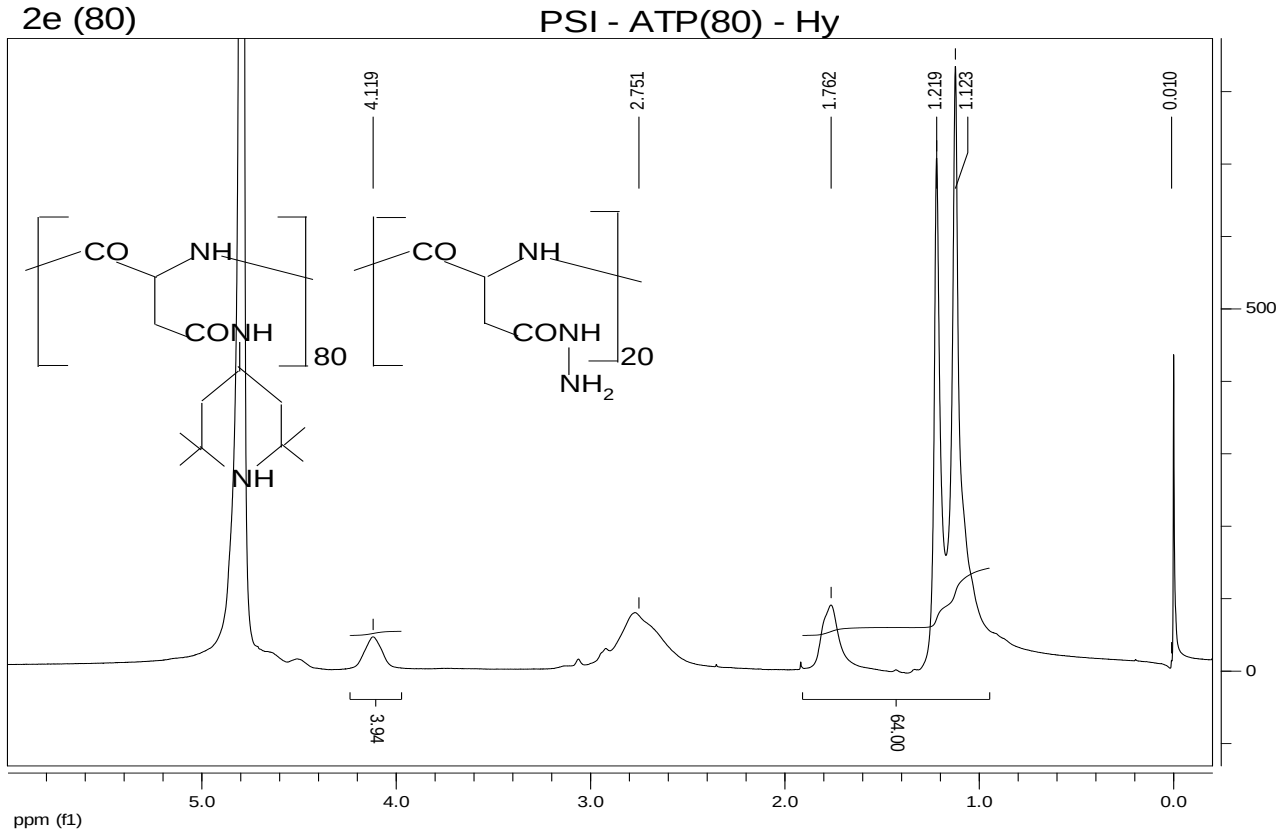
2e (80)
PSI - ATP(80) - Hy
4.119
2.751
1.762
1.219
1.123
0.010
CO
NH
CONH
80
CO
NH
CONH
20
NH2
NH
3.94
64.00
5.0
4.0
3.0
2.0
1.0
0.0
ppm (f1)
500
0

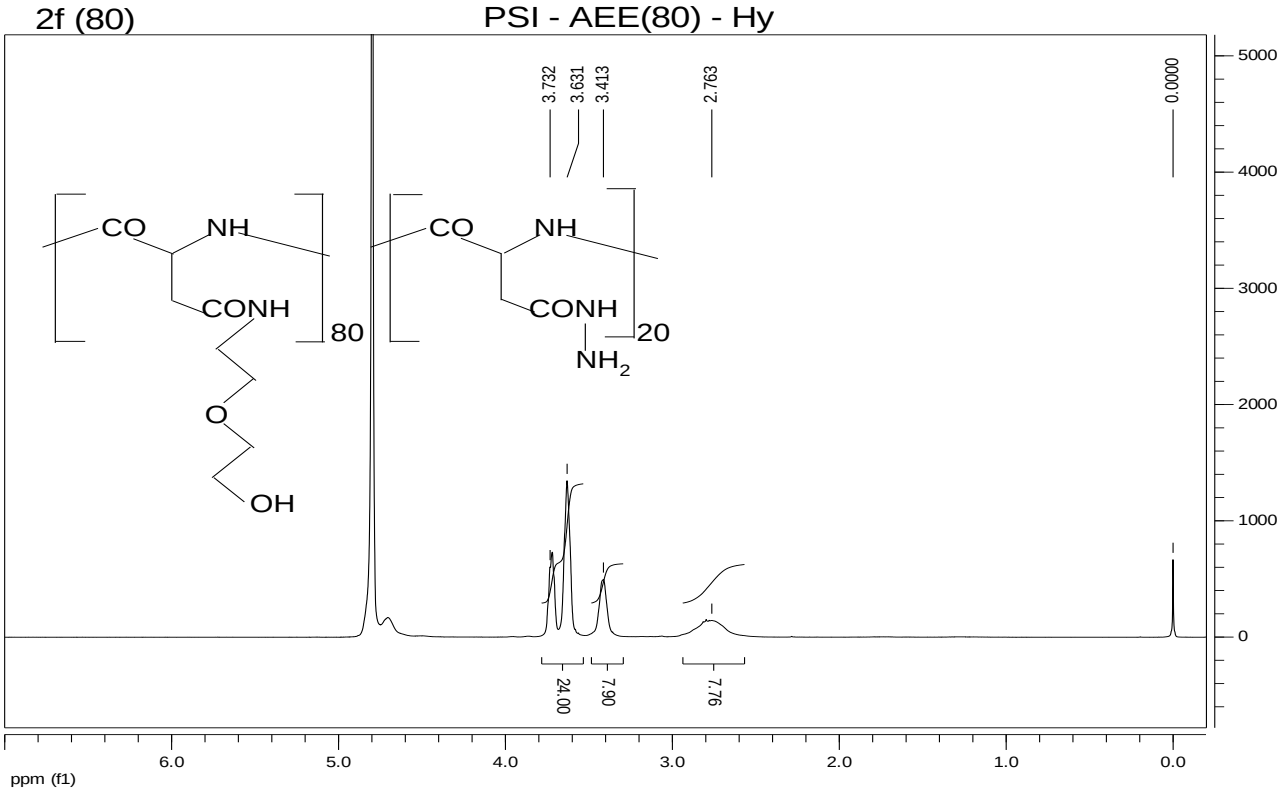
2f (80)
PSI - AEE(80) - Hy
3.732
3.631
3.413
2.763
0.0000
CO
NH
CONH
80
CO
NH
CONH
20
NH2
O
OH
24.00
7.90
7.76
6.0
5.0
4.0
3.0
2.0
1.0
0.0
ppm (f1)
5000
4000
3000
2000
1000
0

2a (90) PSI - DMP(90) - Hy

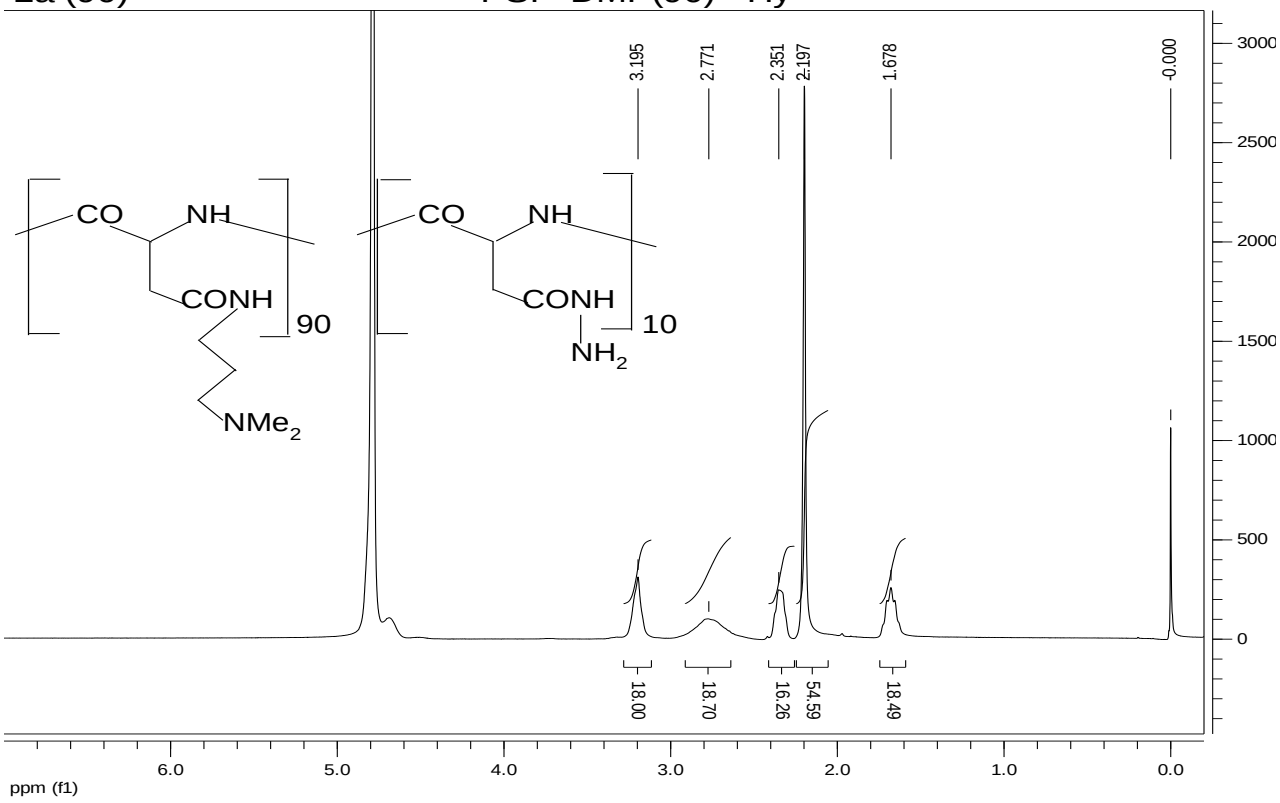

2b (90) PSI - DMEA(90) - Hy

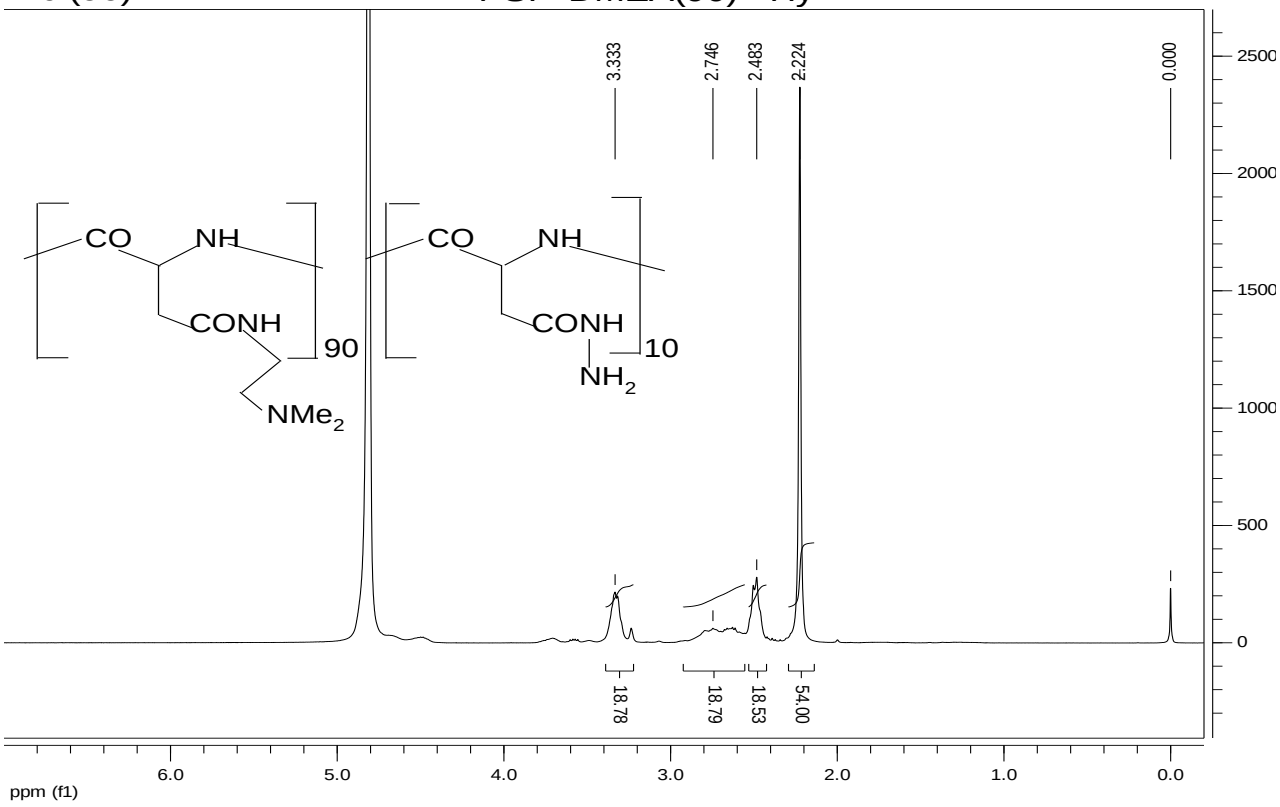

2c (90)

PSI - DEP(90) -Hy

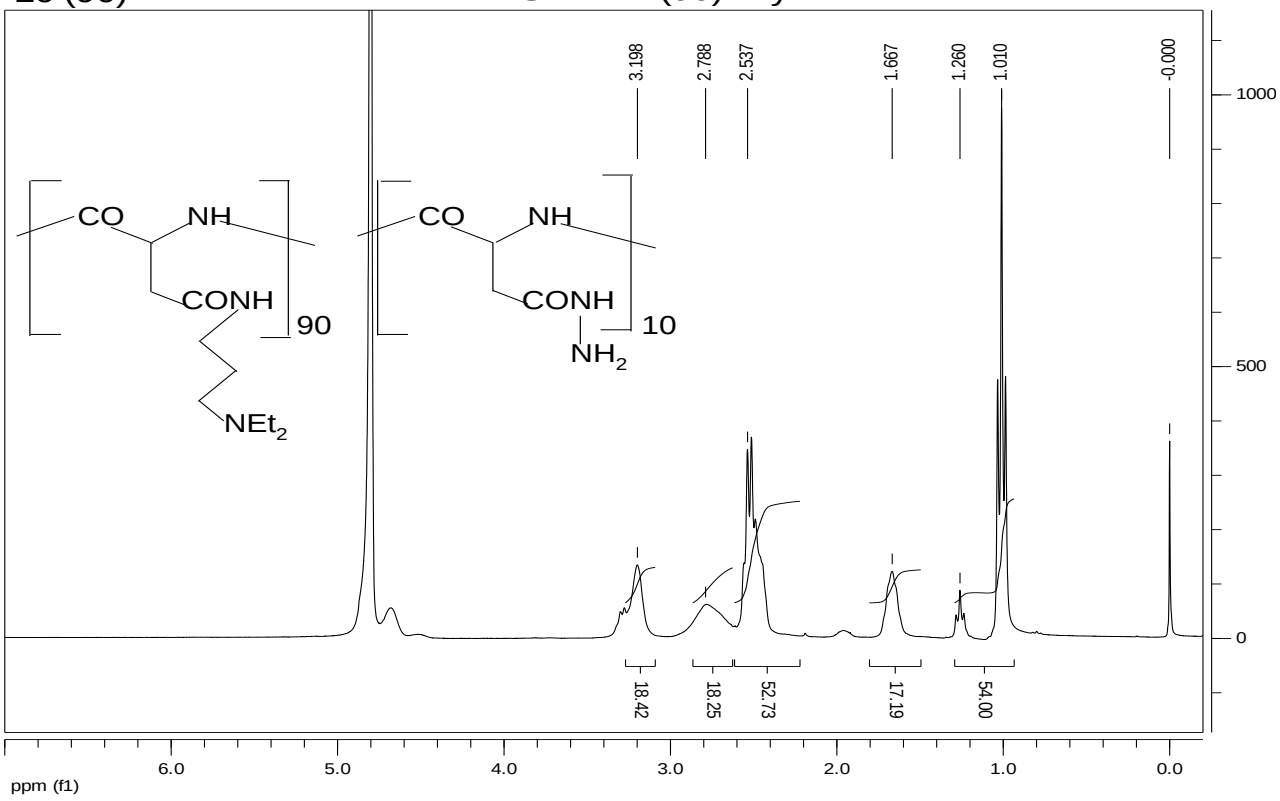

2d (90)

PSI - DEEA(90) - Hy

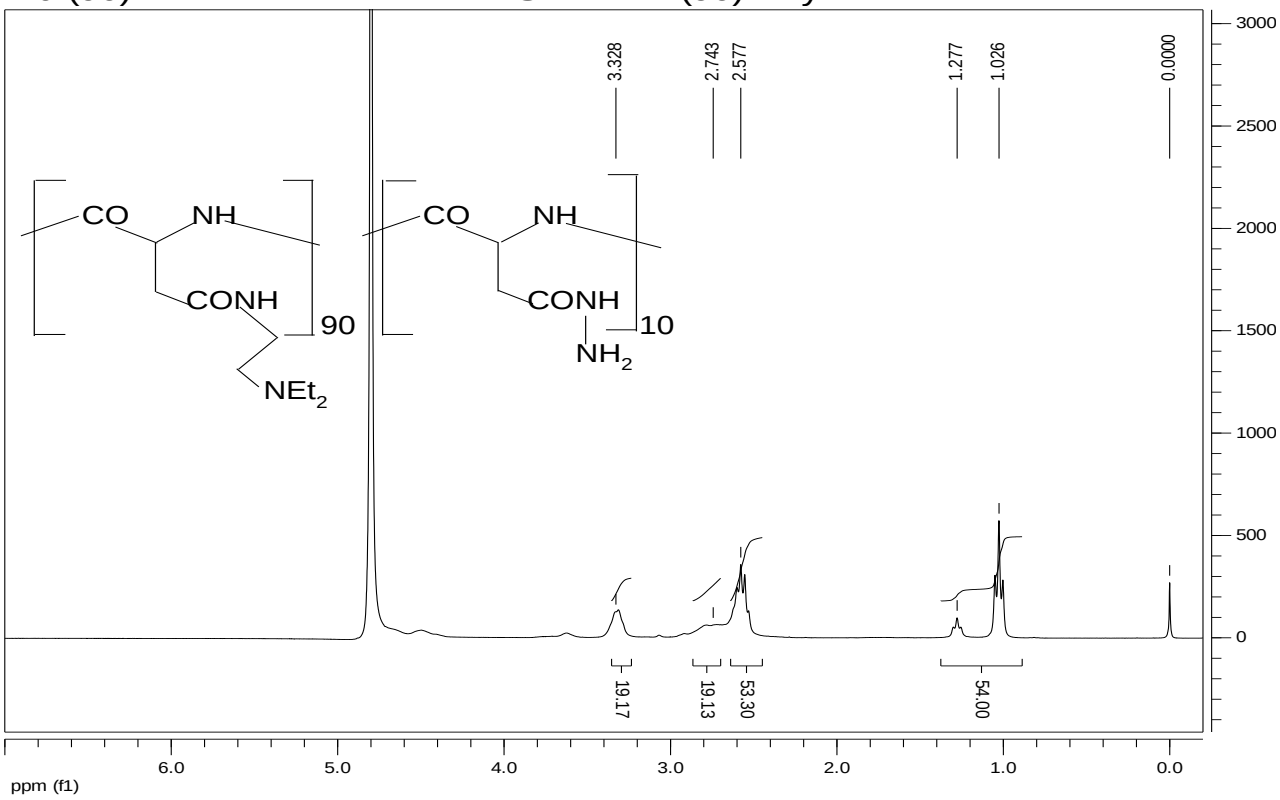

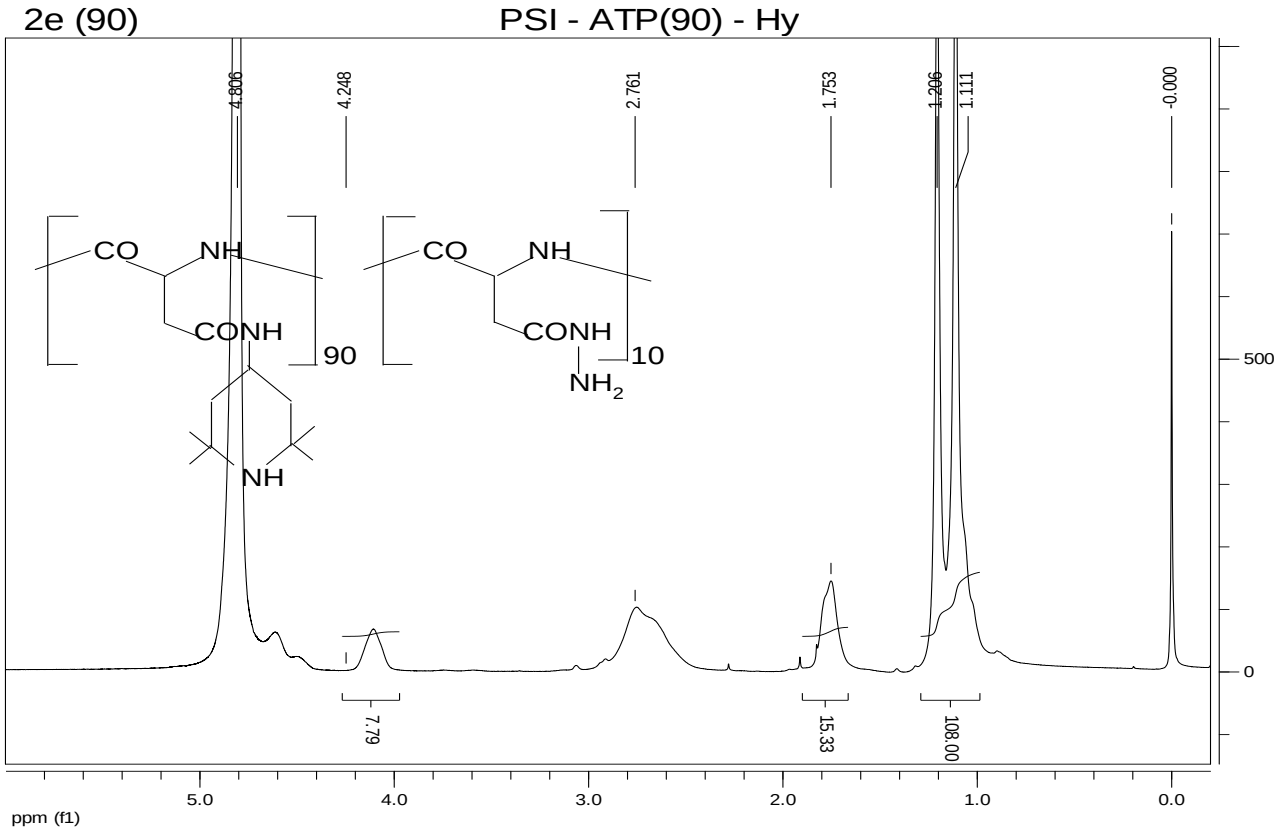
2e (90)
PSI - ATP(90) - Hy
4.806
4.248
2.761
1.753
1.296
1.111
-0.000
CO
NH
CONH
90
10
NH2
NH
7.79
15.33
108.00
500
0
5.0
4.0
3.0
2.0
1.0
0.0
ppm (f1)

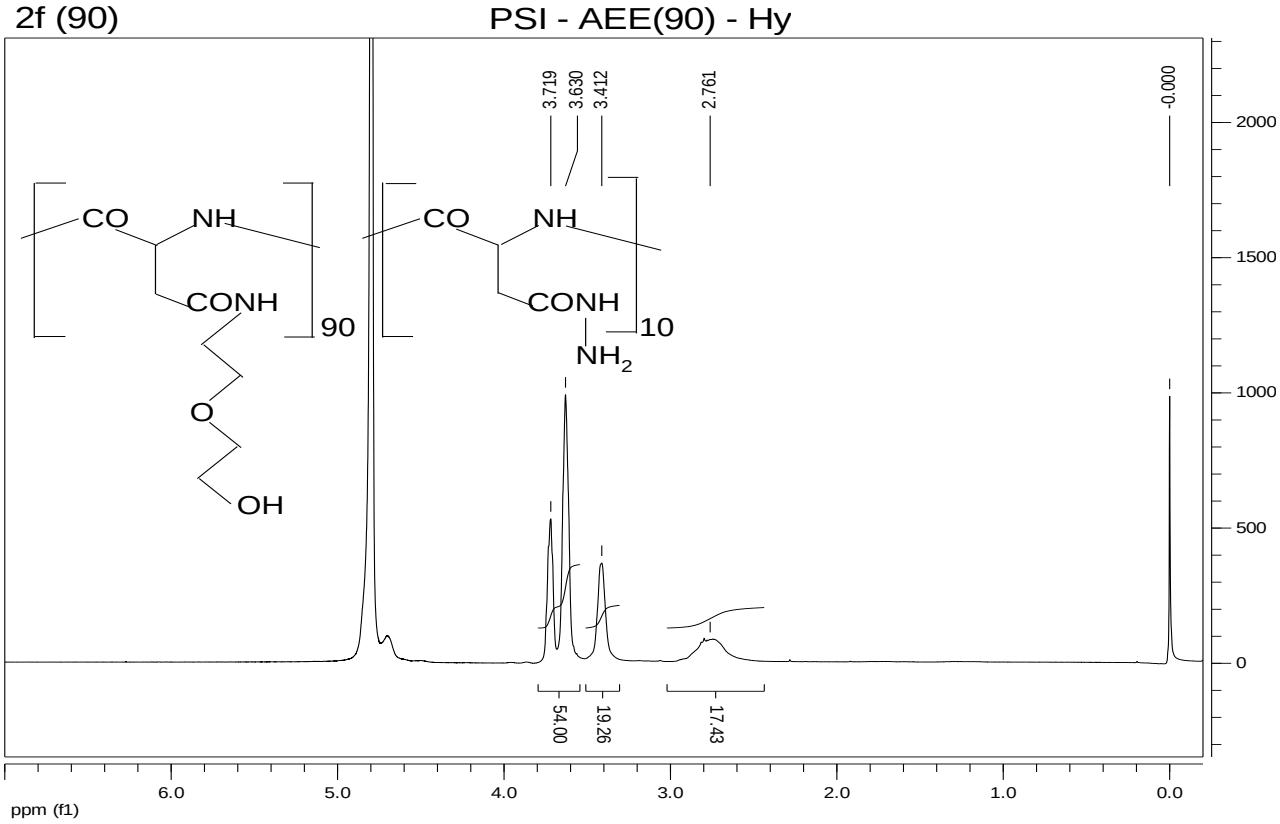
2f (90)
PSI - AEE(90) - Hy
3.719
3.630
3.412
2.761
-0.000
CO
NH
CONH
90
10
NH2
O
OH
54.00
19.26
17.43
2000
1500
1000
500
0
6.0
5.0
4.0
3.0
2.0
1.0
0.0
ppm (f1)

3a (50)

PSI - DMP(40) - AEE(50) - Hy

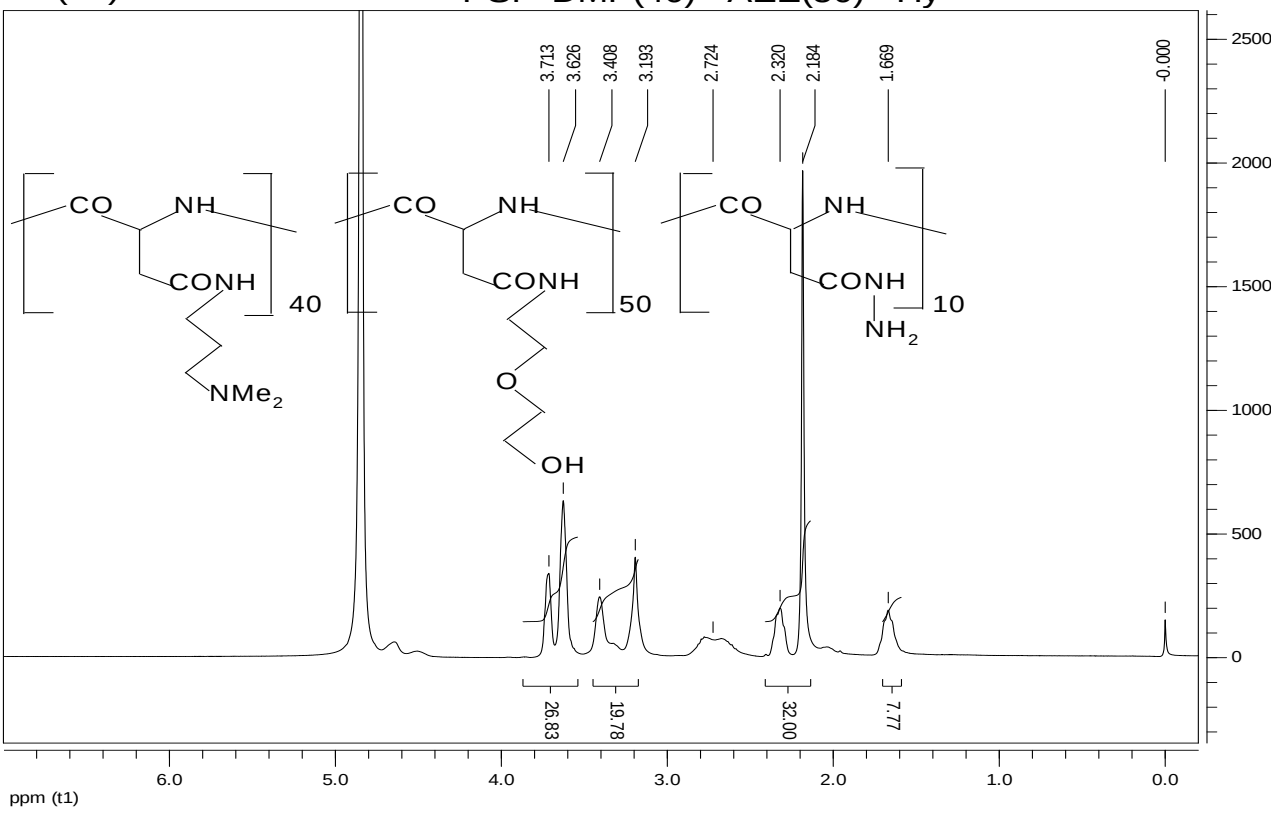

3b (50)

PSI - DMEA(40) - AEE(50) - Hy

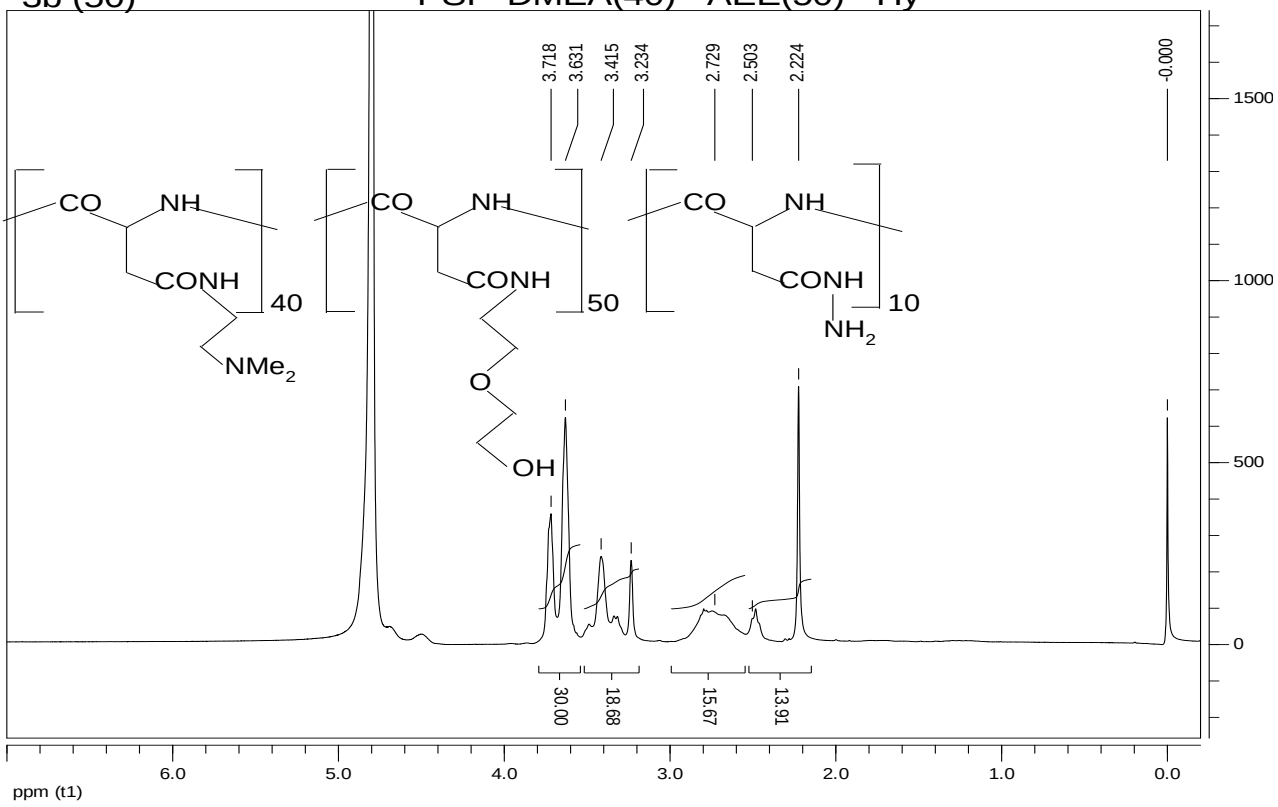

3c (50) PSI - DEP(40) - AEE(50) - Hy

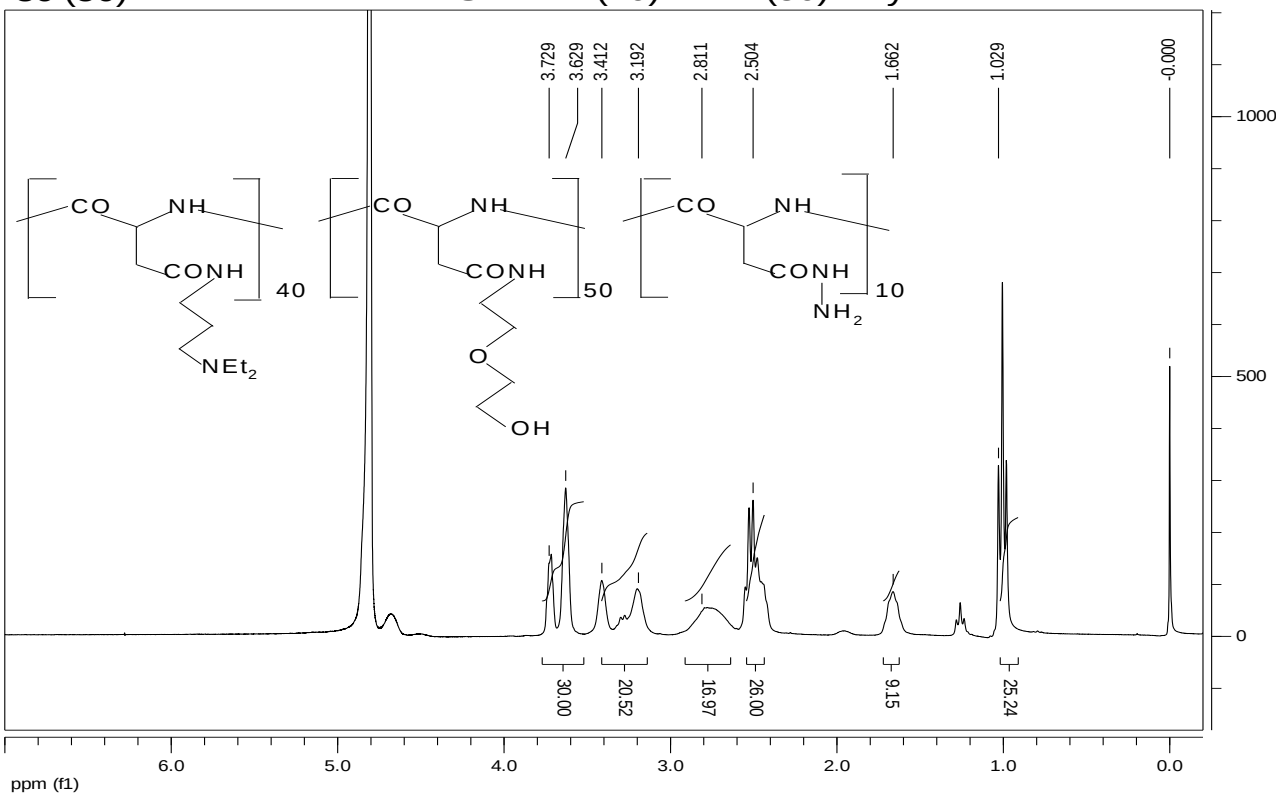

3d (50) PSI - DEEA(40) - AEE(50) - Hy

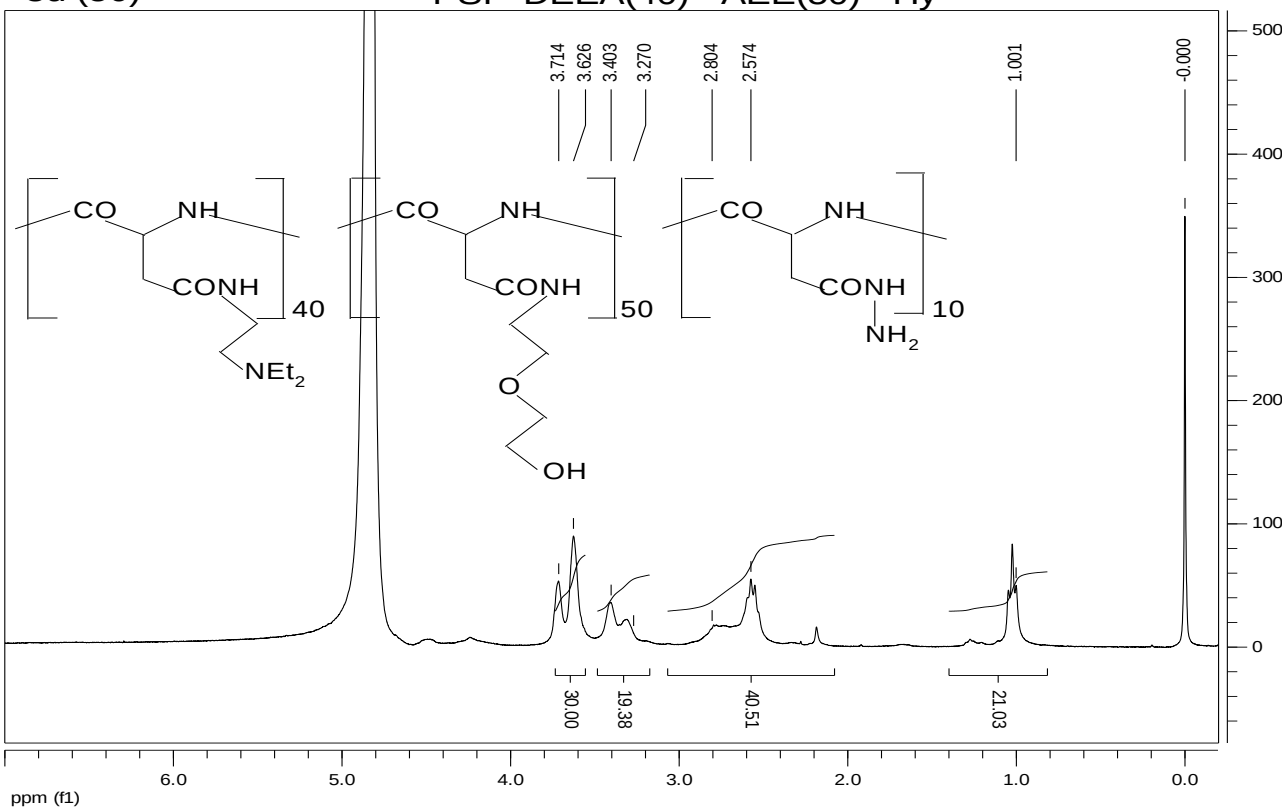

3e (50)

PSI - ATP(40) - AEE(50) - Hy

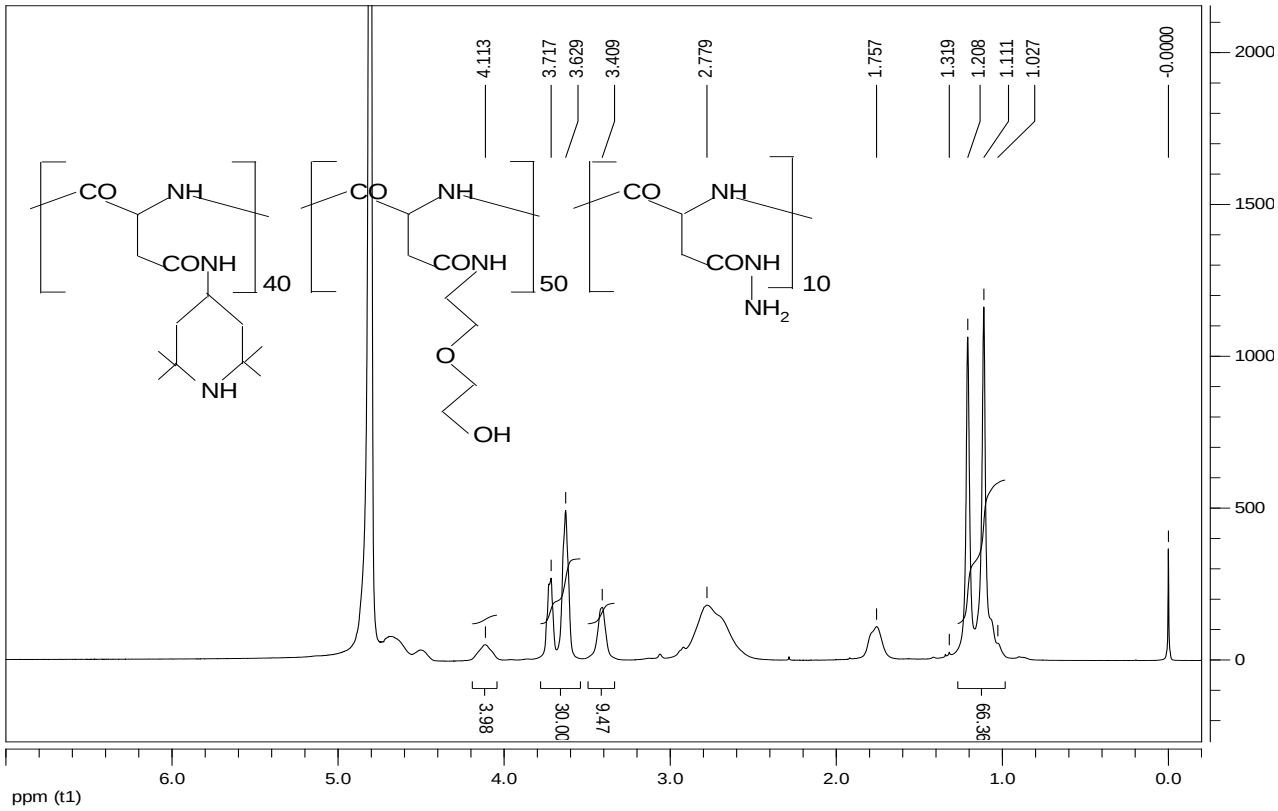

3a (60)

PSI - DMP(60) - AEE(20) - Hy

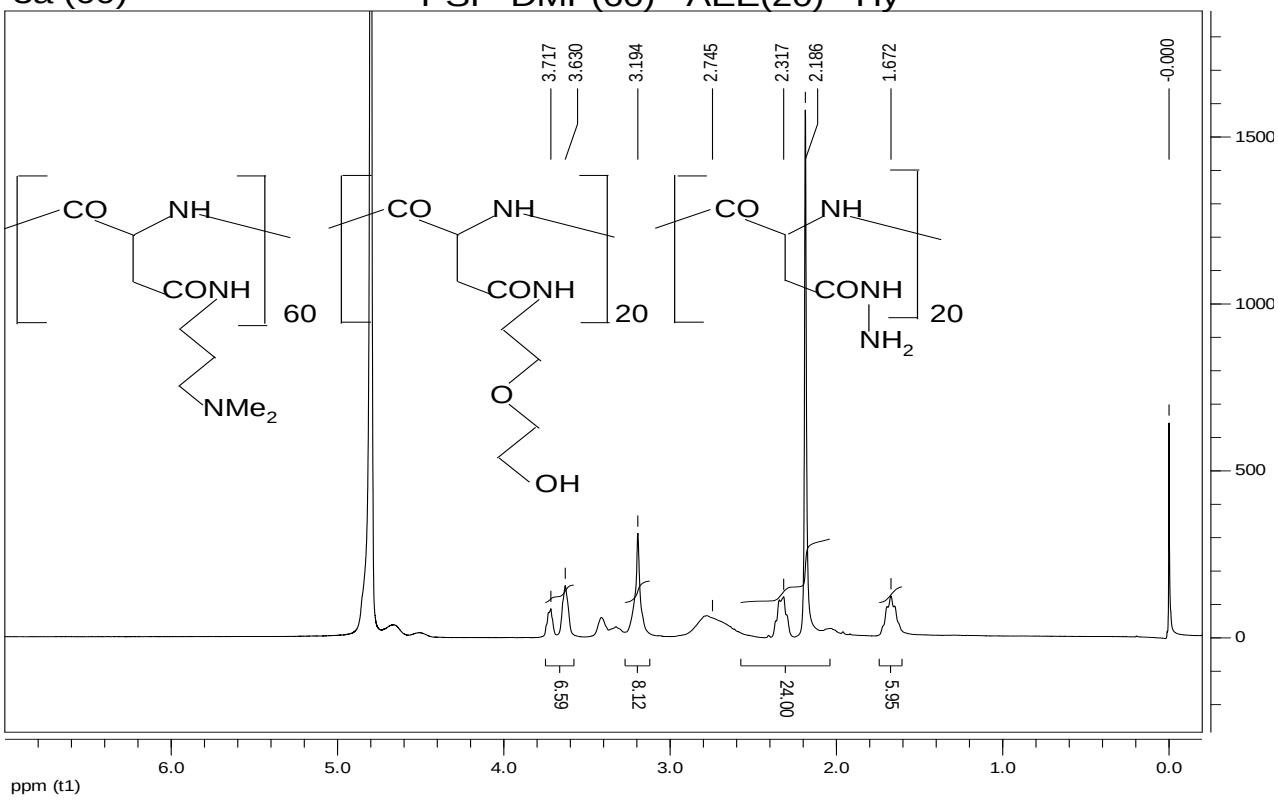

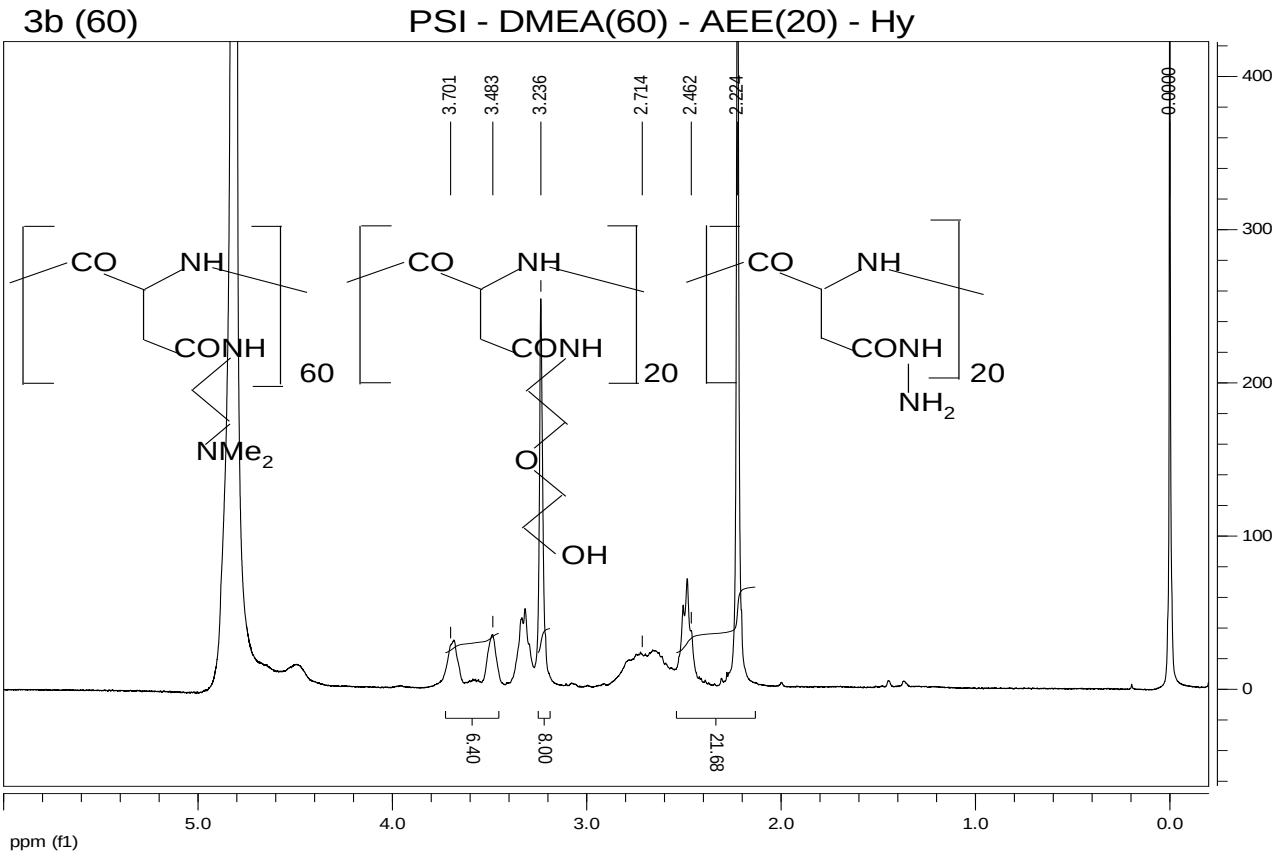
3b (60)
PSI - DMEA(60) - AEE(20) - Hy
3.701
3.483
3.236
2.714
2.462
2.224
0.0000
CO
NH
CONH
60
NMe2
20
O
OH
20
NH2
6.40
8.00
21.68
400
300
200
100
0
5.0
4.0
3.0
2.0
1.0
0.0
ppm (f1)

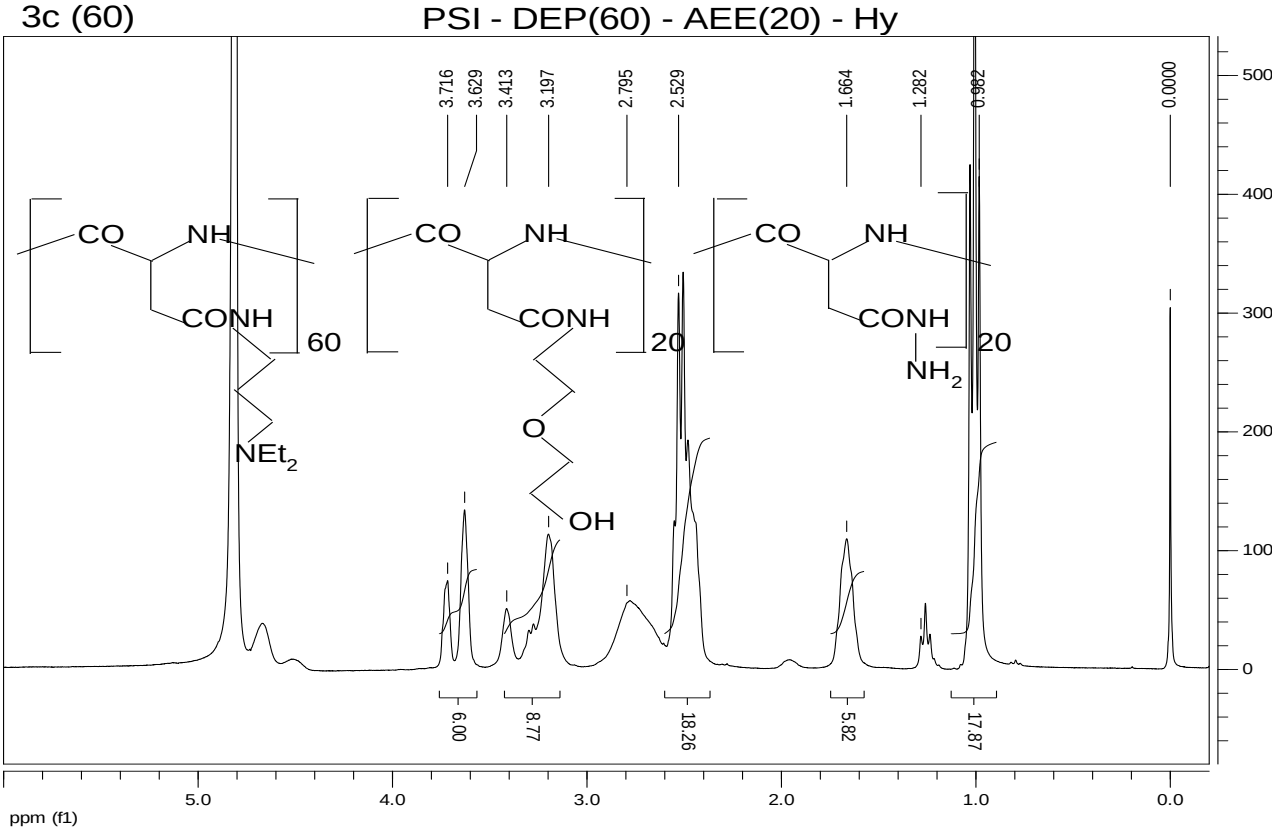
3c (60)
PSI - DEP(60) - AEE(20) - Hy
3.716
3.629
3.413
3.197
2.795
2.529
1.664
1.282
0.982
0.0000
CO
NH
CONH
60
NEt2
20
O
OH
20
NH2
6.00
8.77
18.26
5.82
17.87
500
400
300
200
100
0
5.0
4.0
3.0
2.0
1.0
0.0
ppm (f1)

3e (60)

PSI - ATP(60) - AEE(20) - Hy

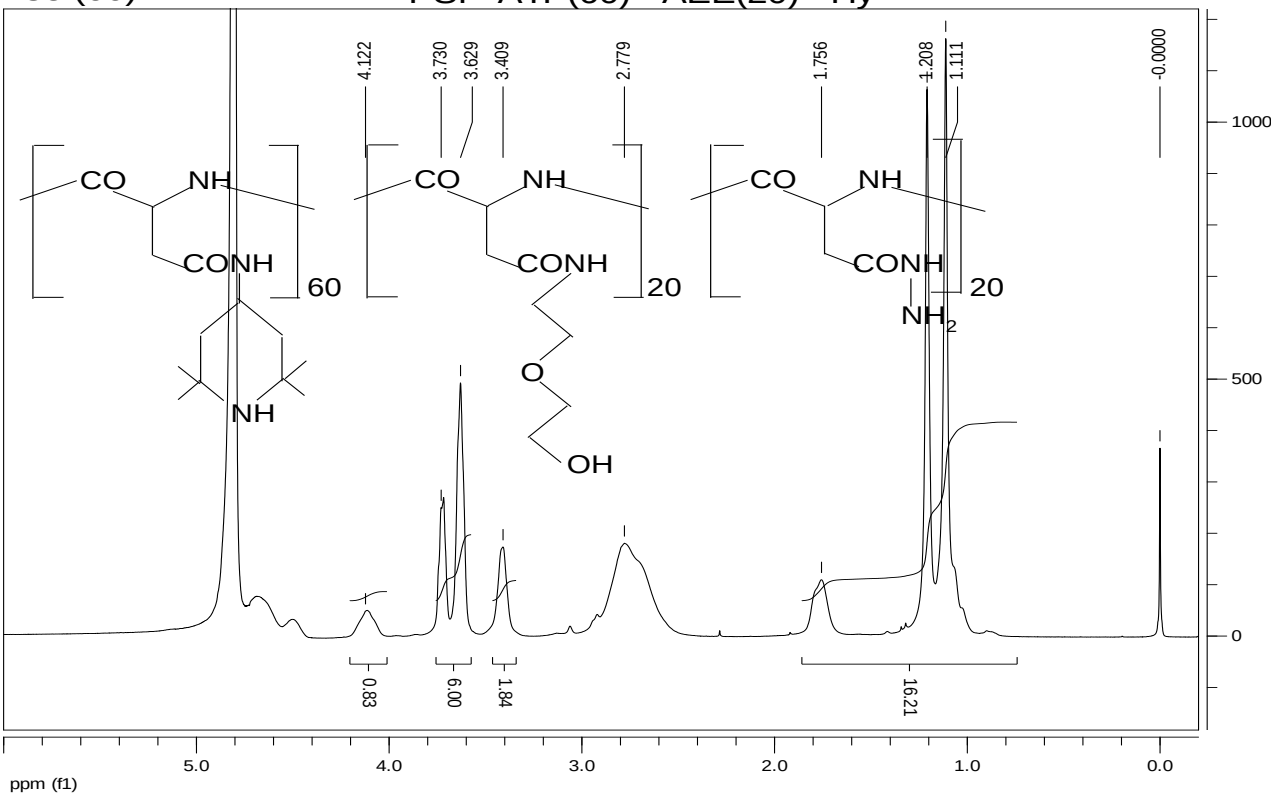

4a (50)

PSI - DMP(40) - ATP(50) - Hy

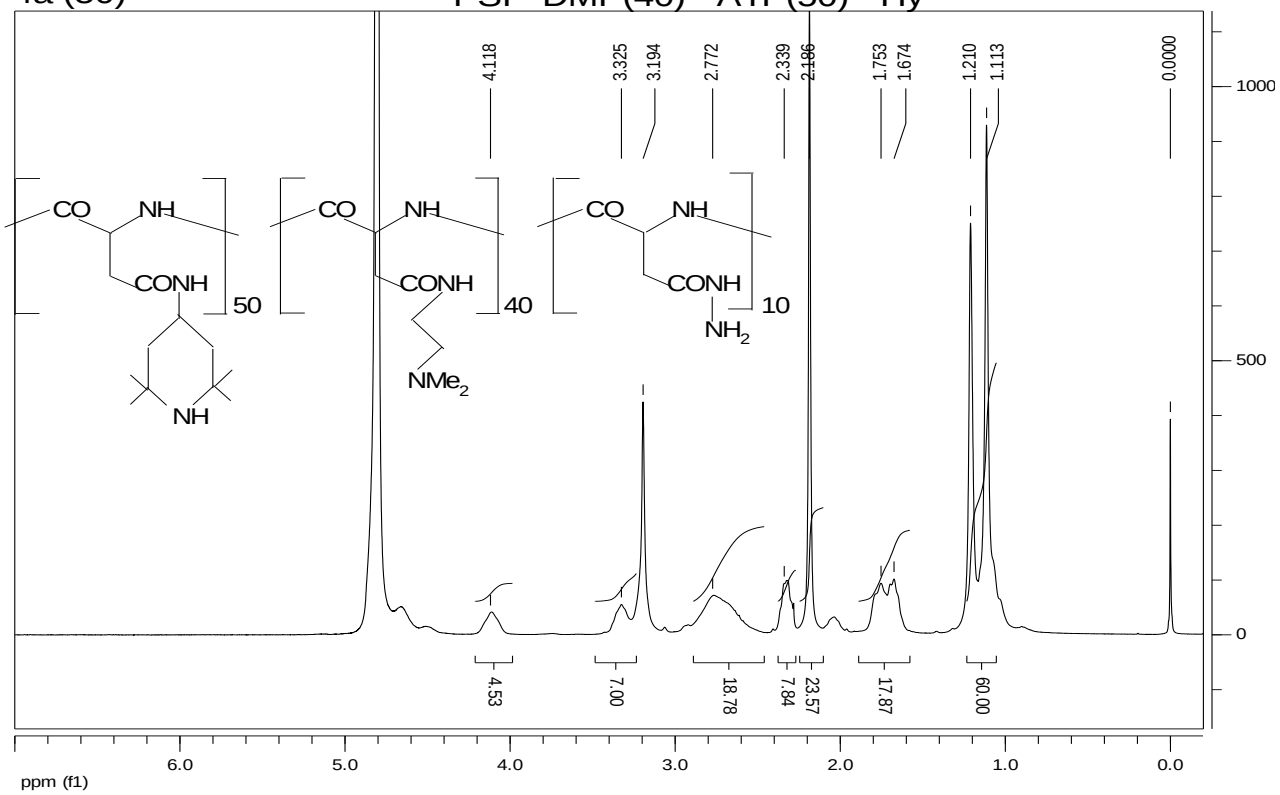

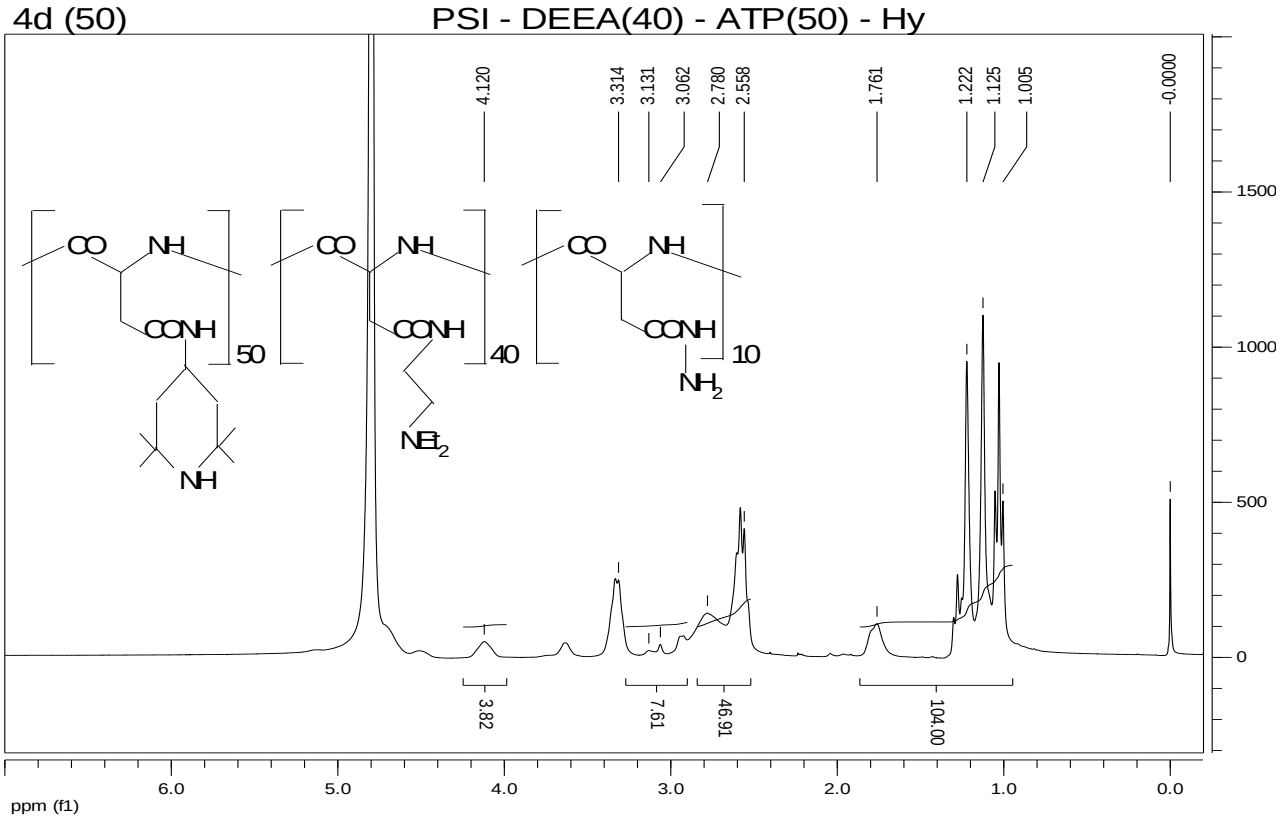
4d (50)
PSI - DEEA(40) - ATP(50) - Hy
4.120
3.314
3.131
3.062
2.780
2.558
1.761
1.222
1.125
1.005
-0.0000
CO
NH
CONH
50
40
10
NH2
NEt2
NH
3.82
7.61
46.91
104.00
1500
1000
500
0
6.0
5.0
4.0
3.0
2.0
1.0
0.0
ppm (f1)

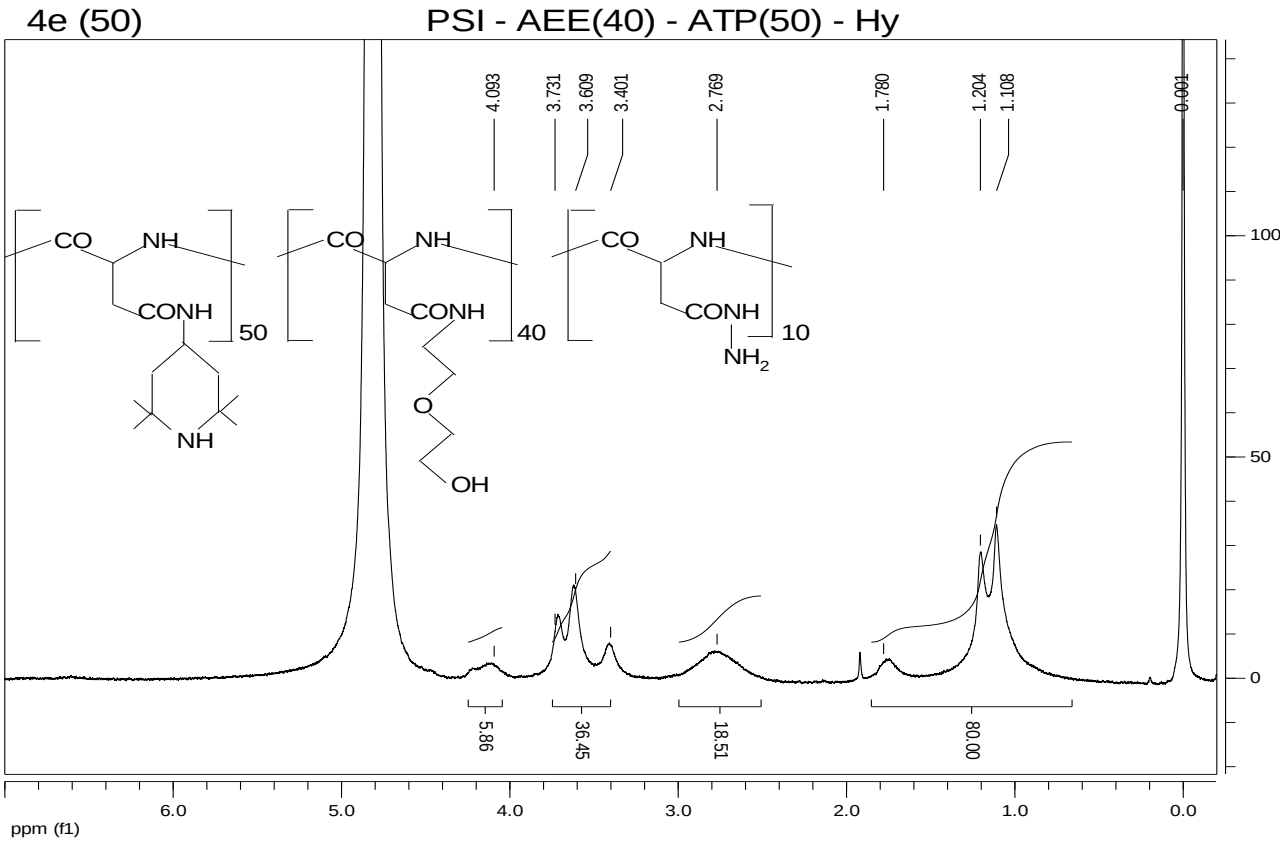
4e (50)
PSI - AEE(40) - ATP(50) - Hy
4.093
3.731
3.609
3.401
2.769
1.780
1.204
1.108
0.001
CO
NH
CONH
50
40
10
NH2
O
OH
NH
5.86
36.45
18.51
80.00
100
50
0
6.0
5.0
4.0
3.0
2.0
1.0
0.0
ppm (f1)

4a (60)

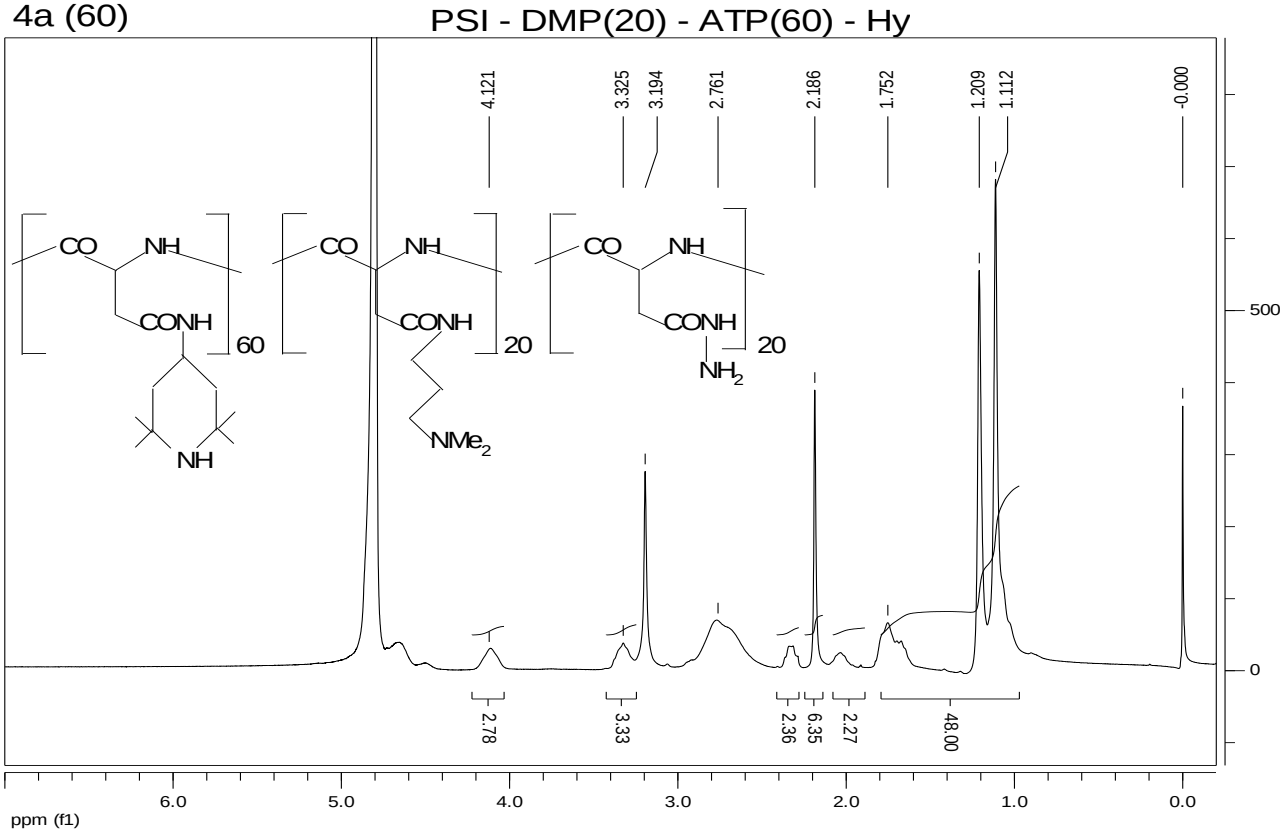
PSI - DMP(20) - ATP(60) - Hy
4.121
3.325
3.194
2.761
2.186
1.752
1.209
1.112
-0.000
CO
NH
CONH
60
20
NMe2
NH2
NH
500
0
2.78
3.33
2.36
6.35
2.27
48.00
6.0
5.0
4.0
3.0
2.0
1.0
0.0
ppm (f1)

4b (60)

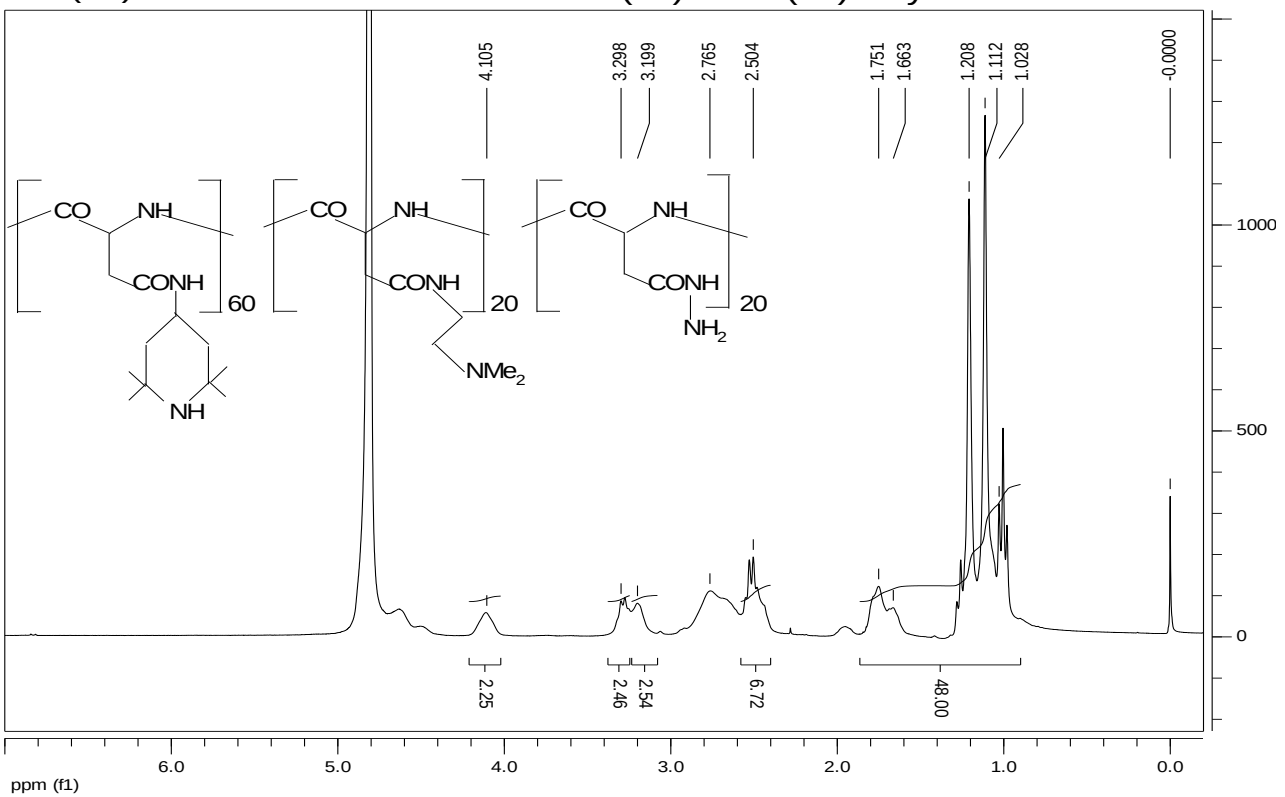
PSI - DMEA(20) - ATP(60) - Hy
4.105
3.298
3.199
2.765
2.504
1.751
1.663
1.208
1.112
1.028
-0.0000
CO
NH
CONH
60
20
NMe2
NH2
NH
1000
500
0
2.25
2.46
2.54
6.72
48.00
6.0
5.0
4.0
3.0
2.0
1.0
0.0
ppm (f1)

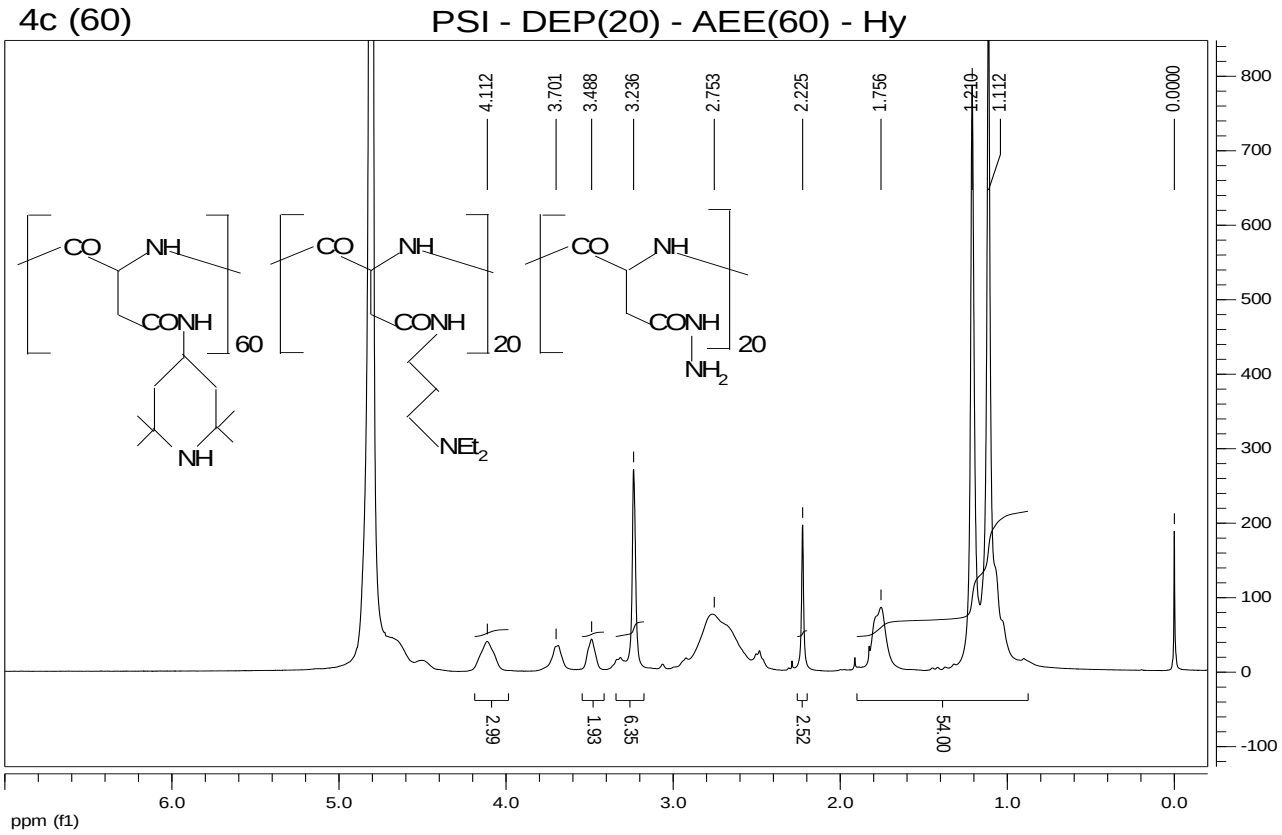
4c (60)
PSI - DEP(20) - AEE(60) - Hy
4.112
3.701
3.488
3.236
2.753
2.225
1.756
1.210
1.112
0.0000
CO
NH
CONH
60
20
NEt2
NH2
2.99
1.93
9.35
2.52
54.00
ppm (f1)

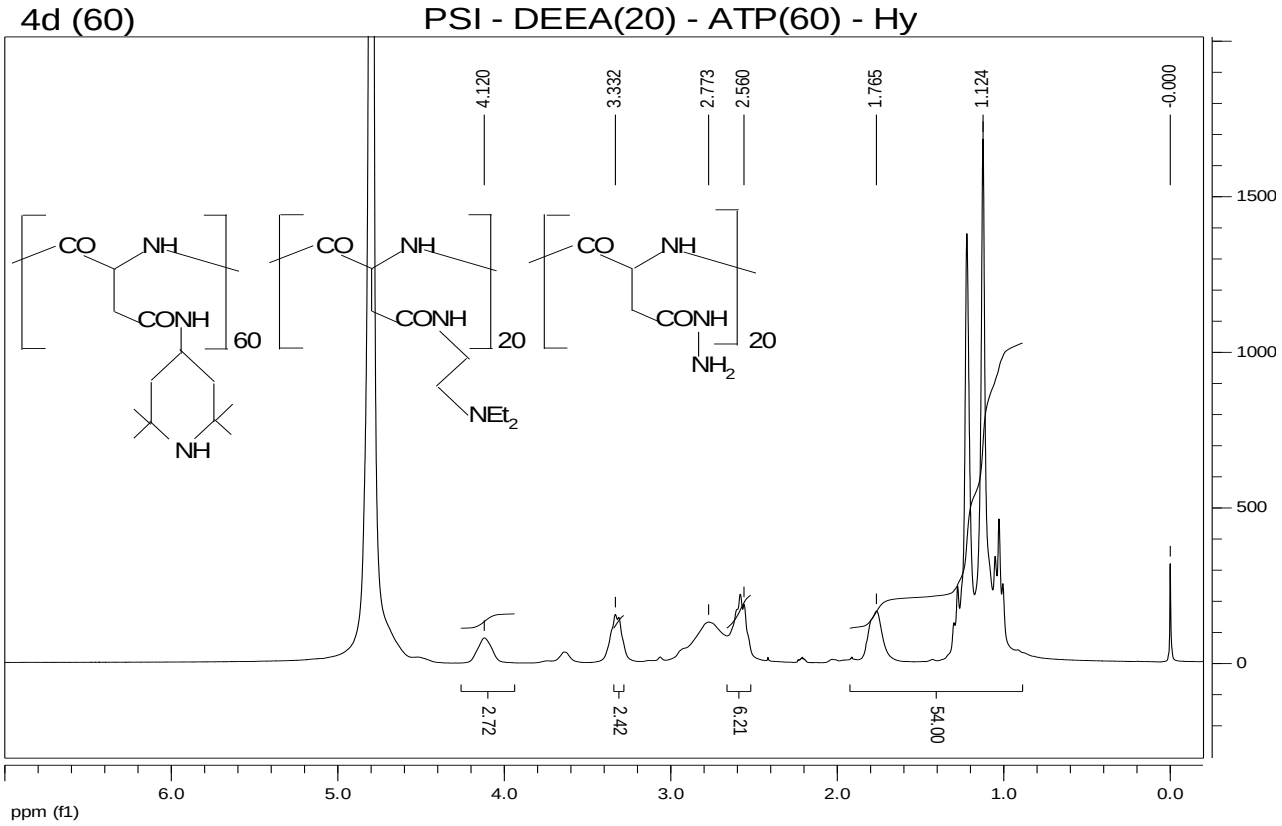
4d (60)
PSI - DEEA(20) - ATP(60) - Hy
4.120
3.332
2.773
2.560
1.765
1.124
-0.000
CO
NH
CONH
60
20
NEt2
NH2
2.72
2.42
6.21
54.00
ppm (f1)

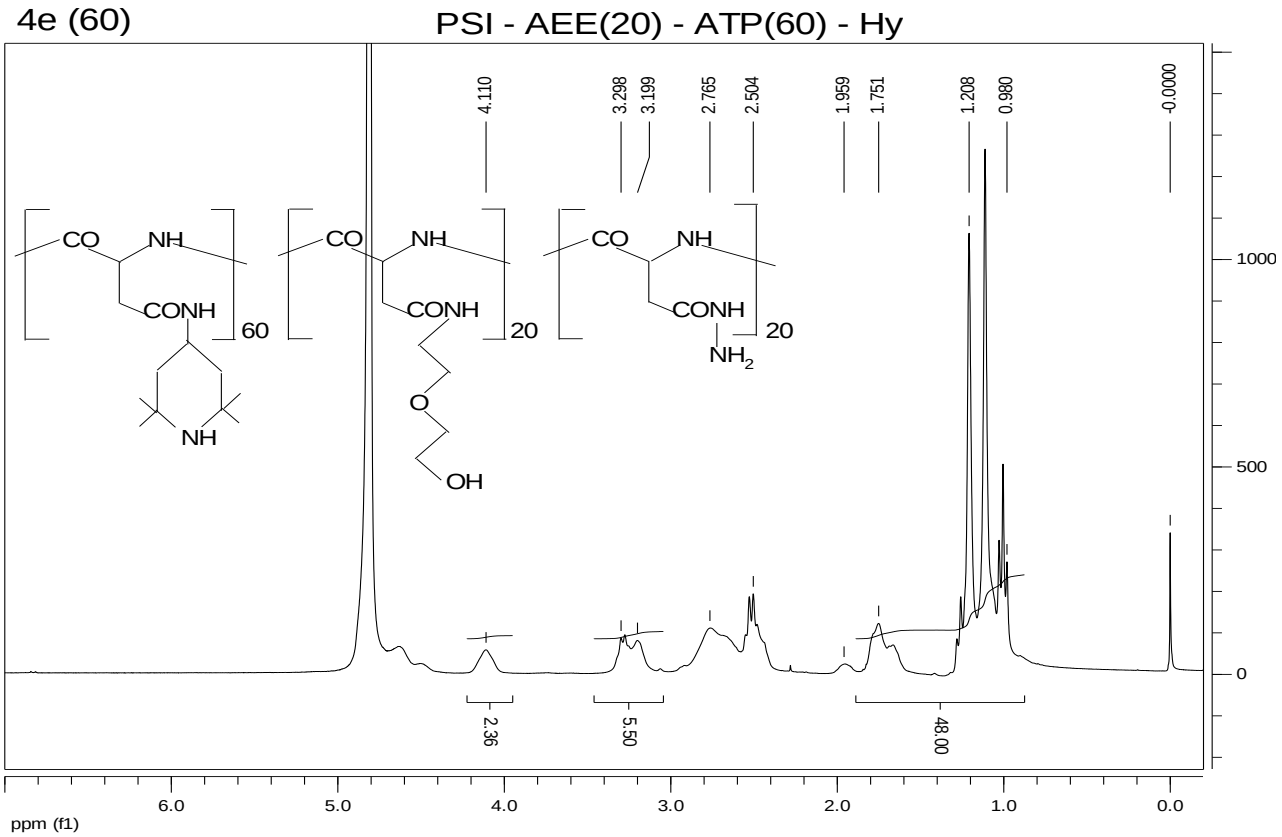
4e (60)
PSI - AEE(20) - ATP(60) - Hy
4.110
3.298
3.199
2.765
2.504
1.959
1.751
1.208
0.980
-0.0000
CO
NH
CONH
60
20
20
NH
O
OH
NH2
1000
500
0
2.36
5.50
48.00
6.0
5.0
4.0
3.0
2.0
1.0
0.0
ppm (f1)

Drugs coupling

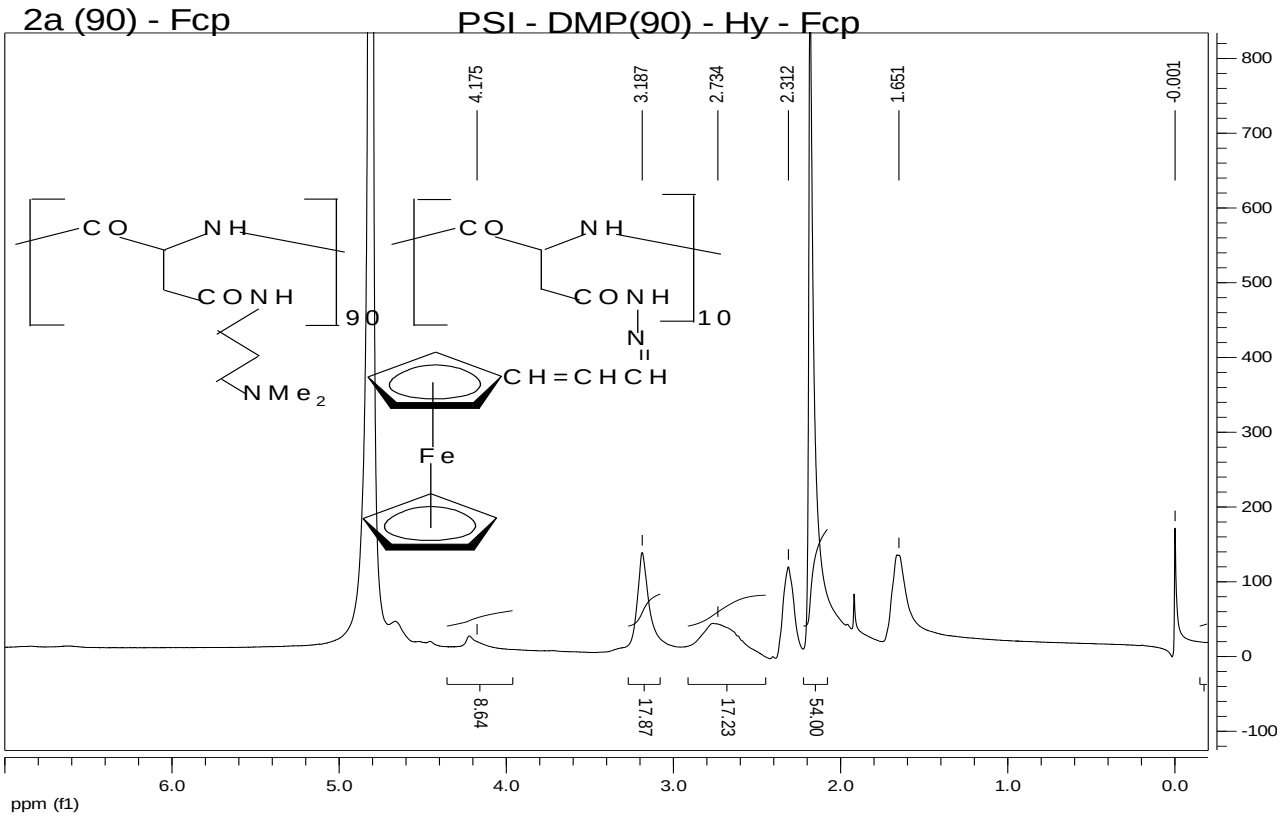

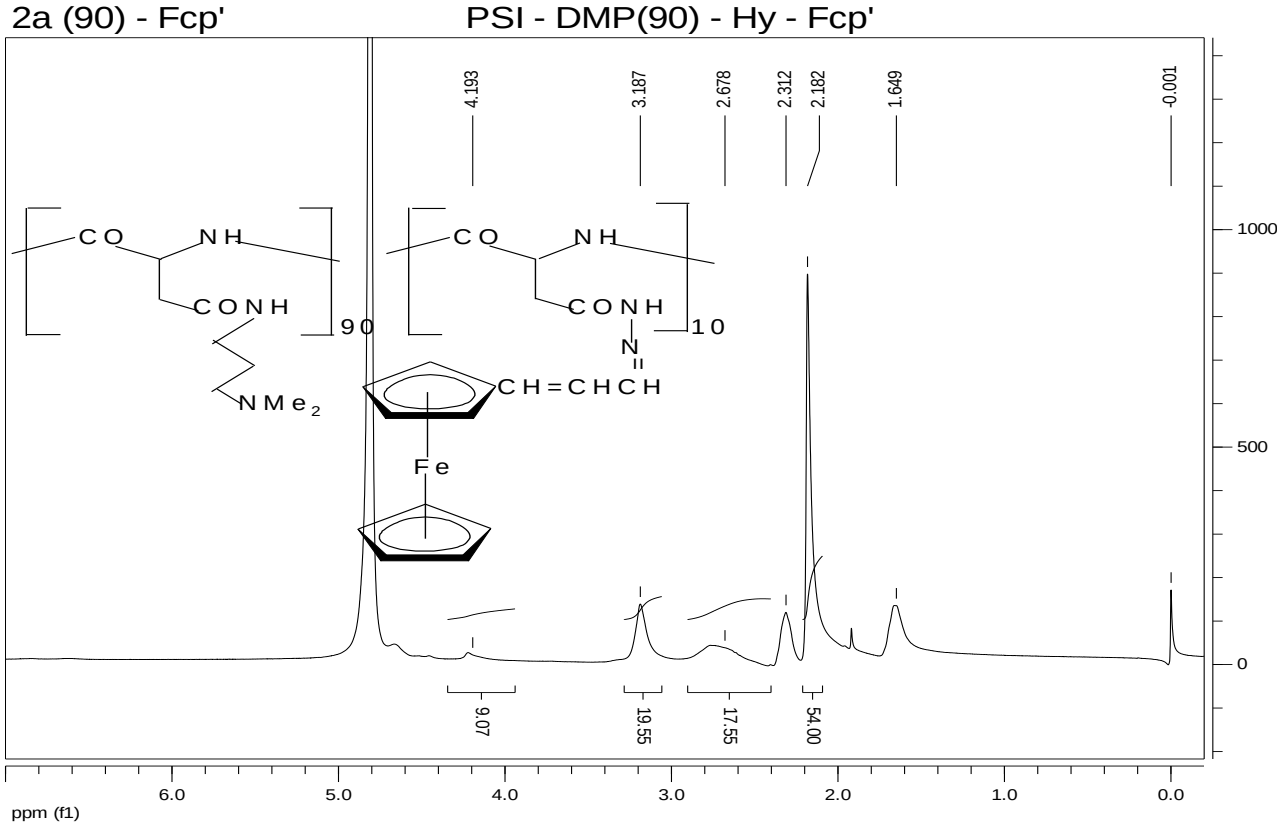

2d (90) - Fcp

PSI - DEEA(90) - Hy - Fcp

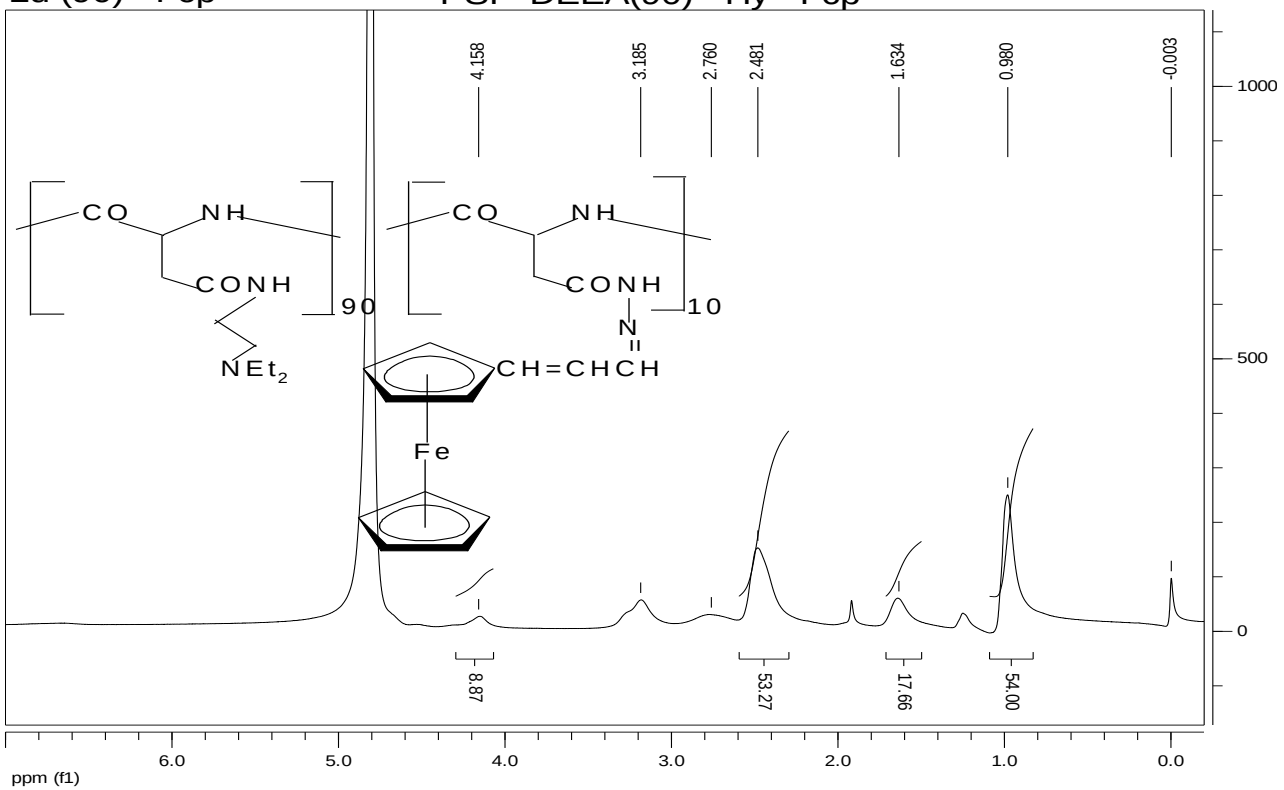

2f (90) - Fcp

PSI - AEE(90) - Hy - Fcp

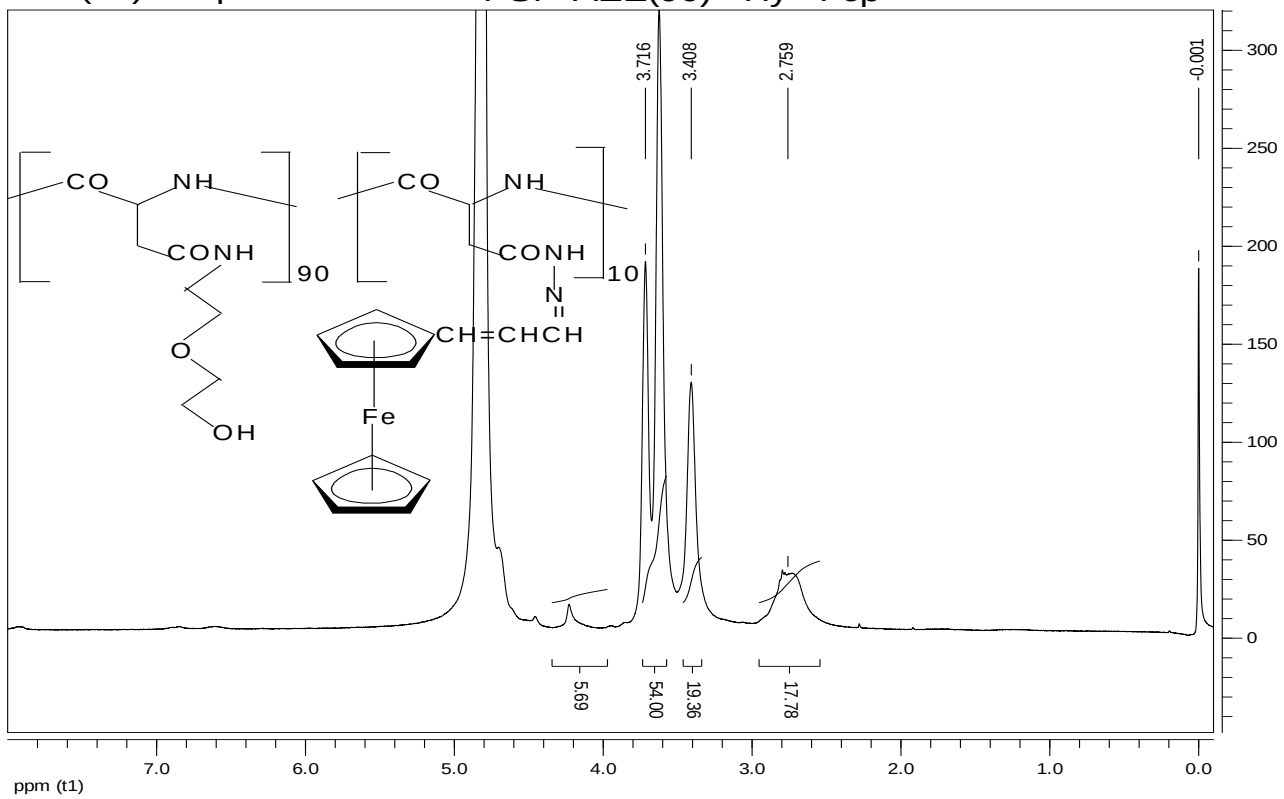

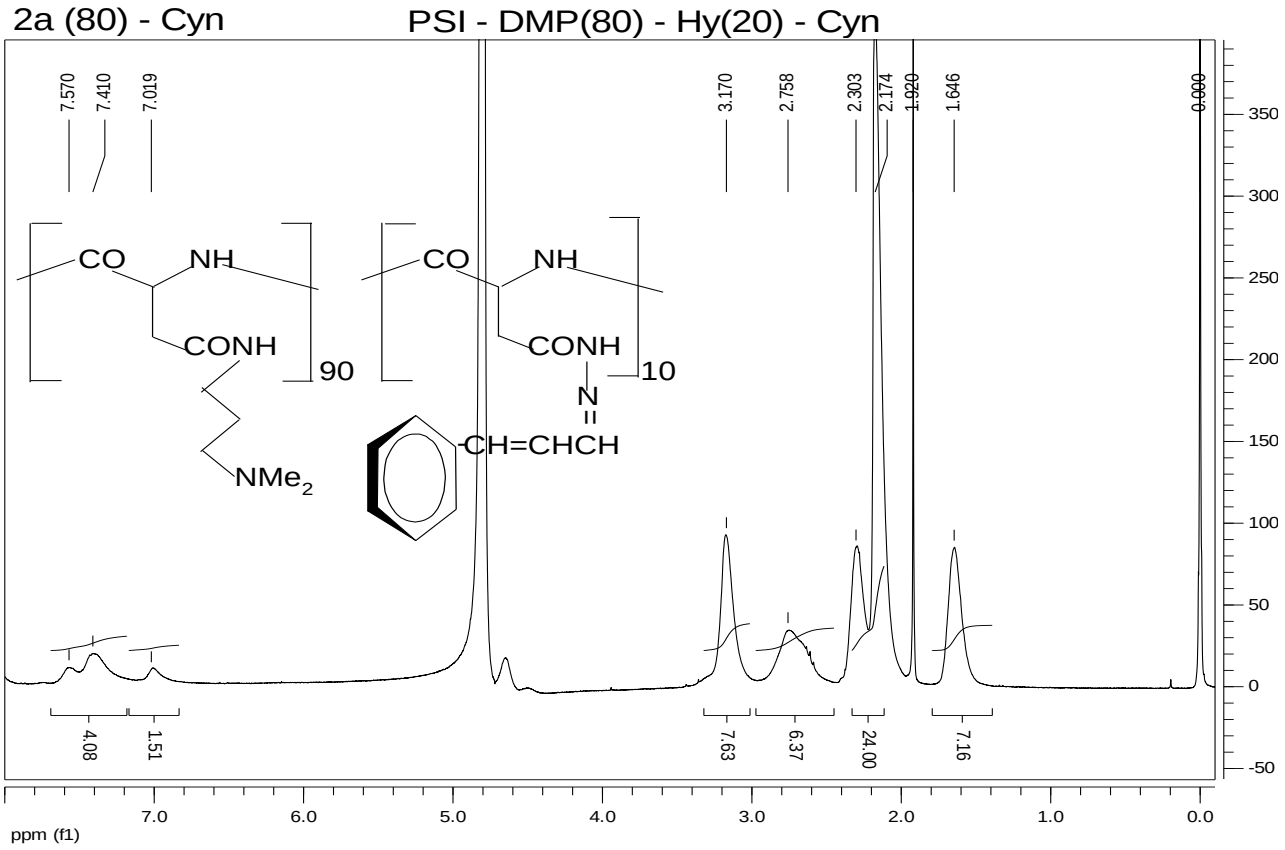
2a (80) - Cyn
PSI - DMP(80) - Hy(20) - Cyn
7.570
7.410
7.019
3.170
2.758
2.303
2.174
1.920
1.646
0.000
CO
NH
CONH
90
10
N
CH=CHCH
NMe2
4.08
1.51
7.63
6.37
24.00
7.16
ppm (f1)

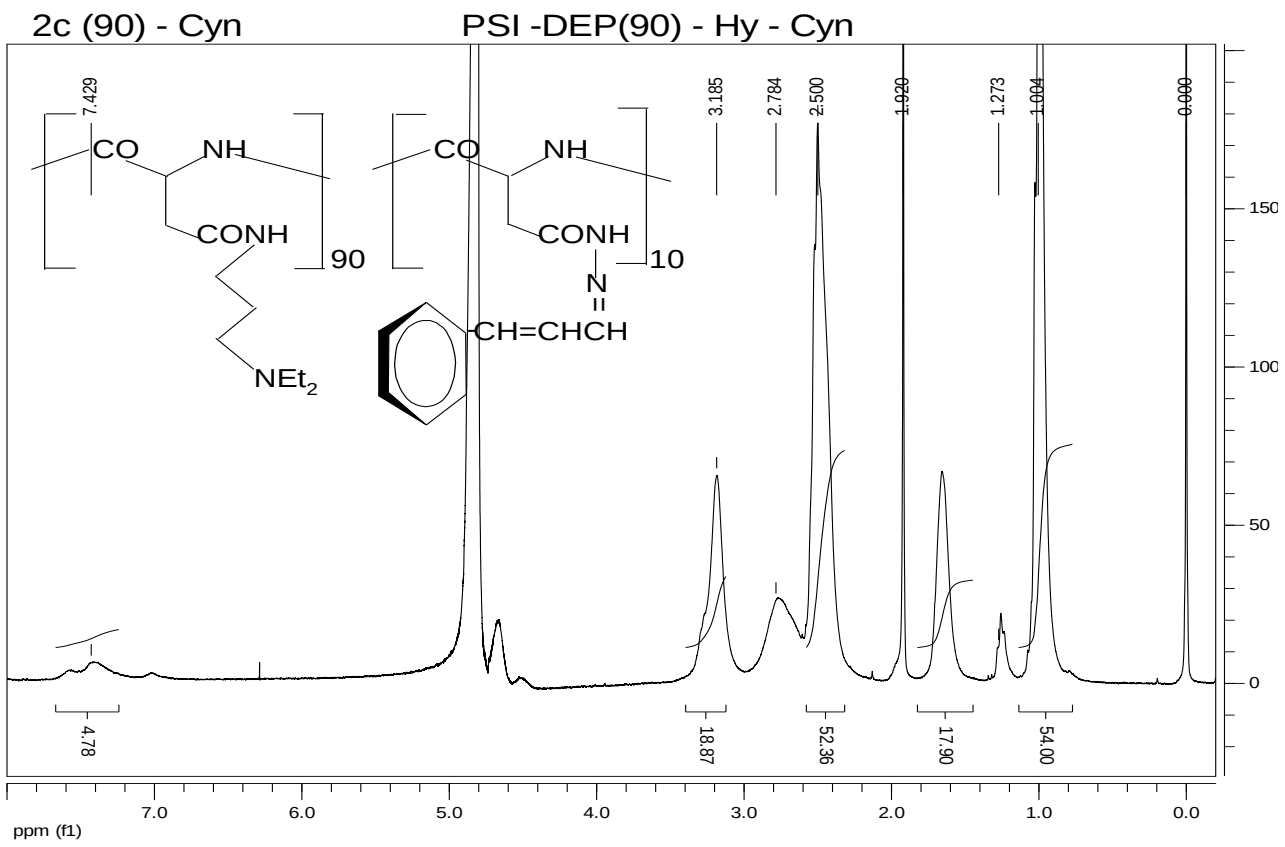
2c (90) - Cyn
PSI -DEP(90) - Hy - Cyn
7.429
3.185
2.784
2.500
1.920
1.273
1.004
0.000
CO
NH
CONH
90
10
N
CH=CHCH
NEt2
4.78
18.87
52.36
17.90
54.00
ppm (f1)

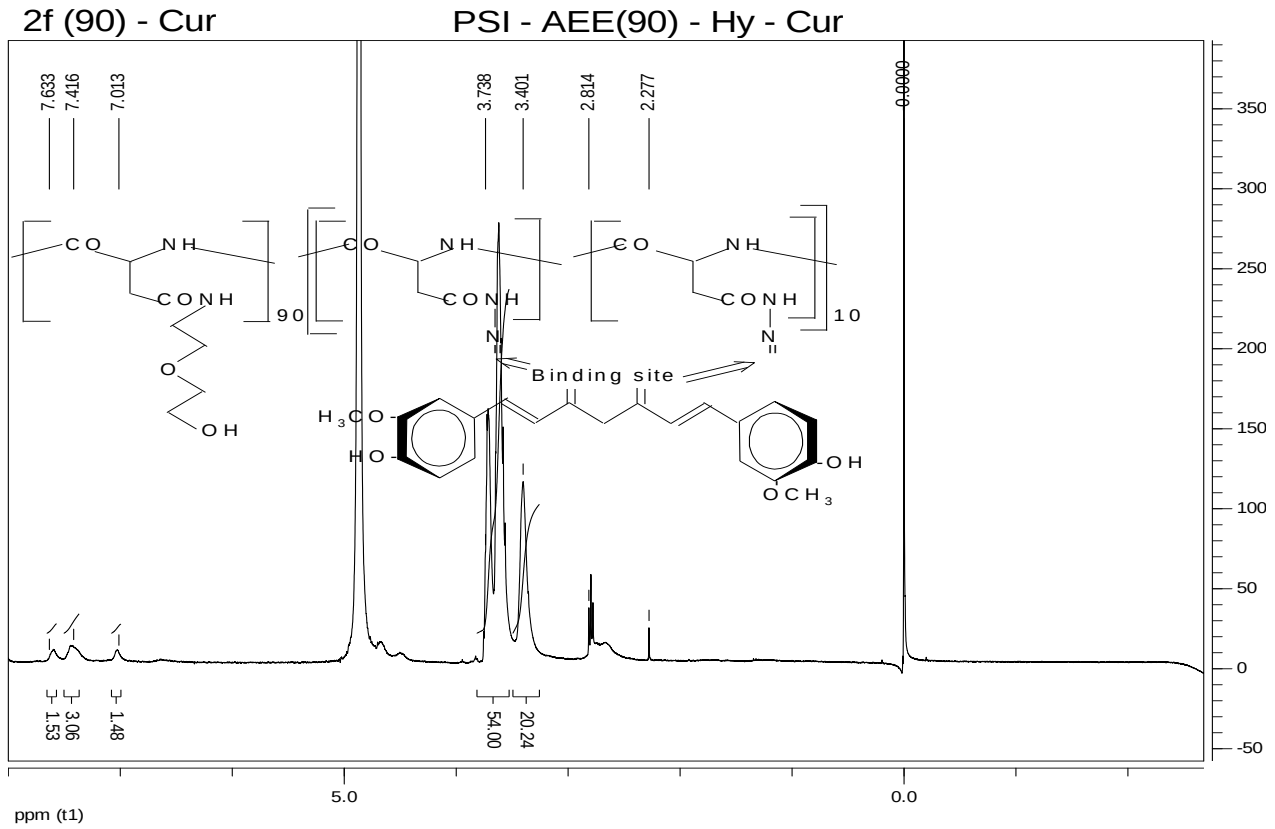
2f (90) - Cur
PSI - AEE(90) - Hy - Cur
7.633
7.416
7.013
3.738
3.401
2.814
2.277
0.0000
90
10
Binding site
1.53
3.06
1.48
54.00
20.24
ppm (t1)

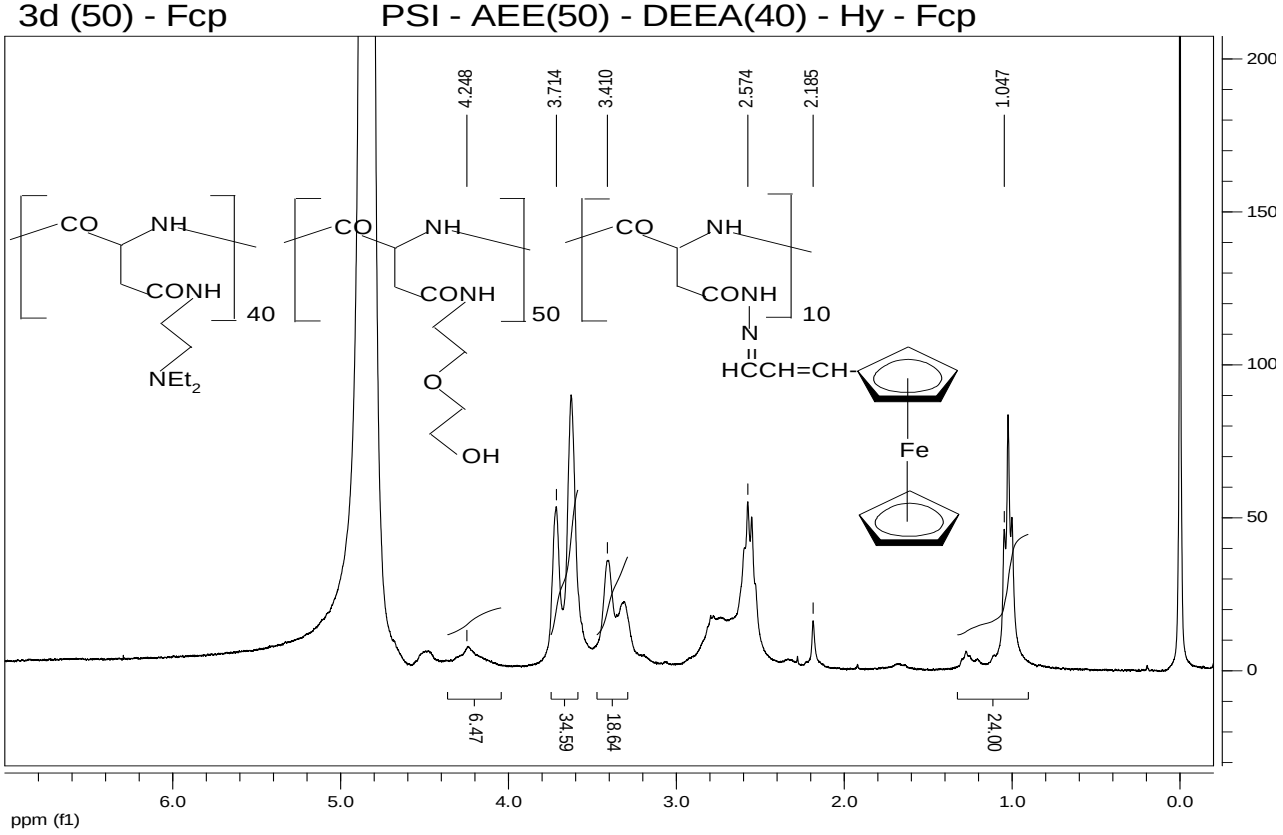
3d (50) - Fcp
PSI - AEE(50) - DEEA(40) - Hy - Fcp
4.248
3.714
3.410
2.574
2.185
1.047
40
50
10
6.47
34.59
18.64
24.00
ppm (f1)

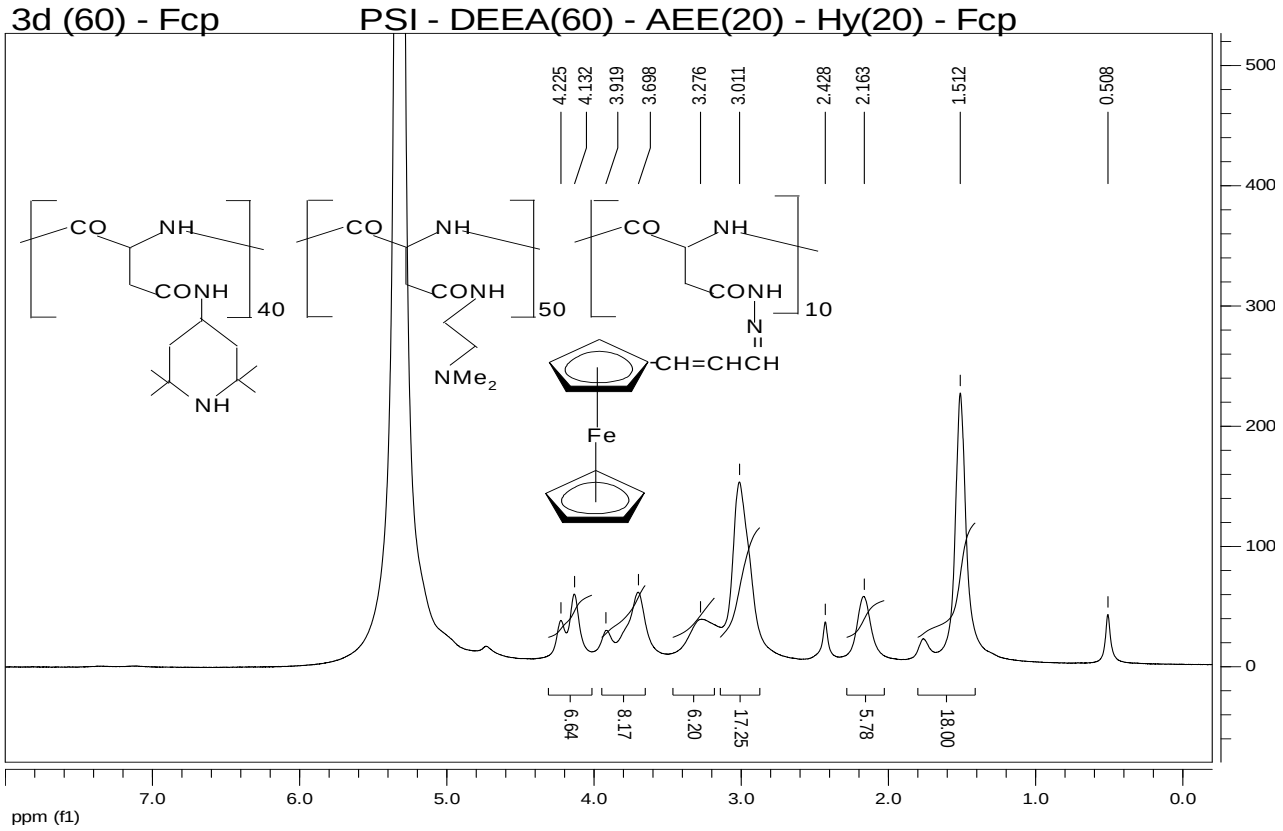
3d (60) - Fcp
PSI - DEEA(60) - AEE(20) - Hy(20) - Fcp
4.225
4.132
3.919
3.698
3.276
3.011
2.428
2.163
1.512
0.508
CO
NH
CONH
40
50
10
NMe2
NH
N=
CH=CHCH
Fe
6.64
8.17
6.20
17.25
5.78
18.00
7.0
6.0
5.0
4.0
3.0
2.0
1.0
0.0
ppm (f1)

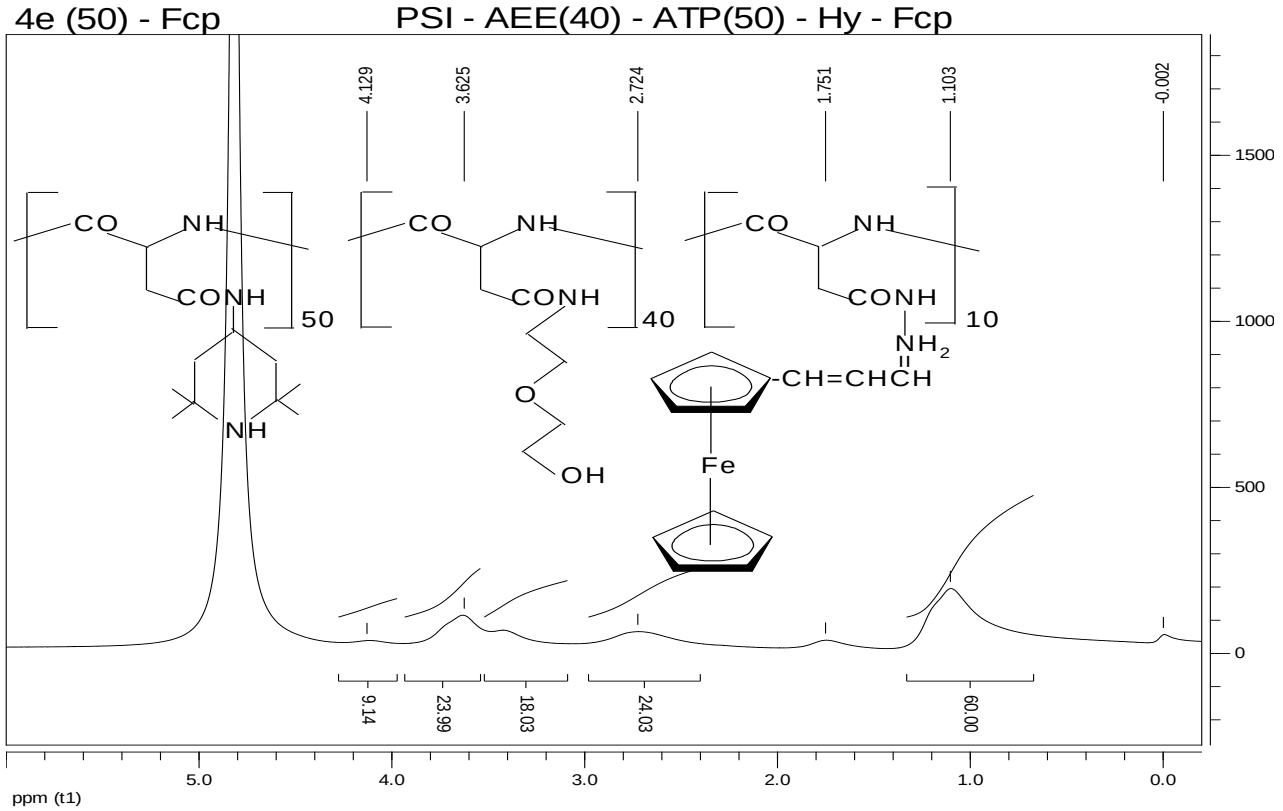
4e (50) - Fcp
PSI - AEE(40) - ATP(50) - Hy - Fcp
4.129
3.625
2.724
1.751
1.103
-0.002
CO
NH
CONH
50
40
10
NH2
O
OH
CH=CHCH
Fe
9.14
23.99
18.03
24.03
60.00
5.0
4.0
3.0
2.0
1.0
0.0
ppm (t1)

4a (60) - Cur PSI - ATP(60) - DMP(20) - Hy(20) - Cur

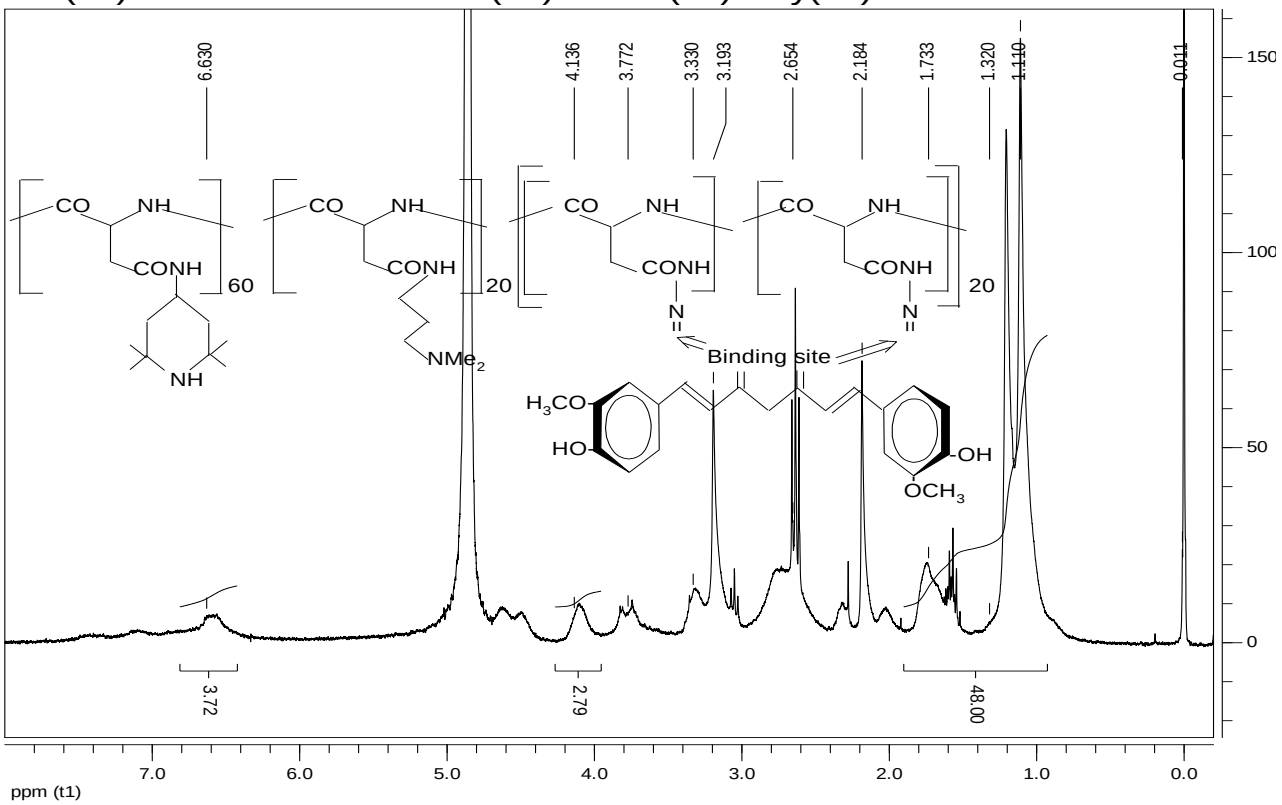

4b (50) - Fca PSI - ATP(50) - DMEA(40) - Hy - Fca

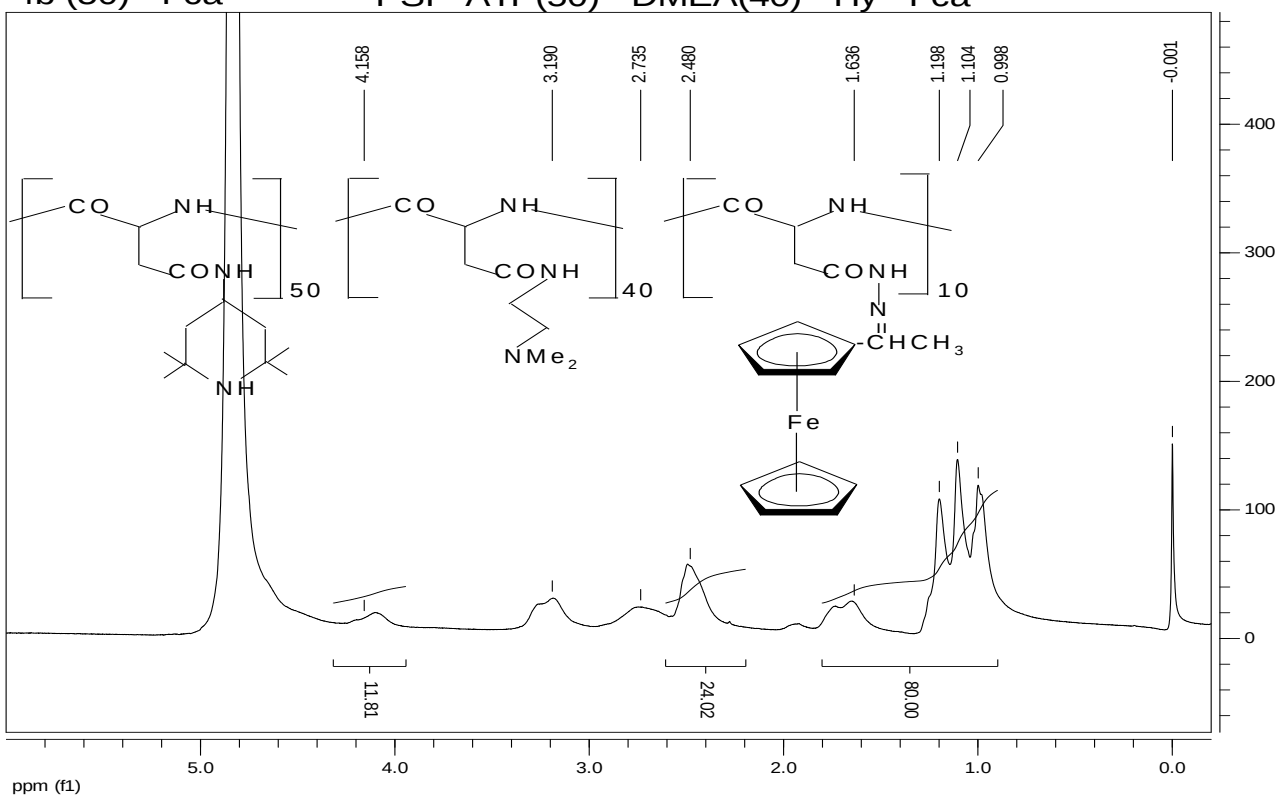

4C (60) - Fcc PSI - ATP(60) - DEP(20) - Hy(20) - Fcc

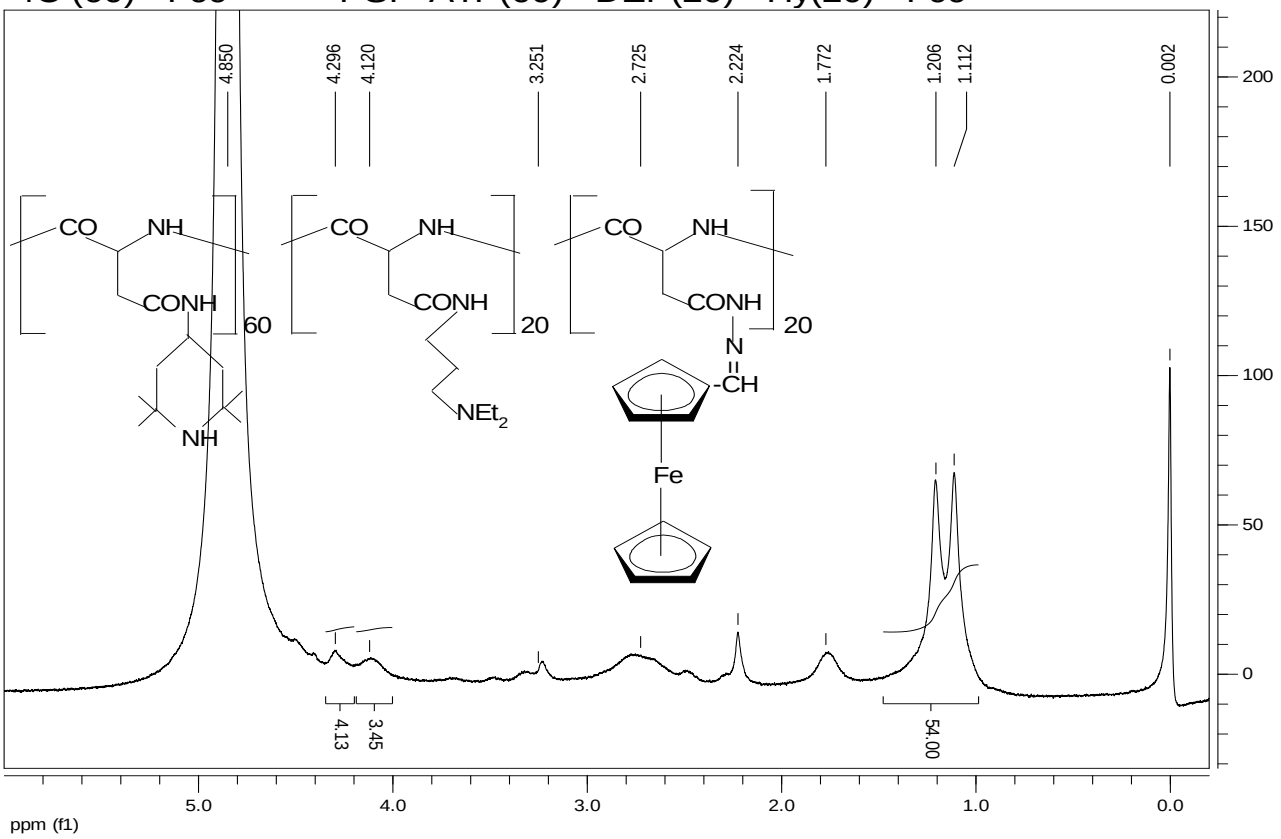

4e (50) - Fcc PSI - ATP(50) - AEE(40) - Hy - Fcc

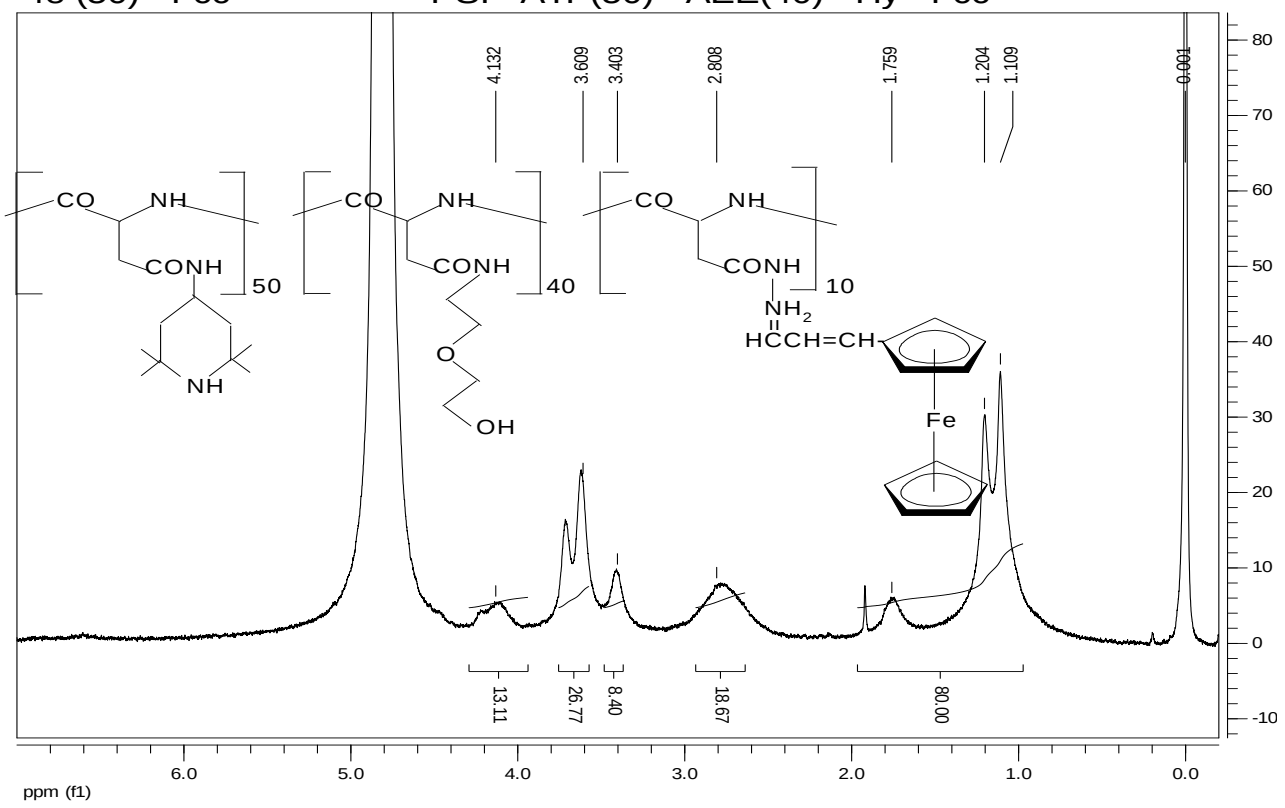

2a (80) - FA - Fcp PSI - DMP(80) - Hy(20) - FA - Fcp

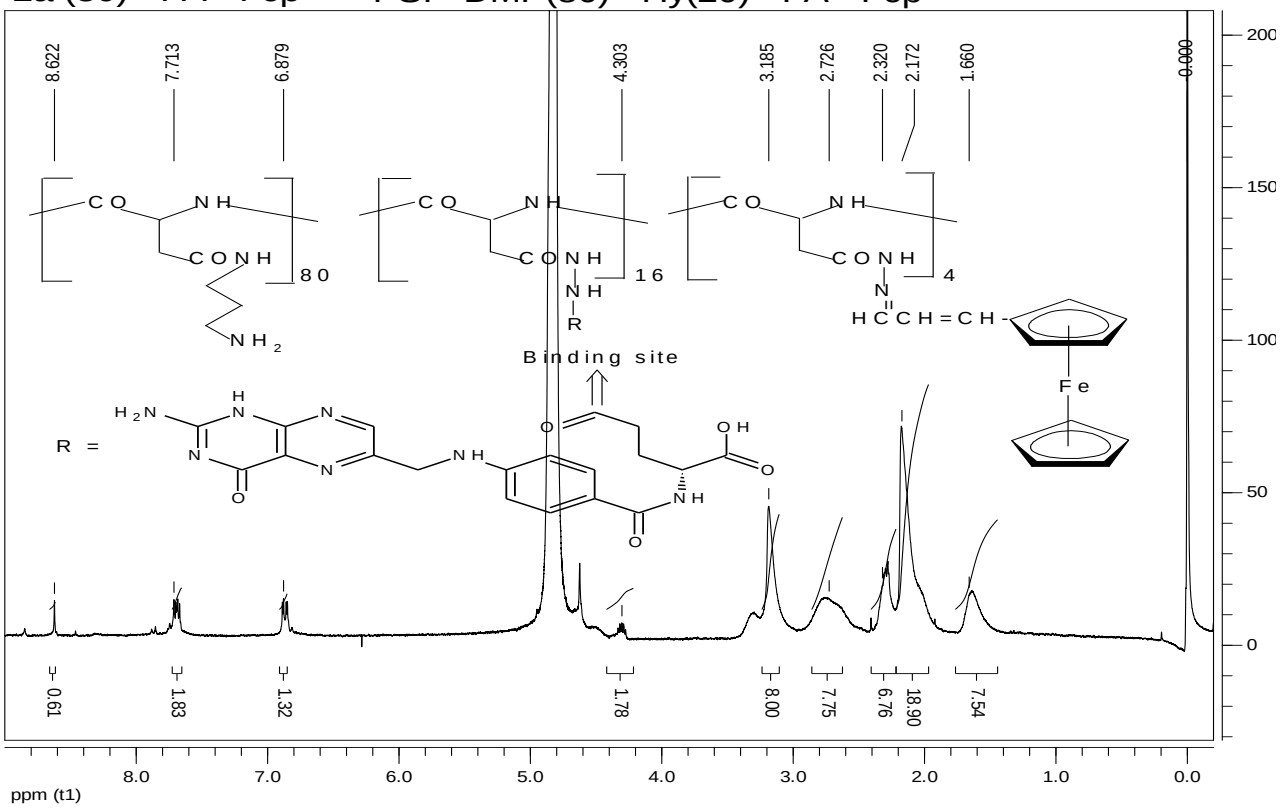

4c (60) - Cur- Fcp PSI - ATP(60) - DEP(20) - Hy(20) - Cur - Fcp

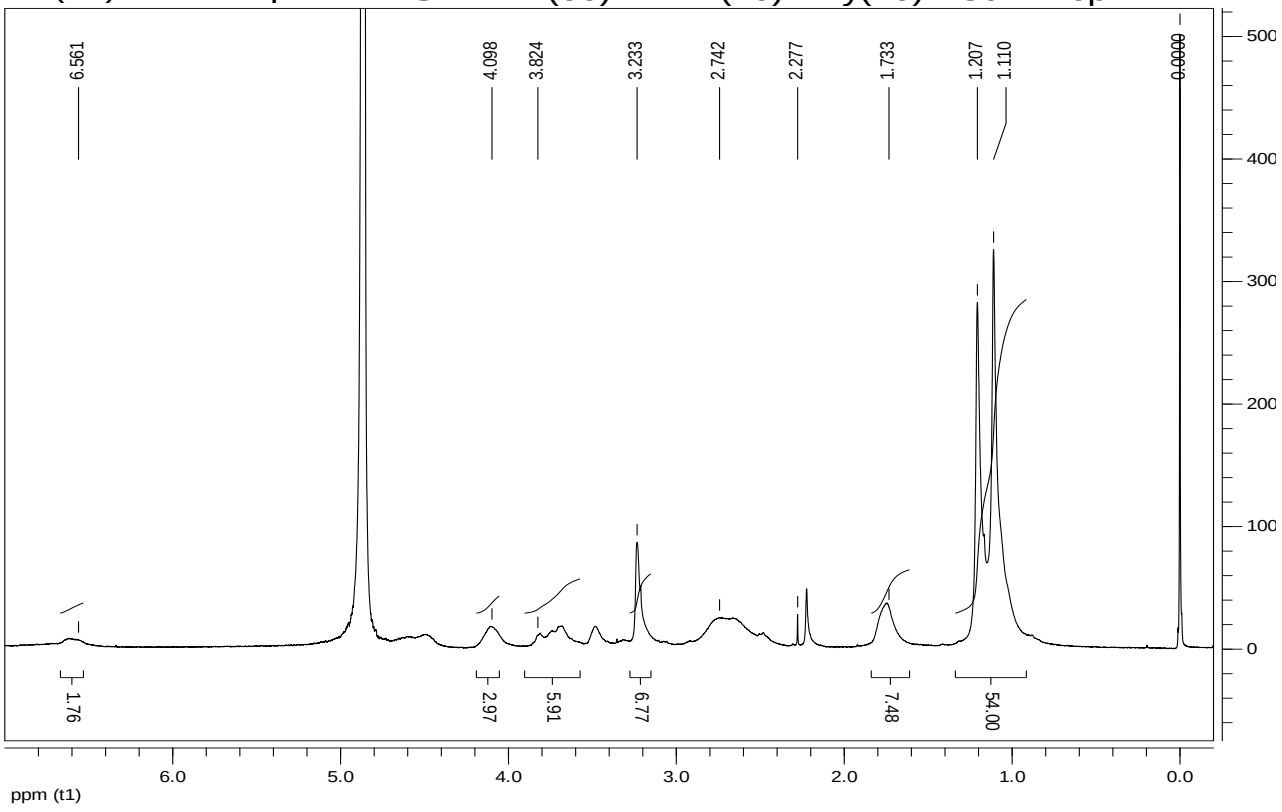

4c (60) – Cur – Fcp structure

4c (60) - Cur- Fcp PSI - ATP(60) - DEP(20) - Hy(20) - Cur - Fcp

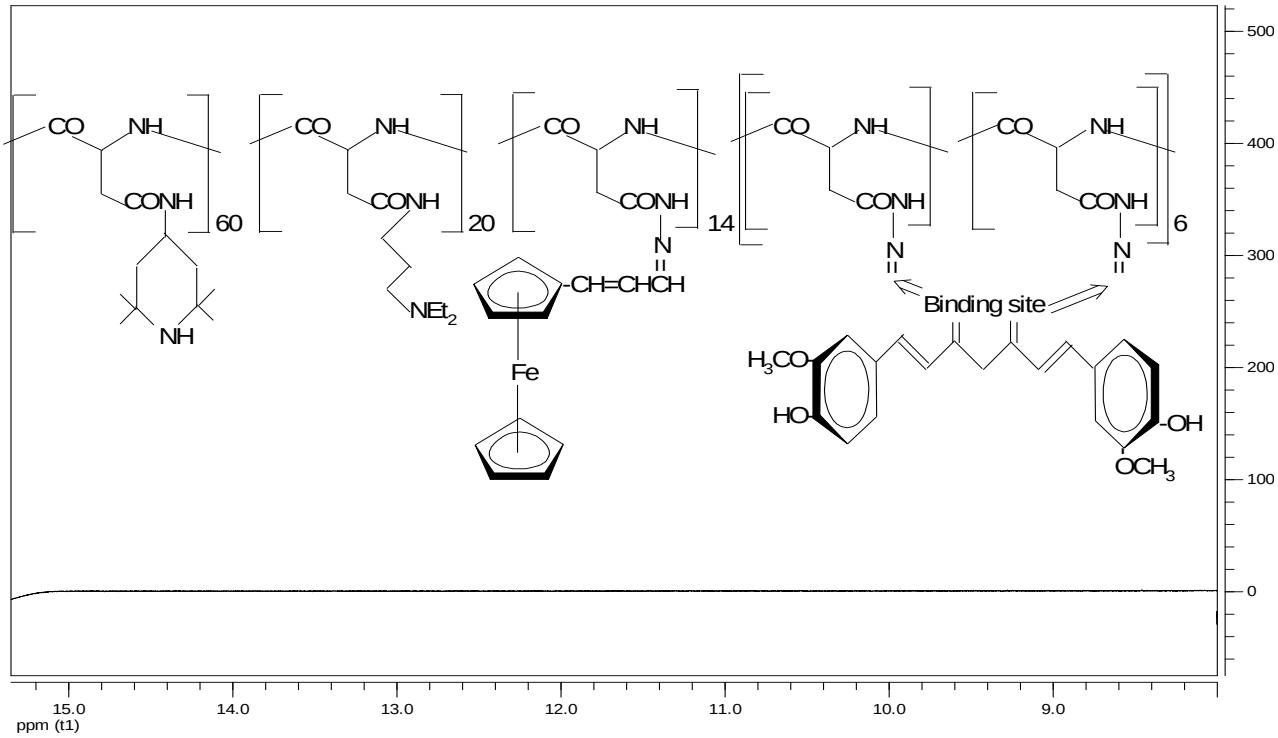

SELECTED IR SPECTRUM

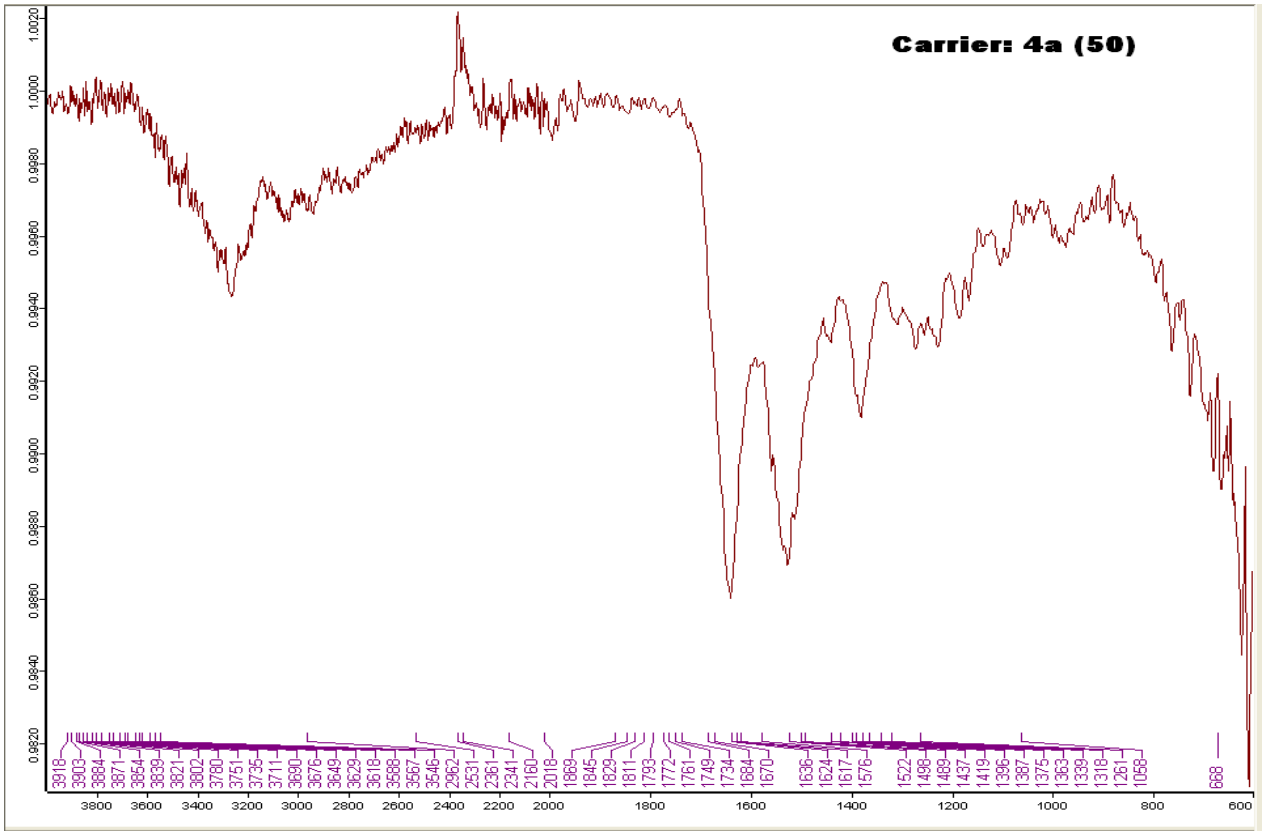
Carrier: 4a (50)
1.0020
1.0000
0.9980
0.9960
0.9940
0.9920
0.9900
0.9880
0.9860
0.9840
0.9820
3918
3903
3884
3871
3854
3839
3821
3802
3780
3751
3735
3711
3690
3676
3649
3629
3618
3588
3567
3546
2962
2531
2361
2341
2160
2018
1869
1845
1829
1811
1793
1772
1761
1749
1734
1684
1670
1636
1624
1617
1576
1522
1498
1489
1437
1419
1396
1387
1375
1363
1339
1318
1261
1058
668
3800
3600
3400
3200
3000
2800
2600
2400
2200
2000
1800
1600
1400
1200
1000
800
600

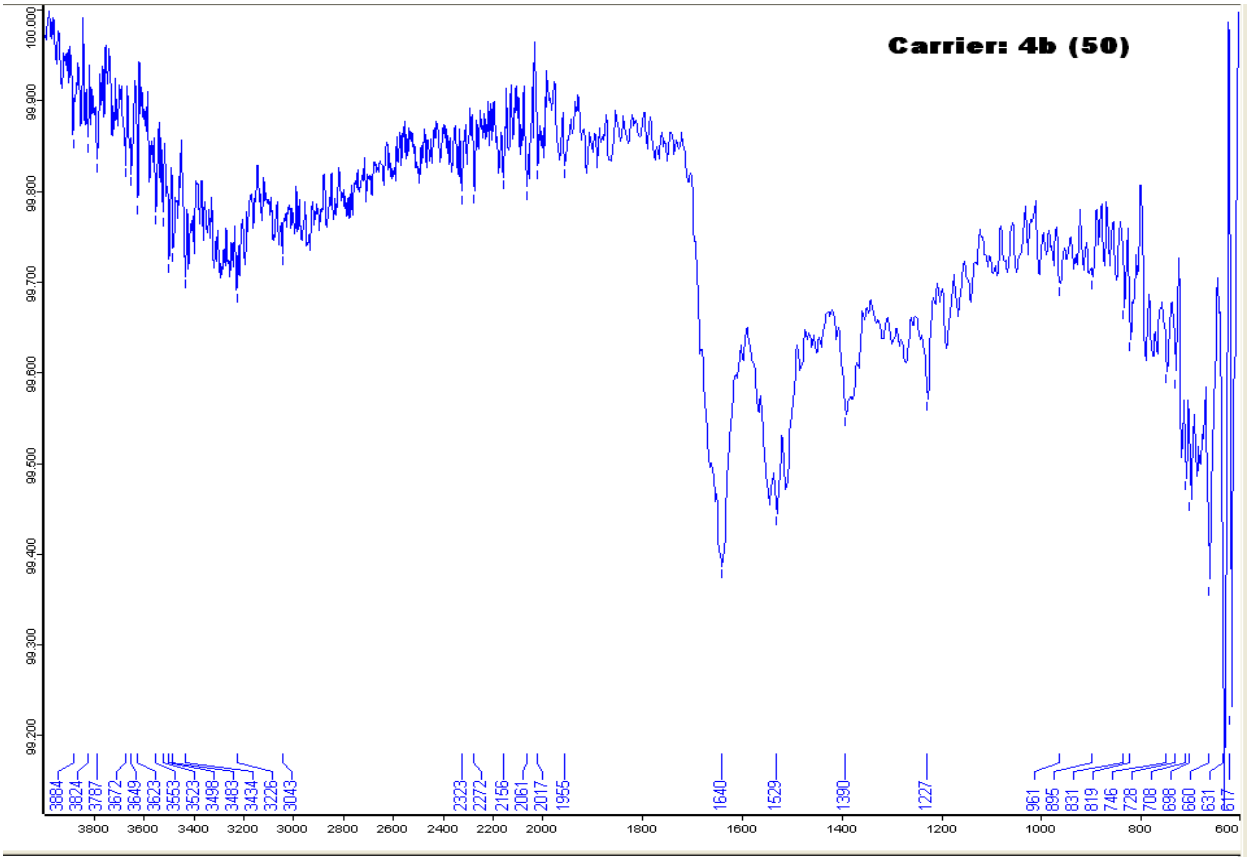
Carrier: 4b (50)
100.000
99.900
99.800
99.700
99.600
99.500
99.400
99.300
99.200
3884
3824
3787
3672
3649
3623
3553
3523
3498
3483
3434
3226
3043
2323
2272
2156
2061
2017
1955
1640
1529
1390
1227
961
895
831
819
746
728
708
698
660
631
617
3800
3600
3400
3200
3000
2800
2600
2400
2200
2000
1800
1600
1400
1200
1000
800
600

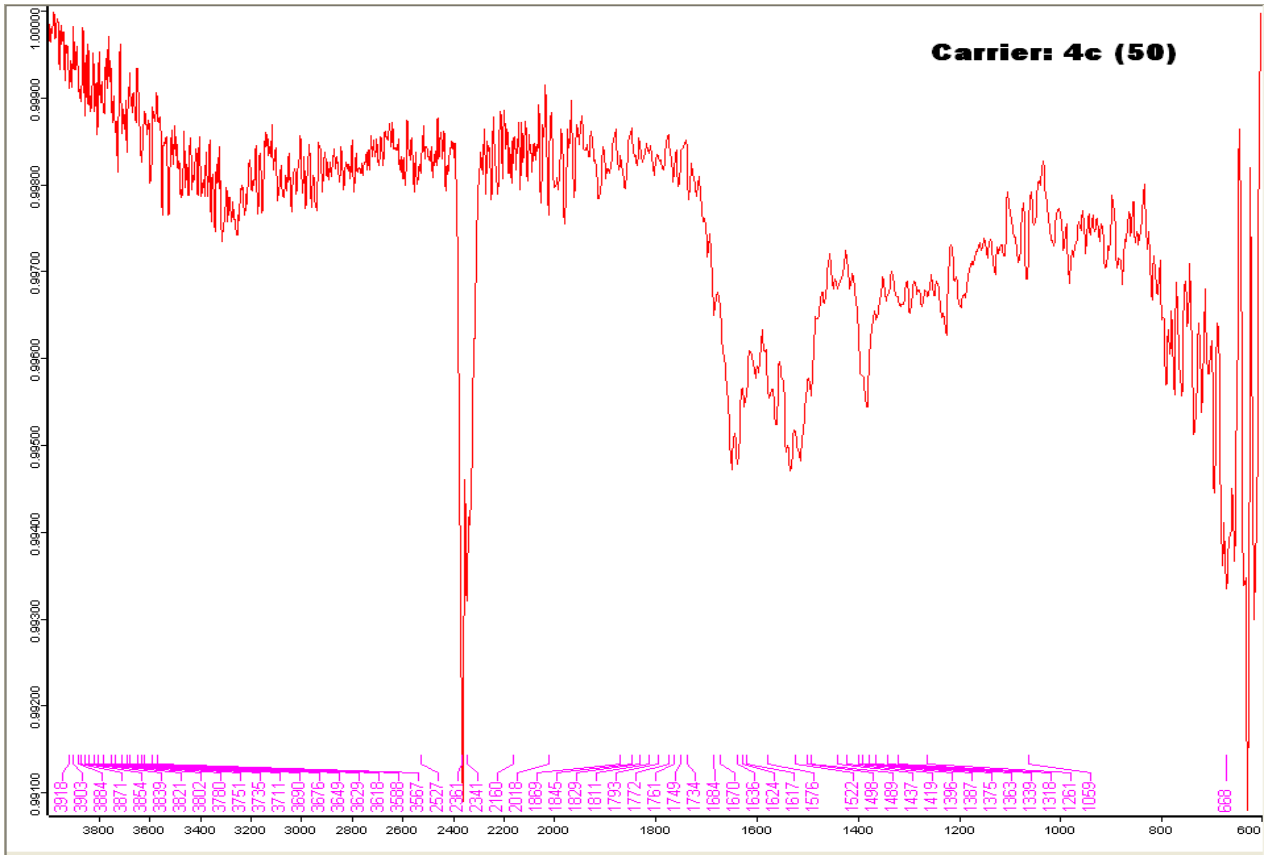
Carrier: 4c (50)
1.00000
0.99900
0.99800
0.99700
0.99600
0.99500
0.99400
0.99300
0.99200
0.99100
3800 3600 3400 3200 3000 2800 2600 2400 2200 2000 1800 1600 1400 1200 1000 800 600
3918 3903 3884 3871 3854 3839 3821 3802 3780 3751 3735 3711 3690 3676 3649 3629 3618 3588 3567 2527 2361 2341 2160 2018 1869 1845 1829 1811 1793 1772 1761 1749 1734 1684 1670 1636 1624 1617 1576 1522 1498 1489 1437 1419 1396 1387 1375 1363 1339 1318 1261 1059 668

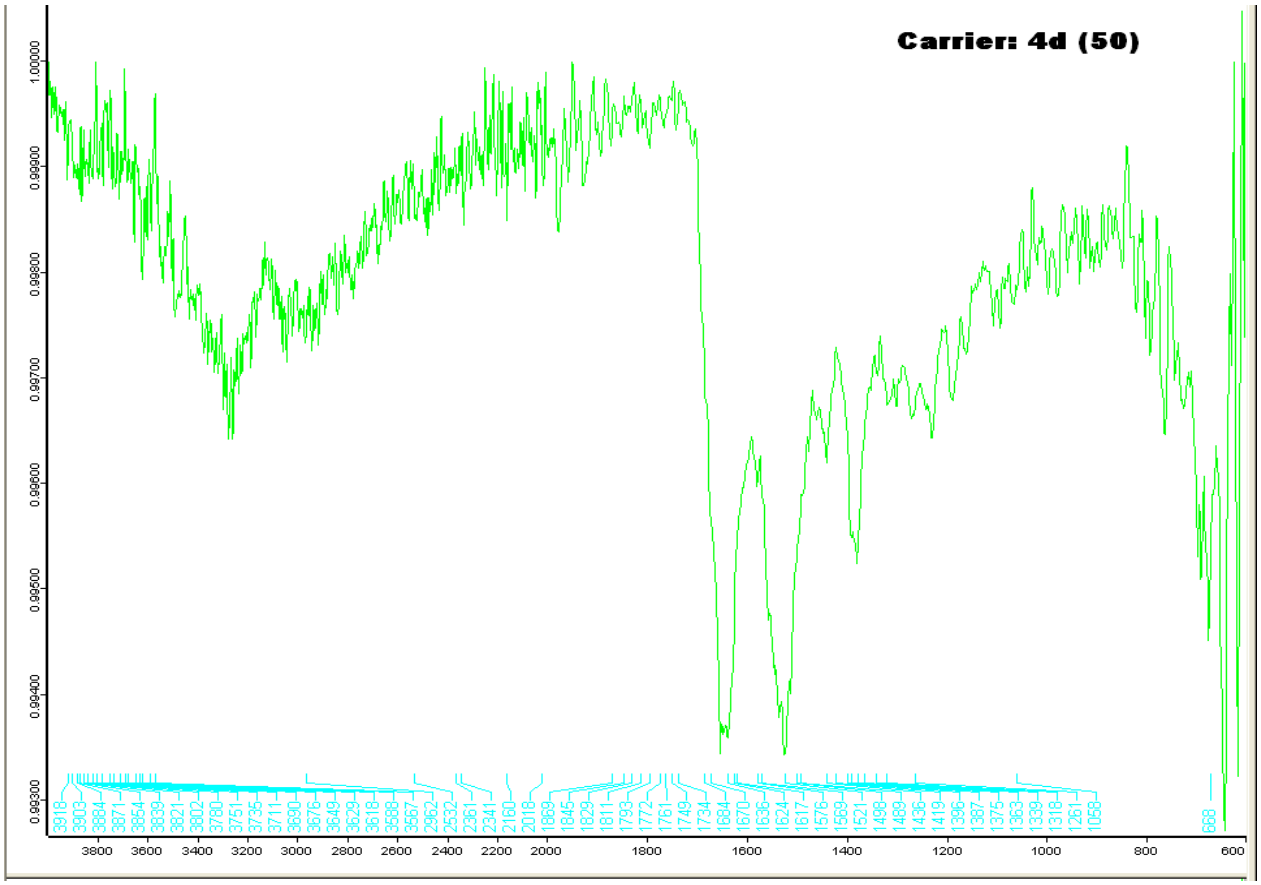
Carrier: 4d (50)
1.00000
0.99900
0.99800
0.99700
0.99600
0.99500
0.99400
0.99300
3800 3600 3400 3200 3000 2800 2600 2400 2200 2000 1800 1600 1400 1200 1000 800 600
3918 3903 3884 3871 3854 3839 3821 3802 3780 3751 3735 3711 3690 3676 3649 3629 3618 3588 3567 2962 2532 2361 2341 2160 2018 1869 1845 1829 1811 1793 1772 1761 1749 1734 1684 1670 1636 1624 1617 1576 1569 1521 1498 1489 1436 1419 1396 1387 1375 1363 1339 1318 1261 1058 668

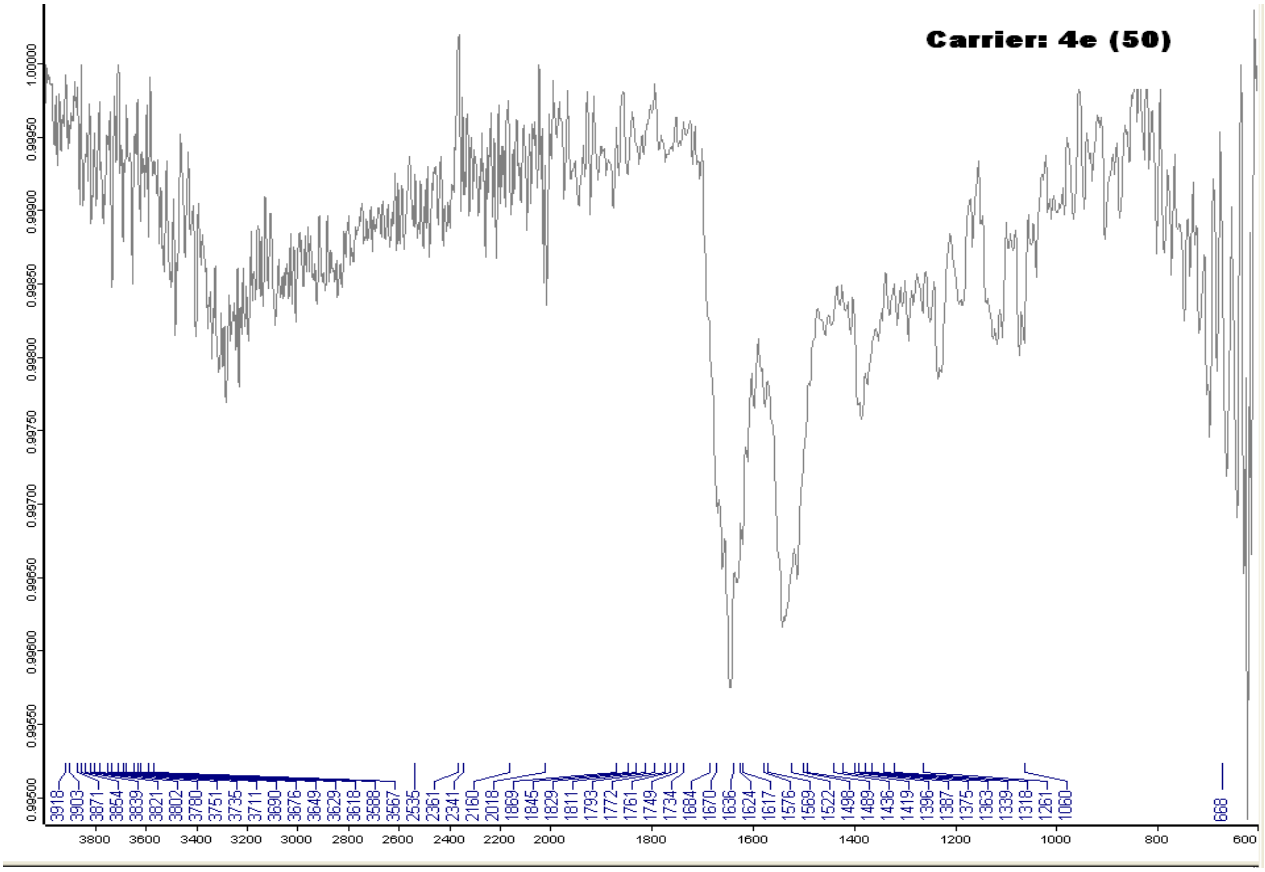
Carrier: 4e (50)
1.00000
0.99950
0.99900
0.99850
0.99800
0.99750
0.99700
0.99650
0.99600
0.99550
0.99500
3800 3600 3400 3200 3000 2800 2600 2400 2200 2000 1800 1600 1400 1200 1000 800 600
3918 3903 3871 3854 3839 3821 3802 3780 3751 3735 3711 3690 3676 3649 3629 3618 3588 3567 2536 2361 2341 2160 2018 1869 1845 1829 1811 1793 1772 1761 1749 1734 1684 1670 1636 1624 1617 1576 1569 1522 1498 1489 1436 1419 1396 1387 1375 1363 1339 1318 1261 1060 668

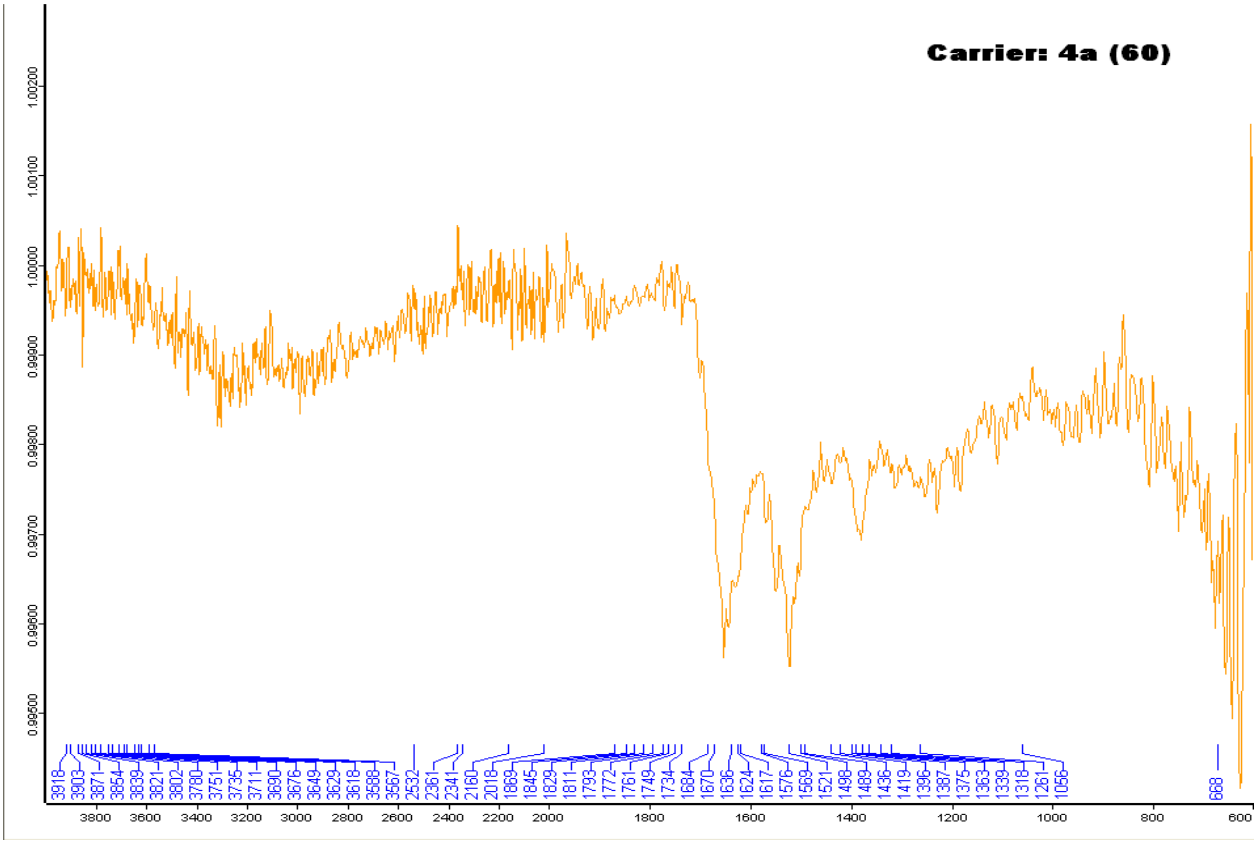
Carrier: 4a (60)
1.00200
1.00100
1.00000
0.99900
0.99800
0.99700
0.99600
0.99500
3800 3600 3400 3200 3000 2800 2600 2400 2200 2000 1800 1600 1400 1200 1000 800 600
3918 3903 3871 3854 3839 3821 3802 3780 3751 3735 3711 3690 3676 3649 3629 3618 3588 3567 2532 2361 2341 2160 2018 1869 1845 1829 1811 1793 1772 1761 1749 1734 1684 1670 1636 1624 1617 1576 1569 1521 1498 1489 1436 1419 1396 1387 1375 1363 1339 1318 1261 1056 668

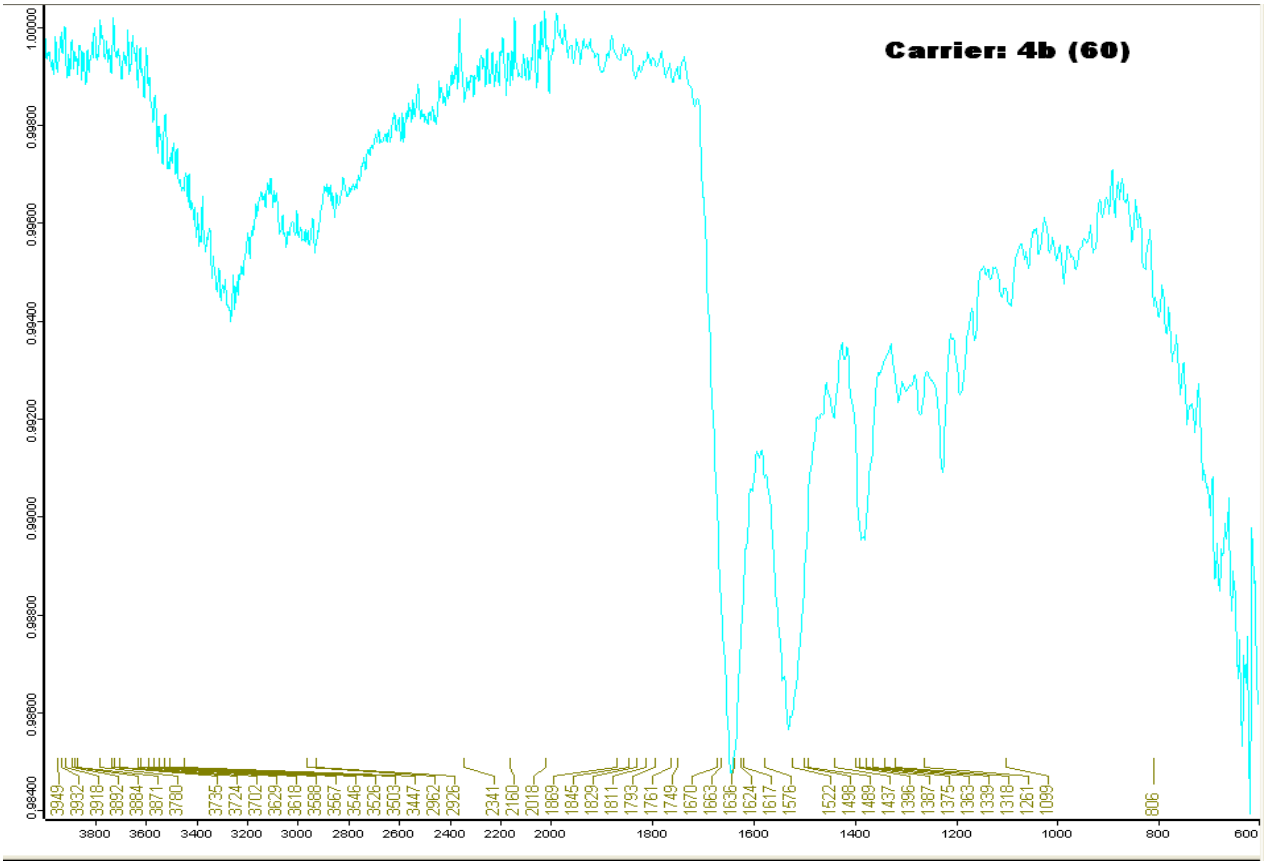
Carrier: 4b (60)

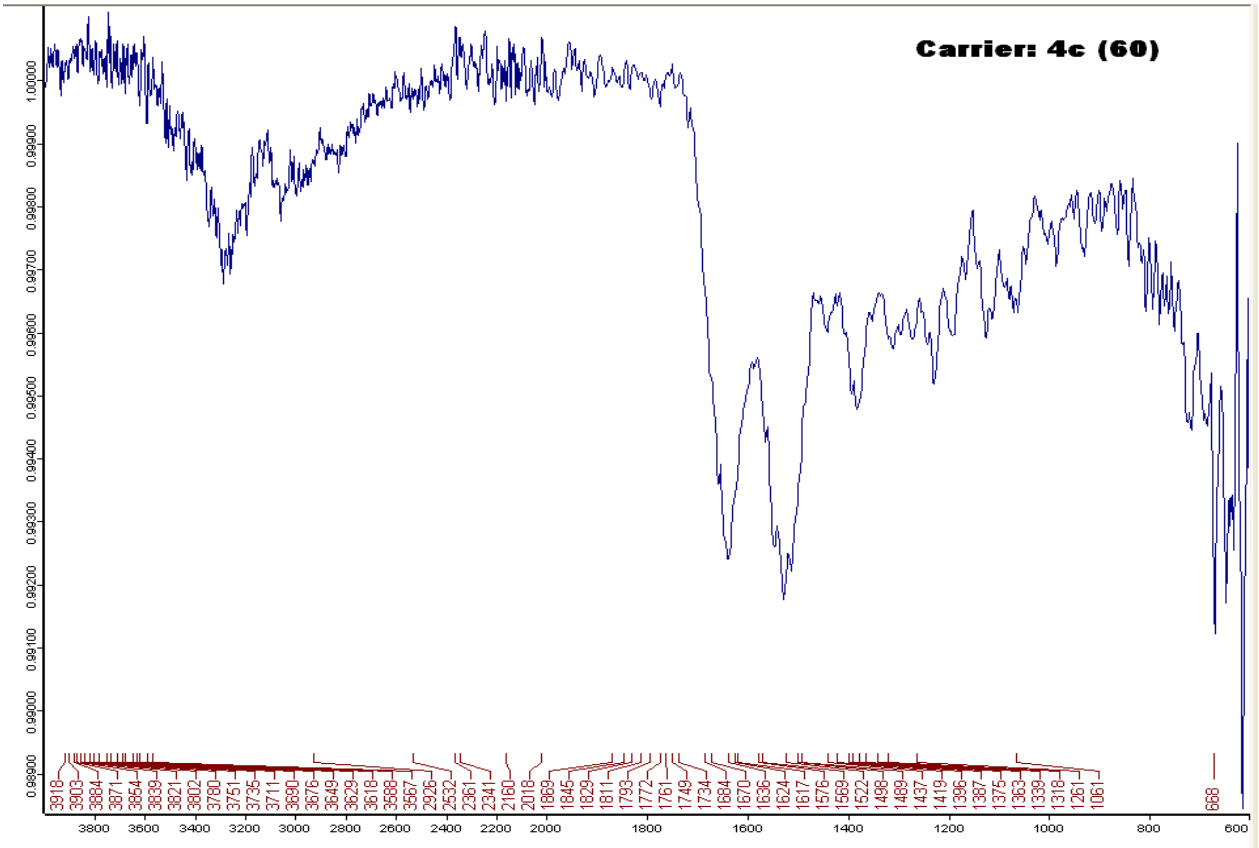
Carrier: 4c (60)

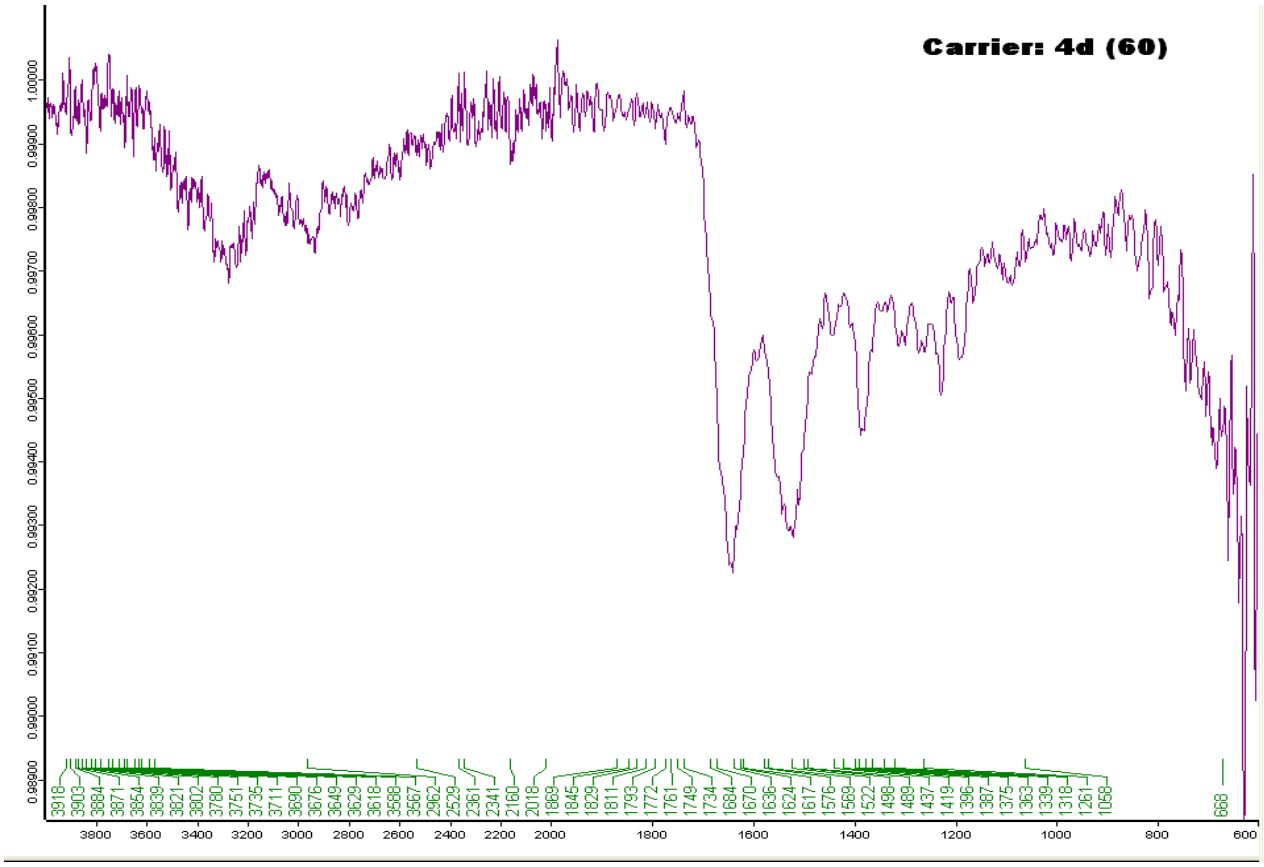
Carrier: 4d (60)
1.00000
0.99900
0.99800
0.99700
0.99600
0.99500
0.99400
0.99300
0.99200
0.99100
0.99000
0.98900
3918 3903 3884 3871 3854 3839 3821 3802 3780 3751 3735 3711 3690 3676 3649 3629 3618 3588 3567 2962 2529 2361 2341 2160 2018 1869 1845 1829 1811 1793 1772 1761 1749 1734 1684 1670 1636 1624 1617 1576 1569 1522 1498 1489 1437 1419 1396 1387 1375 1363 1339 1318 1261 1059
668
3800 3600 3400 3200 3000 2800 2600 2400 2200 2000 1800 1600 1400 1200 1000 800 600

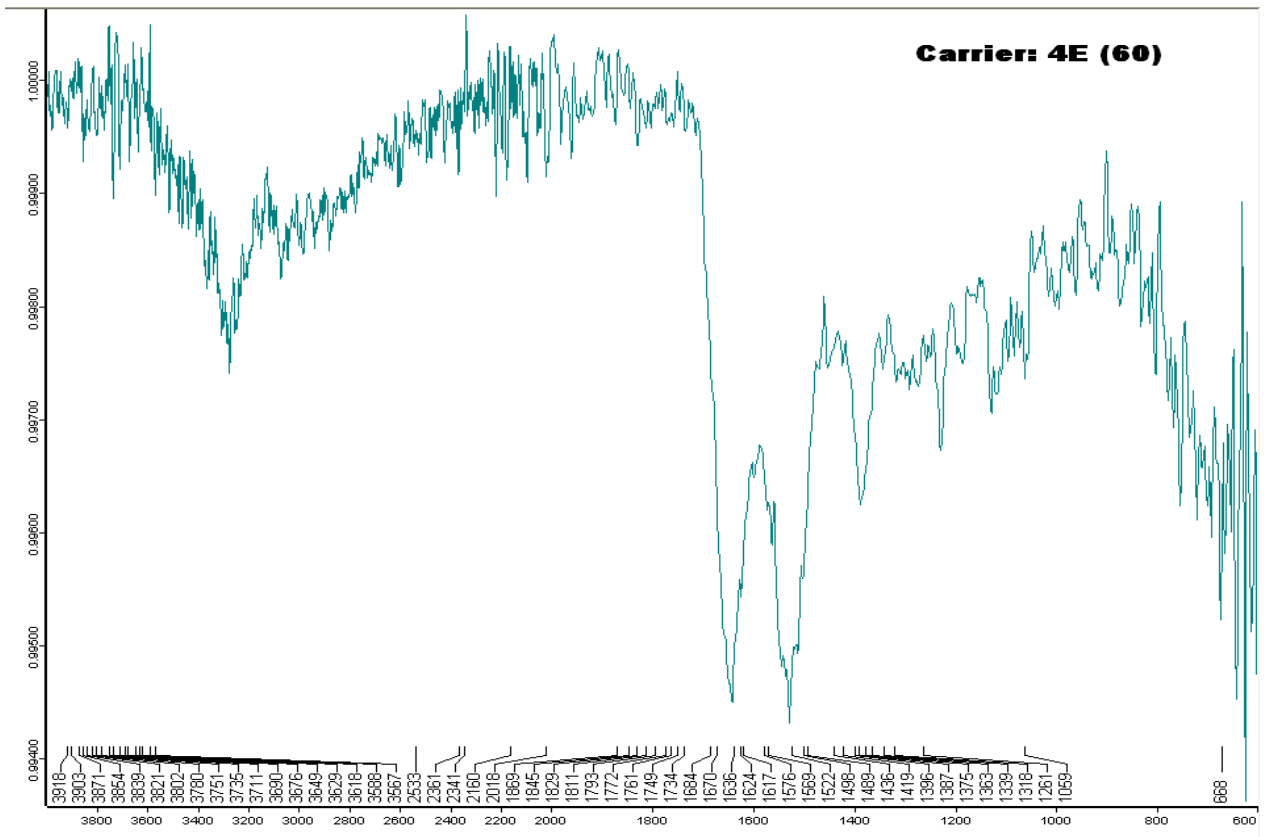
Carrier: 4E (60)
1.00000
0.99900
0.99800
0.99700
0.99600
0.99500
0.99400
3918 3903 3871 3854 3839 3821 3802 3780 3751 3735 3711 3690 3676 3649 3629 3618 3588 3567 2533 2361 2341 2160 2018 1869 1845 1829 1811 1793 1772 1761 1749 1734 1684 1670 1636 1624 1617 1576 1569 1522 1498 1489 1436 1419 1396 1387 1375 1363 1339 1318 1261 1059
668
3800 3600 3400 3200 3000 2800 2600 2400 2200 2000 1800 1600 1400 1200 1000 800 600

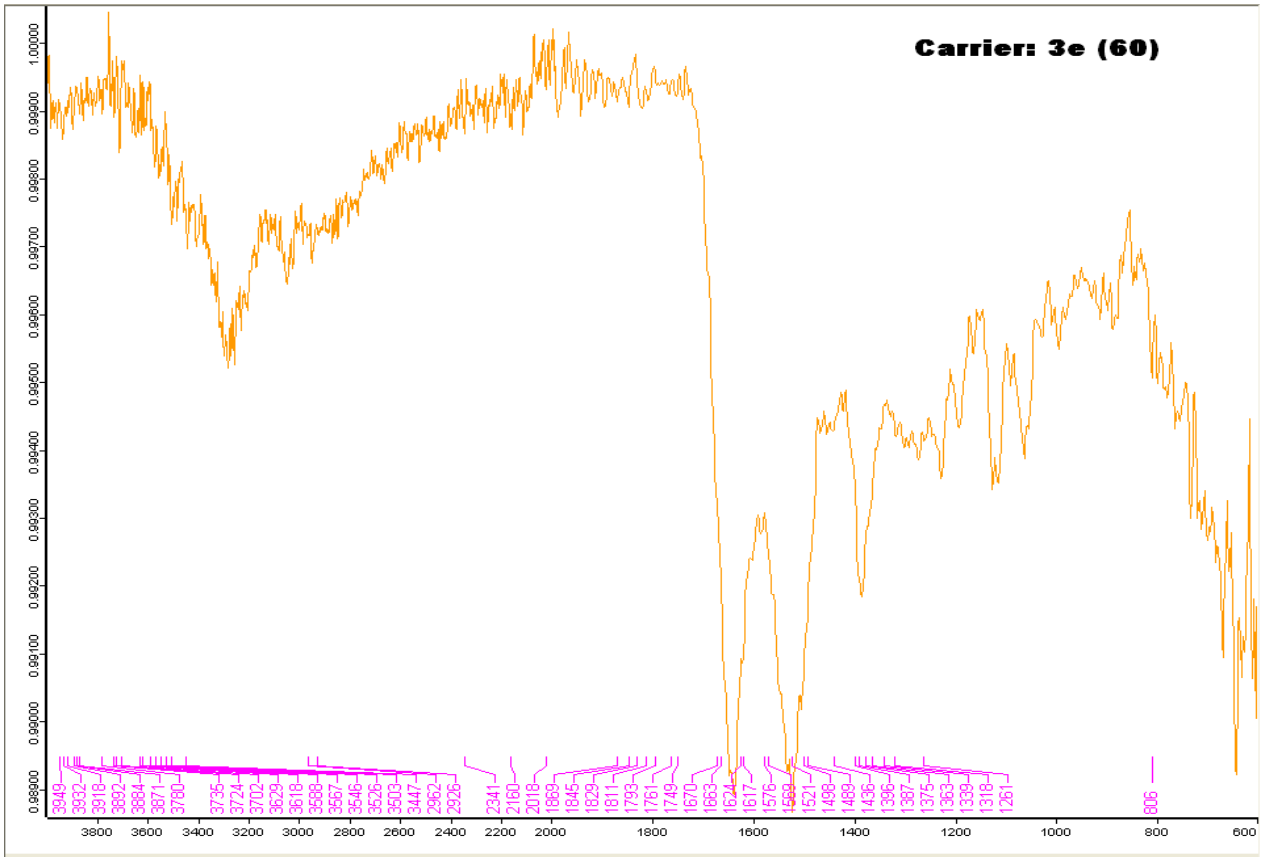
Carrier: 3e (60)
1.00000
0.99900
0.99800
0.99700
0.99600
0.99500
0.99400
0.99300
0.99200
0.99100
0.99000
0.98900
3949
3932
3918
3892
3884
3871
3780
3735
3724
3702
3629
3618
3588
3567
3546
3526
3503
3447
2962
2926
2341
2160
2018
1869
1845
1829
1811
1793
1761
1749
1670
1663
1624
1617
1576
1569
1521
1498
1489
1436
1396
1387
1375
1363
1339
1318
1261
606
3800
3600
3400
3200
3000
2800
2600
2400
2200
2000
1800
1600
1400
1200
1000
800
600

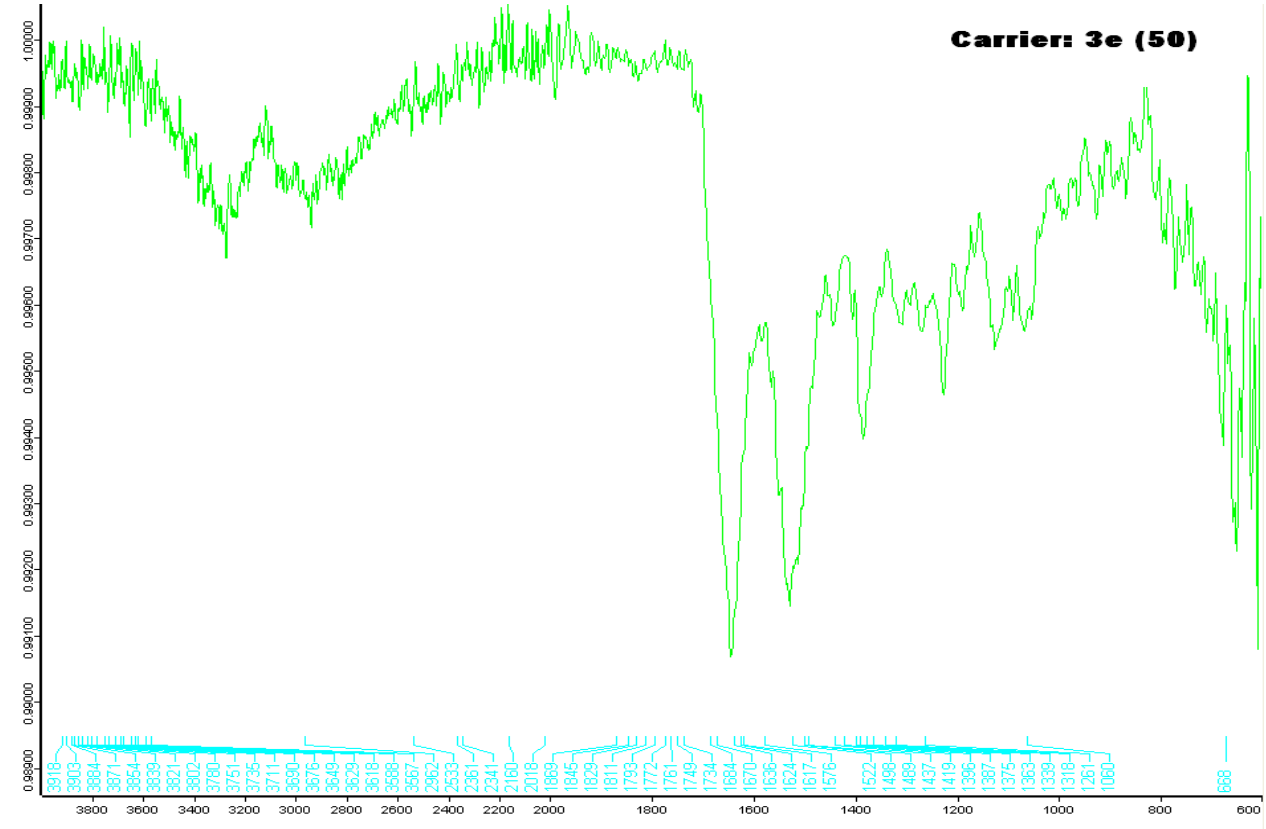
Carrier: 3e (50)
1.00000
0.99900
0.99800
0.99700
0.99600
0.99500
0.99400
0.99300
0.99200
0.99100
0.99000
0.98900
3918
3903
3884
3871
3854
3839
3821
3802
3780
3751
3735
3711
3690
3676
3649
3629
3618
3588
3567
2962
2533
2361
2341
2160
2018
1869
1845
1829
1811
1793
1772
1761
1749
1734
1684
1670
1638
1624
1617
1576
1522
1496
1489
1437
1419
1396
1387
1375
1363
1339
1318
1261
1060
668
3800
3600
3400
3200
3000
2800
2600
2400
2200
2000
1800
1600
1400
1200
1000
800
600

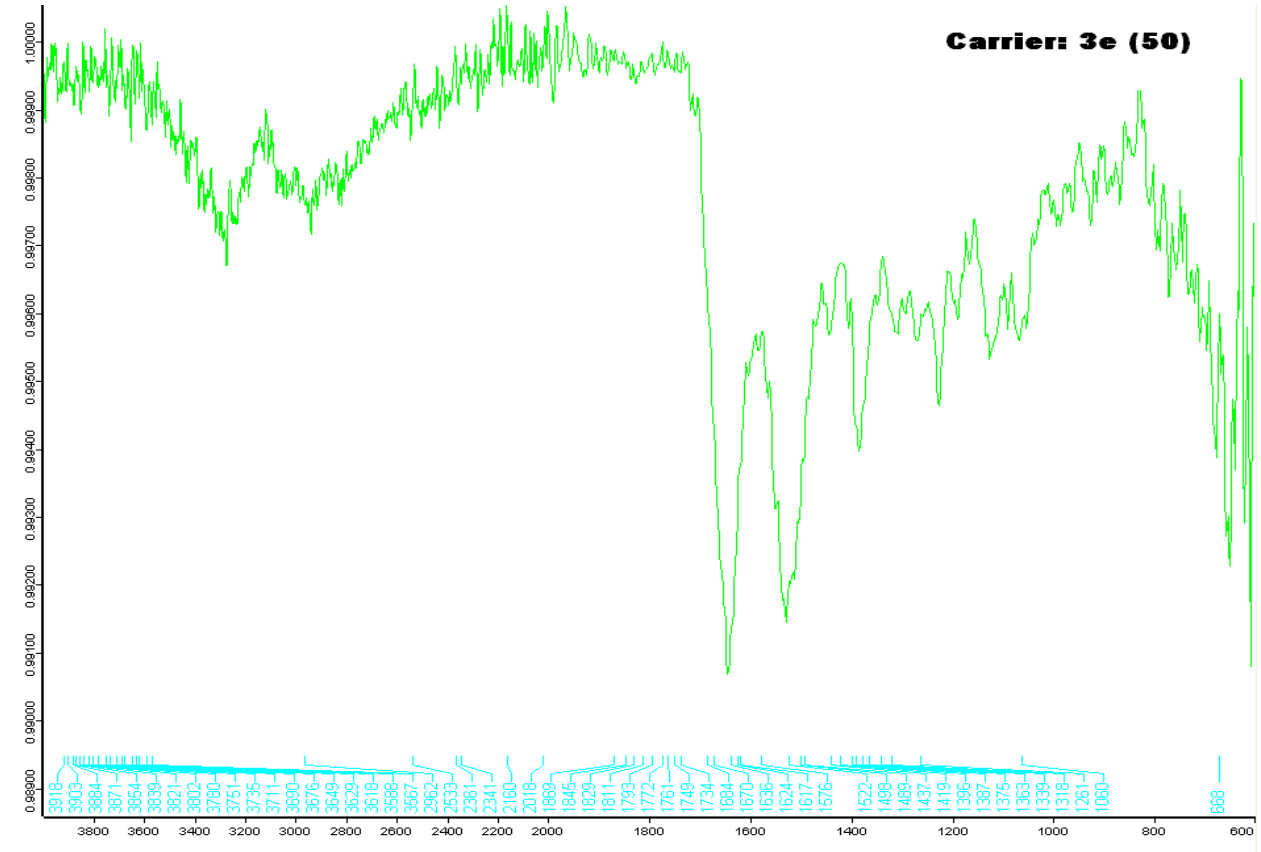
Carrier: 3e (50)
1.00000
0.99900
0.99800
0.99700
0.99600
0.99500
0.99400
0.99300
0.99200
0.99100
0.99000
0.98900
3800 3600 3400 3200 3000 2800 2600 2400 2200 2000 1800 1600 1400 1200 1000 800 600

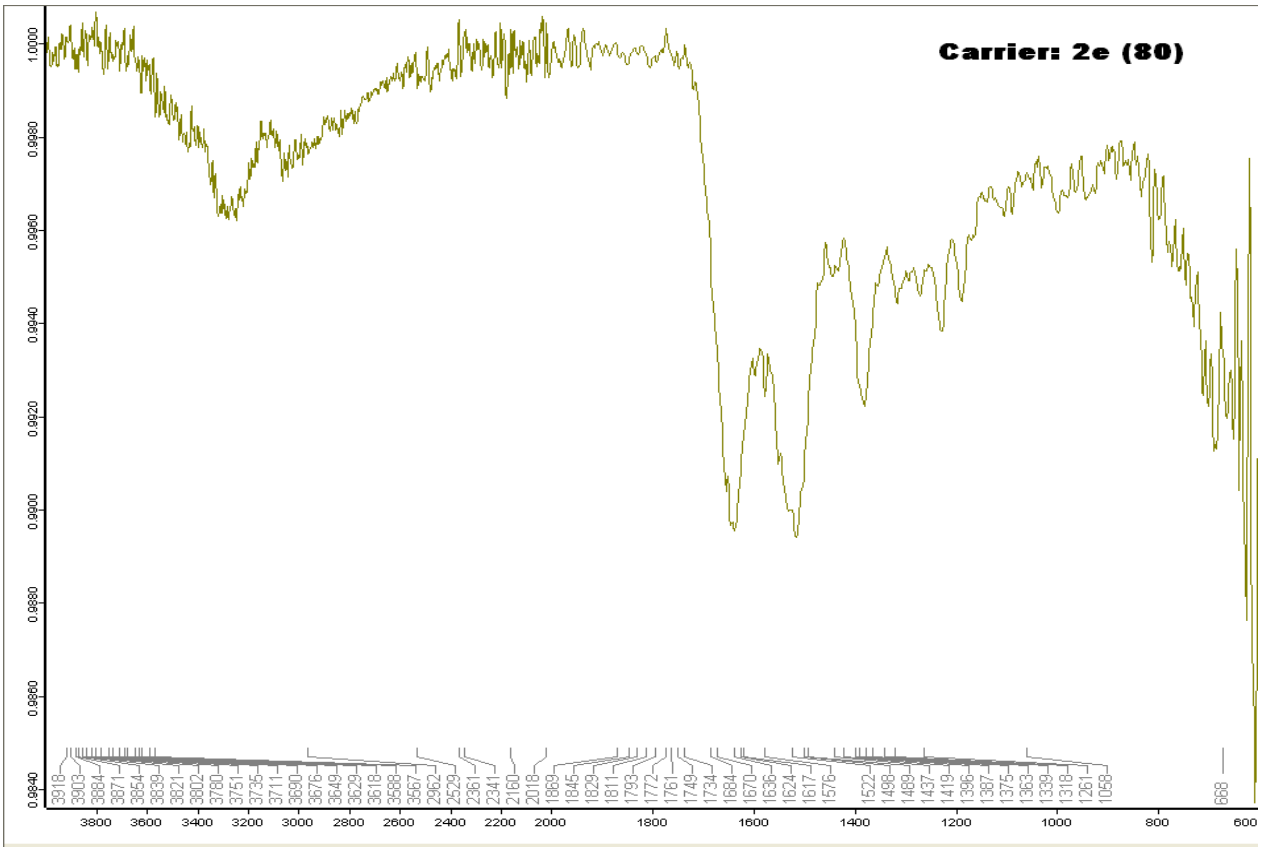
Carrier: 2e (80)
1.0000
0.9980
0.9960
0.9940
0.9920
0.9900
0.9880
0.9860
0.9840
3800 3600 3400 3200 3000 2800 2600 2400 2200 2000 1800 1600 1400 1200 1000 800 600

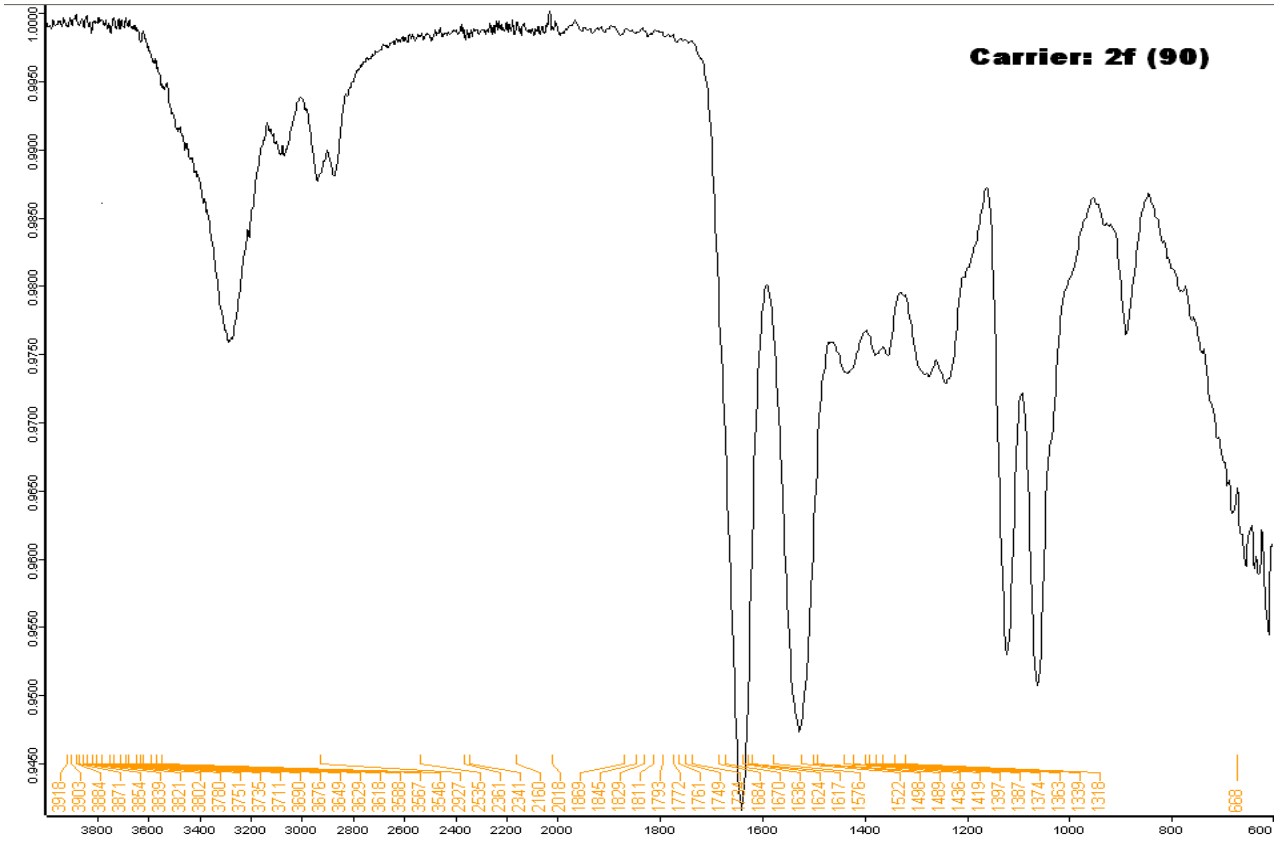
Carrier: 2f (90)

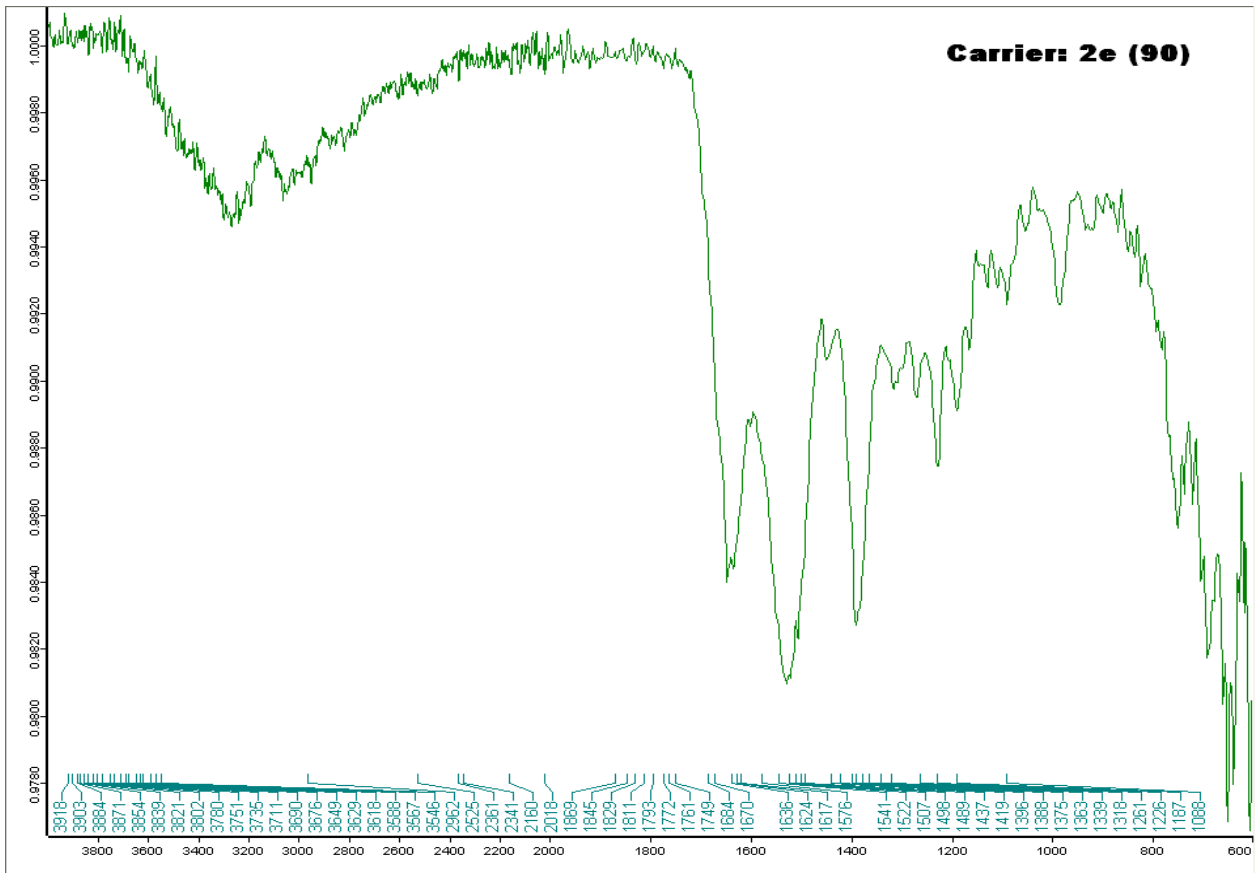
Carrier: 2e (90)

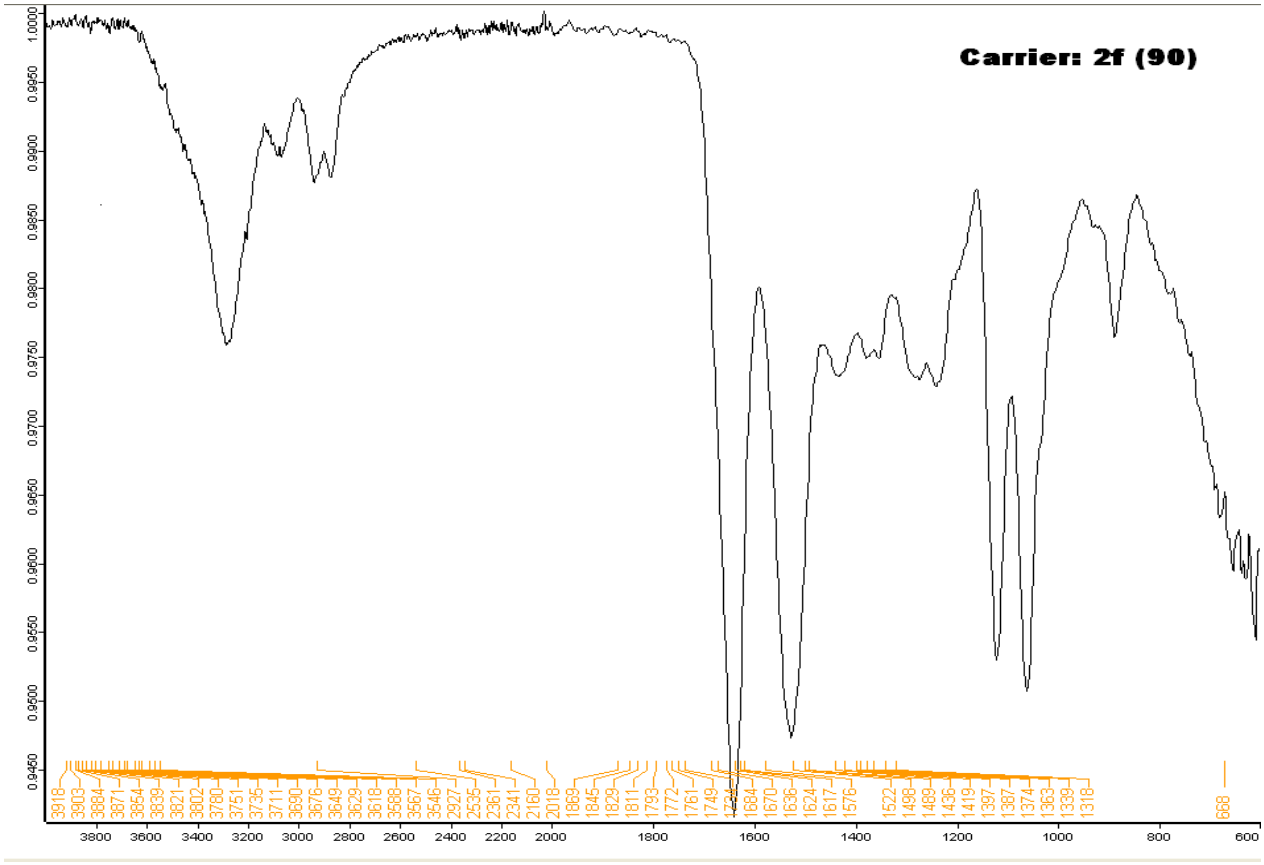
Carrier: 2f (90)

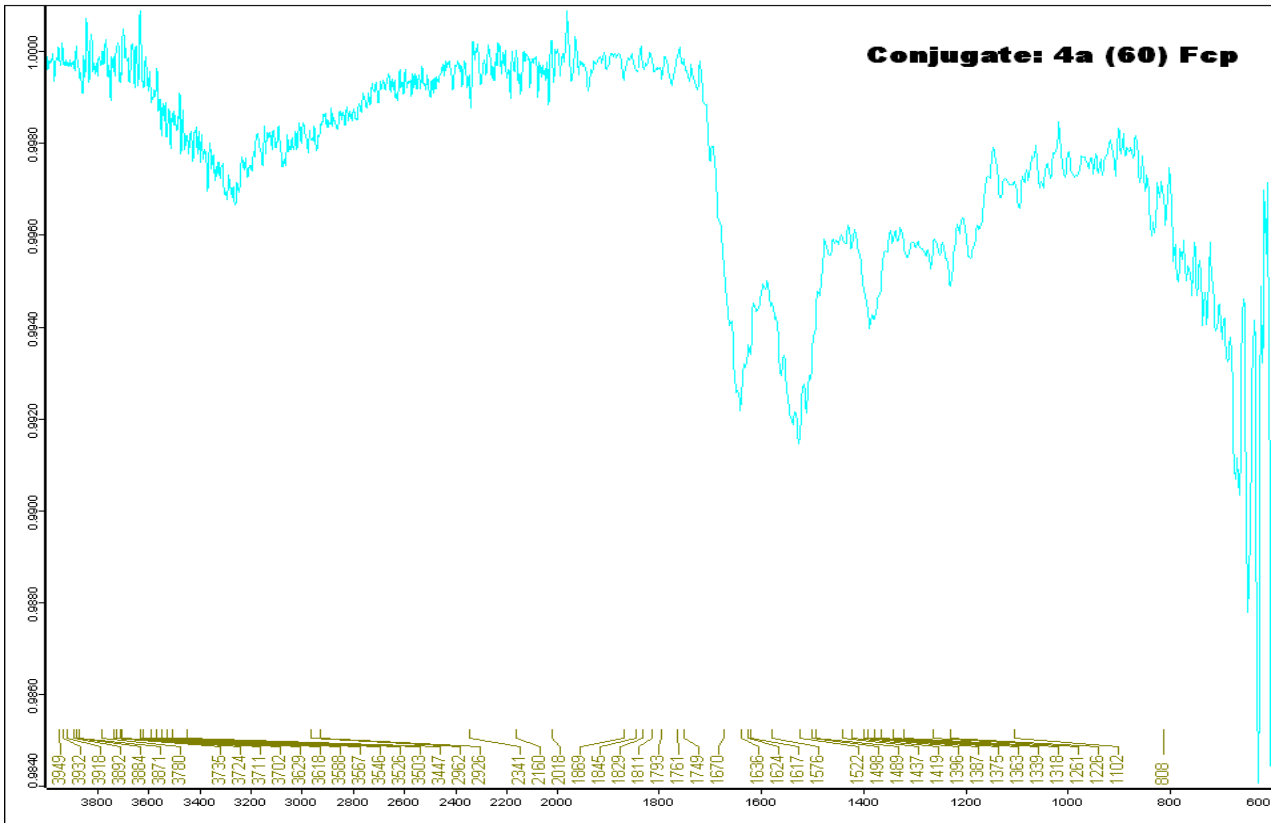
Conjugate: 4a (60) Fcp

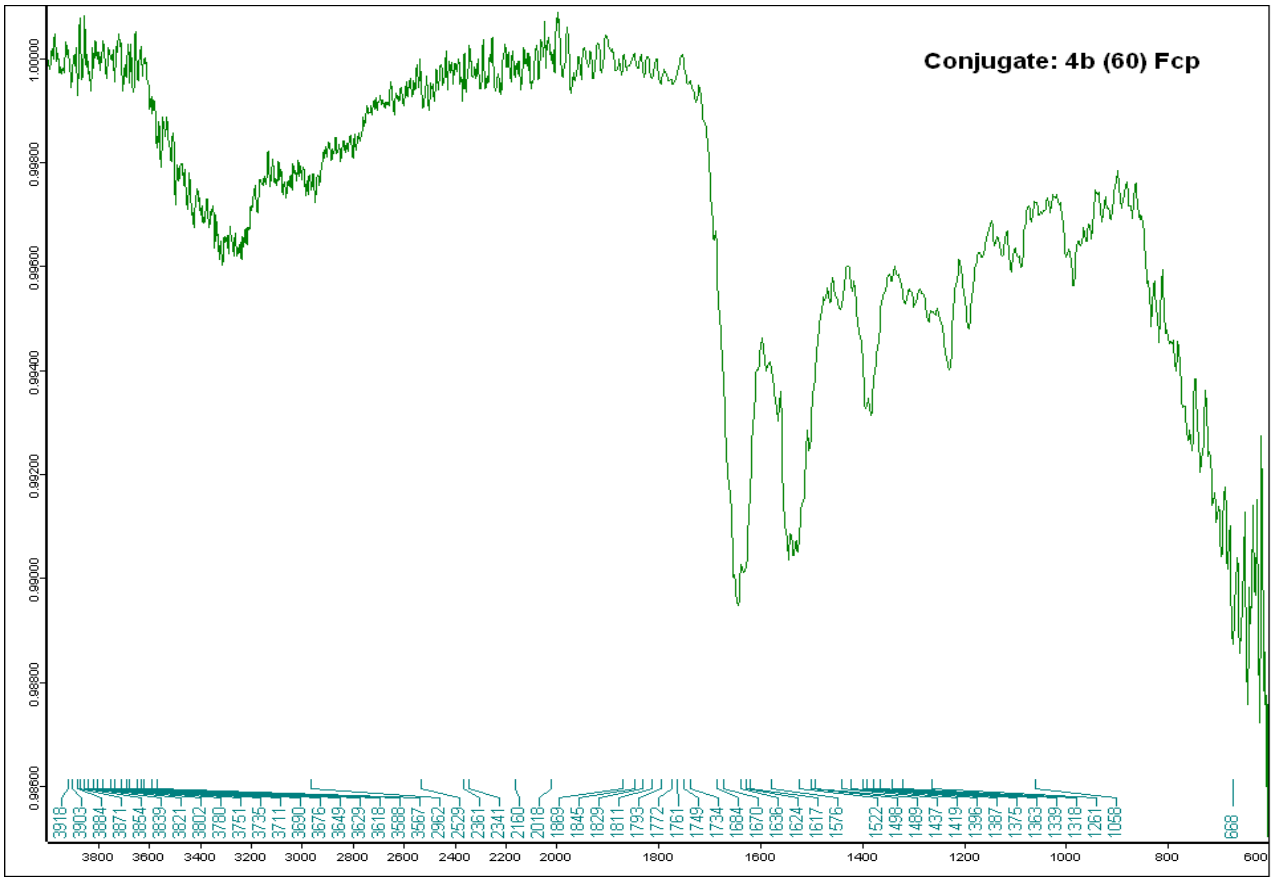
Conjugate: 4b (60) Fcp
1.00000
0.99800
0.99600
0.99400
0.99200
0.99000
0.98800
0.98600
3800 3600 3400 3200 3000 2800 2600 2400 2200 2000 1800 1600 1400 1200 1000 800 600

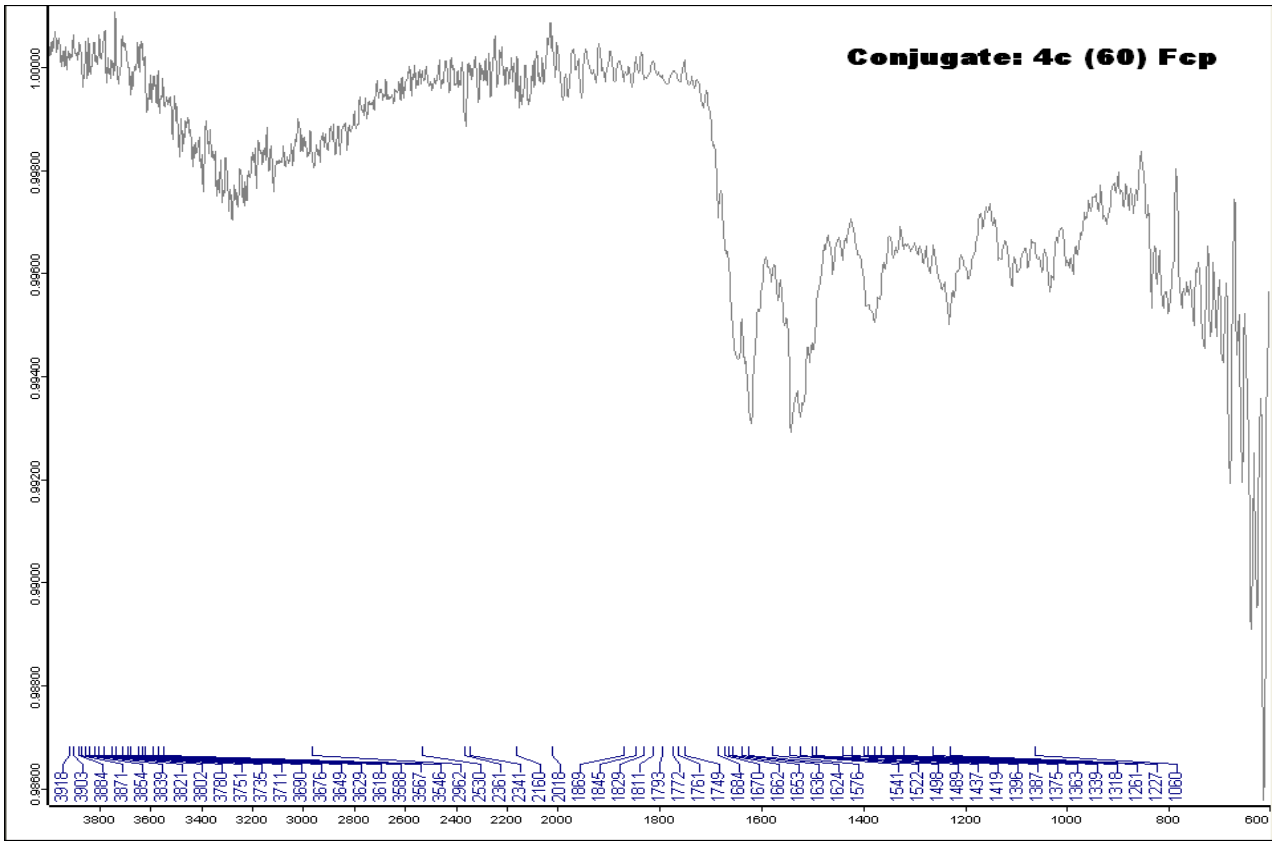
Conjugate: 4c (60) Fcp
1.00000
0.99800
0.99600
0.99400
0.99200
0.99000
0.98800
0.98600
3800 3600 3400 3200 3000 2800 2600 2400 2200 2000 1800 1600 1400 1200 1000 800 600

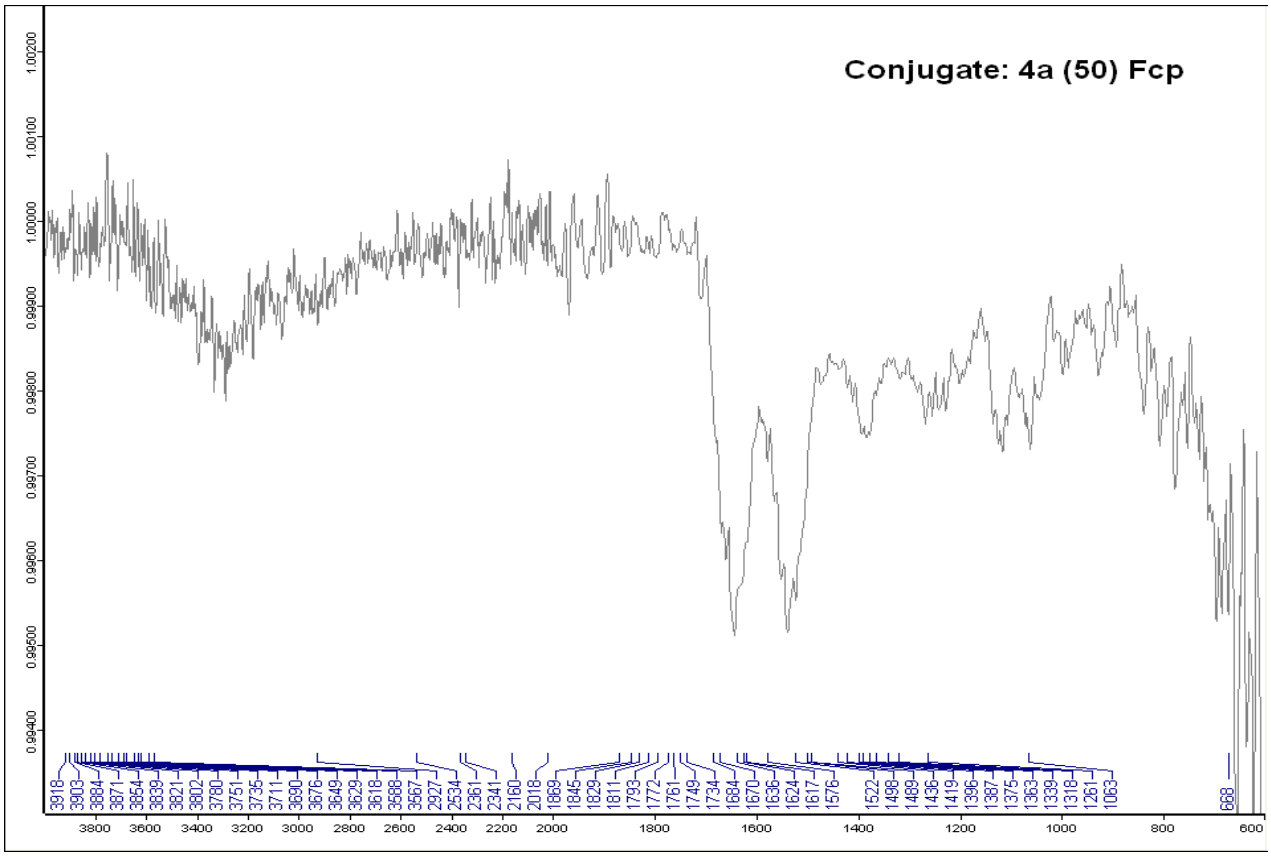
Conjugate: 4a (50) Fcp

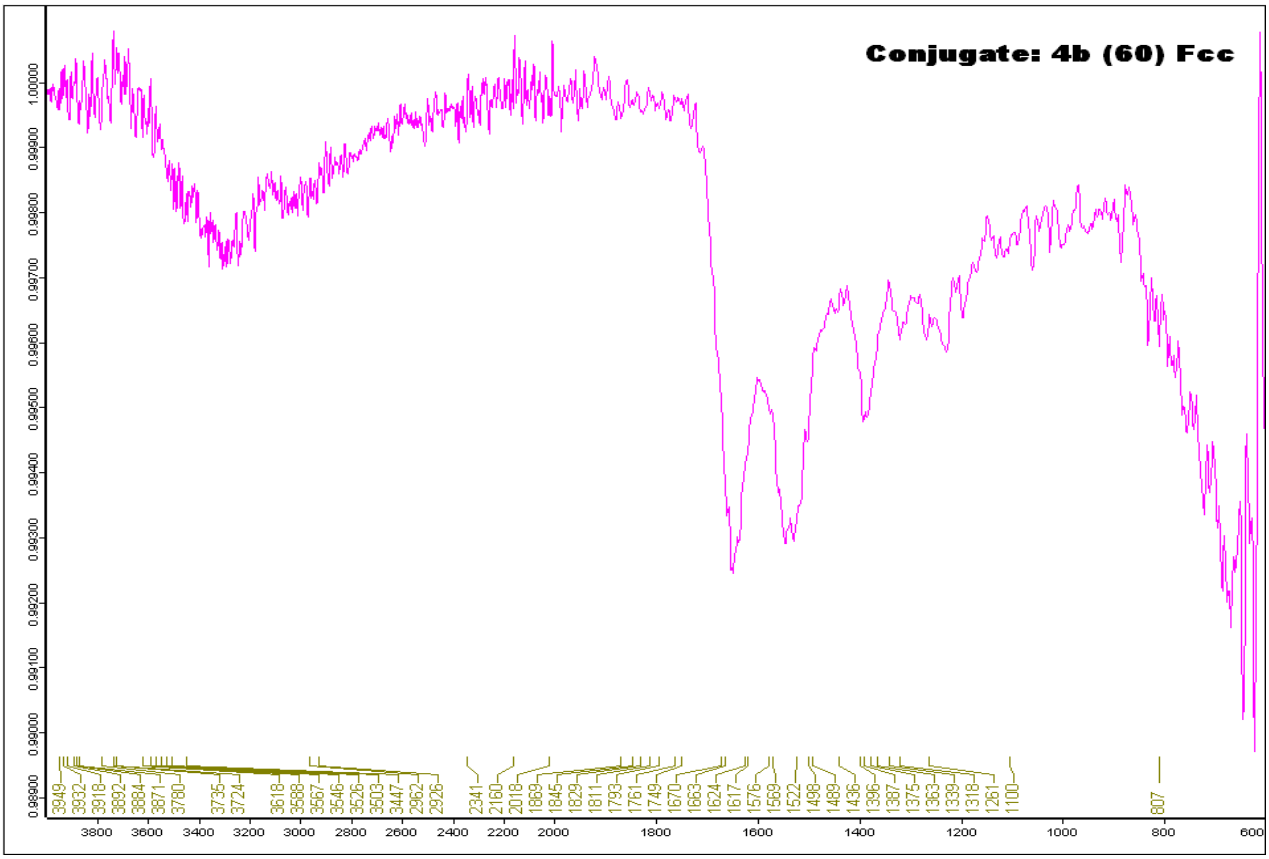
Conjugate: 4b (60) Fcc

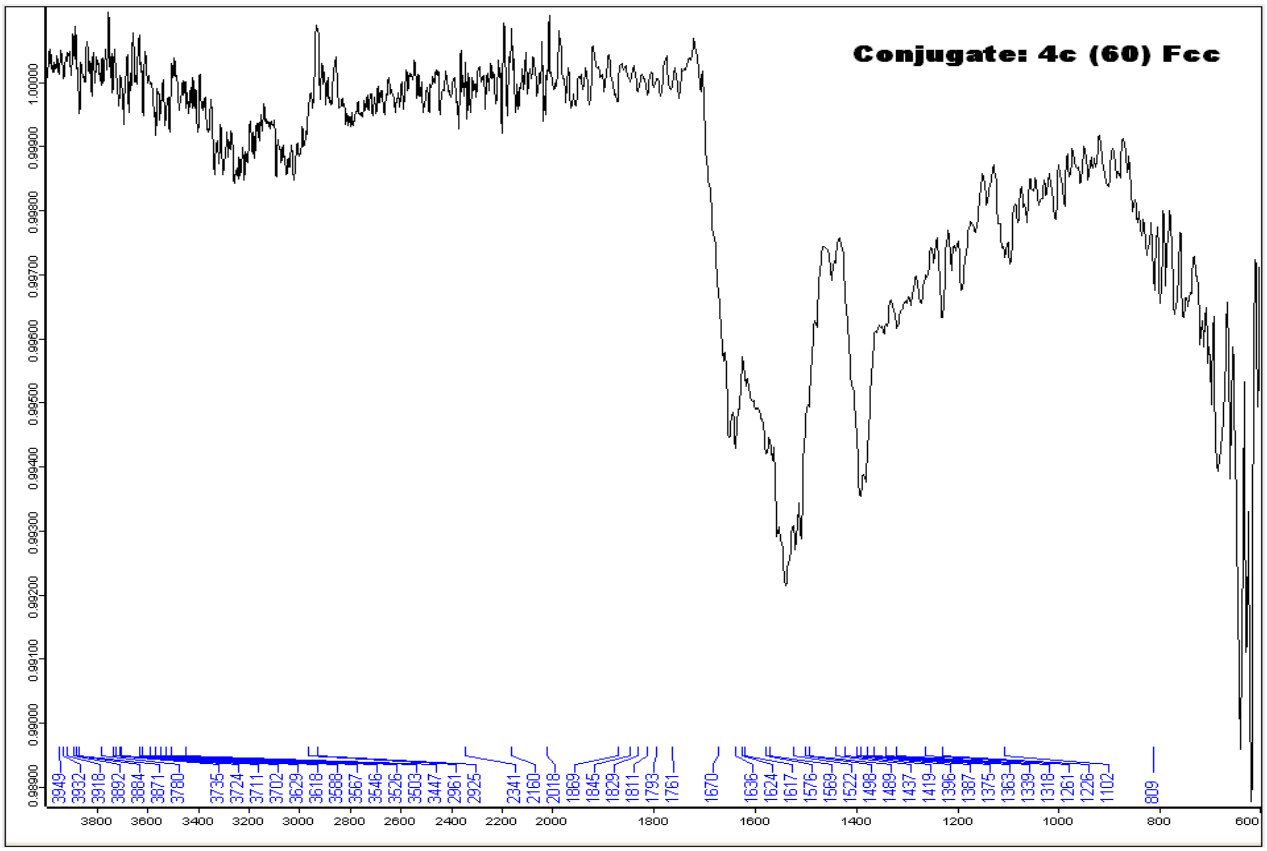
Conjugate: 4c (60) Fcc

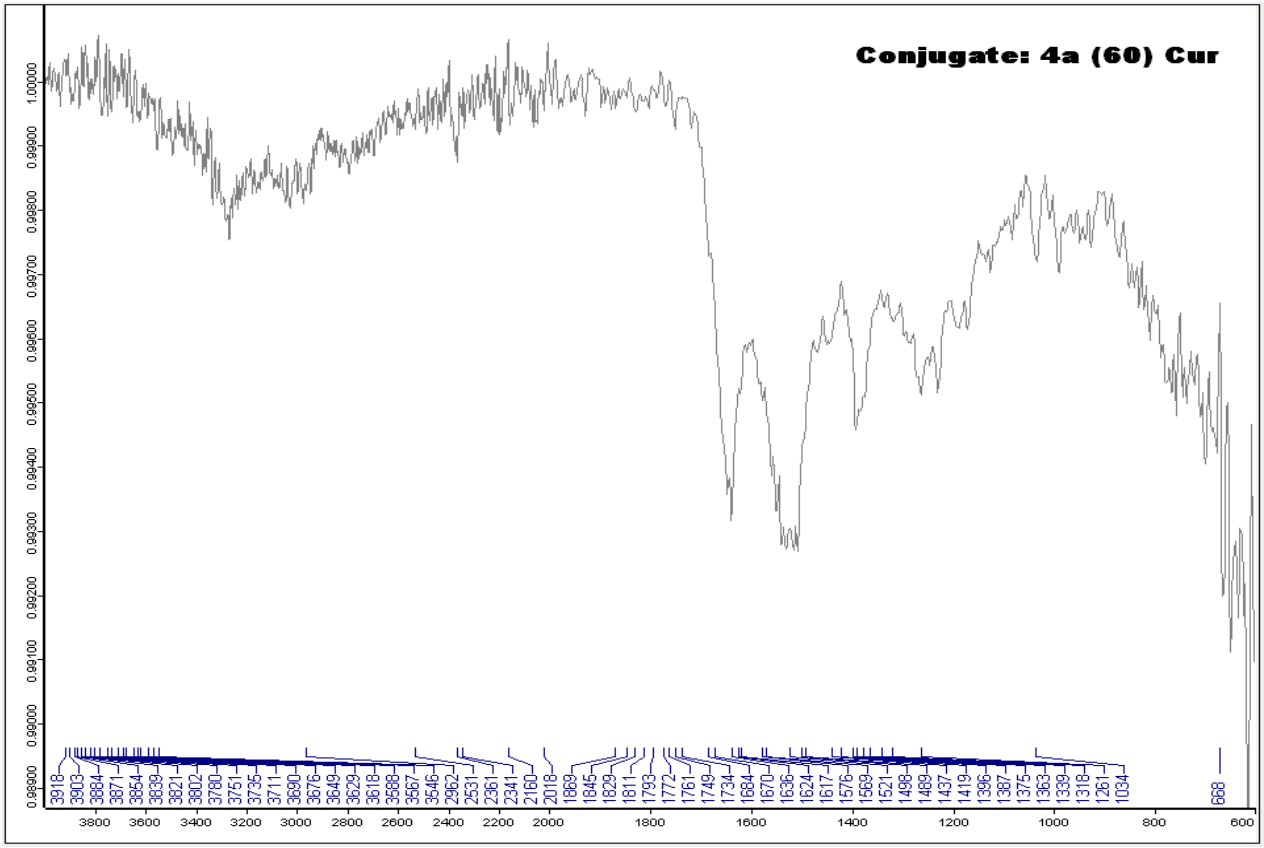
Conjugate: 4a (60) Cur

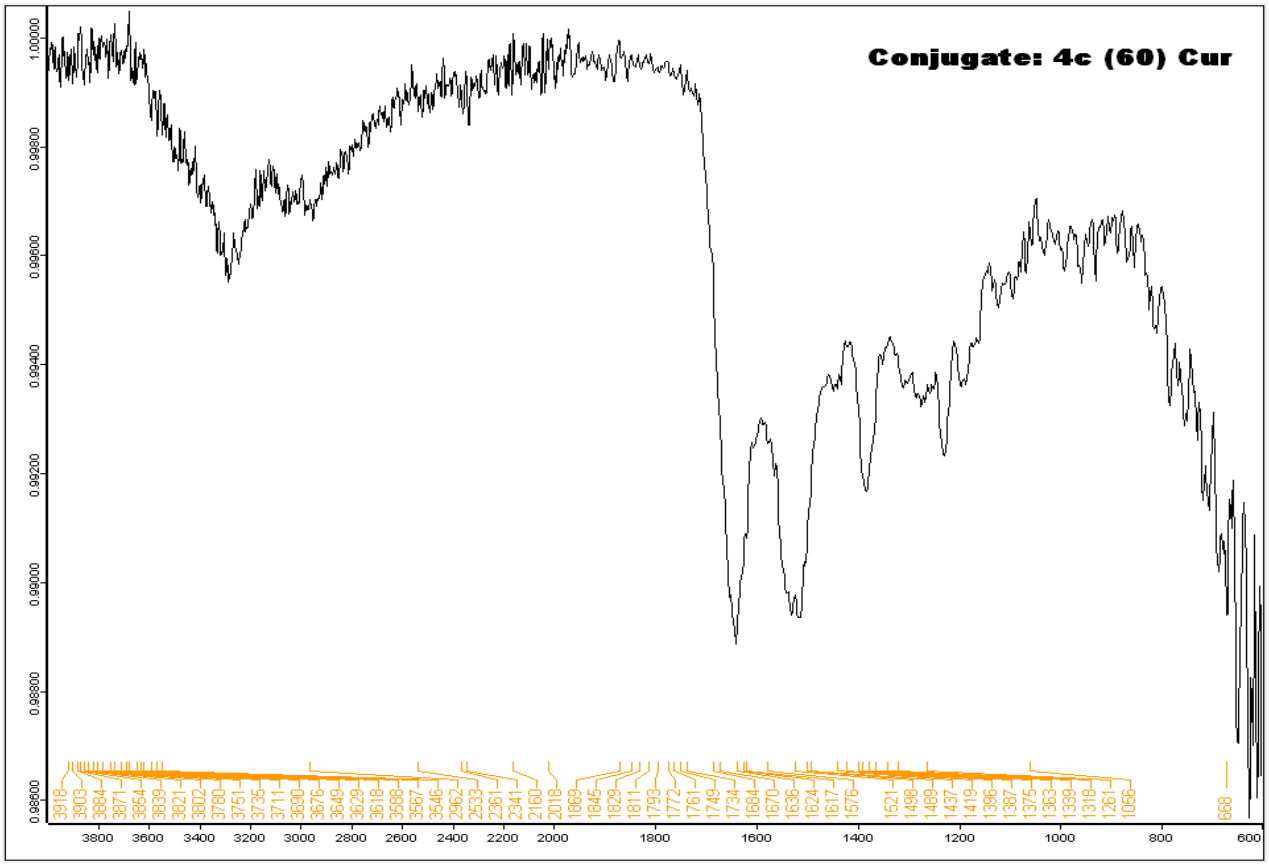
Conjugate: 4c (60) Cur

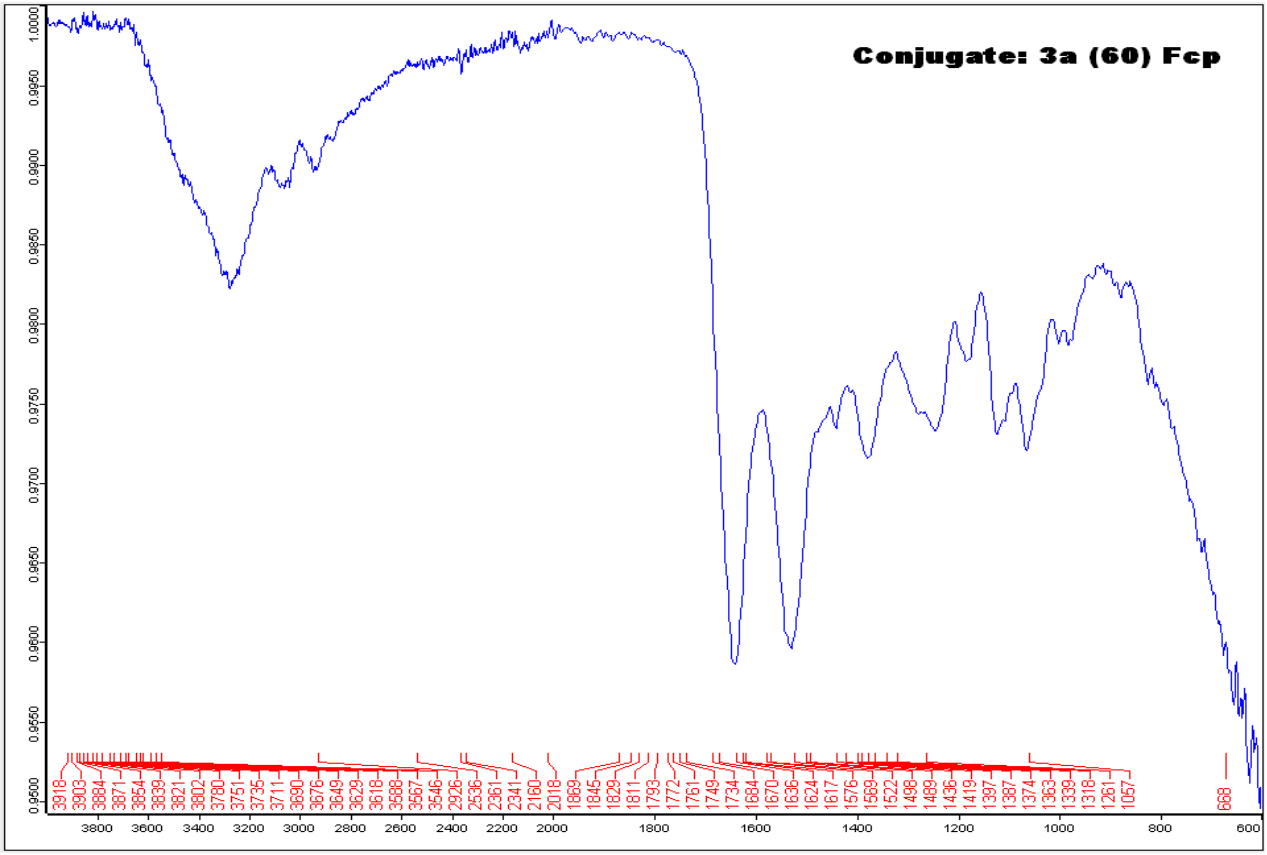
Conjugate: 3a (60) Fcp

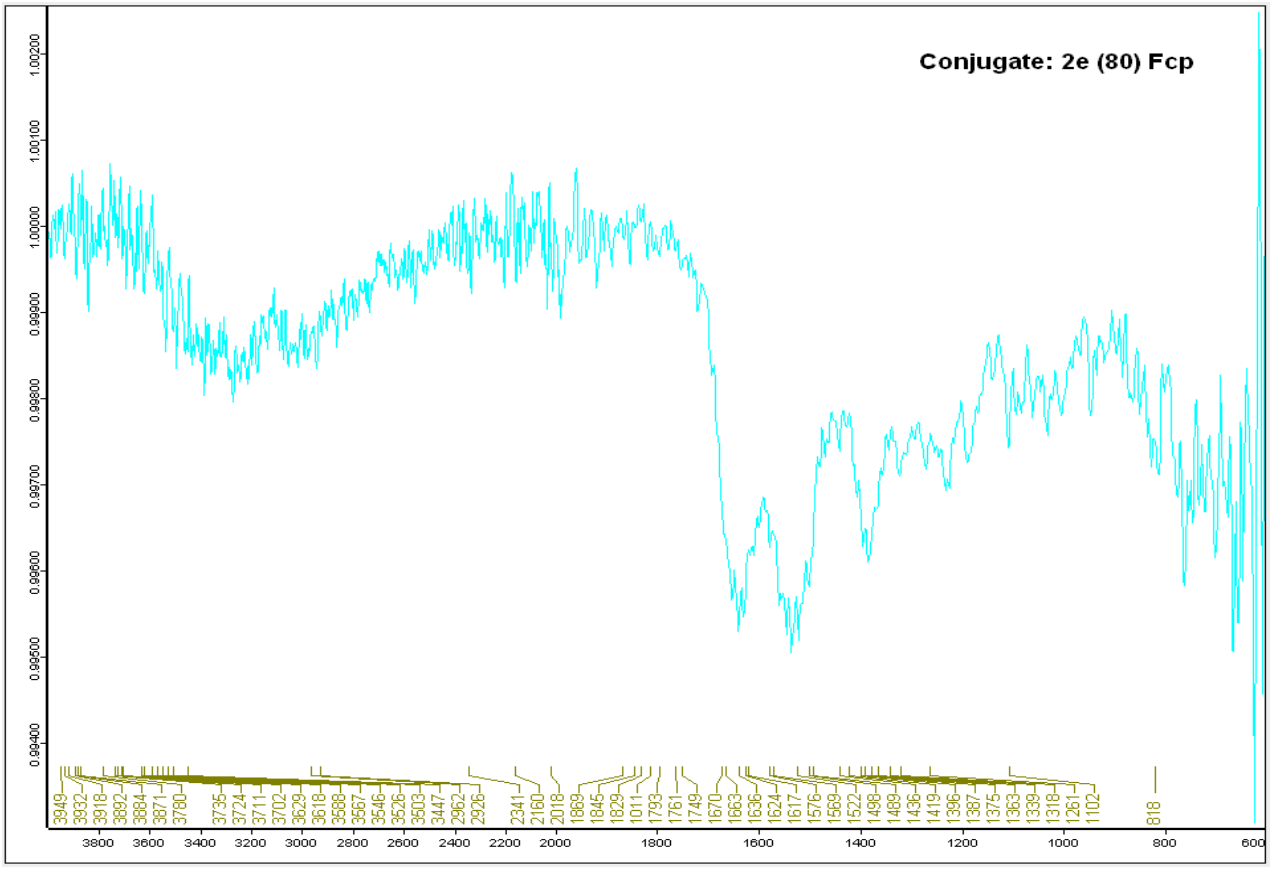
Conjugate: 2e (80) Fcp

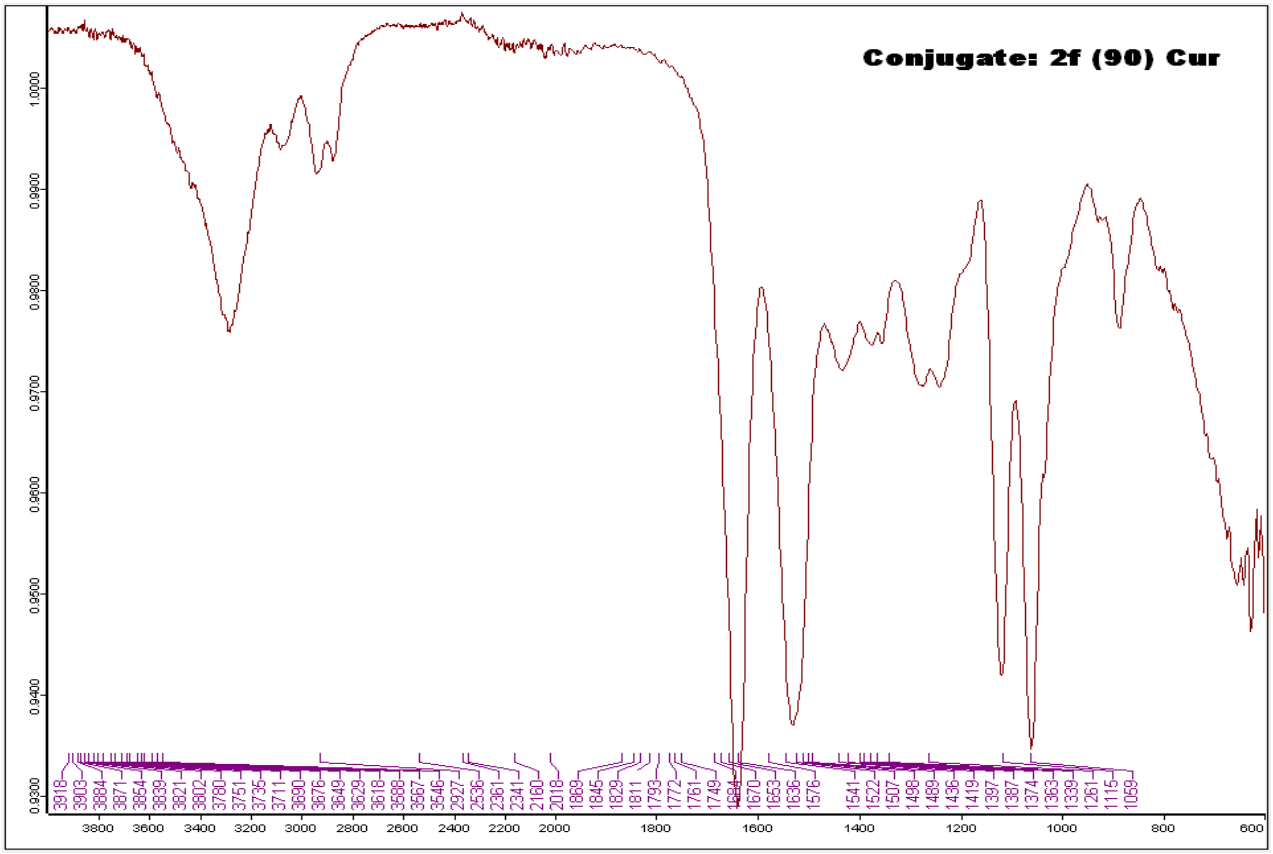
Conjugate: 2f (90) Cur

SELECTED PROCESS PICTURES AND PROPOSED FLOW SHEET

Image 1: Carrier synthesis

Image2: Dialysis process

Image 3: Synthesis of polyaspartamide


Image 4: Freeze drying process

Proposed flow sheet

First step: Carrier synthesis

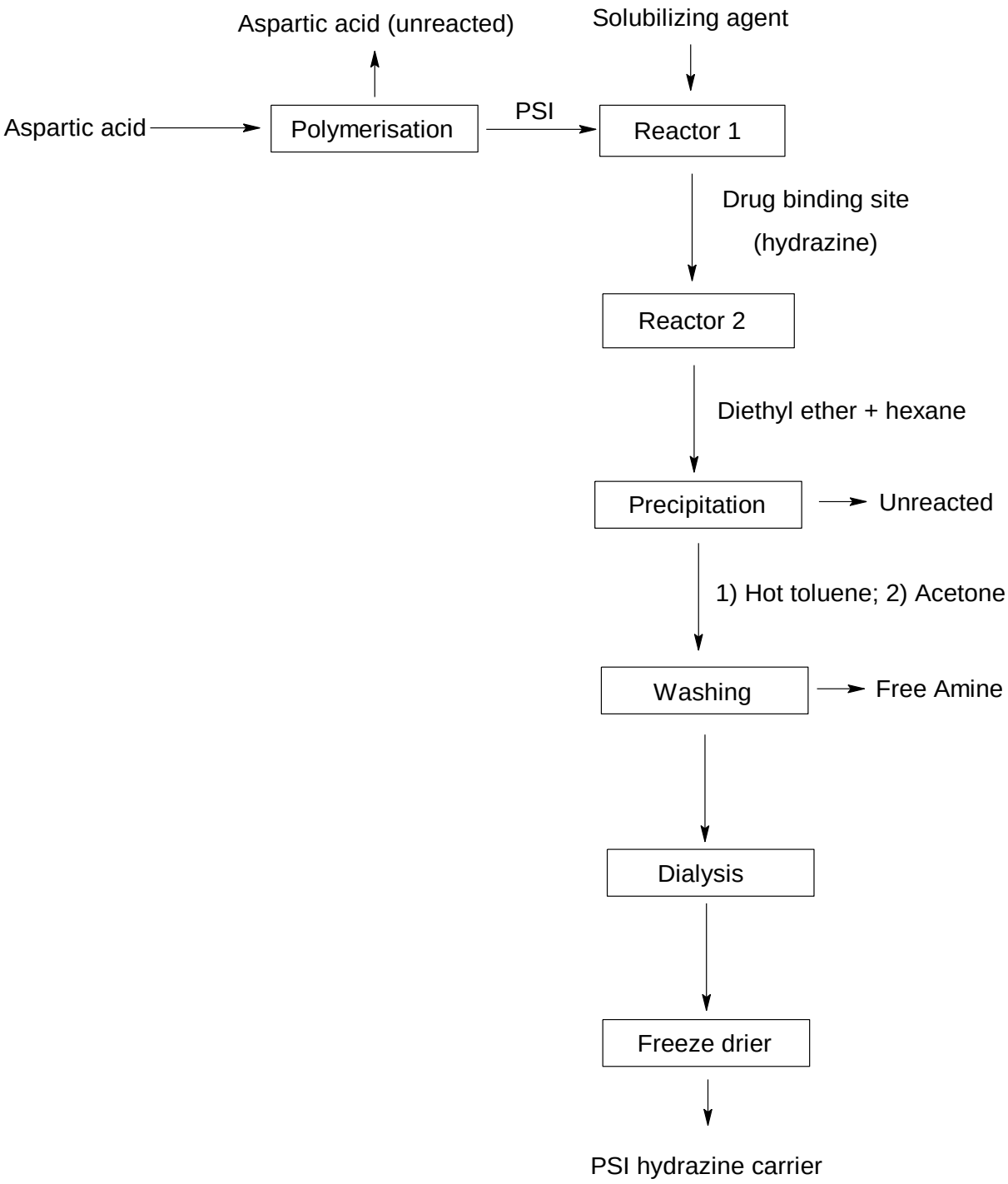

Second step: Drug- carrier conjugation